



**IEA**  
**SOLAR R&D**

**INTERNATIONAL ENERGY AGENCY**

**solar heating and  
cooling programme**

**TASK IX**

**Solar Radiation and  
Pyranometry Studies**

**VALIDATION OF MODELS FOR ESTIMATING  
SOLAR RADIATION ON HORIZONTAL SURFACES**

**VOLUME 1: Report**

**June 1988**

**FINAL REPORT**

**IEA TASK IX**

**VALIDATION OF MODELS FOR ESTIMATING SOLAR  
RADIATION ON HORIZONTAL SURFACES**

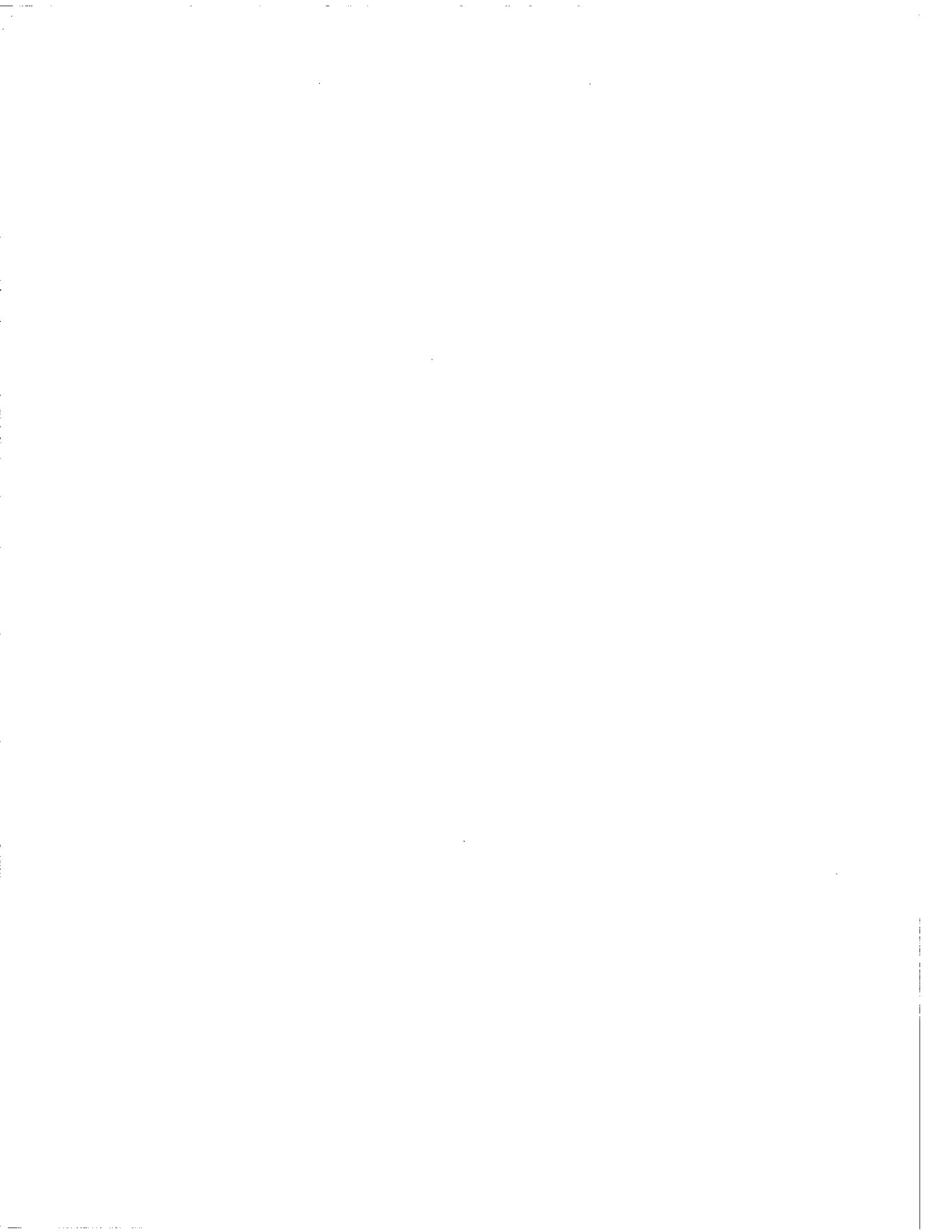
By

J.A. Davies \*  
D.C. McKay \*\*  
G. Luciani \*  
M. Abdel-Wahab \*

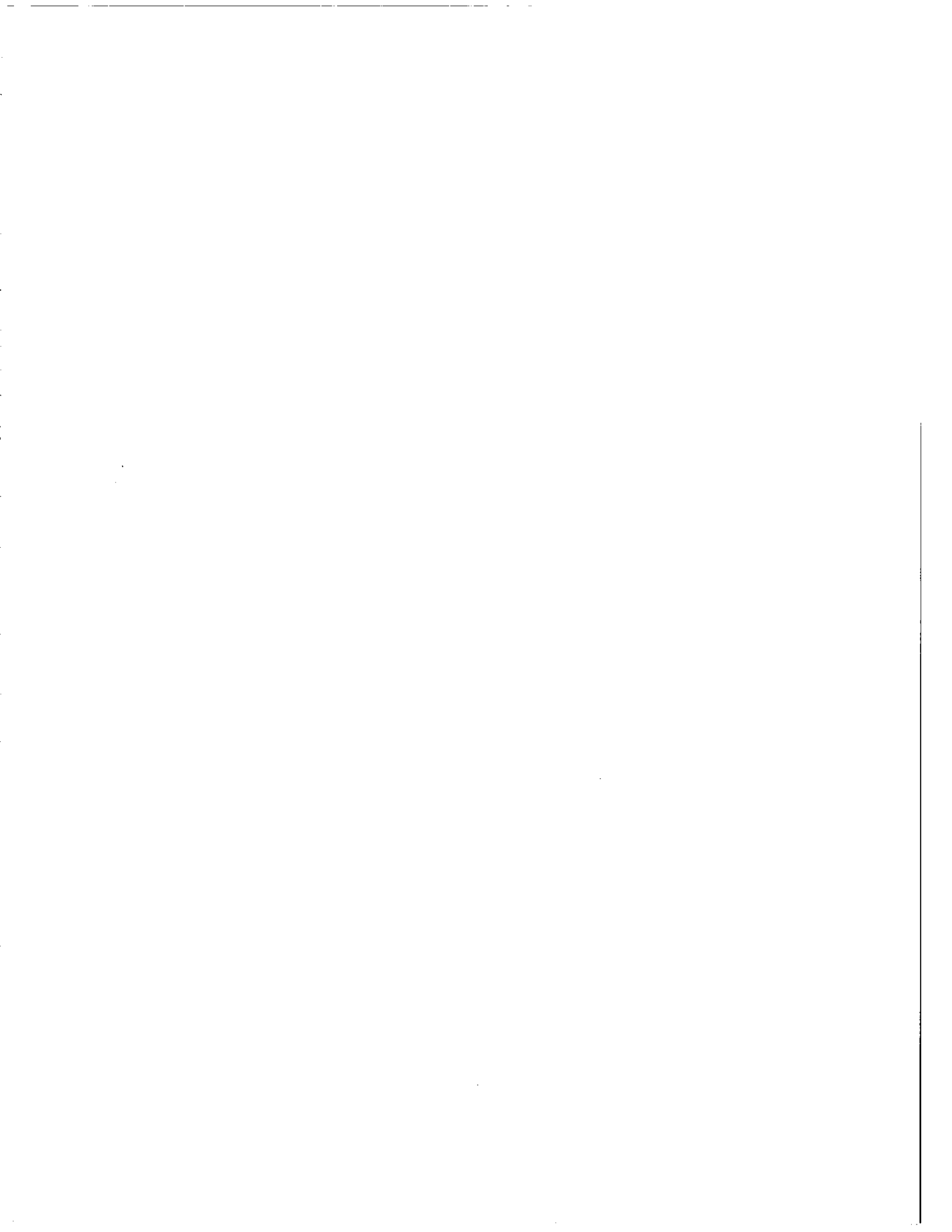
June 1988

\* Department of Geography  
Mc Master University  
Hamilton, Ontario  
CANADA

\*\* Atmospheric Environment  
Service  
4905 Dufferin Street  
Downsview, Ontario  
CANADA



**VOLUME 1 : REPORT**



## EXECUTIVE SUMMARY

The report presents the findings of an international collaborative study performed by Task IX, Solar Radiation and Pyranometry Studies, of the International Energy Agency's Solar Heating and Cooling Program. The overall objective of this study was to evaluate the performance of numerical models which provide estimates of solar irradiance on horizontal surfaces.

Specifically, the study

- evaluated the performance of 12 solar irradiance models over varying time periods from hourly to monthly;
- assessed the influence of temporal averaging (for time scales longer than a day) on the errors associated with the calculation of solar irradiances;
- examined variation in model performance with season and cloudiness; and
- assessed the effect of using estimates of solar irradiance on a horizontal surface to calculate solar irradiance on sloped surfaces.

The models were grouped into three general categories according to the way in which cloud field transmittance is treated: as a function either of fractional sunshine or cloud amount and whether total cloud or cloud layer amounts are used. A fourth category contained models for partitioning radiation into direct beam and diffuse radiation components using the statistical approach of Liu and Jordan (1960). The four categories are as follows:

- Cloud layer models
- Total cloud-based models
- Sunshine-based models
- Liu and Jordan models

The significance of the study resides in its use of data sets representing a range of solar climates and, extending over a number of years. The validation used

15 data sets from Australia, Canada, West Germany, Switzerland, The Netherlands, United Kingdom and the USA.

Three statistical measures were used in the evaluation of the various models. The first was the mean bias error which measures the systematic error. The second was the root mean square error which measures the non-systematic error. The third was the mean absolute error since the mean bias error conceals positive and negative biases.

The models were ranked for each performance statistic, described above, from monthly summaries of hourly and daily solar irradiance statistics. The ranking counts were pooled for all years for each station, and these were then pooled into seven groups; Australia, Europe, Canada, United States, Europe and Canada, North America, All stations.

For comparison, an attempt was made to estimate the best performance that any model can attain. This was achieved by (1) empirically determining  $a$  and  $b$  parameters in the Ångström equation and (2) then using the parameter values to compute daily global radiation. These estimates, which are called *BEST*, provide useful comparisons for all global radiation models.

The results of the validation were as follows:

- **Global radiation.** The two cloud layer models, *JOS* and *MAC*, provided the best hourly and daily estimates with *JOS* usually best. The EURCAN results show that the layer models performed better than the sunshine models. *PAGE* is the best of the sunshine models.
- **Diffuse and direct beam radiation.** The Liu and Jordan models provided the best estimates; *OH* and *EKDH* for hourly radiation and *EKDH* for daily.
- **Variation in model performance with season and cloudiness.** There was no consistent evidence of variations in the performance of the better models (*MAC*, *JOS*, *EKDH* and *EKDD*) with season, cloudiness or atmospheric

transmissivity. This suggests that these models have general applicability.

- **Model performance for different averaging periods.** For all models, the error decreased when data was averaged over longer periods (from 2 to 30 days). The layer models provided the best results for global radiation. With the exception of Australia, the *MAC* model performed the best. For diffuse and direct beam radiation layer model values were similar or even better than values for Liu and Jordan models.
- **Effect of using estimates of incident radiation to calculate radiation sloped surfaces.** When estimated values are used, generally the root mean square error for daily radiation increased by up to a factor of two. In percentage terms, root mean square error values for the different sloped surfaces are similar.

### General

The differences between statistical measures of error for the best and worst performing models may not be sufficiently large to be significant for solar energy or any other purpose. Because there is no clear statement on the required accuracy of radiation estimates for use in certain applications (e.g. solar energy models), it is difficult to assess whether these results or others, are sufficient for recommending one or more models.

The recommendations drawn from the validation are:

- Layer models should be used for estimating global radiation whenever possible.
- Liu and Jordan models, particularly *EKDH* and *EKDD*, are generally best for estimating direct beam and diffuse components.
- Further modelling efforts would benefit from clear guidelines from the solar energy community concerning the required accuracies of radiation estimates that are permissible.



#### 4 *Executive Summary*

Under the same IEA programme, a study was undertaken to validate models which estimate solar irradiance on sloped surfaces. The report; "Calculation of Solar Irradiances for Inclined Surfaces: Verification of Models which use Hourly and Daily Data" is available from Atmospheric Environment Service, 4905 Dufferin Street, Downsview, Ontario, Canada M3H 5T4.

# CONTENTS

## Volume 1

	Executive summary	1
	Contents	5
1	Introduction	7
2	Models	11
3	Data	27
4	Results	39
5	Summary and conclusions	85
6	Availability of models and data	89
7	References	93

## Volumes 2 and 3

	Appendices	Volume
A	Summaries of model performance statistics for daily and hourly radiation estimates	2/3
B	Statistical summaries for each model and year	3
C	RMSE for different averaging periods for each radiation flux, station and model	3
D	Model performance statistics for different atmospheric transmission groupings	3



# CHAPTER 1: INTRODUCTION

Ideally, a network of radiation stations should provide sufficient data to determine spatial and temporal variations of radiation over land masses and adjacent water bodies. The spatial resolution would depend on the spatial density of stations. The practical reality is, however, that in all countries the spatial density is inadequate. Furthermore, there are few stations with extensive, long-term records. Although spatial and temporal limitations apply to the measurement of all meteorological variables, they particularly characterize solar radiation measurement. The dearth of spatial and temporal data on the amounts of solar radiation and its direct beam and diffuse components for solar energy utilization has prompted the development of calculation procedures to provide estimates for places where measurements are not made and for places where there are gaps in the measurement record.

The meteorological and engineering literature is replete with such procedures. Many were developed to satisfy a particular, local need and should not be considered as general models with universal application. Regression - based models generally fall into this category and care should be exercised in applying them beyond the domain for which they were derived. However, the overall forms of these models may be universally applicable so that the user need only verify or revise the numerical values of constants and coefficients for a particular location and time period. Since measurements are needed for this, such calibration of a model is somewhat self defeating.

As part of Task IX of the International Energy Agency's Solar Heating and Cooling Programme, a project was established in 1982 to evaluate selected models which simulate solar irradiance on horizontal surfaces. A selection was made from

models and model forms which either make some claim to generality or may be of general application. The process for evaluating these models was as follows.

A letter requesting models and data sets was sent out in the fall of 1983. From that request and from a review of the scientific literature, twelve models were selected and evaluated with data sets from seven countries at McMaster University in Hamilton, Ontario, Canada. An initial validation was run on the models in the spring and summer of 1984. It consisted of running one year of data through the models to ensure that the study team had coded the models correctly and that the data sets were being read correctly.

In October 1985, the results of this validation were distributed to researchers and individuals who provided models and data sets for the project. The information provided were:

- a summary of models and data worked on before May 1985, and, in particular, questions about the data.
- a computer programme listing containing the model codes and the code for reading the data for the particular country concerned.
- documentation on input and verification data sets for the various locations.
- comparison statistics on a daily and monthly basis for the months of January, July and October.
- explanation of month end statistics.

The questions asked were:

- are the models coded correctly?
- have new algorithms been developed or improvements made for any particular model?
- are there any other data sets that could be used besides the data sets listed?

Based on the comments received, models were updated and corrections were made

to the existing data.

On the basis of the comments received several new models were included. Following revisions, computations were made with more extensive sets of data than in the initial validation. Late in the summer of 1986, a document summarizing the results was distributed to members for comment and for their input on the models' performance. The results and recommendations contained in this report are derived from these sources.

This report consists of three volumes. Volume 1, this volume, discusses the models (Chapter 2), data requirements (Chapter 3) and results (Chapter 4). Chapter 5 presents a summary, conclusions and recommendations. Chapter 6 describes the model source codes and data that are available on magnetic tape. References used in the work are listed in Chapter 7. Volumes 2 and 3 contain complete listings of results.



## CHAPTER 2: MODELS

### 2.1 OVERVIEW OF MODEL FORMS

For most practical purposes, there is little justification for employing formal solutions to the radiative transfer equation to estimate surface global solar radiation and its direct beam and diffuse components. Although the computational requirements for these analytical methods are no longer a serious obstacle because of increased computer power, the required optical information for multiple atmospheric layers is unavailable. Instead, we consider simpler models which are well suited to the available information and can be applied widely.

The models are non-spectral, treat the atmosphere as plane parallel and assume single scattering, although the effect of multiple reflection between ground and atmosphere is generally included. For global radiation  $G$  they follow the general form:

$$(2.1) \quad G = G_0 \psi_c f(\alpha, \beta)$$

where  $G_0$  is a theoretical estimate of cloudless sky global radiation,  $\psi_c$  is the cloud field transmissivity for global radiation and  $f(\alpha, \beta)$  is a function of ground albedo  $\alpha$  and atmospheric reflectivity for surface reflected radiation  $\beta$ , which incorporates multiple reflections between ground and atmosphere. A glossary of symbols used in this report appears in Table 1.

Models can be grouped according to the way in which cloud field transmissivity is treated: as a function either of fractional sunshine or of cloud amount. A further subdivision can be made according to whether total cloud or layer cloud amounts are used. Fractional bright sunshine (the ratio of actual  $n$  to potential number  $N$  of sunshine hours) and cloud amount  $C$  are the most common variables used to calculate cloudy sky transmissivity.



Table 1 Glossary of symbols

$a_w$	water vapour absorptivity
$d$	dust content (particles/cm <sup>3</sup> )
$d_n$	day number (i.e Julian day - 1)
$g$	ratio of forward to total scatter by aerosol
$g'$	$g$ for $m = 1.66$
$h$	solar elevation
$k$	unit air mass aerosol transmissivity
$m$	relative optical air mass
$n$	measured number of sunshine hours
$p$	station pressure
$p_0$	standard sea level pressure (101.3kPa)
$t$	cloud transmissivity
$u_o$	amount of ozone
$u_w$	precipitable water amount
$C$	cloud amount
$C_i$	corrected cloud layer amount
$C_i'$	observed cloud layer amount
$C_{\text{sum}}$	sum of observed cloud layer amounts below the $i$ th level
$CO$	total cloud opacity
$CT_i$	cloud layer type
$D$	diffuse component of global radiation
$\langle D \rangle$	mean measured diffuse radiation
$D_0$	cloudless sky diffuse radiation
$D_a$	diffuse radiation component due to aerosol scattering
$D_r$	diffuse radiation due to Rayleigh scattering
$ET$	equation of time
$G$	global radiation
$\langle G \rangle$	mean measured global radiation
$G_0$	theoretical cloudless sky global radiation
$G^0$	extraterrestrial radiation ( $= I^0 \cos Z$ )
$H$	solar hour angle
$H'$	half day length
$I$	direct beam component of global radiation
$\langle I \rangle$	mean measured direct beam radiation
$I_0$	cloudless sky direct beam radiation
$I_w$	radiation transmitted in the absence of scattering
$I^0$	corrected value of the solar constant
$LAT$	local apparent (true solar) time
$LS$	station longitude
$LSM$	standard meridian for a time zone
$LST$	local standard time
$MBE$	mean bias error
$MAB$	mean absolute error
$N$	potential number of sunshine hours
$RMSE$	root mean square error
$R^*/R'$	ratio of mean to actual sun-earth distance
$T_a$	transmissivity after extinction by aerosol

$T_a'$	$T_a$ for $m = 1.66$
$T_{aa}$	transmissivity after aerosol absorption
$T_{as}$	transmissivity after aerosol scattering
$T_1$	Linke turbidity factor
$T_o$	transmissivity after ozone absorption
$T_r$	transmissivity after Rayleigh scattering
$T(H)$	upper temperature threshold for estimating surface albedo
$T(L)$	lower temperature threshold for estimating surface albedo
$V$	humidity
$X_c$	model estimates of radiation
$X_m$	measured radiation
$Z$	solar zenith angle
$\alpha$	ground albedo
$\alpha_a$	aerosol backscatter coefficient
$\alpha_c$	cloud base albedo
$\alpha_r$	Rayleigh backscatter coefficient (0.0685)
$\alpha(H)$	prescribed albedo for temperatures above $T(H)$
$\alpha(L)$	prescribed albedo for temperatures below $T(L)$
$\beta$	atmospheric reflectivity for surface reflected radiation
$\delta$	solar declination
$\epsilon_i$	$X_c - X_m$
$\theta$	the angle $2\pi d_n/365$
$\tau_a$	aerosol optical depth
$\tau_o$	ozone optical depth
$\tau_w$	water vapour optical depth
$\tau_r$	Rayleigh optical depth
$\varphi$	station latitude
$\psi_c$	cloud field transmittance for global radiation
$\omega$	single scattering albedo for aerosol

Hourly radiation in  $\text{kJ}/\text{m}^2/\text{hr}$   
 Daily radiation in  $\text{MJ}/\text{m}^2/\text{day}$ .

Using cloud amount, (2.1) can be expanded in a geometric series:

$$(2.2a) \quad G = G_0 \psi_c (1 + \alpha\beta + \alpha^2\beta^2 + \dots + \alpha^{n-1}\beta^{n-1}) = G_0 \frac{(1 - C_i + t_i C_i)}{1 - \alpha\beta}$$

This equation allows for transmission through blue sky  $(1 - C)$  and through cloud of transmissivity  $t$  and allows for radiation enhancement by multiple reflections. Monteith (1962) derived (2.2a) somewhat differently. If only one reflection cycle between ground and atmosphere is considered,

$$(2.2b) \quad G = G_0 (b_0 + b_1 C - b_2 C^2)$$

Using the definition of  $\beta$  given by Davies and McKay (1982) the coefficients can be calculated from ground albedo, cloud albedo  $\alpha_c$  and transmissivity, Rayleigh

backscatter  $\alpha_r$  and aerosol backscatter  $\alpha_a$  using

$$\begin{aligned} b_0 &= 1 + \alpha(\alpha_r + \alpha_a) \\ b_1 &= \alpha(\alpha_c - \alpha_r) - (1 - t)b_0 \\ (2.3) \quad b_2 &= \alpha(\alpha_r - \alpha_c)(1 - t) \end{aligned}$$

Alternatively the  $b$  parameters can be determined by regression (Kimura and Stephenson, 1969).

Assuming that  $n/N = 1 - C$ , (2.2) becomes

$$(2.4a) \quad G = G_0 \frac{[ t + (1 - t)\frac{n}{N} ]}{1 - \alpha\beta}$$

which is Ångström's equation with the addition of multiple reflection effects. Equations (2.2) and (2.4a) have usually been applied without the multiple reflection term to daily or mean daily totals of global radiation. Replacement of  $G_0$  with extraterrestrial radiation  $G^0$  is a further simplification that is commonly made. In that case  $t$  and  $1-t$  are replaced with parameters ( $a$  and  $b$ ) determined by regression:

$$(2.4b) \quad G/G^0 = a + bn/N$$

Numerical values of  $a$  and  $b$  can vary regionally and seasonally due to variations in multiple reflection effects (Hay, 1979), atmospheric transmission (Davies, 1965) and methods of measuring sunshine (Painter, 1981). Neglect of variation in cloud transmissivity with cloud type must reduce the short-term application of (2.2) and (2.4). Transmissivity is approximately three times greater for high clouds than for low clouds (Kasten and Czeplak, 1980). Cloud layer models consider this variation explicitly by defining the cloud field transmissivity as

$$(2.5) \quad \psi_c = \prod_{i=1}^n (1 - C_i + t_i C_i)$$

where  $C_i$  is cloud amount, corrected for overlap effects (Davies *et al.*, 1975), and  $t_i$  is the transmissivity of an individual layer. Cloud layer models have the following general form:

$$(2.6) \quad G = G_0 \frac{\prod_{i=1}^n (1 - C_i + t_i C_i)}{1 - \alpha\beta}$$

In most instances, the solar radiation value available at a station, either measured or derived, is global radiation. The direct and diffuse beam components are needed to determine radiation on tilted surfaces. Following the pioneering work of Liu and Jordan (1960), many studies have empirically related daily values of the ratios of diffuse  $D$  to global radiation and global to extraterrestrial radiation:

$$(2.7) \quad D/G = f(G/G_0)$$

The method provides the attractive possibility of calculating diffuse and direct beam radiation simply for stations having a global radiation value.

Equations (2.2)–(2.7) are prototypes for most models. Most were intended for estimating radiation over daily, or longer periods. Few can or are meant to provide hourly values. For global radiation the layer models are best suited in principle for this purpose since they are the most sensitive to changes in cloud layer amounts and allow cloud transmissivity to vary with cloud type. For diffuse and direct beam radiation, the Liu and Jordan models using measured global radiation are best suited for providing hourly estimates. Because all models contain statistical components which describe average states they only provide satisfactory average, not instantaneous, radiation estimates. No model, which estimates radiation from meteorological observations, can provide actual short-term (hourly or daily) values comparable in accuracy with radiation measurements. For this reason this report stresses model performance for different averaging periods.

## 2.2 MODEL FORMULATIONS

The models examined in this report are described within the groups defined previously. They are listed in Table 2 with the acronyms we have used.

Table 2 List of models and abbreviations

Abbreviation	Model
BCLS	Barbaro <i>et al.</i> (1979)
CPR	Collares-Pereira and Rabl (1979)
EKDD	Erbs <i>et al.</i> (1982)
EKDH	Erbs <i>et al.</i> (1982)
JOS	Josefsson (1985)
KAS	Kasten (1983)
KASM	This report
MAC	Davies and McKay (1982)
MON	Monteith (1962)
OH	Orgill and Hollands (1977)
PAGE	Page (1961)
RIET	Rietveld (1978)
BEST	This report

### 2.2.1 Cloud Layer Models

Models developed at the Center for Environment and Man (Atwater and Ball,1978), McMaster University (Davies et al.,1975; Davies and Hay,1980;Davies and McKay,1982), the University of British Columbia (Suckling and Hay,1976,1977) fall into this category. On the basis of earlier evaluations (AES,1980; Davies,1981; Davies and McKay, 1982), the McMaster model was selected for this study. In addition, a new model submitted by Josefsson (1985) was included in the evaluation.

#### 2.2.1.1 The McMaster Model (MAC).

Global radiation is calculated from (2.6) with the theoretical cloudless sky radiation expressed as the sum of a direct beam component  $I_0$  and diffuse components due to Rayleigh  $D_r$  and aerosol  $D_a$  scattering. These are given by

$$(2.8) \quad I_0 = G^0(T_0 T_r - a_w) T_a$$

$$(2.9) \quad D_r = G^0 T_0 (1 - T_r) / 2$$

$$(2.10) \quad D_a = G^0 (T_0 T_r - a_w) (1 - T_a) \omega g$$

where  $G_0$  is the extraterrestrial radiation,  $T_0$  the transmissivity after absorption by ozone;  $T_r$  the transmissivity after Rayleigh scatter;  $a_w$  the absorptivity of water vapour; and  $T_a$  the transmissivity after extinction by aerosol;  $\omega$  the spectrally-averaged single scattering albedo for aerosol and  $g$  the ratio of forward to total scatter by aerosol.

Direct beam radiation is calculated from

$$(2.11) \quad I = I_0(1 - CO)$$

where  $CO$  is total cloud opacity, and diffuse radiation as a residual:

$$(2.12) \quad D = G - I$$

Transmissivity after absorption by ozone and the absorptivity of water vapour were computed from formulae given by Lacis and Hansen (1974). These are expressed in terms of the product of relative optical air mass  $m$  and depth of ozone or water. Depth of ozone was set at a fixed value of 3.5mm. Procedures used for estimating the precipitable water are referenced in Chapter 3. Spectrally-integrated values of transmissivity after Rayleigh scatter as a function of relative optical air mass were obtained as described by Davies (1987). Transmissivity after extinction by aerosol was calculated from

$$(2.13) \quad T_a = \exp(-\tau_a m) = k^m$$

where  $\tau_a$  is a spectrally-averaged aerosol optical depth and  $k$ , therefore, is a unit air mass aerosol transmissivity.

Values of  $\tau_a$  or  $k$  and  $\omega$  must be pre-assigned. For aerosol that only scatters  $\omega = 1$ , but in urban areas aerosols absorb significantly and values of  $\omega$  are less than unity. A fuller discussion of aerosol terms is given in Chapter 3. The ratio of forward to total aerosol scatter is expressed as a function of relative optical air mass using Robinson's (1962) experimentally-based values. Parameterization for cloudless and cloudy sky radiation calculations are summarized in Tables 3 and 4.

The model requires estimates of the fraction of the sky at each level which is

Table 3 MAC parameterization for cloudless sky radiation

$$T_o = 1 - a_o$$

$$a_o = \frac{0.1082X_1}{1+13.86X_1^{0.805}} + \frac{0.00658X_1}{1+(10.36X_1)^3} + \frac{0.00218}{1+0.0042X_1+0.00000323X_1^2}$$

$$X_1 = mu_o, \quad u_o \text{ in mm.}$$

$$a_w = \frac{0.29X_2}{(1+14.15X_2)^{0.635}+0.5925X_2}$$

$$X_2 = mu_w, \quad u_w \text{ in mm}$$

$$m = \frac{35}{(1+1224\cos^2Z)^{0.5}}$$

$$T_r = \frac{X}{(1+X)}$$

$$X = 8.688237ma$$

$$a = 0.0279286(\ln m) - 0.806955$$

$$g = 0.93 - 0.21(\ln m)$$

cloud covered. In most countries, observed cloud layer amounts are expressed as fractions of a total cloud amount which does not exceed one. Davies *et al.* (1975) proposed a scheme to correct amounts above the lowest level for the fraction of sky obscured from the observer's vision. Corrected amounts for layers above the lowest layer are obtained from

$$(2.14) \quad C_i = C_i' / (1 - C_{\text{sum}})$$

where  $C_{\text{sum}}$  is the sum of observed layer cloud amounts below the  $i$ th level.

Cloud transmissivity is obtained from

$$(2.15) \quad t_i = A_i \exp(-B_i m)$$

Table 4 MAC, JOS and BCLS cloud parameterization

<b>MAC</b>					
Cloud	$A_i$	$B_i$	Cloud	$A_i$	$B_i$
Ac	.556	.053	Cu,Cf,Sc	.368	.045
As	.413	.004	St,Sf	.252	.100
Cc,Cs	.923	.089	Ns	.119	-.226
Ci	.871	.020	F	.123	-.031
Cb	.119	-.226	OTF	.163	-.031

<b>JOS</b>			
Cloud	$t_i$	Cloud	$t_i$
Ci	.90	Ns	.15
Cc	.70	Sc	.30
Cs	.60	St,Cu	.25
Ac	.30	Cb	.15
As	.25		

<b>Key</b>			
Ac	Alto cumulus	As	Altostratus
Cc	Cirrocumulus	Cs	Cirrostratus
Ci	Cirrus	Cb	Cumulonimbus
Cu	Cumulus	Cf	Cumulus fractus
Sc	Stratocumulus	St	Stratus
Sf	Stratus fractus	Ns	Nimbostratus
F	Fog	OTF	Other obstructions

<b>BCLS</b>								
$\varphi$	20	25	30	35	40	45	50	55
t	.33	.32	.32	.32	.33	.34	.36	.38



using values of  $A_i$  and  $B_i$  from Haurwitz (1948).

Atmospheric backscatter and surface albedo must be specified for incorporating multiple reflection effects between ground and atmosphere. Atmospheric backscatter is calculated as the sum of components due to Rayleigh scattering  $\alpha_r$ , assumed to apply only to the cloudless portion of the sky, scattering by aerosol  $\alpha_a$  in the atmosphere below cloud base and cloud base albedo  $\alpha_c$ , the product of average cloud albedo and total cloud amount. Hence,

$$(2.16) \quad \beta = \alpha_r(1 - C) + \alpha_a + \alpha_c C$$

where  $\alpha_r = 0.0685$  and

$$(2.17) \quad \alpha_a = (1 - T_a')\omega(1 - g')$$

in which  $T_a'$  and  $g'$  are values of  $T_a$  and  $g$  determined at  $m = 1.66$ , the appropriate air mass for diffuse radiation.

#### 2.2.1.2 Josefsson's Model (JOS)

This model is similar to the McMaster model. The equations for cloudless sky radiation are:

$$(2.18) \quad I_0 = G^0(T_0 T_r T_{as} T_{aa} - a_w)$$

$$(2.19) \quad D_r = G^0 T_0 T_{as} T_{aa} (1 - T_r) / 2$$

$$(2.20) \quad D_a = G^0 (T_0 T_r T_{aa} - a_w) (1 - T_{as}) g$$

where  $T_{as}$  and  $T_{aa}$  are transmissivities after scattering and absorption by aerosol. Global, direct beam and diffuse radiation for cloudy skies are calculated as in the McMaster model.

Parameterization for this model is given in Tables 4 and 5. It differs mainly from the McMaster model in five respects:

- The ratio of forward to total scatter by aerosol is expressed as a linear function of solar elevation  $h$  for  $0^\circ < h < 90^\circ$  and as a constant when  $-5^\circ < h < 0^\circ$ .

- A correction is made for observer overestimation of total cloud amount and amounts in the lowest two layers by

$$(2.21) \quad C_i = (C_i')^{1.6}$$

where  $C_i'$  is observed cloud amount.

- Fixed cloud transmissivities are used.
- Cloud field transmission is reduced by 30% if precipitation occurred during an hour and by 20% if it ended within the hour.
- Atmospheric backscatter is calculated from

$$(2.22) \quad \beta = (\alpha_r + \alpha_a)(1 - C^{1.6} + \alpha_c CO)$$

where  $C$  and  $CO$  are total cloud amount and opacity

---

Table 5 JOS parameterization for cloudless sky radiation

---

$$T_o = 0.95545$$

$$a_w = \frac{0.29X_2}{(1+14.15X_2)^{0.635} + 0.5925X_2}$$

$$X_2 = mu_w, \quad u_w \text{ in mm}$$

$$m = \frac{1}{\cos Z + 0.15(93.885 - Z)^{-1.253}}$$

$$T_r = 0.9768 - 0.0874m + 0.010607552m^2 - 8.46205 \times 10^{-4}m^3 \\ + 3.57246 \times 10^{-5}m^4 - 6.0176 \times 10^{-7}m^5$$

$$\begin{aligned} g &= 0.5248 + 0.007981h, & 0 \leq h \leq 45 \\ g &= 0.8560 + 0.000734h, & 45 < h \leq 90 \\ g &= 0.5 & -5 \leq h \leq 0 \end{aligned}$$

$$T_{aa} = 1 - (1 - \omega)(1 - T_a)$$

$$T_{as} = 1 - \omega(1 - T_a)$$


---

### 2.2.2 Total Cloud-based models

Models developed by Monteith(1962), Hay(1970), Hoyt(1978), Lettau and Lettau (1969), Kimura and Stephenson(1969), ASHRAE(1972), Won (1977) and Kasten (1983) are examples of this group. The Kasten and Monteith models were evaluated.

#### 2.2.2.1 Kasten's model (KAS).

Global radiation is calculated from

$$(2.23) \quad G/G_0 = 1 - aC^b$$

where the cloudless sky radiation is given by

$$(2.24) \quad G_0 = G^0 A \exp(-BT_1 m)$$

Here,  $T_1$  is the Linke turbidity factor, and  $a, b, A, B$  have the values 0.72, 3.2, 0.84, and 0.027 respectively, based on analysis of West German data. Kasten did not include the calculation of direct beam radiation in his model. This modification was made using

$$(2.25) \quad I = G^0 \exp(-T_1 \tau_r m) (1 - C)$$

where  $\tau_r$  is the Rayleigh scattering optical depth as given by Kasten (1980):

$$(2.26) \quad \tau_r = 1/(9.4 + 0.9m).$$

Then, diffuse radiation is the difference between global and direct beam radiation.

A variant of Kasten's model was also evaluated. In this extension (KASM), the cloudless sky formulation for the McMaster model (2.8,2.9,2.10) replaces (2.24). This modification incorporates the variable effects of water vapour absorption explicitly which is desirable for the application of the model in drier atmospheres than western Europe.

#### 2.2.2.2 Monteith's model (MON).

This is (2.2a) with cloudless sky global radiation calculated as in the

McMaster model and using the Berland and Danilchenko (1961) cloud transmissivities. This type of model can be used where only total cloud amount information is available and where there are no empirical cloud transmissivities.

### 2.2.3 Sunshine-based models.

The models of Barbaro *et al.* (1979), Page (1961) and Rietveld (1978) were selected from this group. All three can be applied generally.

#### 2.2.3.1 Barbaro *et al.* (BCLS).

Direct beam and diffuse radiation for cloudless skies are given by

$$(2.27) \quad I_0 = G^0 \exp[a_1 + b_1 u_w - a_3(d - 400)] \exp\{-[a_2 + b_2 u_w + b_3(d - 400)]m\}$$

and

$$(2.28) \quad D_0 = \kappa(I_w - I_0)$$

where  $u_w$  is precipitable water;  $d$  the dust content (particles/cm<sup>3</sup>);  $\kappa$  a zenith angle dependent empirical coefficient given by  $\kappa = 0.5 \cos Z^{0.33}$ ; and  $I_w$  the radiation transmitted in the absence of scattering:

$$(2.29) \quad I_w = G^0 [0.938 \exp(-0.0154 X_1)] + \{0.004 X_1^{2.1} - 1.1086 \times 10^{-5} X_1^3 + 121.948(1 + X_1) / [1 + 10 X_1^2]\} \times 10^{-3}$$

in which  $X_1 = m u_w$ . The following values were used for the  $a$  and  $b$  parameters:

$$\begin{array}{lll} a_1 = -0.13491 & a_2 = 0.13708 & a_3 = 3.68 \cdot 10^{-5}; \\ b_1 = -4.28 \cdot 10^{-3} & b_2 = 2.61 \cdot 10^{-3} & b_3 = 1.131 \cdot 10^{-4}. \end{array}$$

Daily totals of cloudless sky direct beam and diffuse radiation are obtained by integration. Then fractional sunshine is used to calculate daily totals for cloudy skies:

$$(2.30) \quad I = (n/N) I_0$$

$$(2.31) \quad D = (n/N) D_0 + t(1 - n/N)(I_0 + D_0)$$

using cloud transmissivity values of Berland and Danilchenko (1961) (Table 4). In

the absence of sunshine data  $1-C$  can be used for  $n/N$ .

### 2.2.3.2 The Page Model (PAGE).

This model has been widely used in Europe and some other parts of the world. It is a regression model (2.4b) and, therefore, the regression parameters may vary with location and time. We have used the parameter values given by Page (1961):

$$(2.32) \quad G = G^0(0.23 + 0.48n/N)$$

### 2.2.3.3 The Rietveld Model (RIET).

Rietveld (1978) used extensive published regression data to relate both  $a$  and  $b$  in (2.4b) to  $n/N$ :

$$(2.33) \quad a = 0.1 + 0.24n/N$$

and

$$(2.34) \quad b = 0.38 + 0.08N/n$$

In this study,  $a$  and  $b$  were determined from these relationships using mean sunshine values for each month.

## 2.2.4 Liu and Jordan Models

We selected and evaluated the models of Collares–Pereira and Rabl (1979) and Erbs *et al.* (1982), which estimate daily radiation totals, and the models of Orgill and Hollands (1977) and Erbs *et al.* (1982) which estimate hourly values. For brevity,  $K$  will be used to represent  $G/G^0$ , the atmospheric transmissivity for global radiation.

## 2.2.4.1 The Collares–Pereira and Rabl Model (CPR).

From American data for ten stations:

$$(2.35) \quad \begin{aligned} D/G &= 0.99, & K &\leq 0.17 \\ D/G &= 1.88 - 2.72K + 9.43K^2 - 21.856K^3 \\ &+ 14.648K^4, & 0.17 &\leq K \leq 0.8 \end{aligned}$$

where values of  $G^0$  were obtained by integrating (3.2) over the daylight period.

2.2.4.2 The Erbs *et al.* Model (EKDD).

Seasonal correlations were obtained from data for four American stations: Fort Hood, Texas; Livermore, California; Raleigh, North Carolina; Maynard, Maine; and Albuquerque, New Mexico. Data were grouped seasonally according to the hour angle (in radians) at sunrise  $H'$ .

For  $H' < 1.4208$

$$(2.36) \quad \begin{aligned} D/G &= 1.0 - 0.2727K + 2.4495K^2 - 11.9514K^3 \\ &+ 9.3879K^4 & K &< 0.715 \end{aligned}$$

$$(2.37) \quad \begin{aligned} D/G &= 0.143 & K &\geq 0.715 \end{aligned}$$

For  $H' \geq 1.4208$

$$(2.38) \quad \begin{aligned} D/G &= 1.0 + 0.2832K - 2.5557K^2 + 0.8448K^3 \\ & & K &< 0.722 \end{aligned}$$

$$(2.39) \quad \begin{aligned} D/G &= 0.175 & K &\geq 0.722 \end{aligned}$$

## 2.2.4.3 The Orgill and Hollands Model (OH).

For Toronto, Orgill and Hollands (1977) obtained the following relationships

$$(2.40) \quad \begin{aligned} D/G &= 1.0 - 0.249K & K &< 0.35 \end{aligned}$$

$$(2.41) \quad \begin{aligned} D/G &= 1.557 - 1.84K & 0.35 &\leq K \leq 0.75 \end{aligned}$$

$$(2.42) \quad \begin{aligned} D/G &= 0.177 & K &> 0.75 \end{aligned}$$

2.2.4.4 The Erbs *et al.* Model (EKDH).

For the stations identified in 2.2.4.2 the following, seasonally-independent correlations were obtained:

$$(2.43) \quad D/G = 1.0 - 0.09K \quad K \leq 0.22$$

$$(2.44) \quad D/G = 0.9511 - 0.1604K + 4.388K^2 - 16.638K^3 \\ + 12.336K^4 \quad 0.22 < K \leq 0.80$$

$$(2.45) \quad D/G = 0.165 \quad K > 0.80$$

In this and the previous model,  $G^0$  is calculated for the midpoint of the hourly period under consideration.

## CHAPTER 3: DATA

The number of measured or observed variables required as input to the models varies from one for sunshine-based models to at least six for layer models. Table 6 indicates the vital ones for each model, which must be measured or observed. All other variables can be estimated.

### 3.1 OBSERVATIONS AND MEASUREMENTS

Data for 15 stations were used in this study. In most cases, three years of data were processed for each station. Table 7 summarizes the available data. Most participating countries provided selected data sets for the project. However, more extensive data sets were obtained for Australia and the USA, from which selections were made. Four Australian stations were selected to represent the interior and the western, southern and eastern margins. Data were not available for tropical locations. A data set of over 150 station years for the USA was classified according to the availability of radiation data. Four stations were selected.

For the Liu and Jordan models, global radiation measurements are mandatory. The possibility of using model estimates of global radiation will be addressed later. For sunshine-based models, sunshine measurements were not available for American and Australian stations. The complement of observed total cloud amount was used instead. Since this is a major, and probably questionable, approximation, the performance of these models is assessed with data for stations with sunshine measurements. For layer models, cloud layer information was incomplete for Australia and the USA and was estimated (Davies and Uboegbulam, 1979). The cloud information for these stations consists of total and low cloud amounts and cloud types in all layers, usually three. The estimation procedure



Table 6 Essential measured or observed variables for the models

Model	G	n	V	C	C <sub>i</sub>	CT <sub>i</sub>
OH	•					
EKDD	•					
EKDH	•					
PAGE		•				
RIET		•				
KAS				•		
KASM				•		
MON		•	•			
BCLS			•	•		•
MAC			•	•	•	•
JOS			•	•	•	•

G = global radiation  
n = sunshine  
V = surface humidity  
C = total cloud amount  
C<sub>i</sub> = cloud layer amount  
CT<sub>i</sub> = cloud layer type

allocates the difference between total cloud amount and low cloud amount to the layer or layers above. If there are two cloud layers above the lowest, the difference is partitioned equally between them. For some stations, clouds were observed at three hourly intervals. Although cloud amount can be interpolated between observations, cloud type is a discontinuous variable which can not always be interpolated. The difficulty was overcome by evaluating the total cloud transmission function (the  $\pi$  term in 2.5) for hours with cloud observation and linearly interpolating function values for intermediate times without observations.

The data sets from seven countries had different formats. They were decoded according to the information provided by each country. Little information was available on the quality controls that had been applied. We ensured

- adequate radiation data for a worthwhile test;
- that both model calculations and comparisons with measured radiation were made with correct input;
- that Australian and West German data, which were provided on several files for each year, were merged correctly.

Inadequate radiation data for comparisons were mainly a problem with the U.S.A. data sets. Most American station records were rejected for this reason. The selected stations had at least two years with more than 300 days of global radiation measurements in each year. Our computer codes screened input files for missing data so that no calculations were made inadvertently using missing data codes. The initial validation included careful examination of input data and calculated radiation values. There was no evidence of errors in the measured radiation records except for occasions when diffuse radiation exceeded global radiation. In these instances, the diffuse component was set equal to the global radiation since global radiation measurements should be more reliable. This correction was mainly necessary near sunrise and sunset. The controls that were implemented are

Table 7 Stations and available data.

LOCATION AND DATA PERIOD				
Station	Country	Lat	Long	Years
Alice Springs	Australia	-23.82	133.90	1980-1982
Guildford	Australia	-31.92	115.97	1978-1980
Mildura	Australia	-34.23	142.08	1979, 1981, 1982
Rockhampton	Australia	-23.38	150.47	1979, 1981, 1982
De Bilt	Netherlands	52.10	-5.18	1971, 1976, 1979
Hamburg	West Germany	53.63	-10.00	1976-1978
Kew	United Kingdom	51.48	0.30	1975-1977
Zurich	Switzerland	47.48	-8.53	1964-1965
Montreal	Canada	45.50	73.62	1972-974
Winnipeg	Canada	49.90	97.24	1970-1972
Vancouver	Canada	49.18	123.20	1968
Albuquerque	United States	35.03	106.62	1978-1980
Columbia	United States	38.82	92.22	1979-1980
Medford	United States	42.37	122.87	1978-1980
Sterling	United States	38.98	77.47	1979-1980

## AVAILABLE DATA

Station	G	D	I	n	C
Alice Springs	•	•	•		A
Guildford	•	•	•		A
Mildura	•	•	•		A
Rockhampton	•	•	•		A
De Bilt	•	•	•	•	B
Hamburg	•	•	•	•	B
Kew	•	•	•	•	B'
Zurich	•	•	•	•	B
Montreal	•	•	•	•	B
Winnipeg	•			•	B
Vancouver	•			•	B
Albuquerque	•	•	•		A
Columbia	•	•	•		A
Medford	•	•	•		A
Sterling	•	•	•		A

n = sunshine

B = hourly cloud

C = cloud

B' = hourly low cloud and all layer types

A = 3-hourly cloud

documented in the computer codes. The computer codes and results were circulated to member countries for scrutiny to detect errors in decoding data and in implementing models. Few errors were reported. The codes were corrected before subsequent runs.

### 3.2 CALCULATED QUANTITIES

All models required either astronomical variables or quantities that depend on them. These are discussed in the next section. Several models also require information on precipitable water, atmospheric aerosol and surface albedo. Since little information was available for these, estimates were made as described in subsequent sections.

#### 3.2.1 Astronomical parameters.

We adopt a solar constant value of  $1376 \text{ Wm}^{-2}$ . This value refers to the mean Sun–Earth distance  $R^*$  and is adjusted to account for the departure of the actual distance  $R'$  from the mean. The corrected value of the solar constant is

$$(3.1) \quad I^0 = 1376(R^*/R')^2$$

Since radiation is referred to a horizontal surface, it is convenient to start with the extraterrestrial radiation defined by

$$(3.2) \quad G^0 = I^0 \cos Z$$

where  $\cos Z$ , the cosine of the solar zenith angle  $Z$ , is calculated from

$$(3.3) \quad \cos Z = \sin \varphi \sin \delta + \cos \varphi \cos \delta \cos H$$

in which  $\varphi$  is station latitude,  $\delta$  solar declination and  $H$  is solar hour angle, which is given, in degrees, by

$$(3.4) \quad H = 15 |12 - LAT|$$

where  $LAT$  is the local apparent (true solar) time. Local apparent time is determined from local standard time  $LST$ , the equation of time  $ET$  (in minutes),

and the station longitude  $LS$  and standard meridian  $LSM$  for the time zone:

$$(3.5) \quad LAT = LST + ET/60 + (LSM - LS)/15$$

Values for  $(R^*/R')^2$ ,  $\delta$  and  $ET$  are calculated, following Spencer (1971), from day number  $d_n$  (= Julian day - 1). Day number defines the angle (radians)

$$(3.6) \quad \theta = 2\pi d_n/365$$

Then

$$(3.7) \quad (R^*/R')^2 = 1.00011 + 0.034221\cos\theta + 0.00128\sin\theta \\ - 0.000719\cos 2\theta + 0.000077\sin 2\theta$$

$$(3.8) \quad \delta = 0.006918 - 0.399912\cos\theta + 0.070257\sin\theta \\ - 0.006759\cos 2\theta + 0.000907\sin 2\theta \\ - 0.002697\cos 3\theta + 0.001480\sin 3\theta$$

and

$$(3.9) \quad ET = 0.000075 + 0.001868\cos\theta - 0.032077\sin\theta \\ - 0.14615\cos 2\theta - 0.040840\sin 2\theta$$

According to Spencer (1971), these approximations produce maximum errors of  $<10^{-4}$  for  $(R^*/R')^2$ ,  $< 3'$  for  $\delta$  and  $< 35''$  for  $ET$ .

Daily totals of extraterrestrial radiation follow by integrating (3.2) between sunrise and sunset. This yields

$$(3.10) \quad G^0 = (24/\pi)(3.6 \times 10^{-3})I^0(H' \sin\varphi \sin\delta + \cos\varphi \cos\delta \sin H')$$

where  $H'$ , the half-day length, is defined as

$$(3.11) \quad \cos H' = -\tan\varphi \tan\delta$$

The maximum number of sunshine hours in a day is

$$(3.12) \quad N = 2H'$$

Because the Campbell-Stokes sunshine recorder fails to respond to bright sunshine at zenith angles larger than  $85^\circ$  (Hay, 1979), a more appropriate value for the maximum number of hours is twice the number of hours between solar noon and a zenith angle of  $85^\circ$ . Using (2.10) this can be calculated from

$$(3.13) \quad N' = (1/7.5)\cos^{-1}[(\cos 85^\circ - \sin\varphi\sin\delta)/(\cos\varphi\cos\delta)]$$

Hourly radiation calculations require values of the relative optical air mass. To allow for refraction effects at large zenith angles one of the following formulae (Kasten, 1966; Rogers, 1967) are used:

$$(3.14a) \quad m(\text{Kasten}) = 1/[\cos Z + 0.15/(93.885 - Z)^{1.253}]$$

$$(3.14b) \quad m(\text{Rogers}) = 35/(1224\cos^2 Z + 1)^{0.5}$$

A correction for atmospheric pressure is made by multiplying by  $p/p_0$  where  $p$  is station pressure and  $p_0$  is standard sea level pressure (101.3kPa).

Where necessary, meteorological data recorded in local time were converted to local apparent time. For example, Canadian radiation and sunshine data are provided as hourly integrated values in *LAT* for the hour at the end of the integration period. Hourly meteorological data are in *LST*. The two records could only be aligned approximately. Each hourly meteorological observation was converted to the *LAT* for the centre of the nearest integration period for radiation. The procedure consists of adding 0.5 to the integer portion of the *LAT* of the hourly observation. This is done for the first observation (0000*LST*) and successive values are obtained by incrementing by 1. Then radiation and sunshine data are shifted to correspond with the derived times of hourly observation. Maximum difference between radiation and observation times by the method is 30 minutes.

### 3.2.2 Precipitable water

Four models (MAC, JOS, KASM, MON) determine water vapour absorption from precipitable water. Although this quantity can be calculated easily from sounding data, such data are uncommon and estimates must be made from surface humidity. The approximation produces little error. Atwater and Ball (1976) reported differences for American stations of no more than 1% between model estimates using precipitable water from sounding data and model estimates using an

empirical function of surface humidity. This agreement did not arise necessarily because the empirical formula estimated precipitable water accurately, but, sufficiently accurately, because layer model estimates of global radiation are not very sensitive to substantial error in precipitable water (Davies et al.,1975).

In this study, precipitable water was calculated from either surface dew point temperature or relative humidity by the following methods:

Region/Country	Method
UK	Monteith (1961)
Europe	Tomasi (1981)
Australia	Monteith (1961)
Canada	Won (1977)
USA	Atwater and Ball (1976)

### 3.2.3 Cloud opacity estimates

Cloud opacity is recorded hourly by meteorological observers in North America. It is a visual estimate of the effective cloud cover of the sky. Thus, a complete cloud cover of fairly transparent cirrus may effectively only cover 20% of the sky, and its opacity would be recorded as 2 tenths. For European and Australian stations, we adopted arbitrarily a procedure used by Zelinka (personal communication) in Switzerland which estimates total cloud opacity by reducing total cloud amount when cirrus is present. When cirrus occurs in a layer, the layer cloud amount is reduced to a third of the observed value.

### 3.2.4 Aerosol terms

In atmospheres which are significantly affected by mankind's pollution, such as much of Europe and North America, the aerosol attenuation of global radiation is significant and approaches in magnitude attenuation by water vapour (Ball and

Robinson, 1982). Its effect can not be safely ignored in calculations with models which attempt to mimic the physical processes which attenuate radiation. However, there is little empirical information which can be used in models, and aerosol effects can only be incorporated crudely. European work has commonly used Linke's turbidity factor to specify aerosol attenuation. In North America, it is not used. The different traditions have produced different parameterizations. However, the relationship between the Linke parameter and other indices is easily shown.

In radiative transfer aerosol properties are uniquely specified by three variables:

- optical depth  $\tau_a$ , which is proportional to the aerosol loading;
- single scattering albedo  $\omega$ , which is a measure of the total radiation attenuation by aerosol due to scattering;
- asymmetry factor, which is a measure of the direction of scatter.

From Beer's law:

$$(3.15) \quad I = I^0 \exp[-(\tau_r + \tau_o + \tau_a + \tau_w)m]$$

where  $\tau_r$ ,  $\tau_o$  and  $\tau_w$  are spectrally-integrated optical depths for Rayleigh scattering ozone absorption and water vapour absorption. Linke's factor is defined by dividing the term in square brackets by  $\tau_r$ :

$$(3.16) \quad I = I^0 \exp\left\{-\left[1 + \frac{(\tau_o + \tau_a + \tau_w)}{\tau_r}\right] \tau_r m\right\}$$

$$(3.17) \quad = I^0 \exp[-T_1 \tau_r m]$$

in which

$$(3.18) \quad T_1 = 1 + (\tau_o + \tau_a + \tau_w) / \tau_r$$

Aerosol and water vapour attenuation is expressed as the number of Rayleigh atmospheres that would give the same total attenuation of the direct beam radiation. Since the unit air mass transmittance is defined by

$$(3.19) \quad k = \exp(-\tau_a)$$



$$(3.20) \quad \tau_a = (T_1 - 1)\tau_r - \tau_o - \tau_w = -\ln k$$

Aerosol information is required by the MAC, JOS, KAS, KASM, MON and BCLS models. MAC, JOS, MON and KASM use  $k$  and KAS uses  $T_1$ . MAC, JOS, MON and KASM approximate aerosol transmittance. In JOS, it is formally defined by:

$$(3.21) \quad T_a = T_{aa}T_{as} = \exp(-\tau_{aa})\exp(-\tau_{as}) = \exp[-(1 - \omega)\tau_a]\exp(-\omega\tau_a)$$

For small optical depth ( $\tau < 0.1$ ):

$$(3.22) \quad 1 - T_a = 1 - \exp(-\tau_a) \simeq \tau_a$$

$$(3.23) \quad T_{aa} \simeq 1 - (1 - \omega)\tau_a \simeq 1 - (1 - \omega)(1 - T_a)$$

$$(3.24) \quad T_{as} = 1 - \omega\tau_a = 1 - \omega(1 - T_a)$$

Similarly in MAC,

$$(3.25) \quad (1 - T_a)\omega g \simeq [1 - \exp(-\omega\tau_a)]g$$

since

$$(3.26) \quad 1 - \exp(-\omega\tau_a) \simeq \omega\tau_a \simeq \omega(1 - T_a)$$

These approximations were used in this study but they may introduce errors in urbanized areas where  $\tau_a$  is not negligible. For future use, we recommend that the exponential functions are retained.

A constant value of 0.75 was used for  $\omega$  in MAC, JOS, KASM and MON. Tables 3 and 5 indicate how  $g$  was calculated. Values of  $\tau_a$ , however, were assigned fixed values for each station after several trials in the initial validation. No attempt was made to include seasonal variation since such information was unavailable. Furthermore, experimentally-determined optical depths may not characterize typical conditions but atypical cloudless sky conditions. A value for  $T_1$  was also determined by trial and error although, for Hamburg, data on the seasonal variation of  $T_1$  were provided. Later, we will show differences in results obtained using a constant  $T_1$  and a seasonally varying  $T_1$ .

Values of  $k$ ,  $T_1$  and  $d$  (for the BCLS model) that were used in our

calculations for each station are given in Table 8.

Table 8 Aerosol parameter values used in calculating radiation fluxes. Values of  $\tau_a$  are in brackets after  $k$

Station	$k$	$T_1$	$d$
Alice Springs	1.0 (0)	1.5	200
Guildford	1.0 (0)	2.0	200
Mildura	1.0 (0)	2.0	200
Rockhampton	1.0 (0)	2.0	200
De Bilt	0.91 (0.09)	4.1	400
Hamburg	0.94 (0.06)	4.1	100
Kew	0.87 (0.14)	5.0	400
Zurich	0.90 (0.11)	4.1	200
Montreal	0.91 (0.09)	3.5	200
Winnipeg	0.98 (0.02)	1.5	50
Vancouver	0.98 (0.02)	1.5	50
Albuquerque	0.91 (0.09)	1.0	100
Columbia	0.95 (0.05)	1.0	100
Medford	0.95 (0.05)	1.0	100
Sterling	0.90 (0.11)	2.5	100

Virtually identical model results can be obtained for the European stations using  $k = 0.91$  and for Winnipeg and Vancouver using  $k = 1$ .

### 3.2.5 Surface albedo

Albedo was calculated from hourly measured reflected and incident global radiation for Hamburg. For Canadian stations and Zurich it was estimated from temperature, between two fixed values,  $\alpha(L)$  for temperature below  $T(L)$  and  $\alpha(H)$  for temperature above  $T(H)$  (Davies and McKay, 1982). For  $T(L) < T < T(H)$

$$(3.27) \quad \alpha = \alpha(L) + \frac{T - T(L)}{T(H) - T(L)} [\alpha(H) - \alpha(L)]$$

where  $T(L)$  and  $T(H)$  are  $-6$  and  $3$ , and  $\alpha(L)$  and  $\alpha(H)$  are  $0.6$  and  $0.2$ . At all other stations a fixed albedo of  $0.2$  was generally used. In the USA, albedo was increased to  $0.6$  if snow was present.



## CHAPTER 4: RESULTS

### 4.1 PERFORMANCE INDICATORS

Let  $\epsilon = X_c - X_m$ , where  $X$  refers to global, diffuse or direct beam radiation and the subscripts  $c$  and  $m$  to model estimates and measurements, respectively.

The variance of a set of  $N$  daily or hourly  $\epsilon_i$ :

$$(4.1) \quad \sigma(\epsilon)^2 = \frac{1}{N} \sum_i (\epsilon_i - \bar{\epsilon})^2$$

has two components:

$$(4.2) \quad \sigma(\epsilon)^2 = (RMSE)^2 - (MBE)^2$$

where  $\bar{\epsilon}$  is the mean value of  $\epsilon$ , and  $RMSE$  and  $MBE$  are the root mean square error and mean bias error, which are defined by

$$(4.3) \quad (RMSE)^2 = \frac{1}{N} \sum_i \epsilon_i^2$$

and

$$(4.4) \quad MBE = \frac{1}{N} \sum_i \epsilon_i$$

$MBE$  measures systematic error and  $RMSE$  measures non-systematic error. Since the  $MBE$  may conceal significant positive and negative biases, the mean absolute error was also computed from

$$(4.5) \quad MAB = \frac{1}{N} \sum_i |\epsilon_i|$$

The statistical measures were calculated for each month and year for both hourly and daily totals of global, diffuse and direct radiation. They are expressed in both absolute units,  $MJ/m^2$  for daily totals and  $kJ/m^2$  for hourly totals, and as fractions of mean measured radiation for a month or year. Appendix A lists all of these results. Model performance, as defined by these statistics, was also determined for different averaging periods to demonstrate likely errors for various

model applications and to indicate the minimal averaging period which is needed to attain a desired level of accuracy. The statistics described above were used to rank models according to performance.

In addition, we have attempted to estimate the best performance that any model can attain. This is achieved (1) by empirically determining  $a$  and  $b$  parameters in the Ångström equation (2.4b) for each month in each year at each station, and (2) by using the parameter values for a given month to compute daily global radiation for that month. These estimates, which are called *BEST*, provide useful comparisons for all global radiation models.

#### 4.2 RANKING OF MODELS

Models were ranked for each performance statistic (*MAB*, *MBE*, *RMSE*) from monthly summaries of hourly and daily radiation statistics. For each statistic a weighting of 8 was assigned to the model with the best performance, 7 to the one with the second best, and so on. The ranking counts were pooled for all years for each station, and these were then pooled into seven groups:

AUS	: Australia
EUR	: Europe
CAN	: Canada
USA	: United States
EURCAN	: Europe and Canada
NAM	: North America
ALL	: All stations.

EURCAN combines stations with measured sunshine and, therefore, provides the fairest assessment of the performance of sunshine-based models.

Total counting scores and model rankings (*BEST* omitted) from these are given in Table 9. The findings of this analysis are summarized for each flux.

Table 9a Summary of counting statistics and model rankings.

<b>DAILY GLOBAL RADIATION</b>									
	MAC	KAS	JOS	KASM	MON	PAGE	BCLS	RIET	BEST
<b>Counts</b>									
AUS	1845	1653	2607	1500	2157	780	442	1551	3017
EUR	2003	1761	1897	1359	848	1528	912	1052	2896
CAN	1247	438	1328	594	796	955	853	735	1802
USA	1516	658	1525	645	1881	962	1009	925	2327
NAM	2763	1096	2853	1239	2677	1917	1862	1660	4129
EURCAN	3250	2199	3225	1953	1644	2483	1765	1787	4698
ALL	6611	4510	7357	4098	5682	4225	3216	4263	10042
<b>Rankings</b>									
AUS	3	4	1	6	2	7	8	5	
EUR	1	3	2	5	8	4	7	6	
CAN	2	8	1	7	5	3	4	6	
USA	3	7	2	8	1	5	4	6	
NAM	2	8	1	7	3	4	5	6	
EURCAN	1	4	2	5	8	3	7	6	
ALL	2	4	1	7	3	6	8	5	
<b>HOURLY GLOBAL RADIATION</b>									
	MAC	KAS	JOS	KASM	MON				
<b>Counts</b>									
AUS	2503	2465	3003	2368	2621				
EUR	2610	2526	2535	2254	1955				
CAN	1632	1159	1715	1304	1480				
USA	2056	1489	2096	1627	2272				
NAM	3688	2648	3811	2931	3752				
EURCAN	4242	3685	4250	3558	3435				
ALL	8801	7639	9349	7553	8328				
<b>Rankings</b>									
AUS	3	4	1	5	2				
EUR	1	3	2	4	5				
CAN	2	5	1	4	3				
USA	3	5	2	4	1				
NAM	3	5	1	4	3				
EURCAN	1	3	2	4	5				
ALL	2	4	1	5	3				

Table 9b Summary of counting statistics and model rankings.

<b>DAILY DIFFUSE RADIATION</b>									
	MAC	KAS	JOS	KASM	OH	EKDH	BCLS	CPR	EKDD
<b>Counts</b>									
AUS	2244	1505	1920	900	994	1813	293	1006	2285
EUR	981	1144	1356	1034	2470	2396	39	2268	2352
CAN	329	223	453	267	640	694	10	500	556
USA	1142	870	1261	1147	1421	1786	59	1205	1682
NAM	1471	1093	1714	1414	2061	2480	69	1705	2238
EURCAN	1310	1367	1809	1301	3110	3091	49	2767	2908
ALL	4696	3742	4990	3348	5525	6690	401	4978	6875
<b>Rankings</b>									
AUS	2	5	3	8	7	4	9	6	1
EUR	8	6	5	7	1	2	9	4	3
CAN	6	8	5	7	2	1	9	4	3
USA	7	8	4	6	3	1	9	5	2
NAM	6	8	4	7	3	1	9	5	2
EURCAN	7	6	5	8	1	2	9	4	3
ALL	6	7	4	8	3	2	9	5	1
<b>HOURLY DIFFUSE RADIATION</b>									
	MAC	KAS	JOS	KASM	OH	EKDH			
<b>Counts</b>									
AUS	2440	1896	2148	1405	1722	2269			
EUR	1724	1860	1975	1785	2807	2719			
CAN	499	395	595	447	703	727			
USA	1560	1243	1646	1504	1852	2095			
NAM	2059	1638	2241	1951	2555	2822			
EURCAN	2223	2255	2570	2232	3510	3446			
ALL	6223	5394	6364	5141	7084	7810			
<b>Rankings</b>									
AUS	1	4	3	6	5	2			
EUR	6	4	3	5	1	2			
CAN	4	6	3	5	2	1			
USA	4	6	3	5	2	1			
NAM	4	6	3	5	2	1			
EURCAN	6	4	3	5	1	2			
ALL	4	5	3	6	2	1			

Table 9c Summary of counting statistics and model rankings.

<b>DAILY DIRECT BEAM RADIATION</b>									
	MAC	KAS	JOS	KASM	OH	EKDH	BCLS	CPR	EKDD
<b>Counts</b>									
AUS	1783	1199	1732	1783	1276	2035	1237	1269	2429
EUR	1108	1489	1431	1108	2478	2303	772	2266	2193
CAN	478	271	312	478	644	696	222	512	537
USA	1633	511	1434	1633	1438	1784	856	1262	1882
NAM	2111	782	1746	2111	2082	2480	1078	1774	2419
EURCAN	1586	1760	1743	1586	3122	2999	994	2778	2730
ALL	5002	3470	4909	5002	5836	6818	3087	5309	7041
<b>Rankings</b>									
AUS	3	9	5	3	6	2	8	7	1
EUR	7	5	6	7	1	2	9	3	4
CAN	5	8	7	5	2	1	9	4	3
USA	3	9	6	3	5	2	8	7	1
NAM	3	9	7	3	5	1	8	6	2
EURCAN	7	5	6	7	1	2	9	3	4
ALL	5	8	7	5	3	2	9	4	1
<b>HOURLY DIRECT BEAM RADIATION</b>									
	MAC	KAS	JOS	KASM	OH	EKDH			
<b>Counts</b>									
AUS	2142	1792	2064	2142	2180	2623			
EUR	1828	2189	2135	1828	2850	2698			
CAN	631	458	511	631	718	742			
USA	1864	1295	1762	1864	1934	2145			
NAM	2495	1753	2273	2495	2652	2887			
EURCAN	2459	2647	2646	2459	3568	3440			
ALL	6464	5734	6472	6464	7682	8208			
<b>Rankings</b>									
AUS	3	6	5	3	2	1			
EUR	5	3	4	5	1	2			
CAN	3	6	5	3	2	1			
USA	3	6	5	3	2	1			
NAM	3	6	5	3	2	1			
EURCAN	5	3	4	5	1	2			
ALL	4	6	3	4	2	1			



#### 4.2.1 Global radiation

- As expected, *BEST* estimated daily radiation with least error.
- In general, the two cloud layer models (*JOS*, *MAC*) provided the best hourly and daily (after *BEST*) estimates with *JOS* usually best. The counting scores show that these models perform similarly, which is to be expected since differences between the models are slight.
- The EURCAN results show that the layer models performed better than the sunshine models. *PAGE*, the best of the sunshine models, and *KAS* perform similarly.
- The attempt to generalize the Kasten model by introducing water vapour absorption explicitly (*KASM*) did not improve the model's performance.
- There is one surprising regional discrepancy. *MON* is the best performer for USA but the worst for EUR and EURCAN.
- The *BCLS* model performed surprisingly poorly although it is similar in principle to the Monteith model and both used the same cloud transmissivities in this study.
- Rankings using hourly and daily radiation are the same.
- The EURCAN results indicate that Rietveld's procedure for estimating the  $a$  and  $b$  parameters for the Ångström equation did not improve upon radiation estimates from Page's model which uses fixed parameter values.

#### 4.2.2 Diffuse and direct beam radiation

- As expected, Liu and Jordan models provided the best estimates; OH and *EKDH* for hourly radiation and *EKDD* for daily. However, daily estimates from *EKDH* were superior for North America.
- *CPR* did not perform as well as the other models of this type. In Australia,

both *CPR* and *OH* failed to match the performance of the layer models.

- Layer model performance, except in Australia, does not match the Liu and Jordan models. However, the latter require measured global radiation as input. Layer model estimates improve significantly, and possibly to the point of acceptance, for radiation averaged over periods longer than a day.

### 4.3 SUMMARY OF STATISTICS.

Appendix B presents annual statistics for each flux and model for daily and hourly radiation. These statistics are summarized in Table 10. Daily statistics extracted for each month are plotted in Figure 1. Cloud and sunshine model results are grouped together only for Europe and Canada, while a full set of cloud model results is given for all stations. In Table 10 models have been listed in the order of their rankings in Table 9. The following are noteworthy:

- *JOS* and *MAC* have very similar statistics.
- Results for *KAS* and *KASM* are very similar. Thus, the explicit parameterization of cloudless sky attenuation in *KASM* had little effect. Clearly, the cloud transmission function, common to both models, is the limiting factor.
- For estimating global radiation, there is merit in using cloud layer information even when it is incomplete. The effect of using incomplete cloud data is discussed later in this chapter.
- Differences between the statistical measures of error for the best and worst performing models may not be sufficiently large to be significant for solar energy or any other purpose. Without clear guidelines on the required accuracy of radiation estimates, it is impossible to assess whether these results are sufficient for recommending one or more models. Since the performance of *BEST* in estimating global radiation is not much better than



Figure 1 Monthly statistics for daily radiation



FIG. 1.1: MEAN ABSOLUTE BIAS

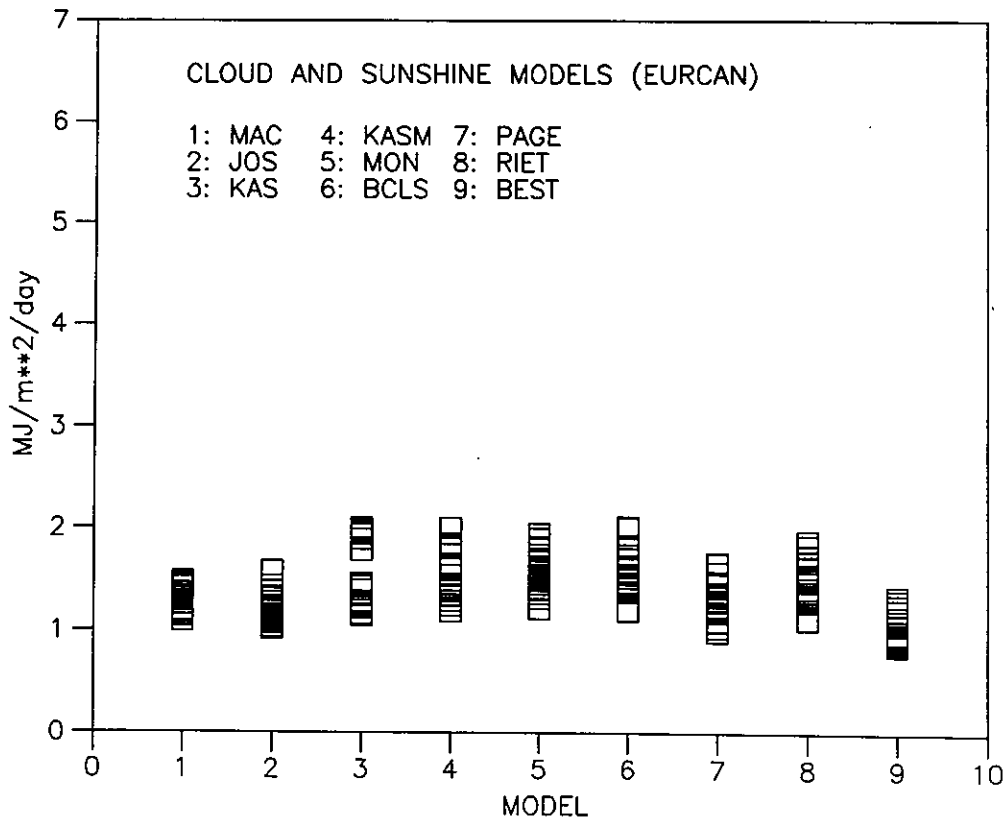
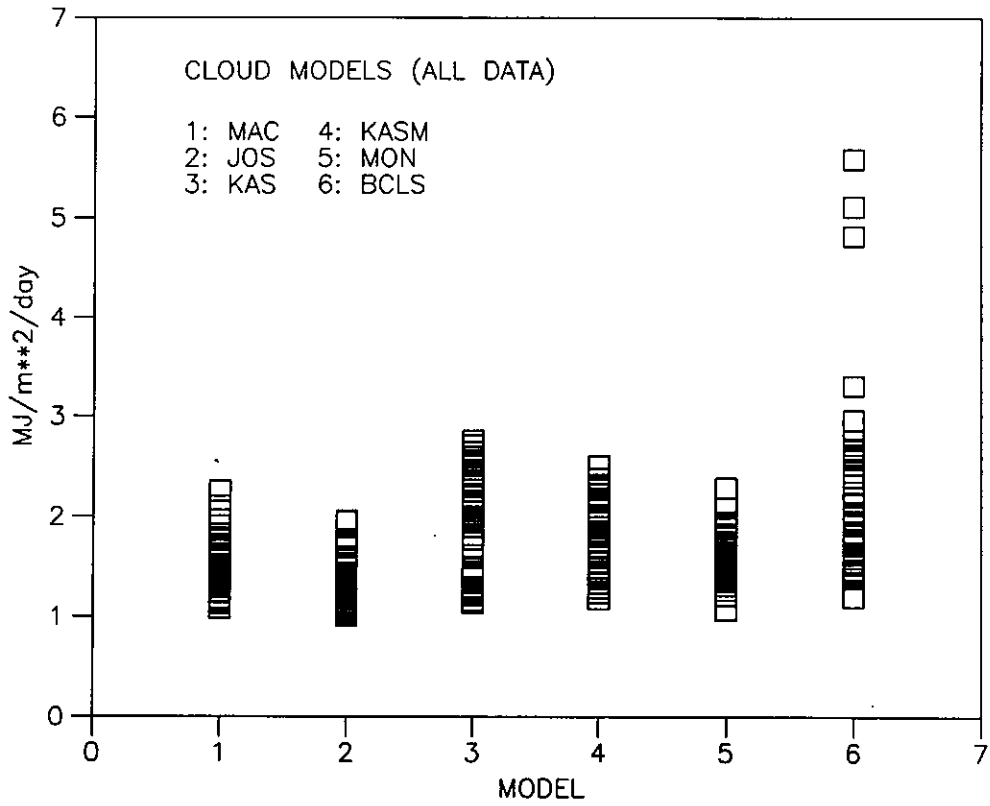




FIG. 1.2: MEAN BIAS ERROR

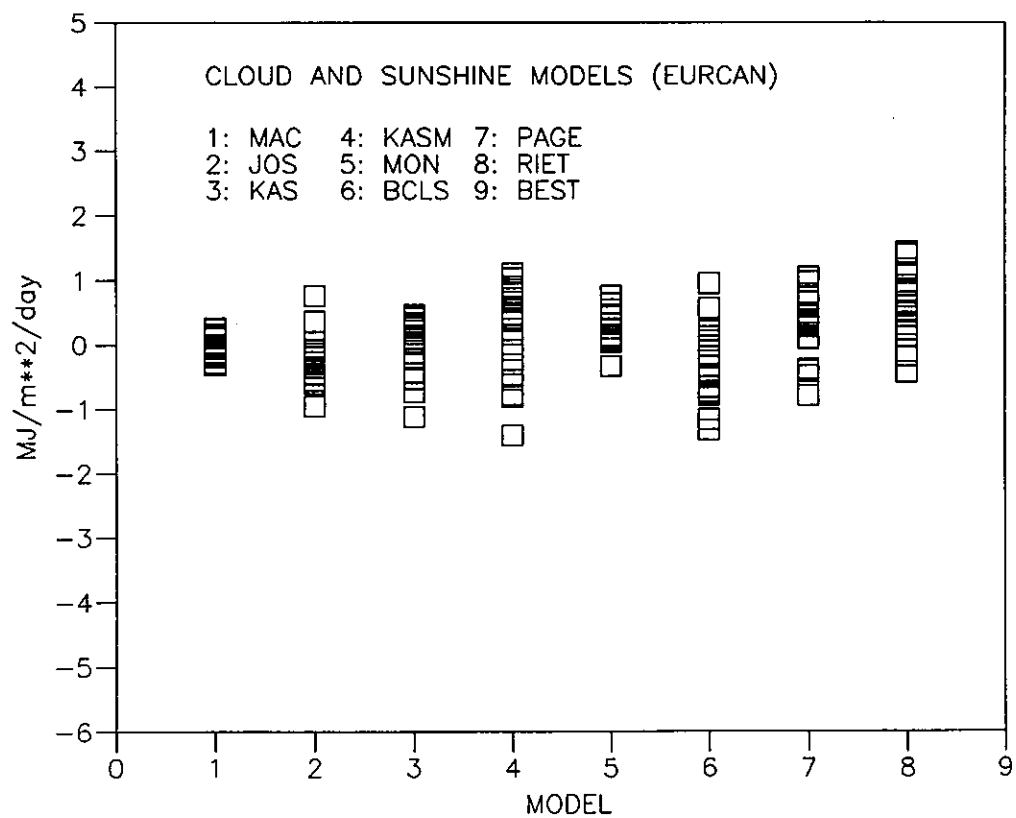
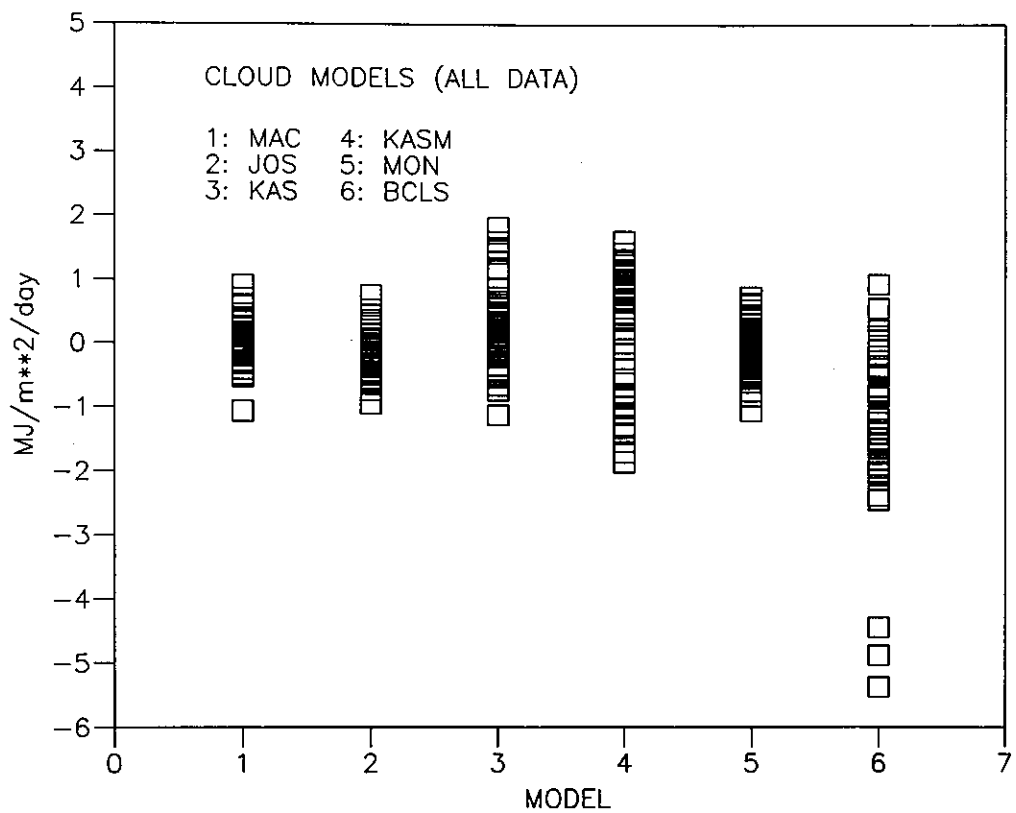






FIG. 1.3: ROOT MEAN SQUARE ERROR

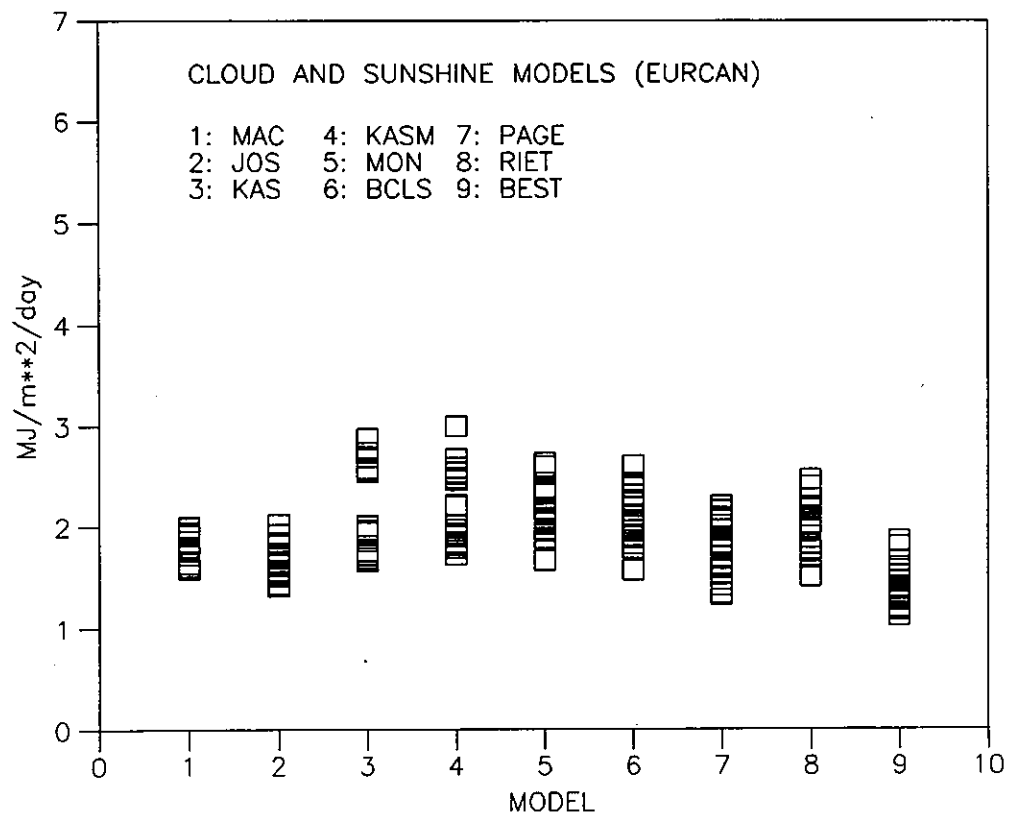
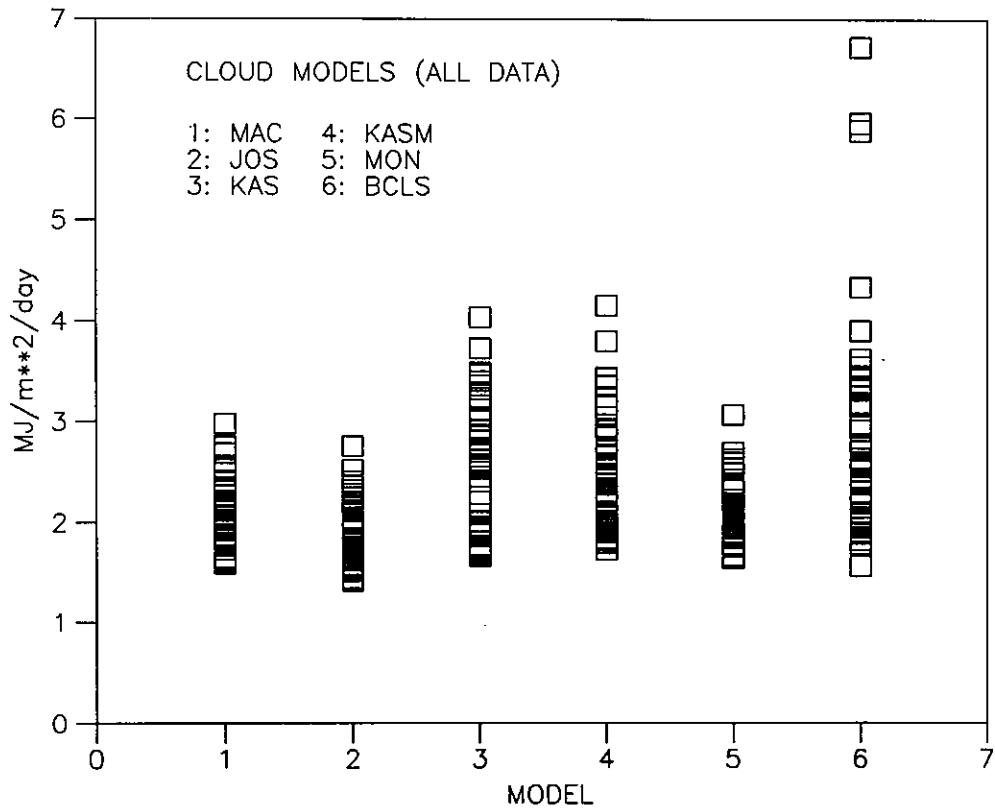




FIG. 1.4: MEAN ABSOLUTE BIAS

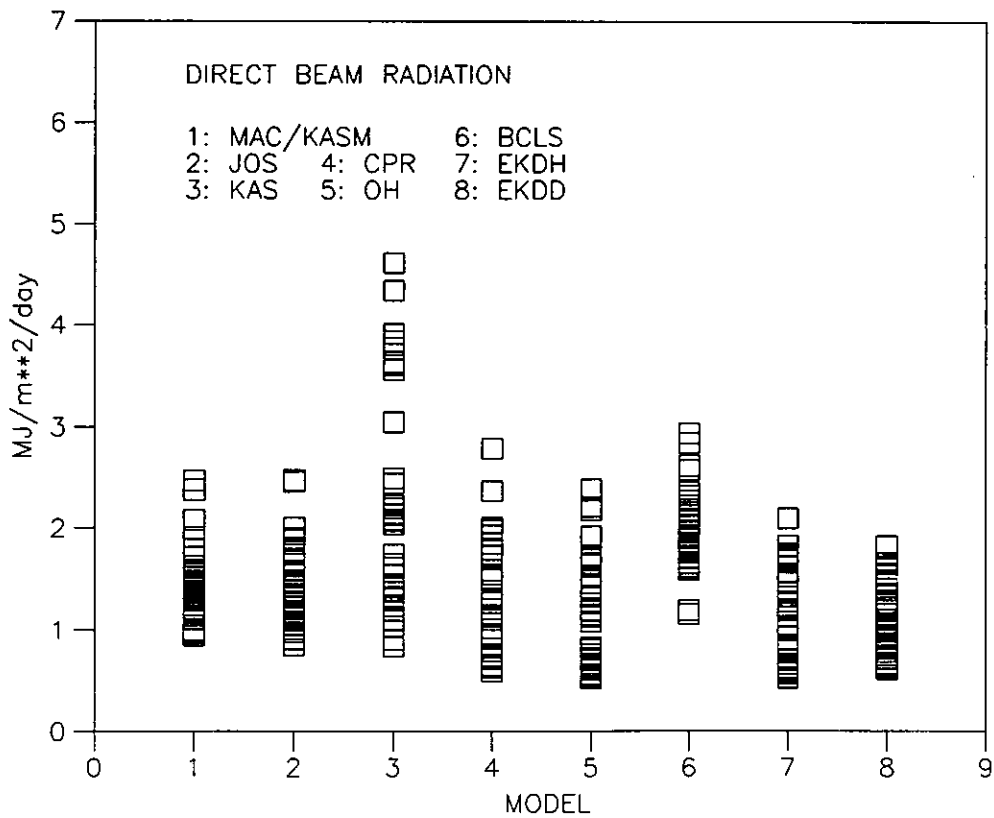
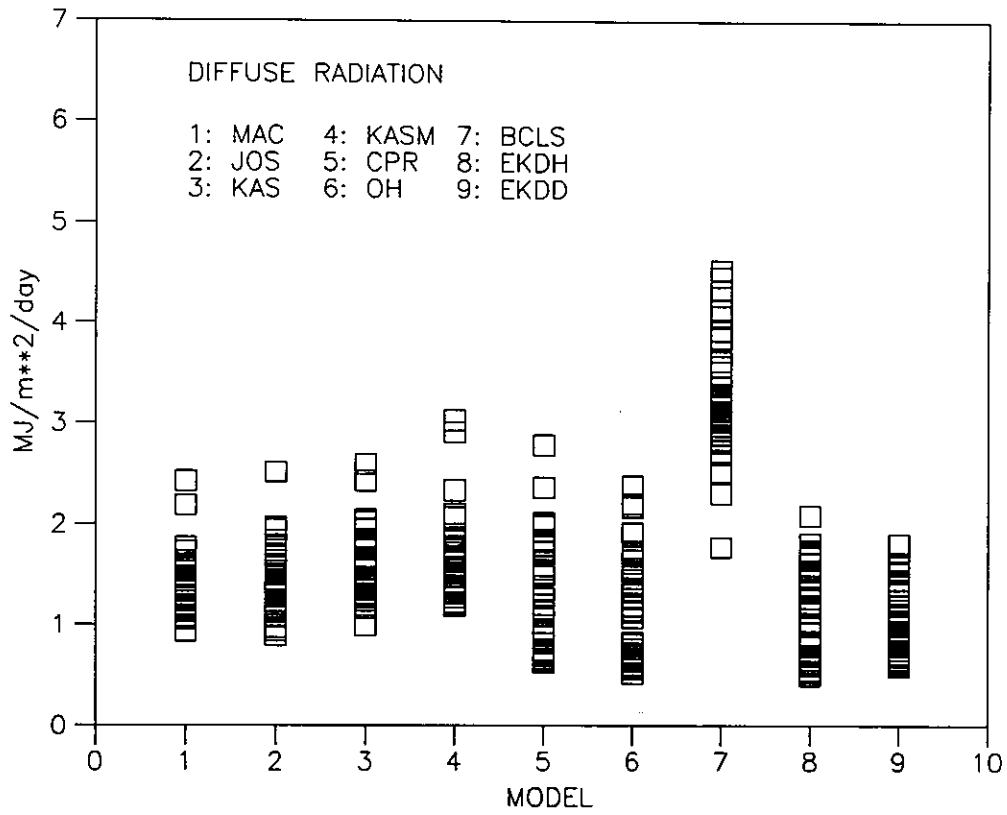




FIG. 1.5: MEAN BIAS ERROR

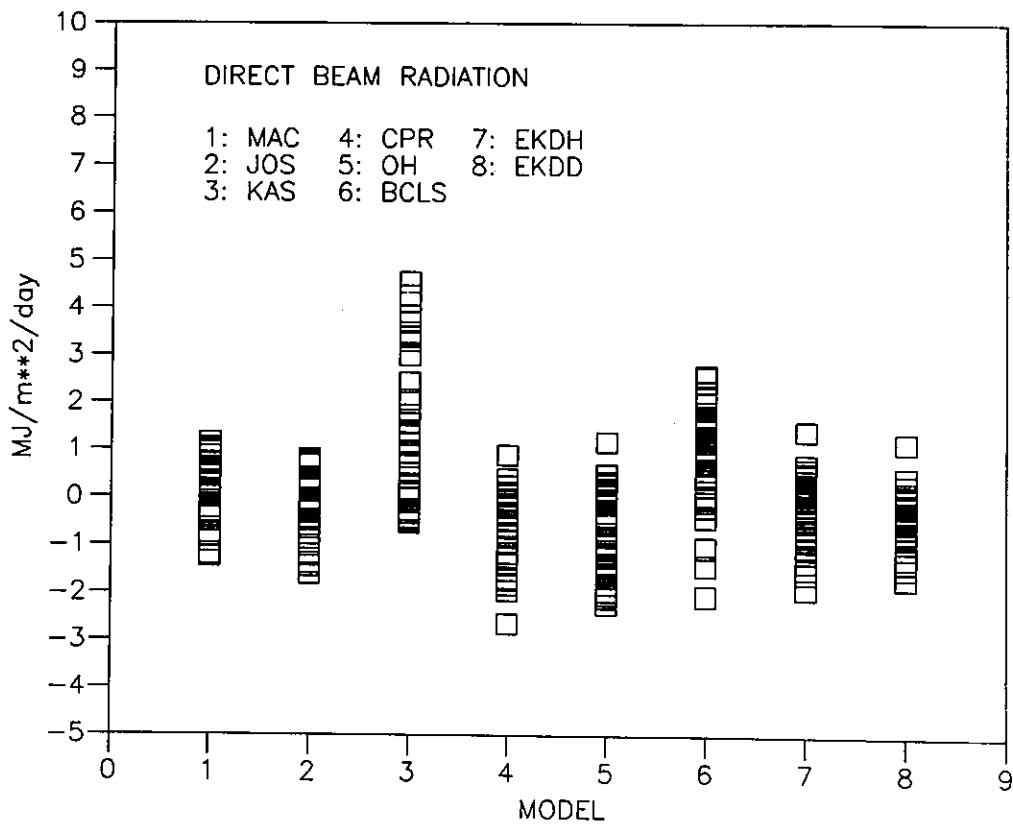
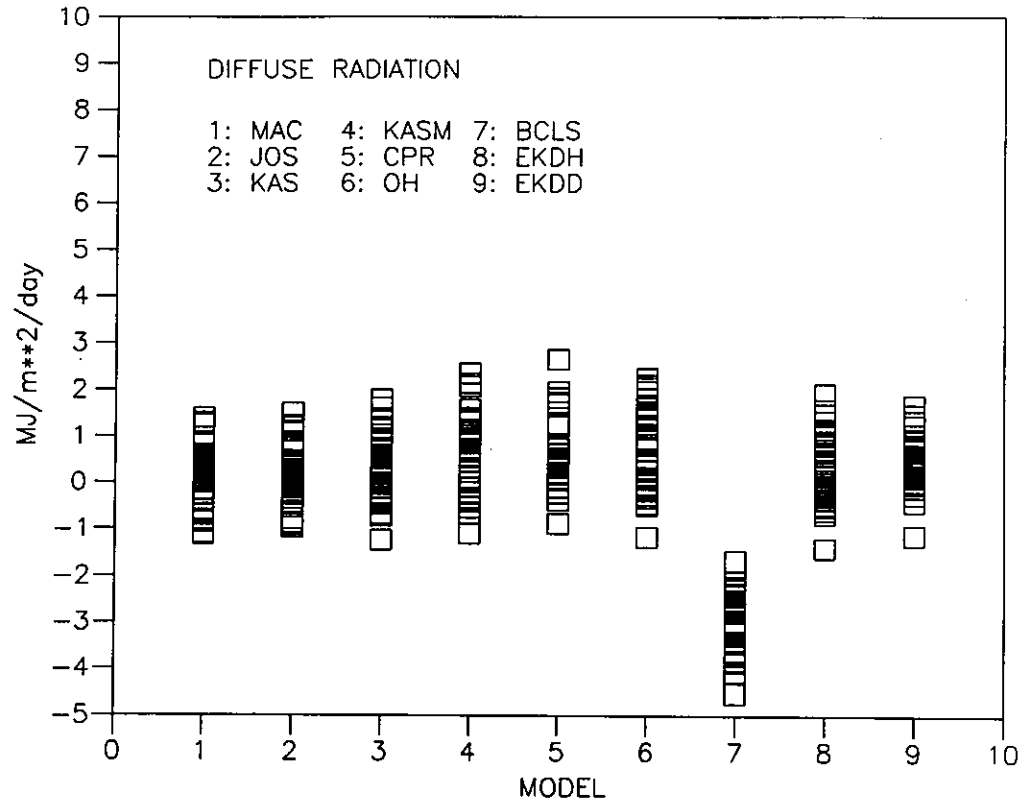




FIG. 1.6: ROOT MEAN SQUARE ERROR

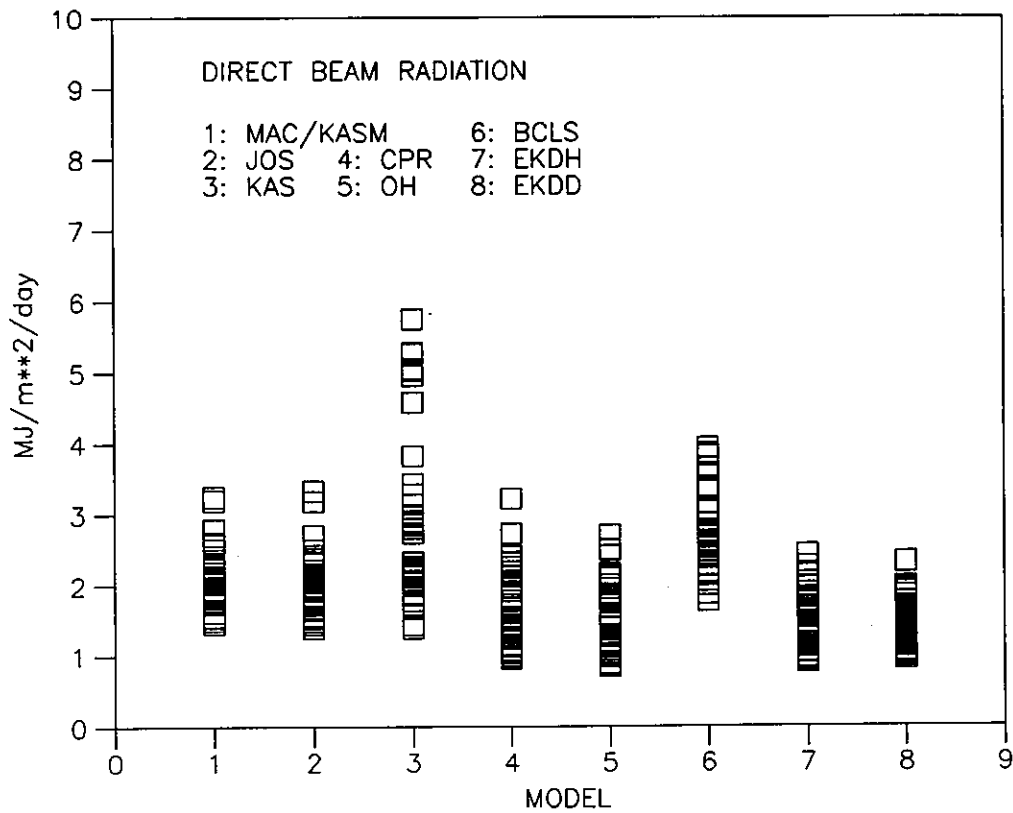
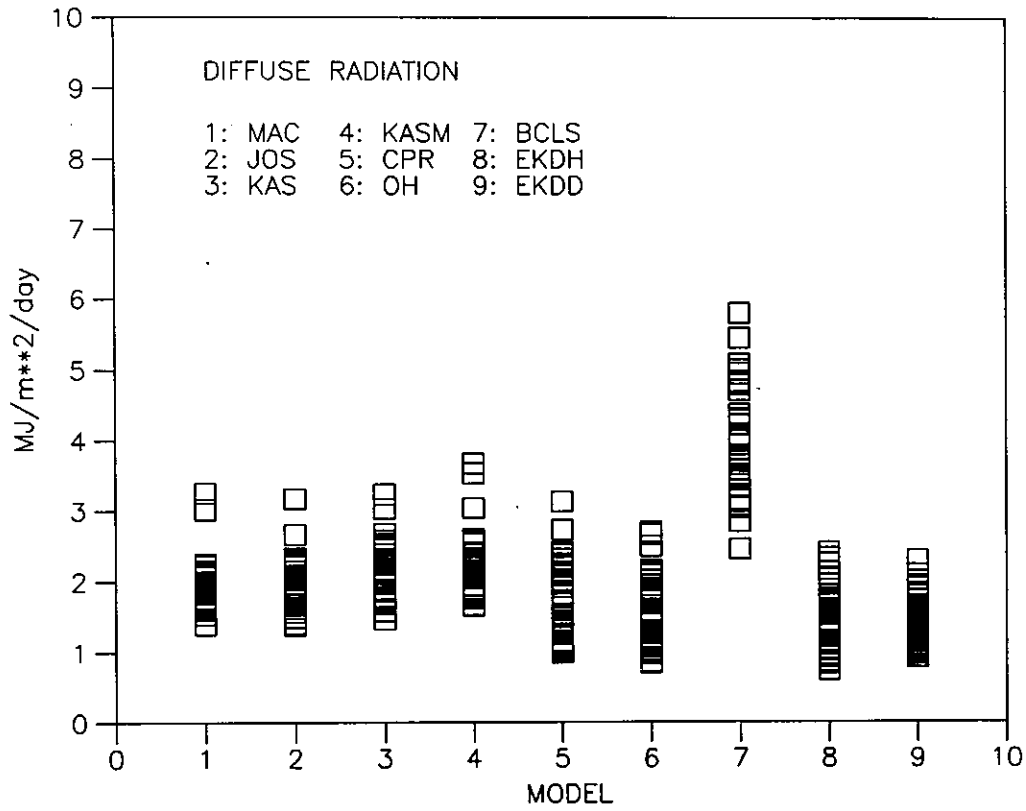






Table 10a Statistical summary for global radiation.  
 $\langle G \rangle$  is the mean measured radiation

	MAB	MBE	RMSE
<b>DAILY GLOBAL</b>			
<b>CLOUD AND SUNSHINE MODELS— EURCAN</b>			
$\langle G \rangle = 10.99 \text{ MJ/m}^2/\text{day}$			
BEST	1.04	-0.00	1.42
JOS	1.20	-0.24	1.67
MAC	1.27	-0.01	1.76
PAGE	1.32	0.23	1.75
KAS	1.54	-0.03	2.14
KASM	1.56	0.22	2.19
RIET	1.51	0.62	1.99
BCLS	1.61	-0.43	2.10
MON	1.58	0.30	2.15
<b>CLOUD MODELS — ALL DATA</b>			
$\langle G \rangle = 14.89 \text{ MJ/m}^2/\text{day}$			
JOS	1.37	-0.18	1.90
MAC	1.51	0.06	2.08
MON	1.58	0.00	2.14
KAS	1.86	0.30	2.52
KASM	1.79	0.12	2.54
BCLS	2.24	-1.35	2.90
<b>HOURLY GLOBAL</b>			
<b>CLOUD AND SUNSHINE MODELS — EURCAN</b>			
$\langle G \rangle = 910 \text{ kJ/m}^2/\text{hr}$			
JOS	172.6	-19.0	266.4
MAC	177.5	0.4	270.7
KAS	196.7	-1.2	302.0
KASM	194.8	19.5	305.1
MON	197.2	25.8	286.6
<b>CLOUD MODELS — ALL DATA</b>			
$\langle G \rangle = 1225 \text{ kJ/m}^2/\text{hr}$			
JOS	192.8	-13.6	299.2
MAC	201.5	6.2	308.1
MON	205.3	1.6	303.1
KAS	227.3	25.8	346.1
KASM	215.9	11.7	344.7

Table 10b Statistical summary for diffuse and direct beam radiation.  $\langle D \rangle$  and  $\langle I \rangle$  are the respective mean measured values

	MAB	MBE	RMSE
<b>DAILY DIFFUSE</b>			
	$\langle D \rangle = 5.45 \text{ MJ/m}^2/\text{day}$		
EKKD	1.03	0.42	1.41
EKDH	1.11	0.33	1.47
OH	1.23	0.60	1.60
CPR	1.29	0.77	1.69
JOS	1.43	0.13	1.93
MAC	1.41	0.06	1.93
KAS	1.59	0.33	2.12
KASM	1.68	0.59	2.23
BCLS	3.29	-2.98	4.05
<b>HOURLY DIFFUSE</b>			
	$\langle D \rangle = 443 \text{ kJ/m}^2/\text{hr}$		
EKDH	119.9	28.4	181.6
OH	128.9	50.8	186.7
JOS	174.3	7.8	261.6
MAC	169.8	1.8	256.6
KAS	195.3	-3.7	285.2
KASM	193.2	32.7	289.3
<b>DAILY DIRECT BEAM</b>			
	$\langle I \rangle = 9.49 \text{ MJ/m}^2/\text{day}$		
EKDD	1.04	-0.38	1.42
EKDH	1.11	-0.30	1.49
OH	1.23	-0.57	1.60
CPR	1.28	-0.73	1.69
MAC	1.42	0.15	2.09
JOS	1.42	-0.16	2.07
KAS	2.17	1.27	3.02
BCLS	1.93	0.94	2.73
<b>HOURLY DIRECT BEAM</b>			
	$\langle I \rangle = 731 \text{ kJ/m}^2/\text{hr}$		
EKDH	120.5	-25.6	184.1
OH	128.9	-47.9	188.4
JOS	180.9	-13.0	296.1
MAC	182.1	13.1	298.3
KAS	240.7	107.8	362.8

that of the layer models, one interpretation of the results is that models are close to the limit of prediction. The difference in *RMSE* between *JOS* (1.67 MJ/day) and *BEST* (1.42 MJ/day) for EURCAN may not be sufficient to justify further modelling efforts. The performance of models which use surface meteorological measurements and observations is probably limited more by the inadequacy of this information than by modifiable defects in the models themselves. Nor do models which use satellite information provide surface global radiation estimates which are always superior to layer model estimates (Davies et al.,1984).

- There is little to recommend sunshine-based models. Even though the Ångström equation can be easily tuned to a location's climatic conditions by simple regression, it requires the existence of radiation measurements in the first place to produce the prediction equation and faith that the regression can be applied to sunshine data for another place or time. Its computational simplicity is irrelevant in these times of the microprocessor. All models used in this study are computationally simple. We see little virtue in further empirical studies with this equation.
- Although Liu and Jordan models are the consistently best performers in estimating diffuse and direct beam radiation, the differences in uncertainty between this group and the layer models is about 25% for daily estimates. The magnitude of this difference may be offset by the Liu and Jordan models' requirement for measured global radiation.

#### 4.4 MODEL PERFORMANCE FOR DIFFERENT AVERAGING PERIODS.

While *MBE* does not change for a data set when data are averaged over groupings of different size, the value of the *RMSE* will decrease. If the *RMSE* is a strictly random error, it will decrease according to the square root of  $N$ , the length of the averaging period. Whether the *RMSE* is strictly random error is not important, here. However, the fact that the error will decrease when data are averaged may be important since it allows an averaging period to be selected which will ensure a *RMSE* within a required limit. *RMSE* was computed for all models and all fluxes for all years for averaging periods of: 2,3,4,5,6,7,8,9,10,15,20,25 and 30 days (Appendix C).

*RMSE* results for 30-day means of all data for each station are given in Table 11 and plotted in Figure 2. Global radiation results for sunshine-based models at locations where sunshine was estimated from cloud amount are italicized. These show:

- Clearer superiority of layer models over others for global radiation.
- With the exception of Australian stations, the MAC model has smallest *RMSE* for global radiation.
- The best *RMSE* values for global radiation are 3–5 times larger than those for *BEST*.
- For diffuse and direct beam radiation, layer model values for many stations are similar or even better than values for Liu and Jordan models. Thus, monthly estimates of these components from the two types of models have comparable accuracy. This is an important result for applications where monthly radiation estimates are sufficient.

Table 11 RMSE ( $\text{MJ}/\text{m}^2/\text{day}$ ) for 30-day averaging periods (calculated from all data for each station)

GLOBAL RADIATION										
STATION	MEAS	MAC	KAS	JOS	KASM	MON	PAGE	BCLS	RIET	BEST
Alice Sp.	22.36	1.09	1.04	0.92	1.33	0.91	2.87	2.34	1.48	0.21
Guildford	18.37	0.82	1.59	0.63	1.42	0.56	1.56	2.38	0.77	0.33
Mildura	19.06	0.79	0.72	0.48	1.05	0.50	1.98	2.20	0.94	0.12
Rockhamp.	19.33	1.34	1.83	1.05	1.63	1.27	2.43	5.55	1.84	0.15
De Bilt	9.95	0.39	0.56	0.40	0.81	0.67	0.42	1.43	0.80	0.10
Hamburg	9.79	0.53	0.57	0.64	1.04	0.76	0.56	0.96	0.91	0.13
Kew	9.74	0.55	0.69	0.66	1.19	0.68	1.11	0.90	1.55	0.11
Zurich	10.99	0.46	0.45	0.40	0.56	0.82	0.97	1.53	0.65	0.18
Montreal	12.12	0.52	0.82	0.87	0.67	0.66	0.83	0.91	1.43	0.17
Winnipeg	13.11	0.45	1.40	0.68	1.44	0.71	1.24	0.95	1.54	0.23
Vancouver	11.92	0.64	0.69	0.72	0.55	0.80	0.63	0.84	0.88	0.15
Albuquer.	20.18	0.50	1.22	0.67	1.63	0.83	2.27	1.49	1.07	0.14
Columbia	15.26	0.78	1.29	0.78	1.74	0.85	1.46	3.48	1.24	0.36
Medford	15.44	0.64	1.45	0.71	1.86	0.80	1.70	2.08	1.67	0.15
Sterling	13.81	0.51	0.82	0.77	1.14	0.45	0.70	2.61	0.92	0.19
DIFFUSE RADIATION										
STATION	MEAS	MAC	KAS	JOS	KASM	OH	EKDH	BCLS	CPR	EKDD
Alice Sp.	4.52	0.85	0.93	0.91	1.59	1.82	1.50	2.29	2.24	1.28
Guildford	5.35	0.75	0.76	0.68	1.38	1.77	1.34	3.64	1.57	1.13
Mildura	4.97	0.75	0.87	0.68	1.33	1.57	1.24	3.03	1.68	1.04
Rockhamp.	5.99	0.73	1.78	1.11	2.25	2.03	1.55	4.77	1.69	1.45
De Bilt	6.23	1.31	0.41	1.03	0.50	0.64	0.85	4.08	0.46	0.46
Hamburg	5.41	0.91	0.98	0.50	0.87	0.41	0.50	3.50	0.38	0.35
Kew	5.45	0.61	1.46	0.40	1.37	0.49	0.36	3.11	0.56	0.58
Zurich	5.86	0.95	0.45	0.56	0.54	0.45	0.62	3.33	0.35	0.39
Montreal	5.50	0.75	0.74	0.56	0.83	0.54	0.47	3.06	0.76	0.70
Albuquer.	4.99	1.32	0.75	1.34	1.26	1.25	0.95	3.03	1.59	1.00
Columbia	6.78	1.02	0.36	1.32	1.02	1.28	1.48	4.71	1.08	1.18
Medford	5.45	0.43	0.78	0.51	0.75	0.88	0.73	3.26	0.88	0.64
Sterling	6.05	0.75	1.13	0.90	1.06	0.67	0.68	4.27	0.64	0.51
DIRECT BEAM RADIATION										
STATION	MEAS	MAC	KAS	JOS	KASM	OH	EKDH	BCLS	CPR	EKDD
Alice Sp.	18.05	1.18	2.22	1.27	1.18	1.82	1.49	1.62	2.23	1.27
Guildford	12.24	0.60	1.77	0.51	0.60	1.78	1.35	0.88	1.58	1.14
Mildura	14.22	0.73	1.25	0.76	0.73	1.57	1.24	1.03	1.68	1.04
Rockhampt	13.49	1.46	1.34	1.54	1.46	2.03	1.55	2.34	1.69	1.45
De Bilt	4.12	1.42	0.82	1.08	1.42	0.68	0.89	2.52	0.49	0.49
Hamburg	4.42	1.03	0.91	0.83	1.03	0.47	0.58	2.69	0.46	0.42
Kew	3.82	0.52	0.65	0.37	0.52	0.38	0.45	3.57	0.33	0.37
Zurich	5.33	0.77	0.32	0.45	0.77	0.45	0.62	1.47	0.35	0.41
Montreal	6.57	0.67	0.83	0.88	0.67	0.53	0.46	2.50	0.75	0.71
Albuquer.	14.96	1.02	4.50	1.44	1.02	1.10	0.80	1.58	1.45	0.83
Columbia	7.53	1.25	4.65	1.03	1.25	1.29	1.51	1.73	1.09	1.18
Medford	9.39	0.50	4.27	0.58	0.50	0.91	0.76	1.07	0.91	0.66
Sterling	7.35	1.07	2.50	0.96	1.07	0.85	0.80	1.93	0.83	0.68



Figure 2 RMSE values for 30-day mean radiation





FIG 2.1: ROOT MEAN SQUARE ERROR

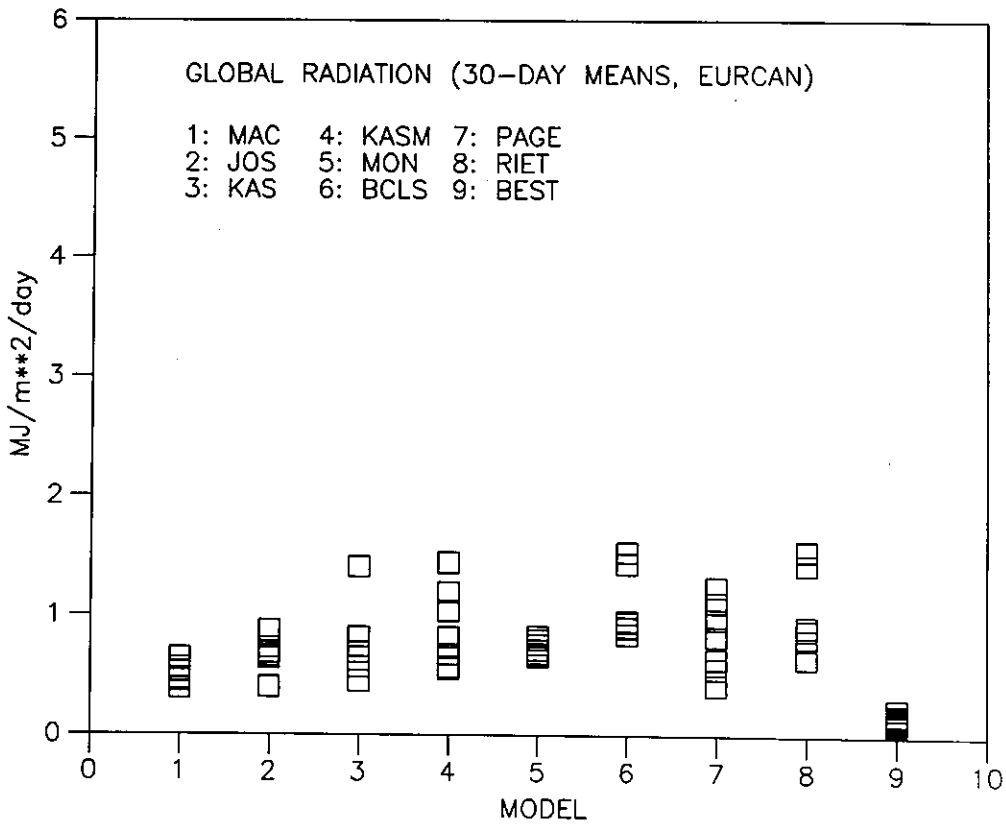
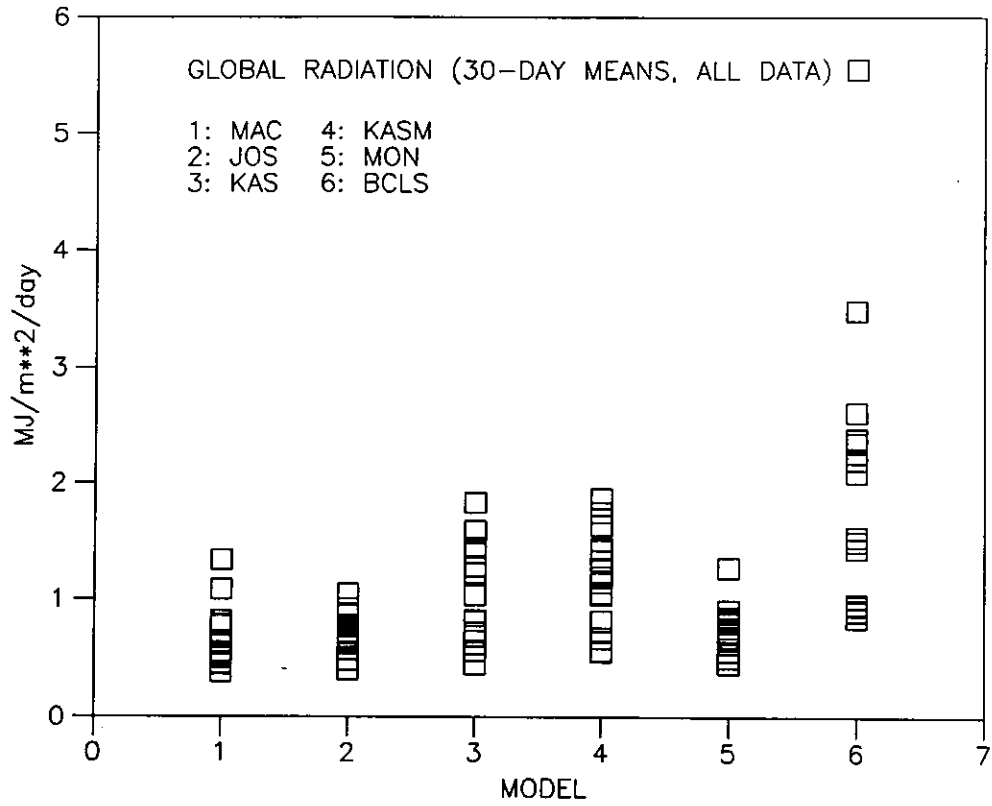
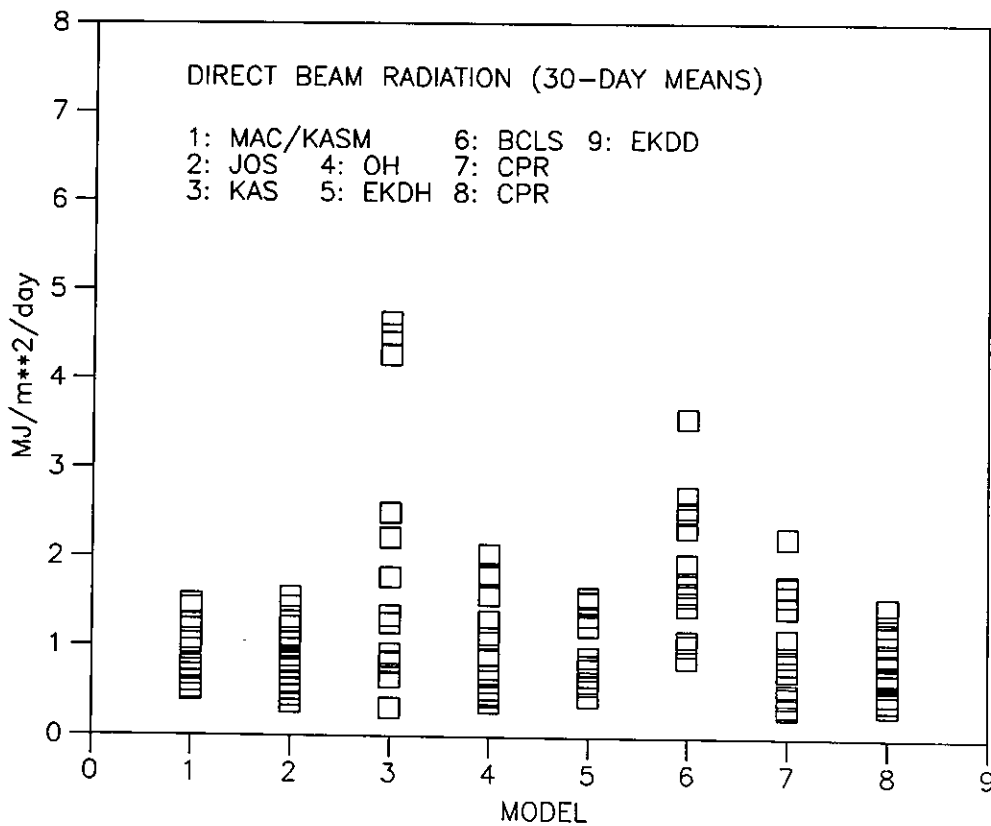
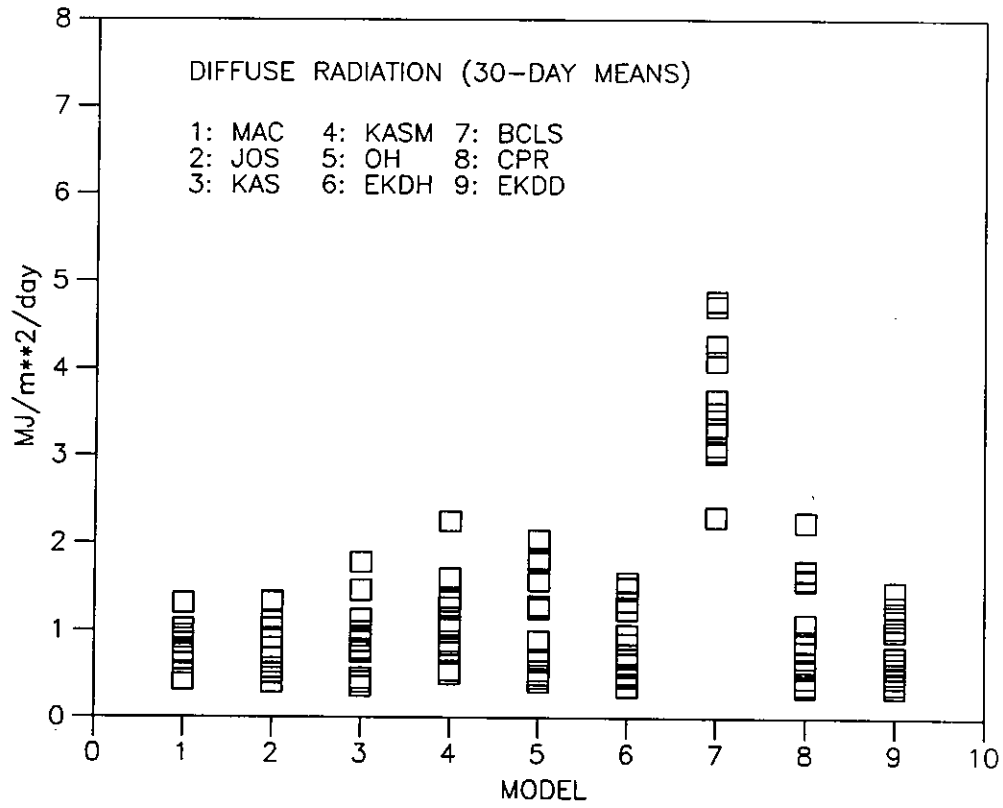




FIG 2.2: ROOT MEAN SQUARE ERROR





#### 4.5 MONTHLY VARIATION IN THE PERFORMANCE OF SELECTED MODELS

The monthly performance of the four best models (*MAC*, *JOS*, *EKDD*, *EKDH*), is shown for representative stations (Alice Springs, Mildura, Albuquerque, Medford, Montreal, Winnipeg, Hamburg, Kew and Zurich). The analysis used the data in Appendix A and, therefore, can be extended to other models. Measured and model values of radiation for all years were combined for each station to compute means and error statistics. Results for global radiation are plotted in Figure 3a and for diffuse and direct beam radiation in Figure 3b. In all figures, measured radiation is plotted with a solid line and model estimates with a dashed line. Values of *MBE* are plotted as crosses and *RMSE* as vertical error bars. There is no separate error diagram for direct beam radiation since *MBE* values differ from diffuse radiation *MBE* only in sign, while *RMSE* values are the same as for diffuse.

The main purpose in examining monthly variation in model performance is to determine whether there are seasonal biases, which, in the case of the cloud layer models, could indicate inadequacies in the parameterization of cloud transmissivities, aerosol attenuation and water vapour absorption. Figure 3a suggests the parameterizations are adequate. Alice Springs has the largest difference between measured and calculated radiation. Although both *MAC* and *JOS* overestimate increasingly between winter and mid-summer, the overestimation is well within 10% of the measured radiation. Since calculations for both models did not use aerosol or precipitable water information for specific sites, the general lack of seasonal bias is a notable result.

Results for *EKDD* and *EKDH* are very similar (Figure 3b). Because these regression models have been fitted to data from several stations, they fit mean



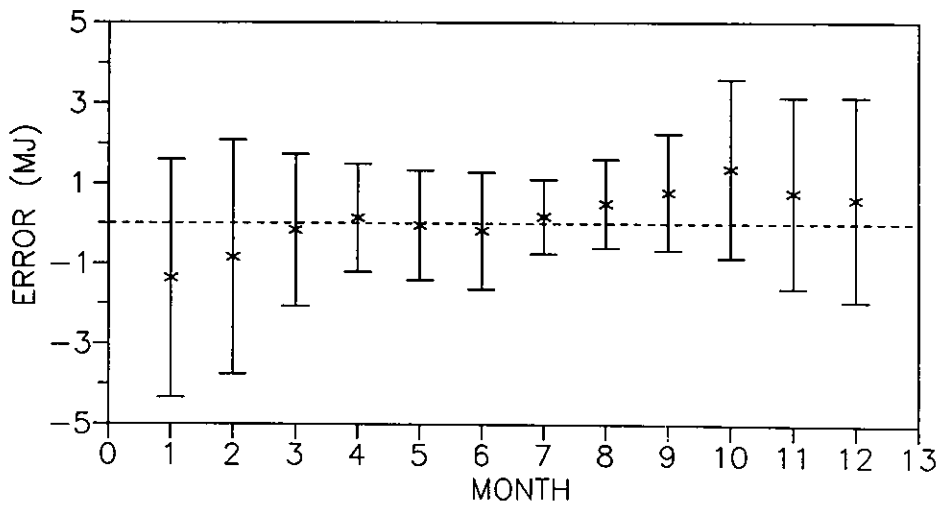
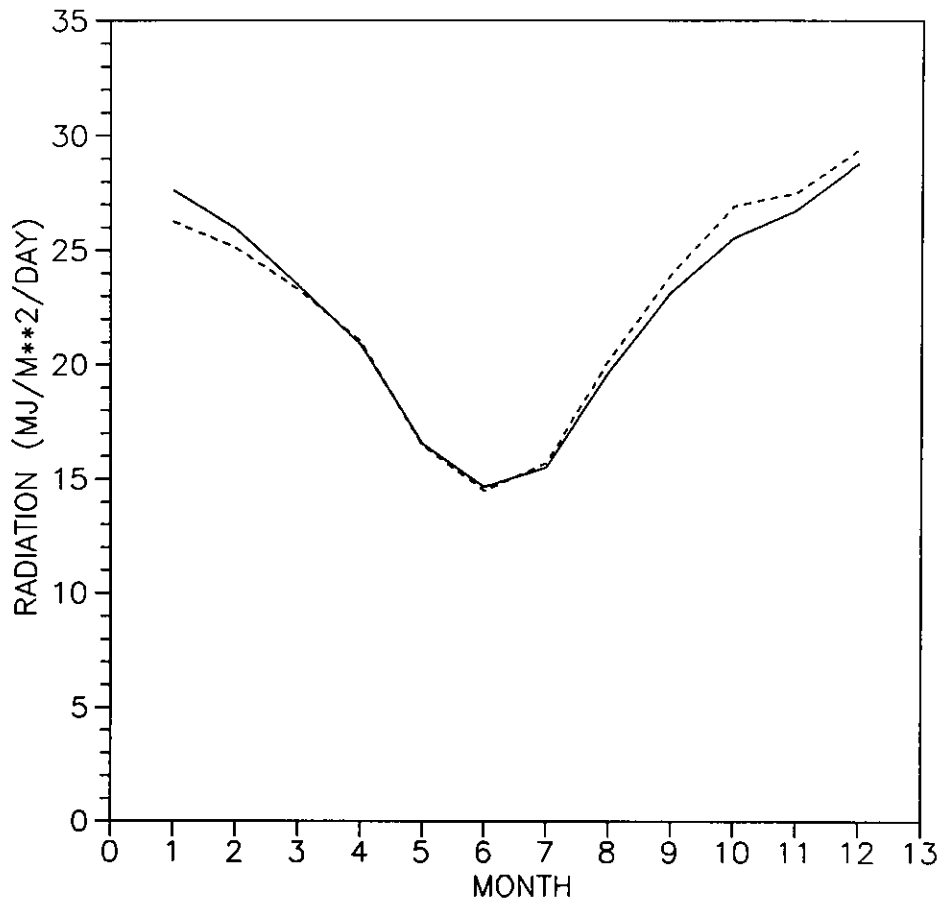
Figure 3a Monthly variation in measured radiation (solid line) and layer model estimates (dashed line) for selected stations. MBE values are shown as crosses and RMSE values as vertical bars

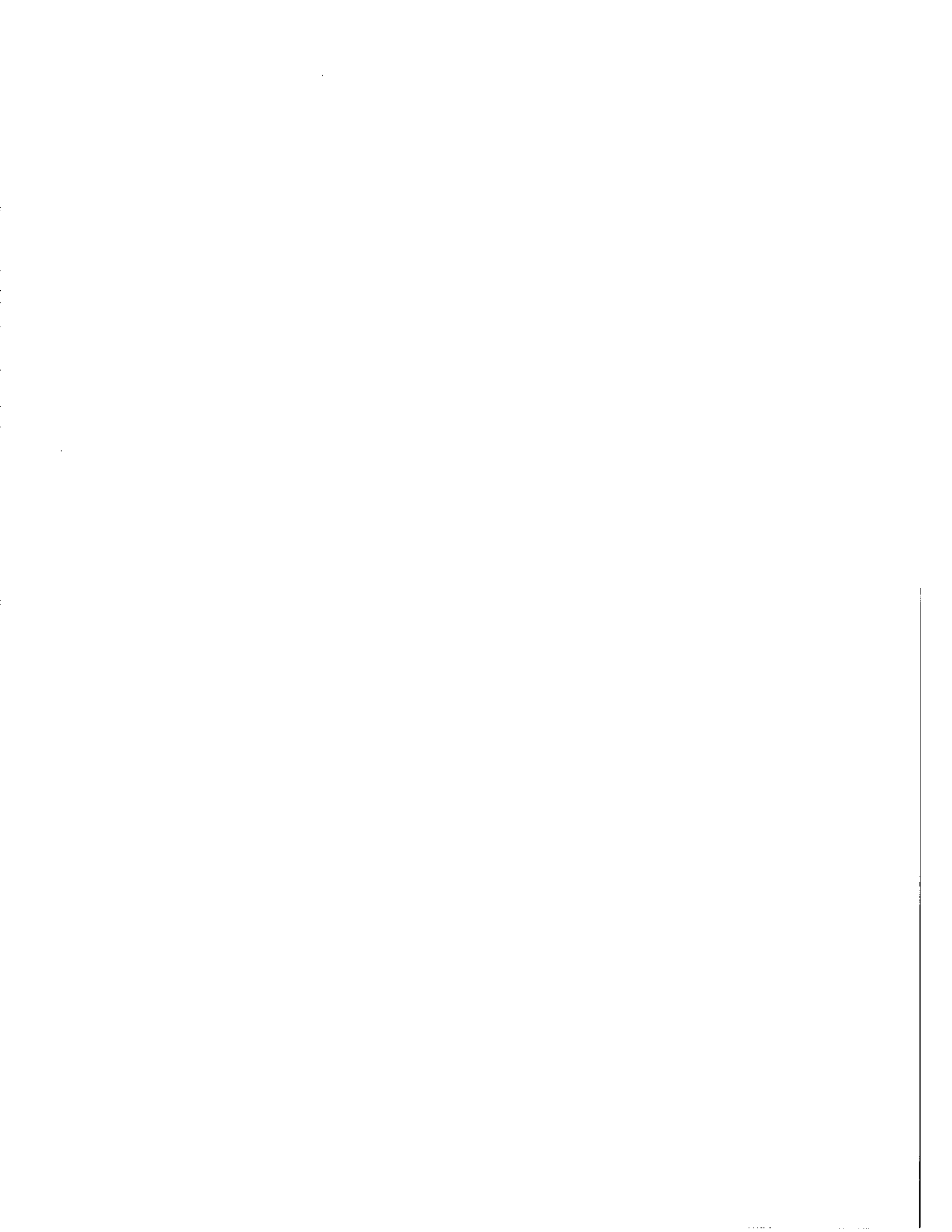




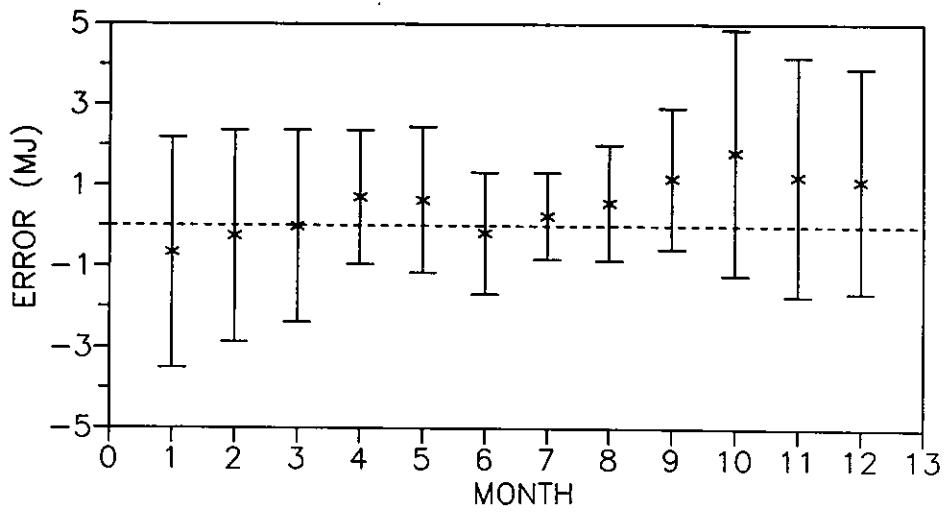
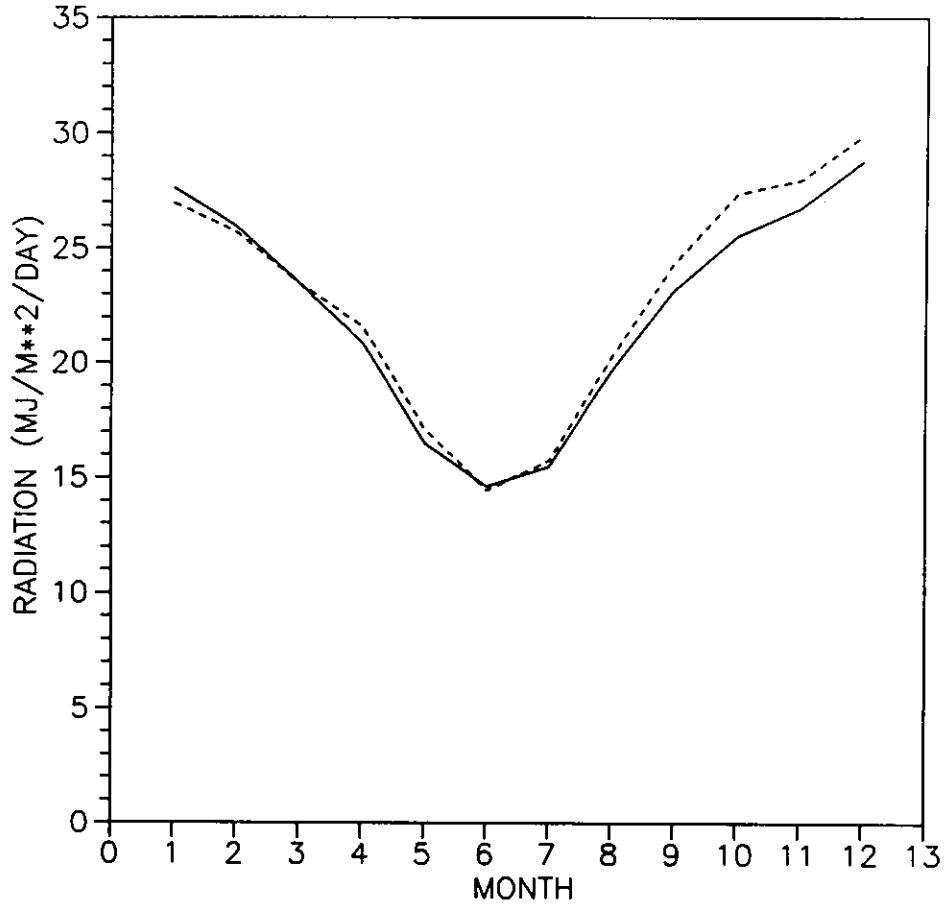
GLOBAL RADIATION: JOS MODEL

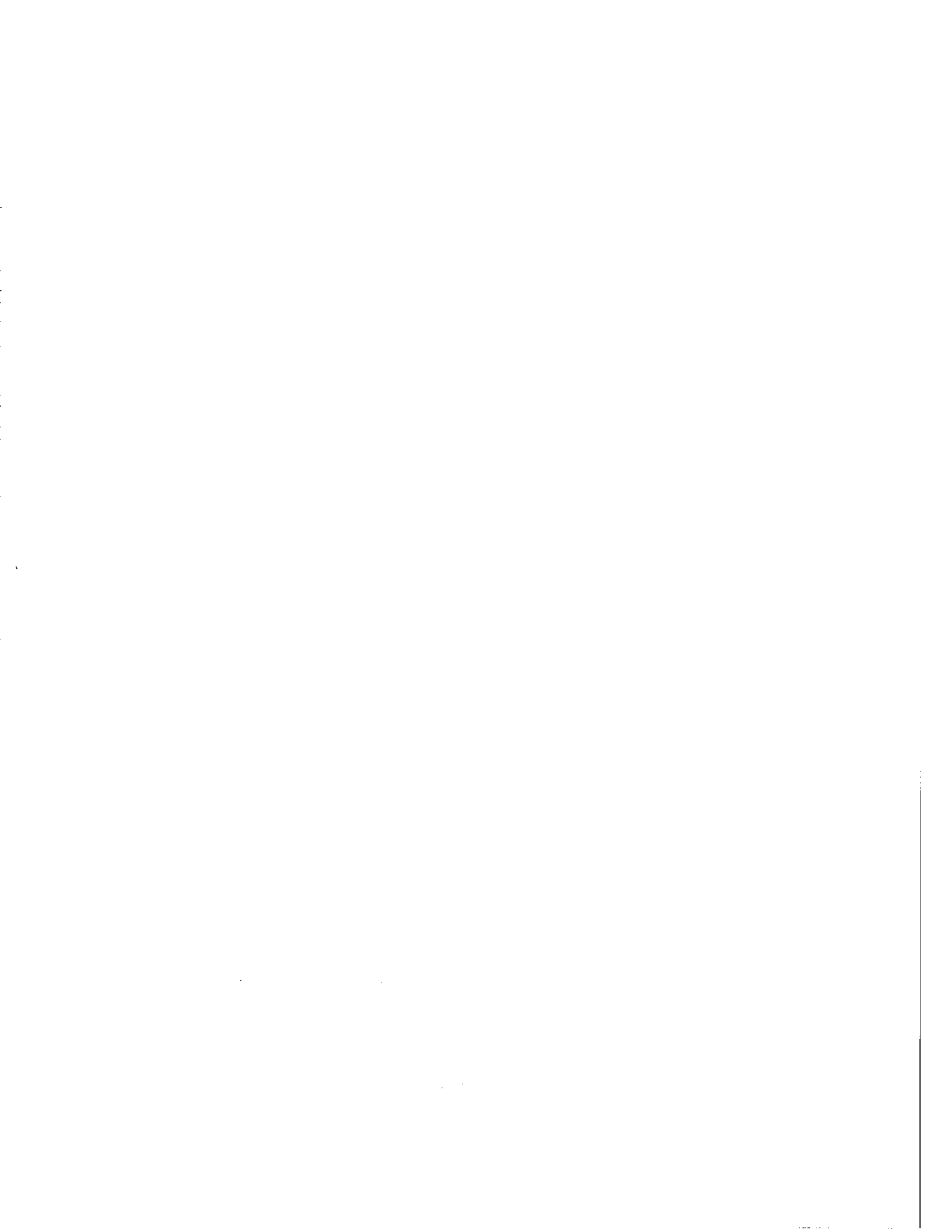
ALICE SPRINGS





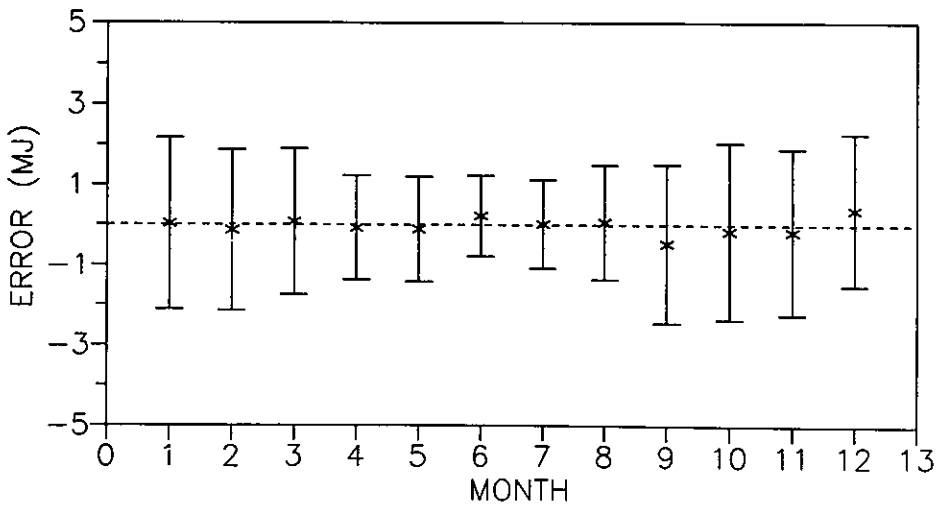
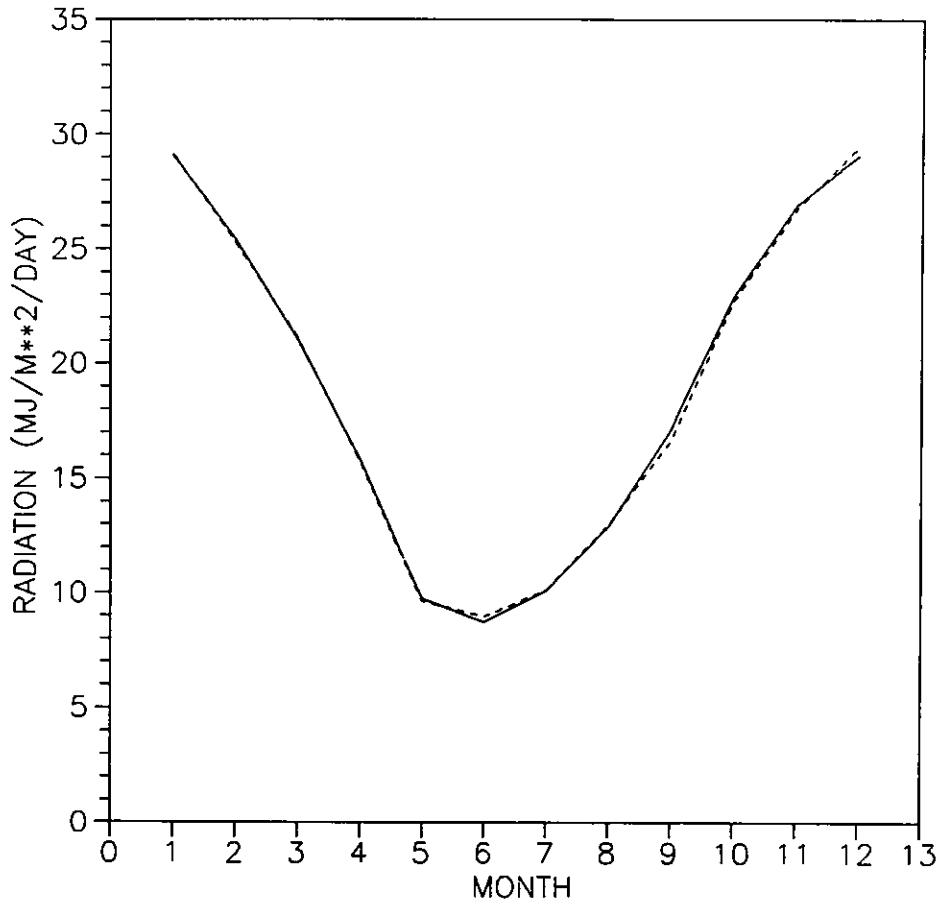
GLOBAL RADIATION: MAC MODEL  
ALICE SPRINGS





GLOBAL RADIATION: JOS MODEL

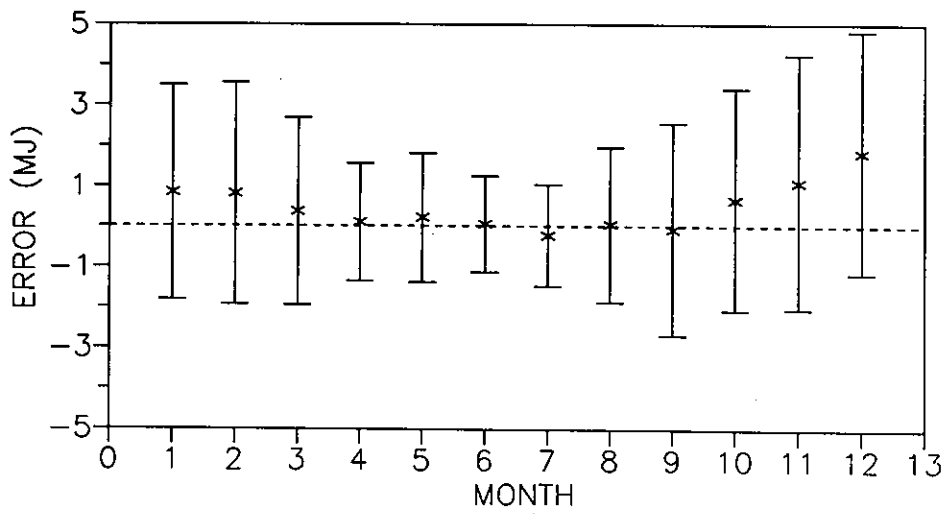
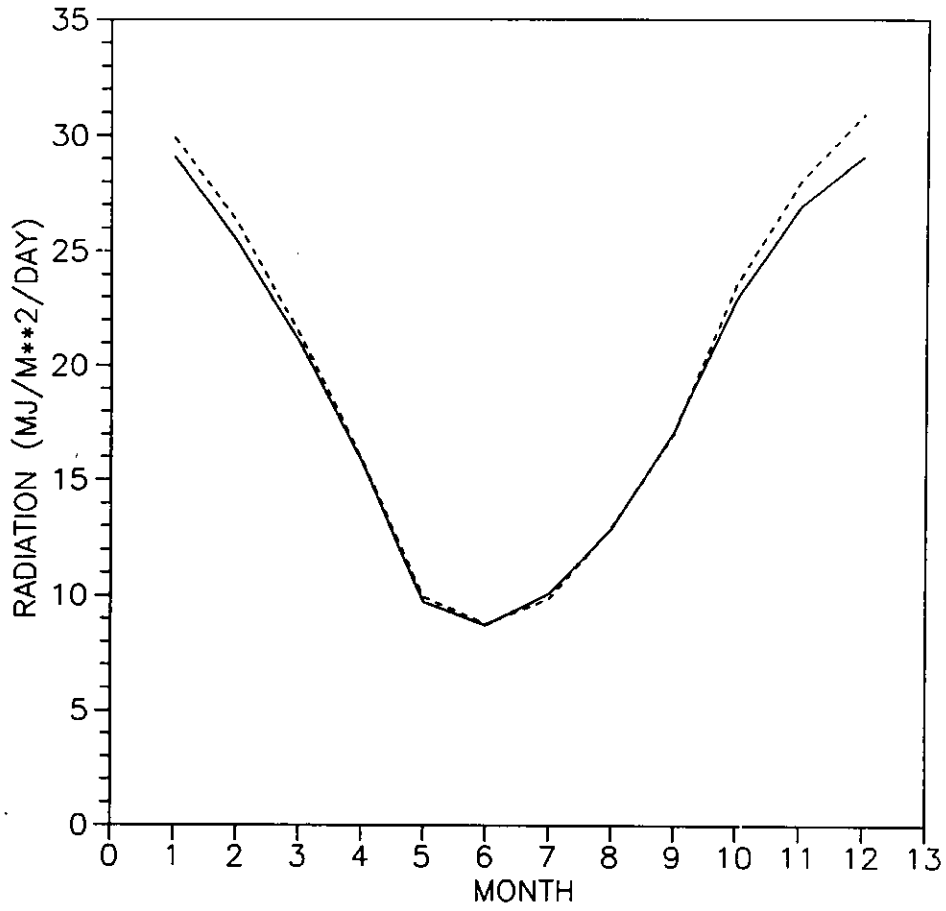
MILDURA





GLOBAL RADIATION: MAC MODEL

MILDURA

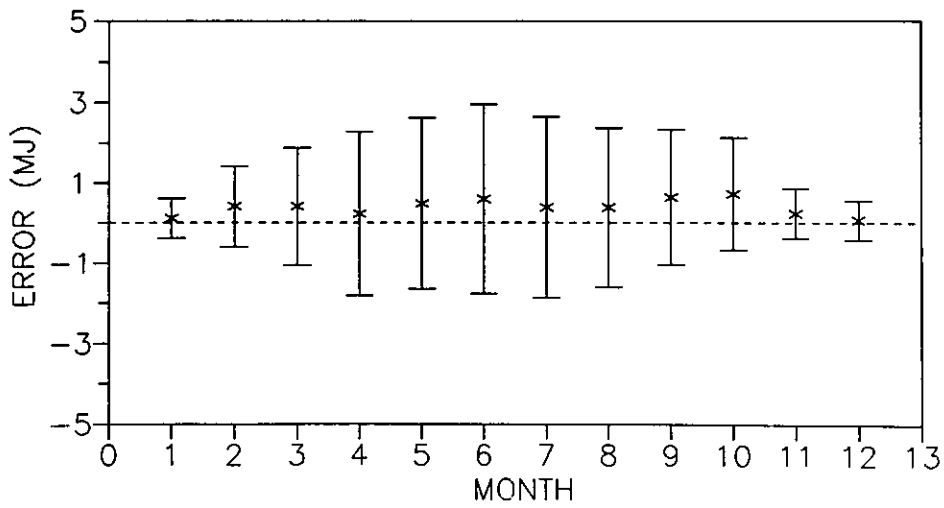
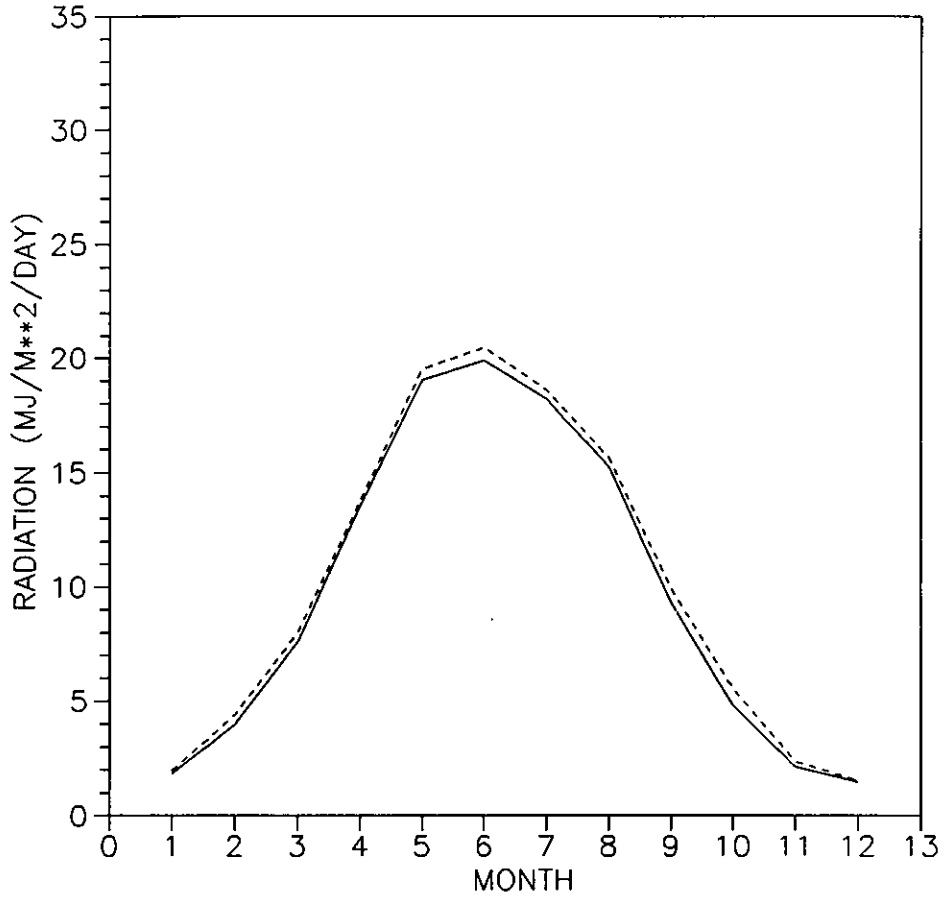


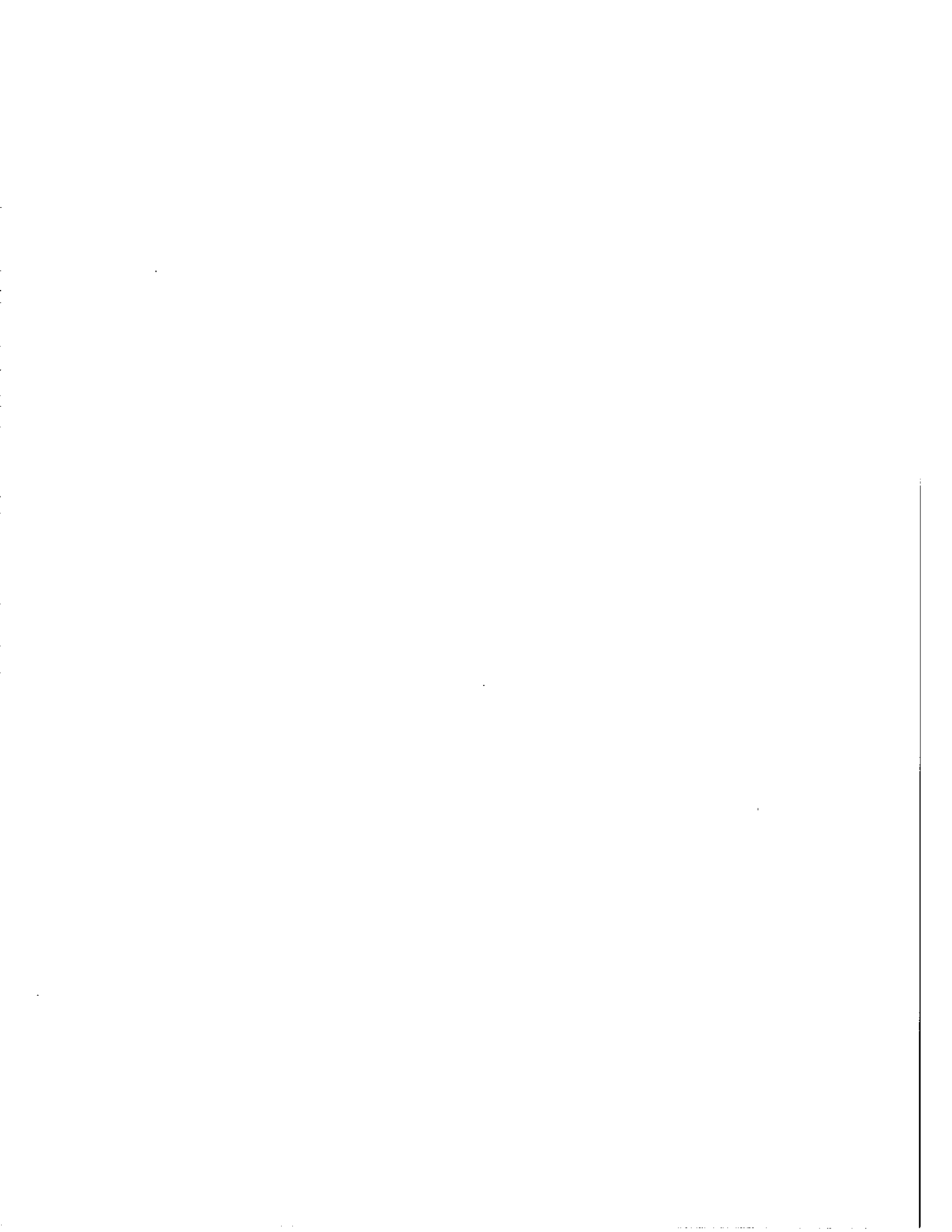




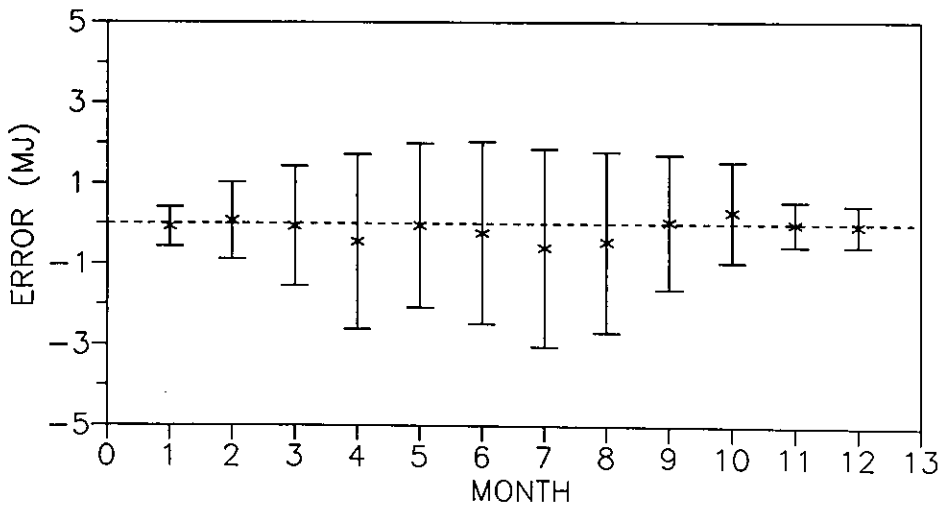
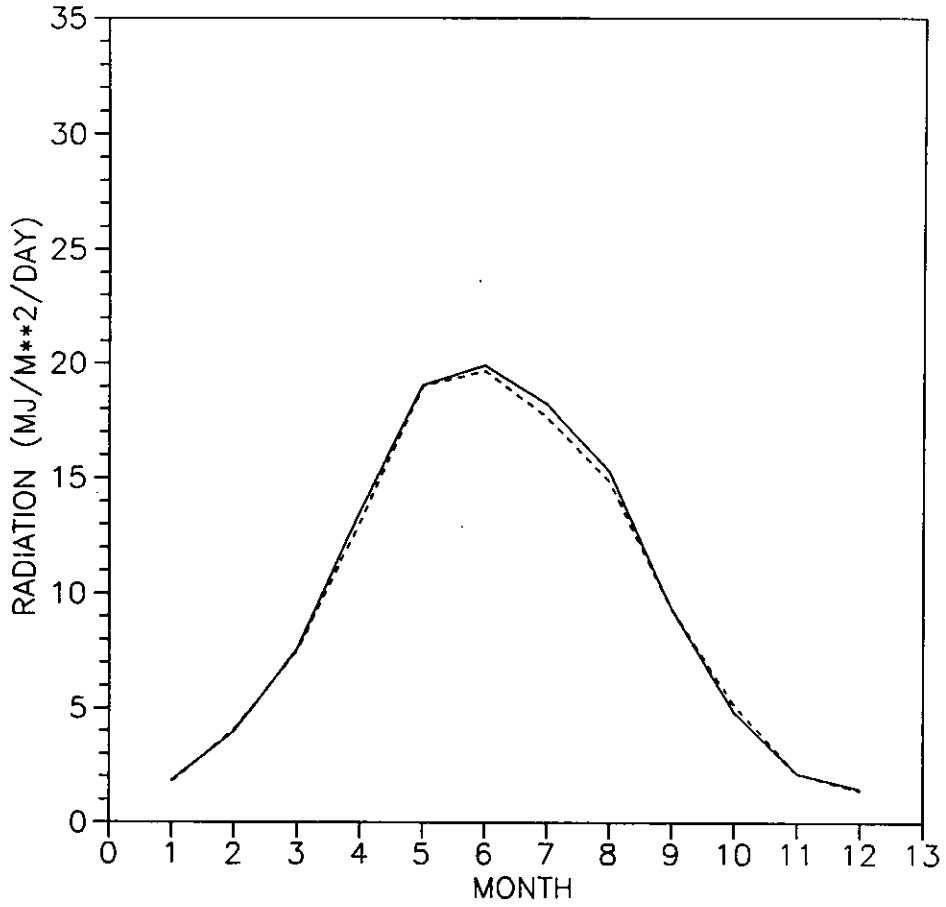
GLOBAL RADIATION: JOS MODEL

HAMBURG





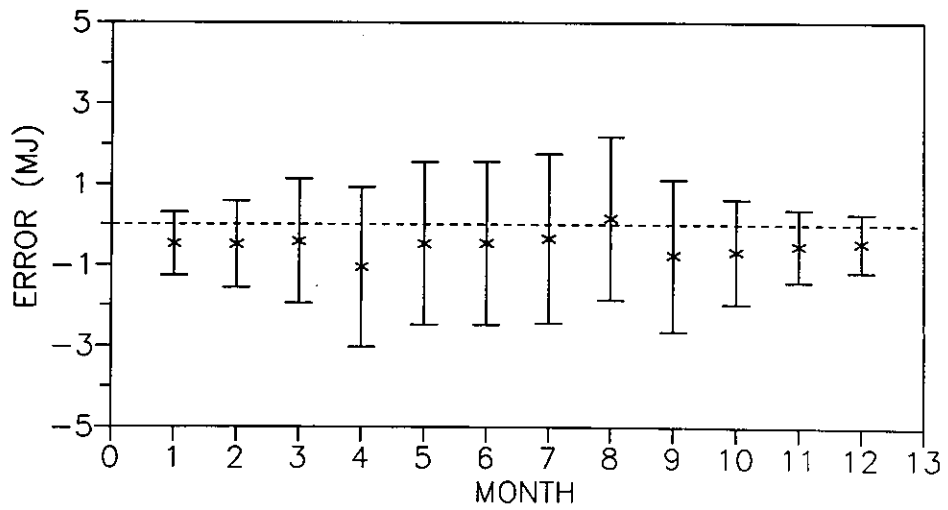
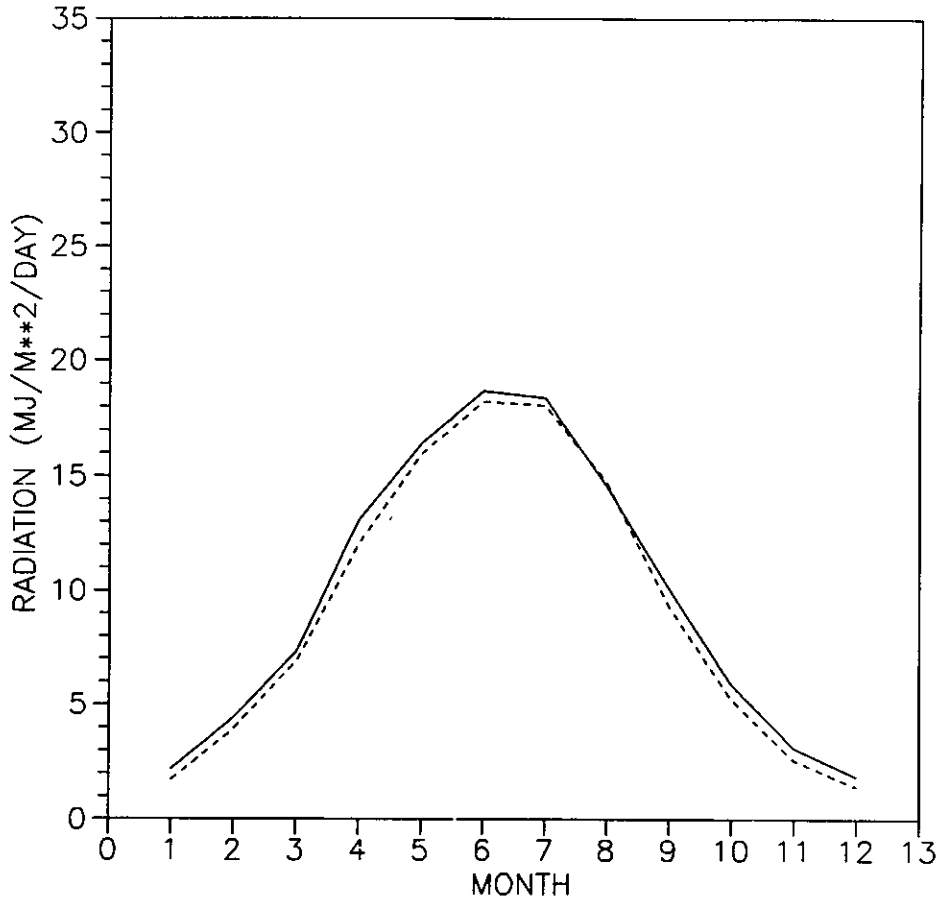
GLOBAL RADIATION: MAC MODEL  
HAMBURG





GLOBAL RADIATION: JOS MODEL

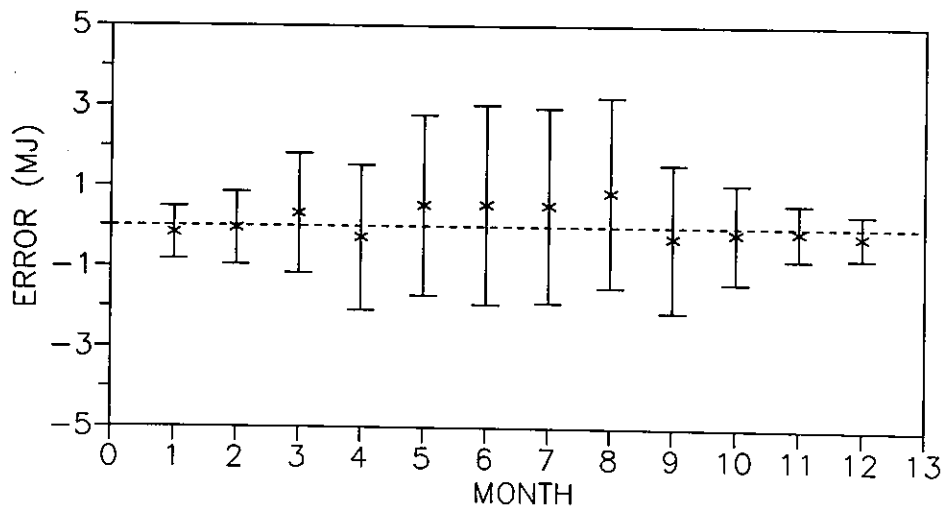
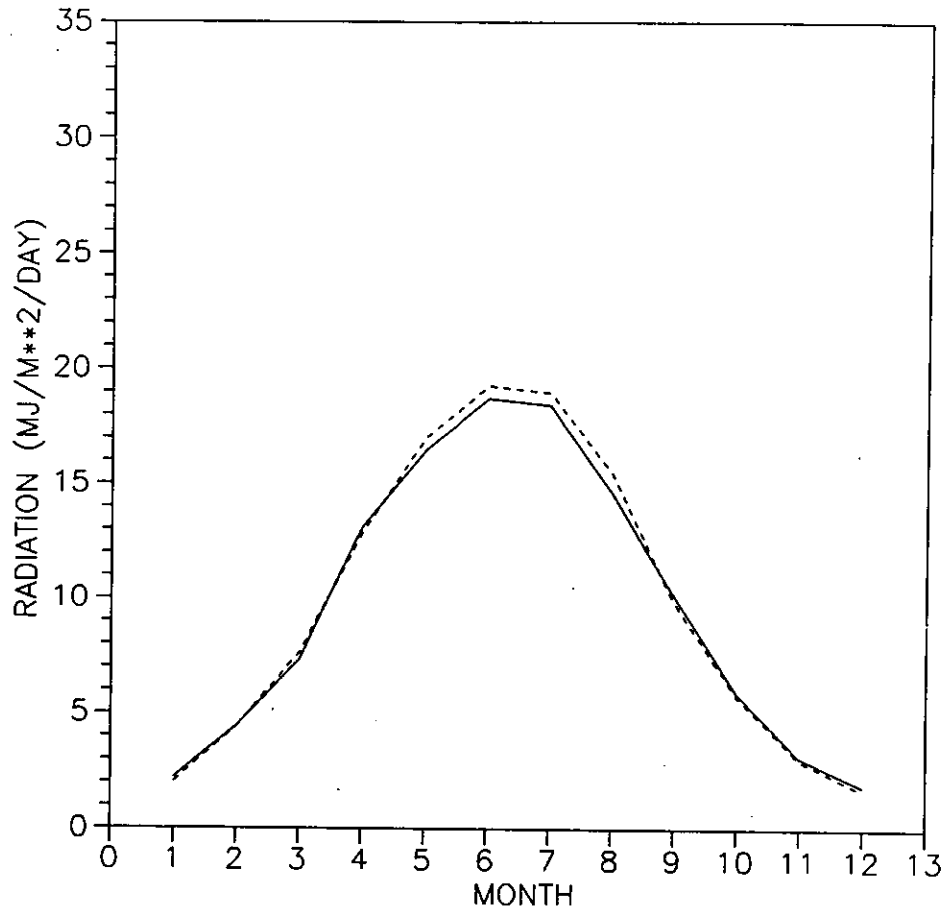
KEW





GLOBAL RADIATION: MAC MODEL

KEW

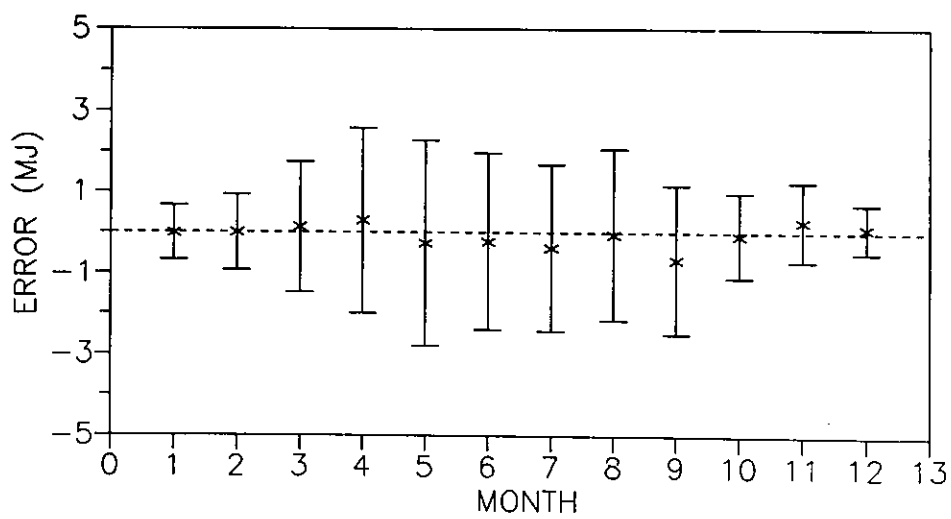
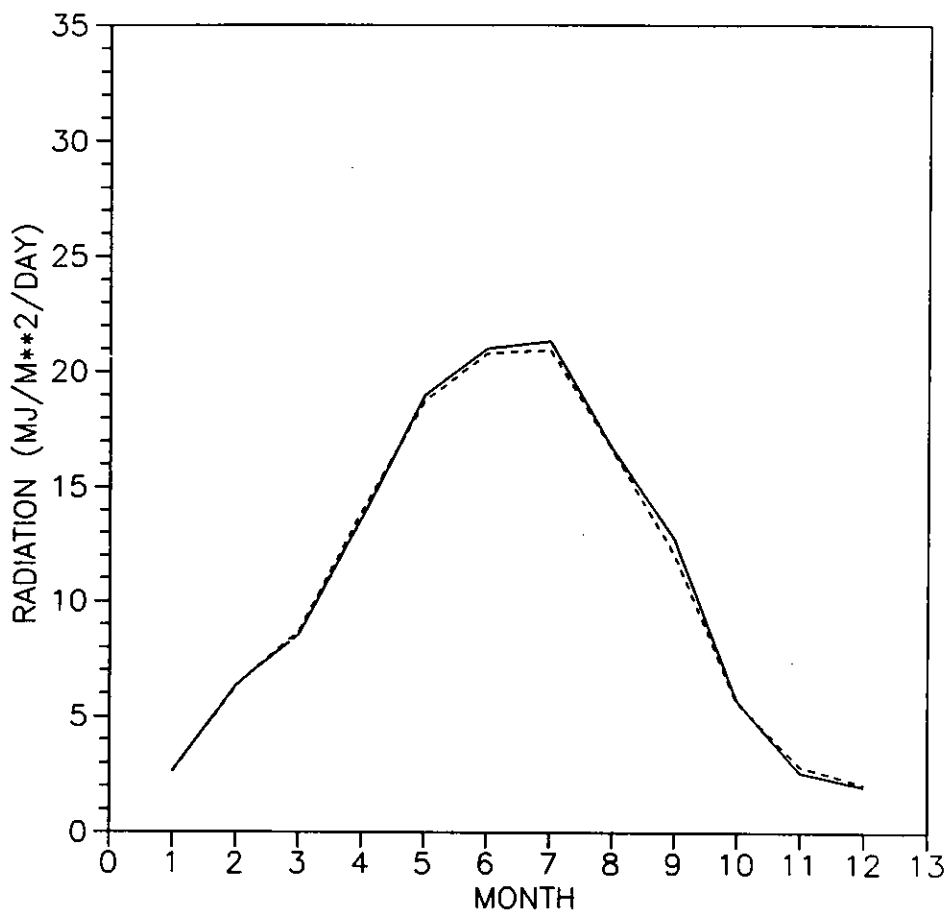


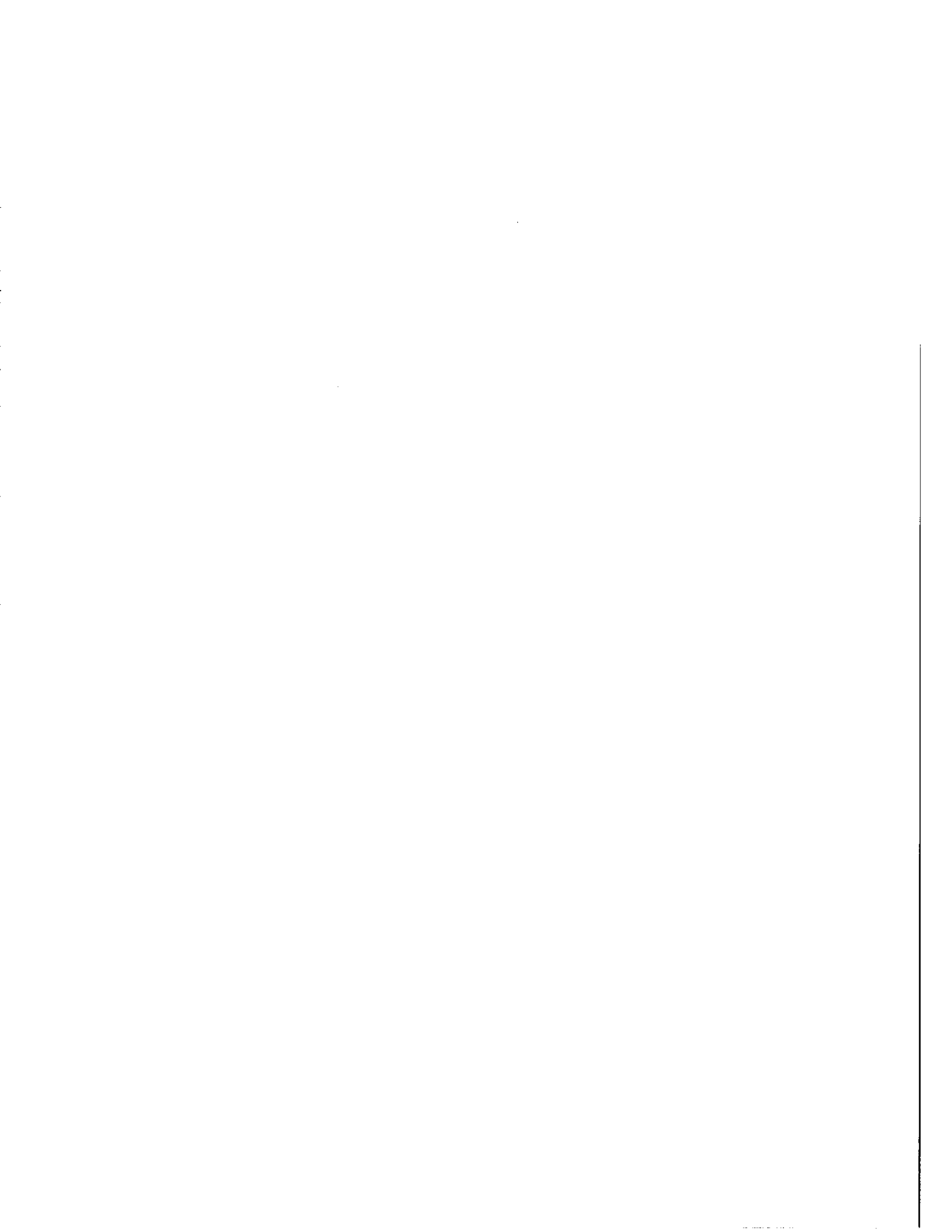




GLOBAL RADIATION: JOS MODEL

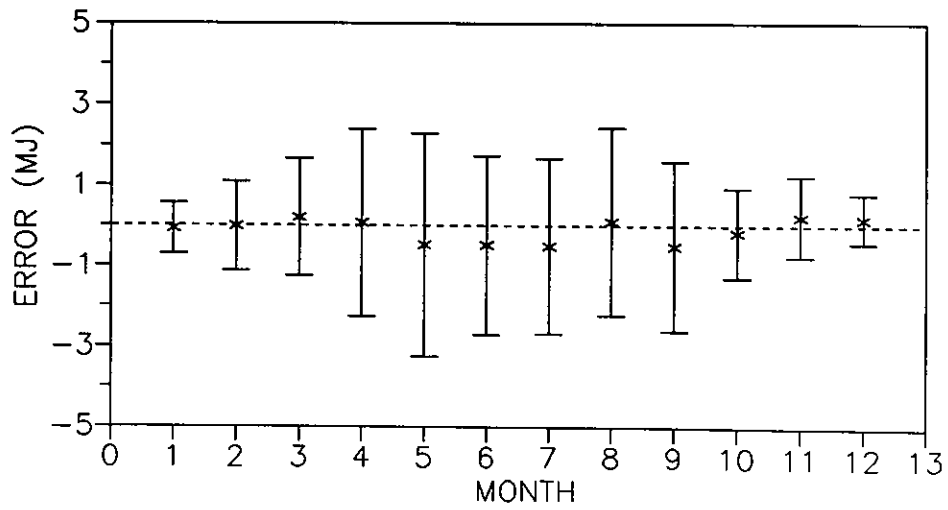
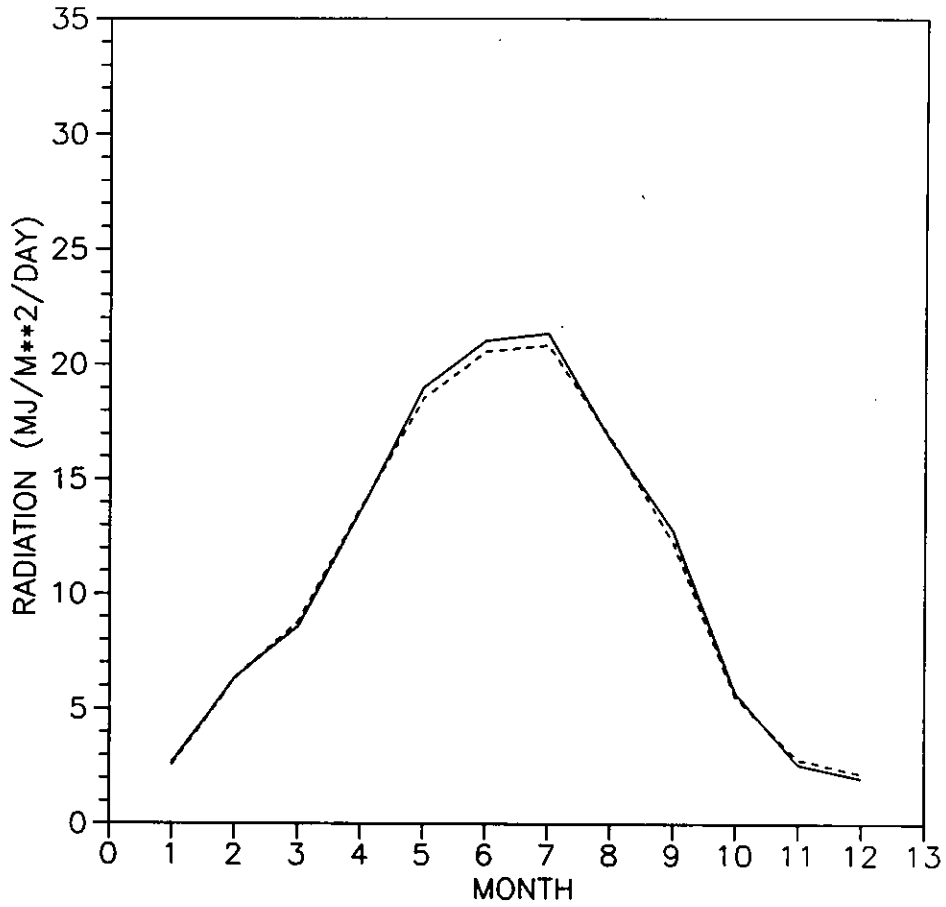
ZURICH





GLOBAL RADIATION: MAC MODEL

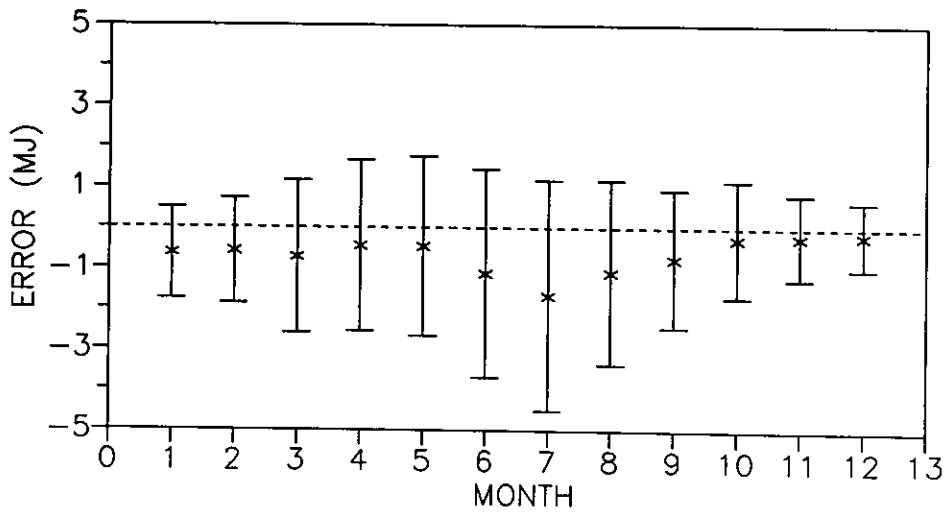
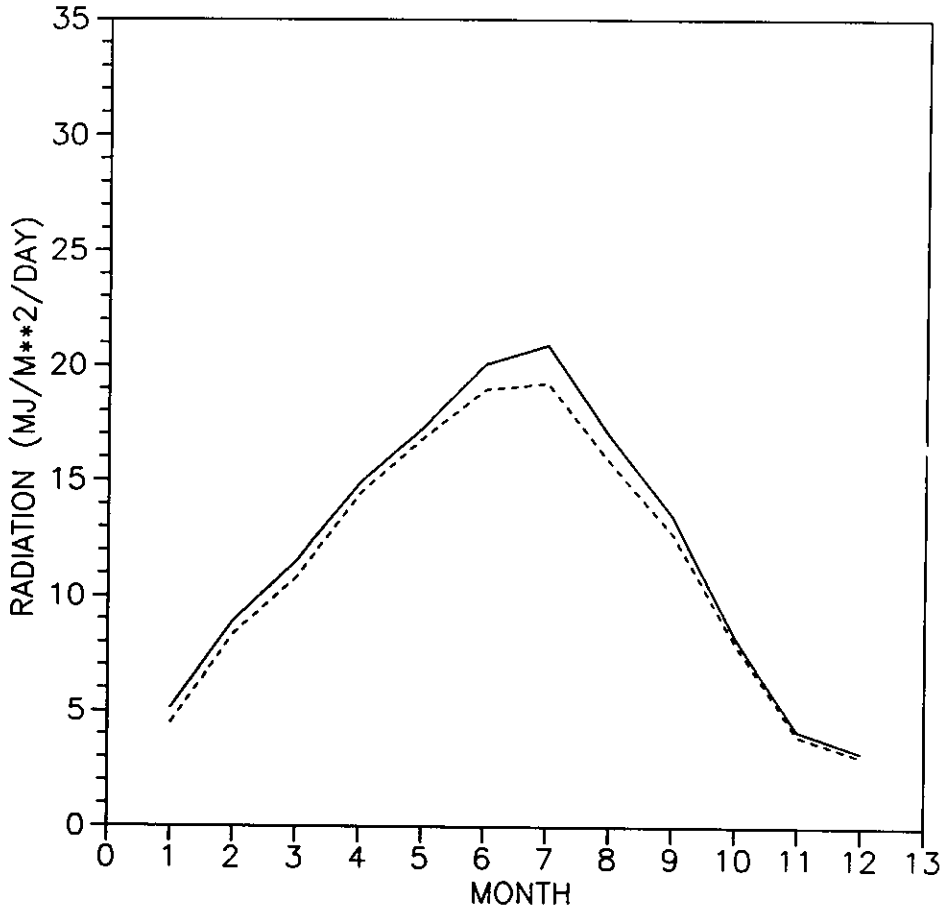
ZURICH





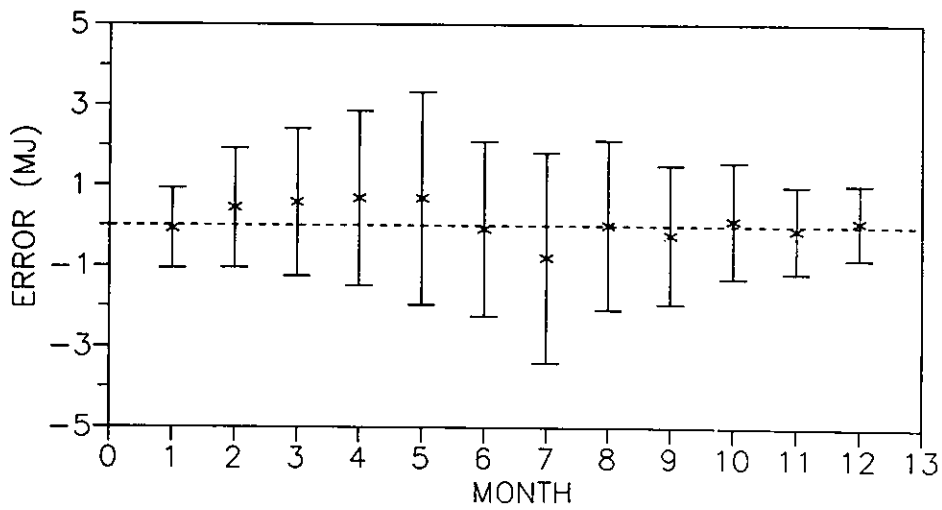
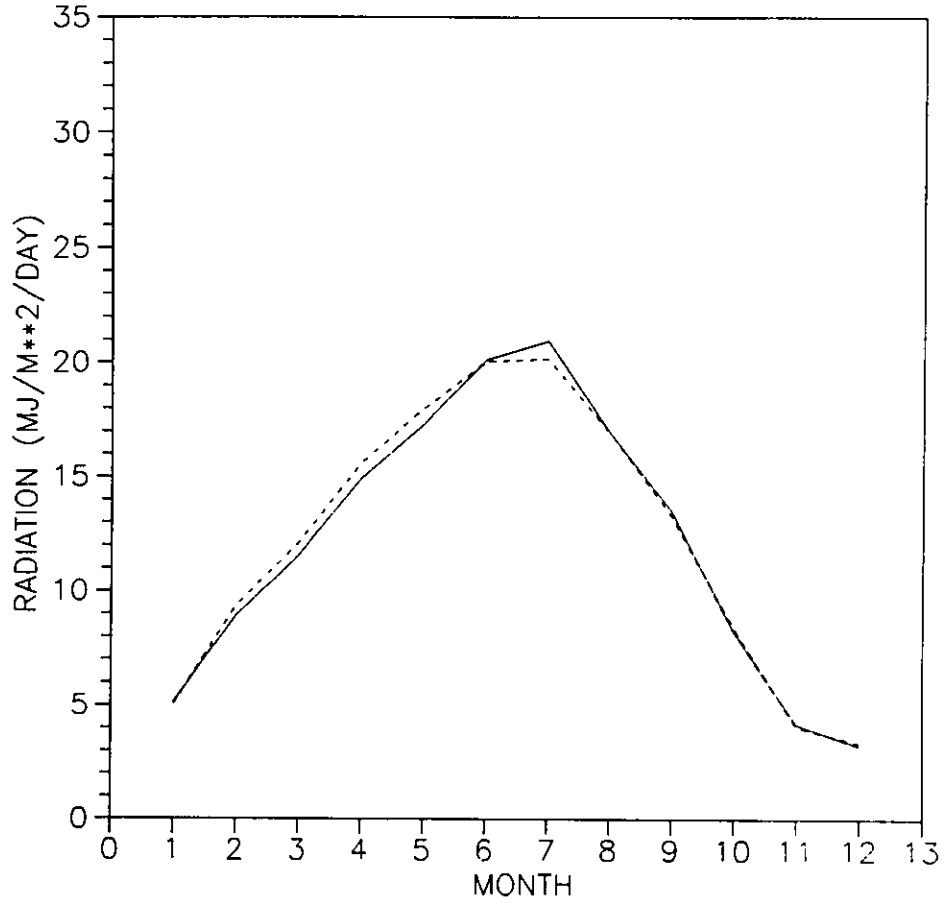
GLOBAL RADIATION: JOS MODEL

MONTREAL

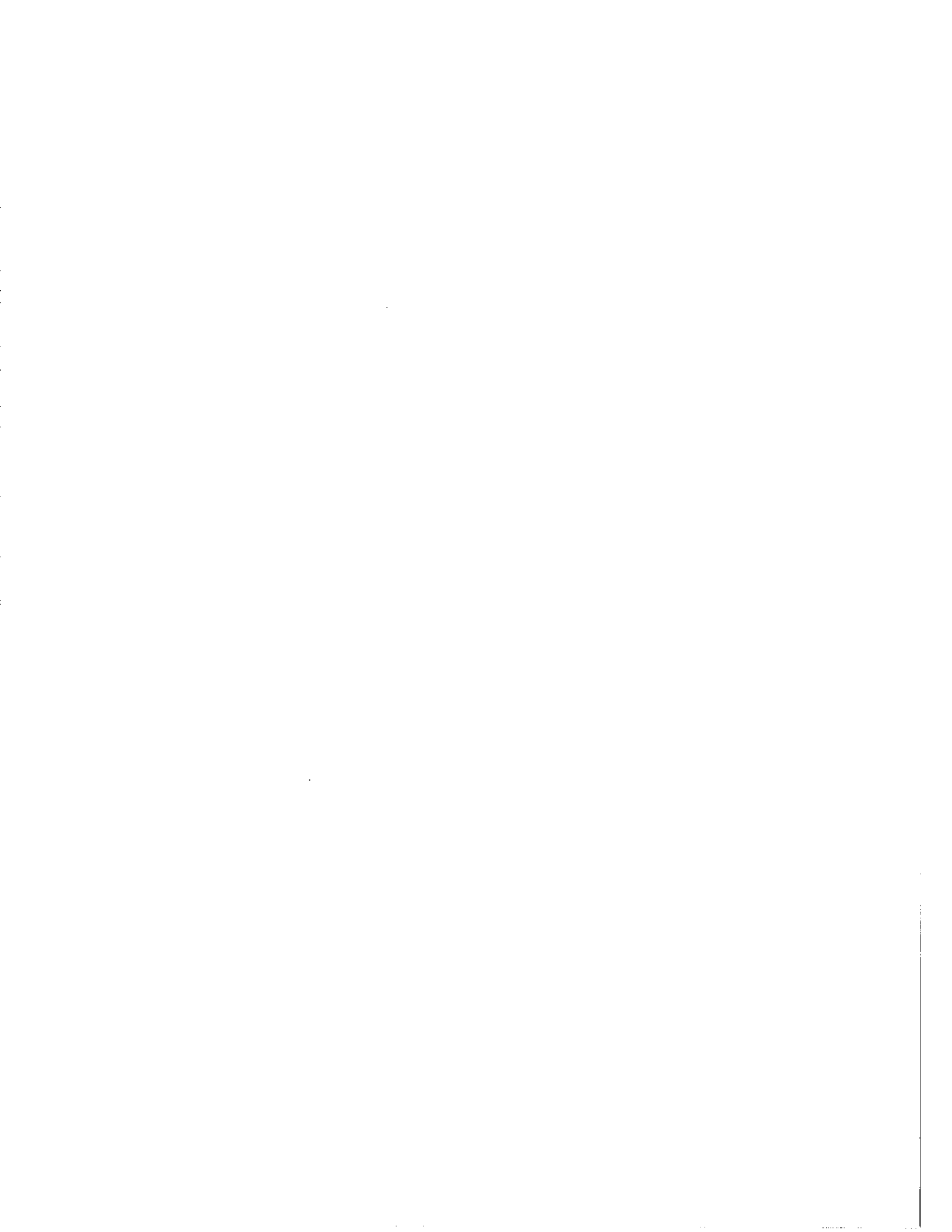




GLOBAL RADIATION: MAC MODEL  
MONTREAL

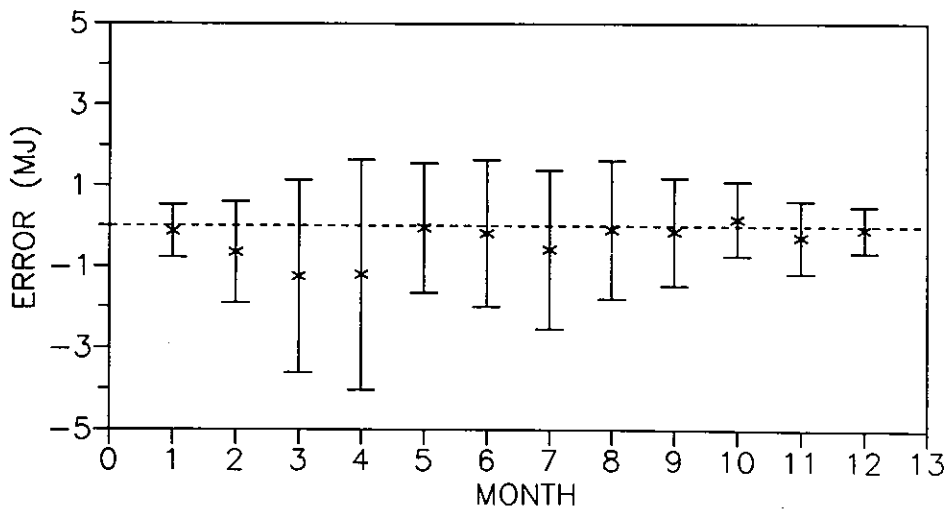
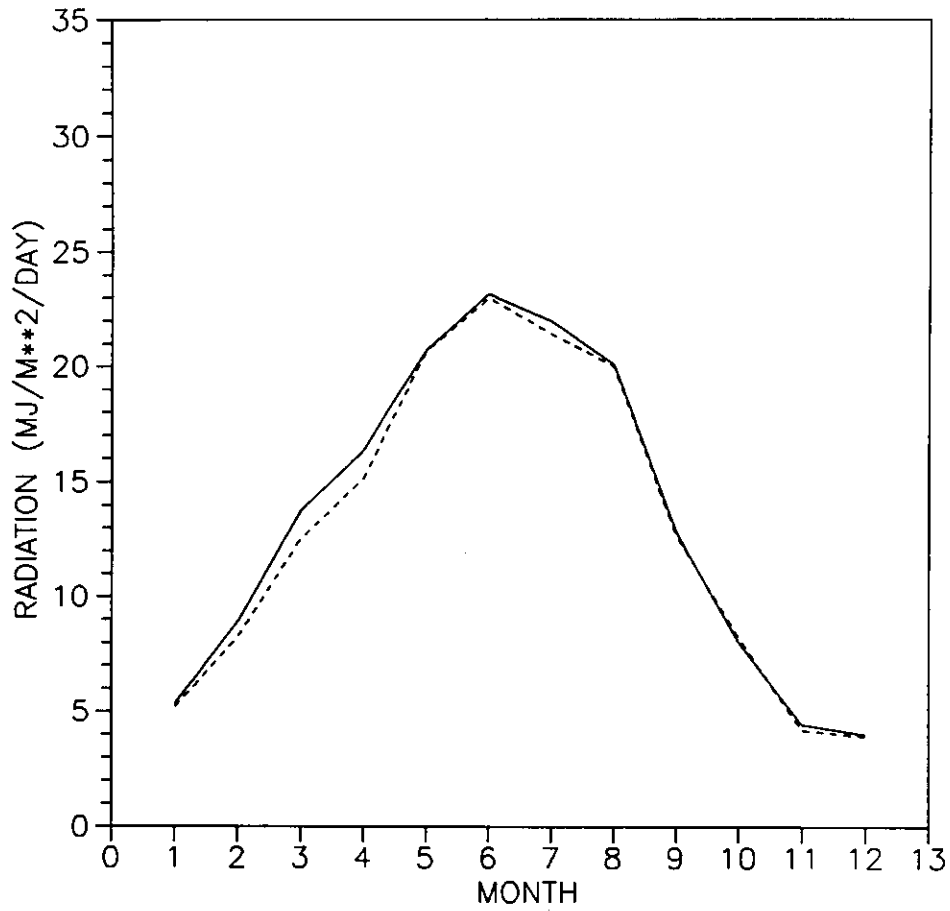


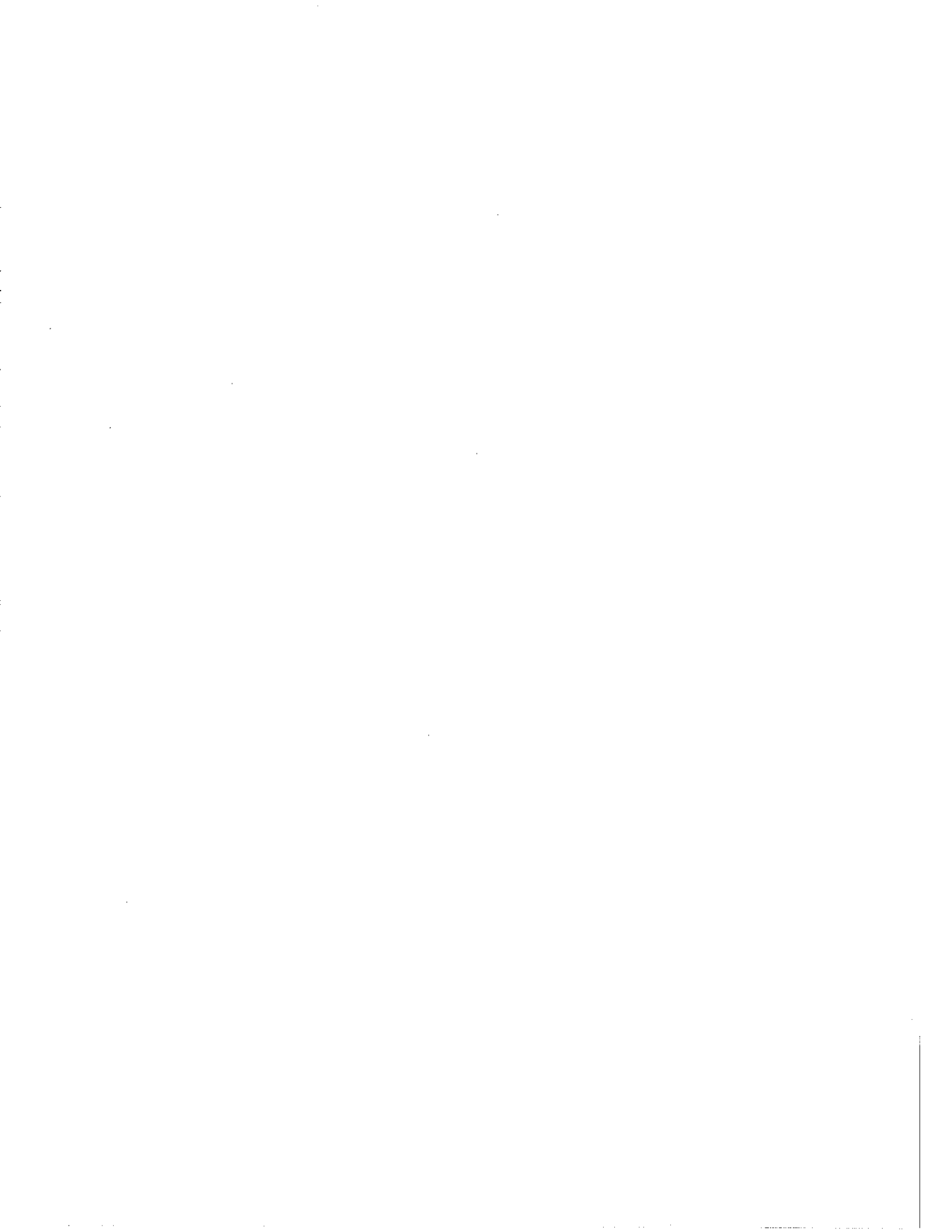




GLOBAL RADIATION: JOS MODEL

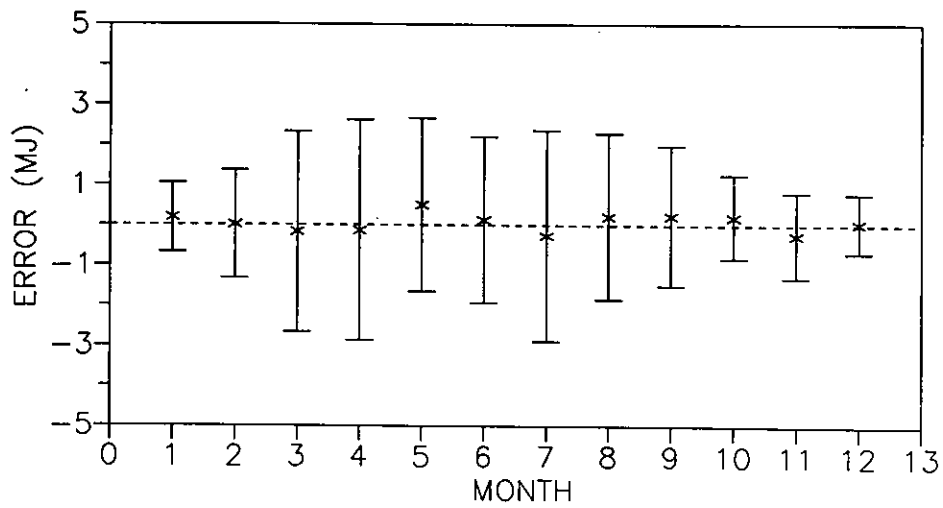
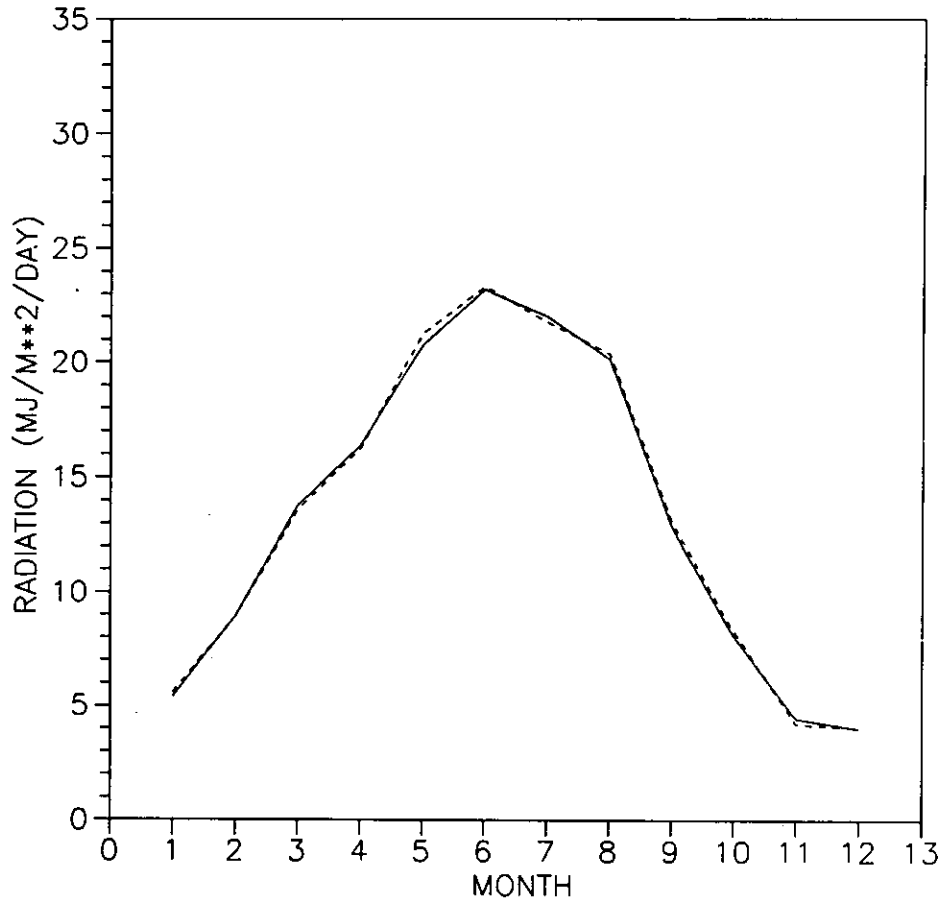
WINNIPEG





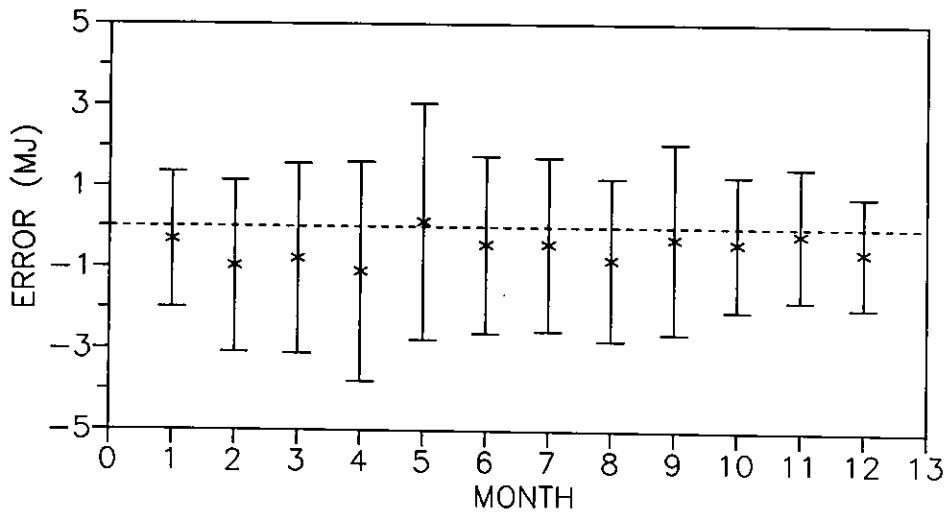
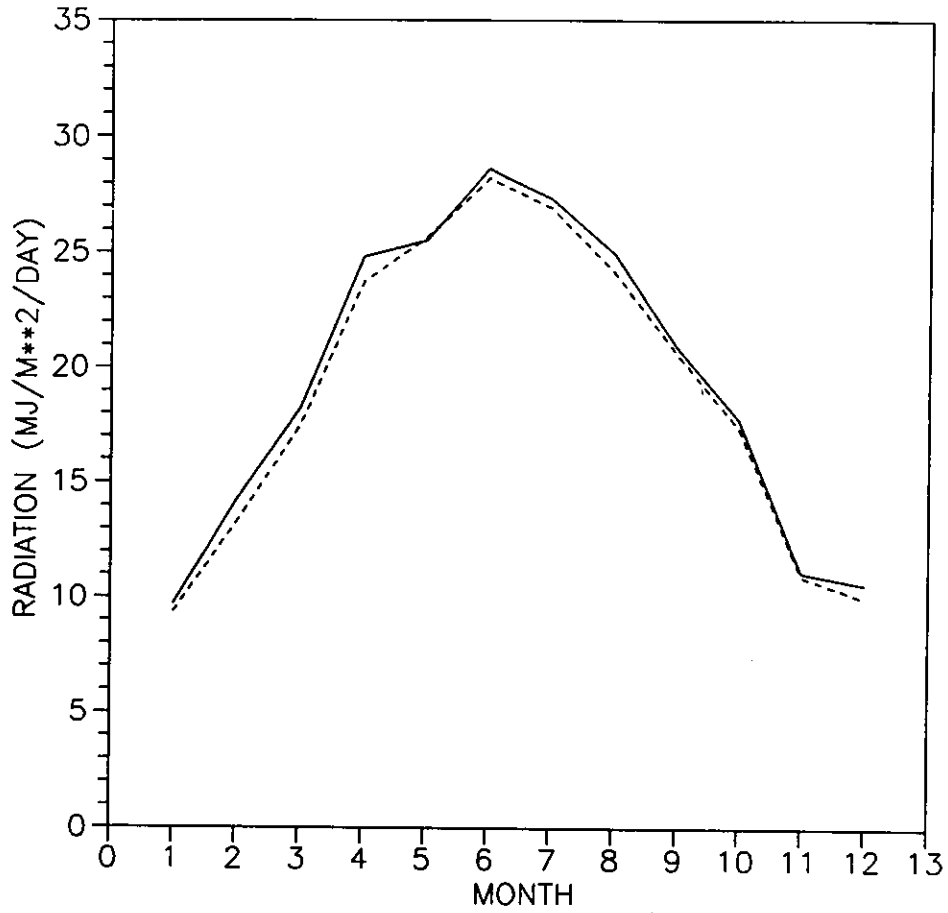
GLOBAL RADIATION: MAC MODEL

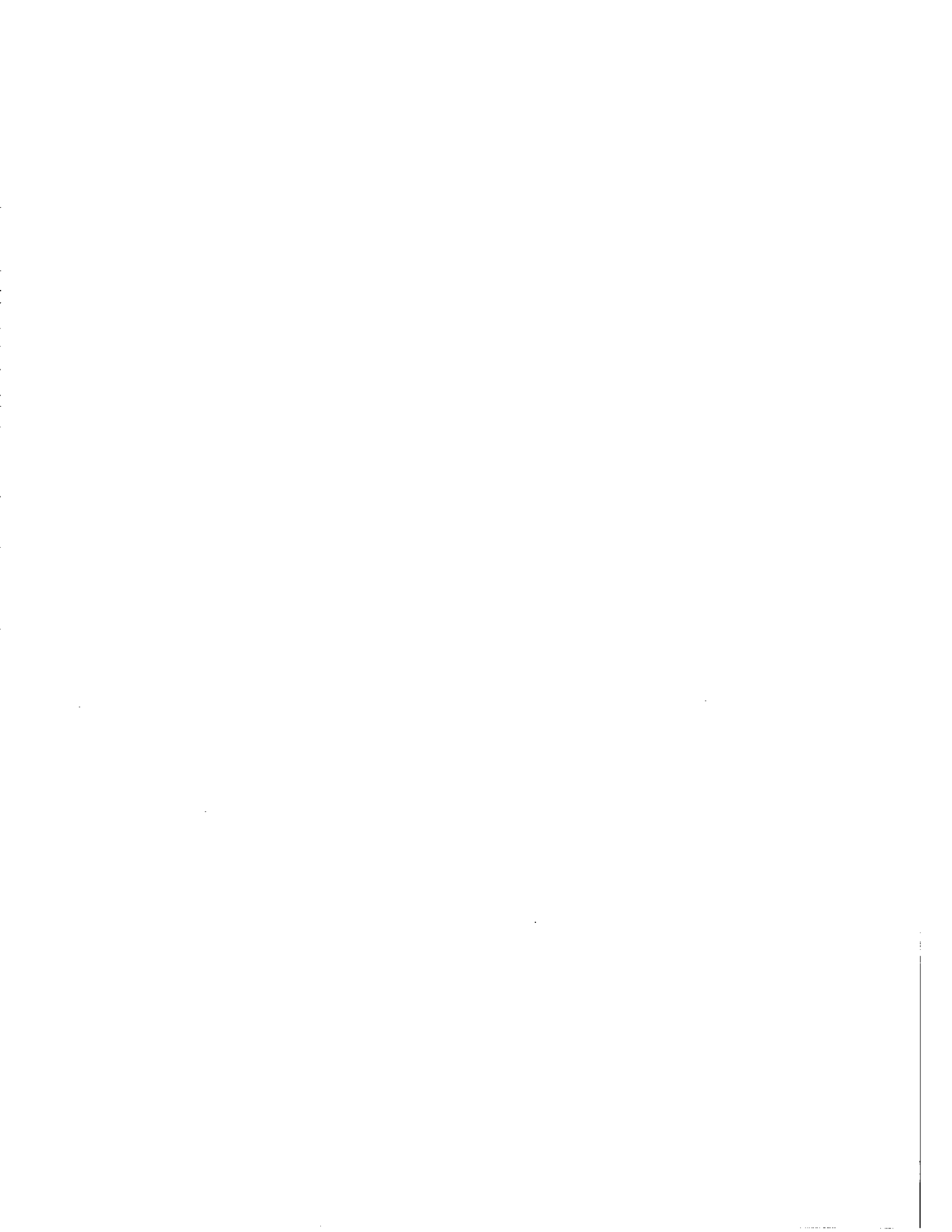
WINNIPEG



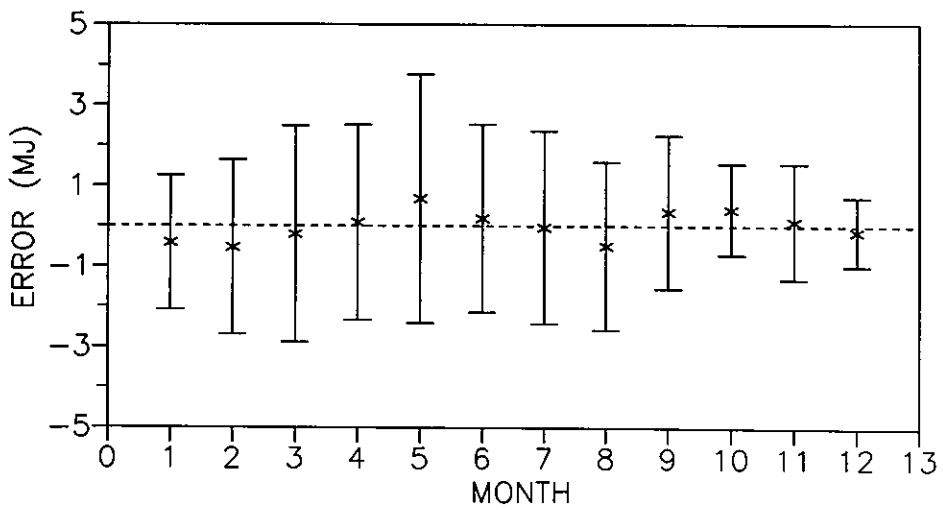
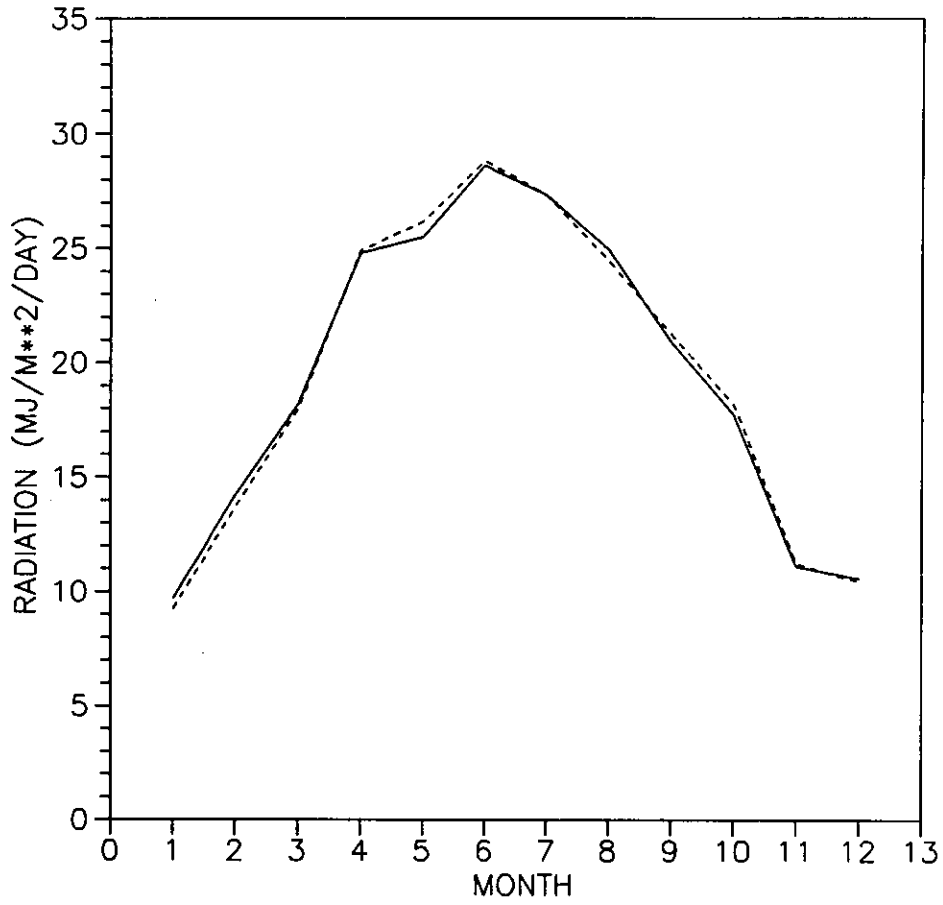


GLOBAL RADIATION: JOS MODEL  
ALBUQUERQUE

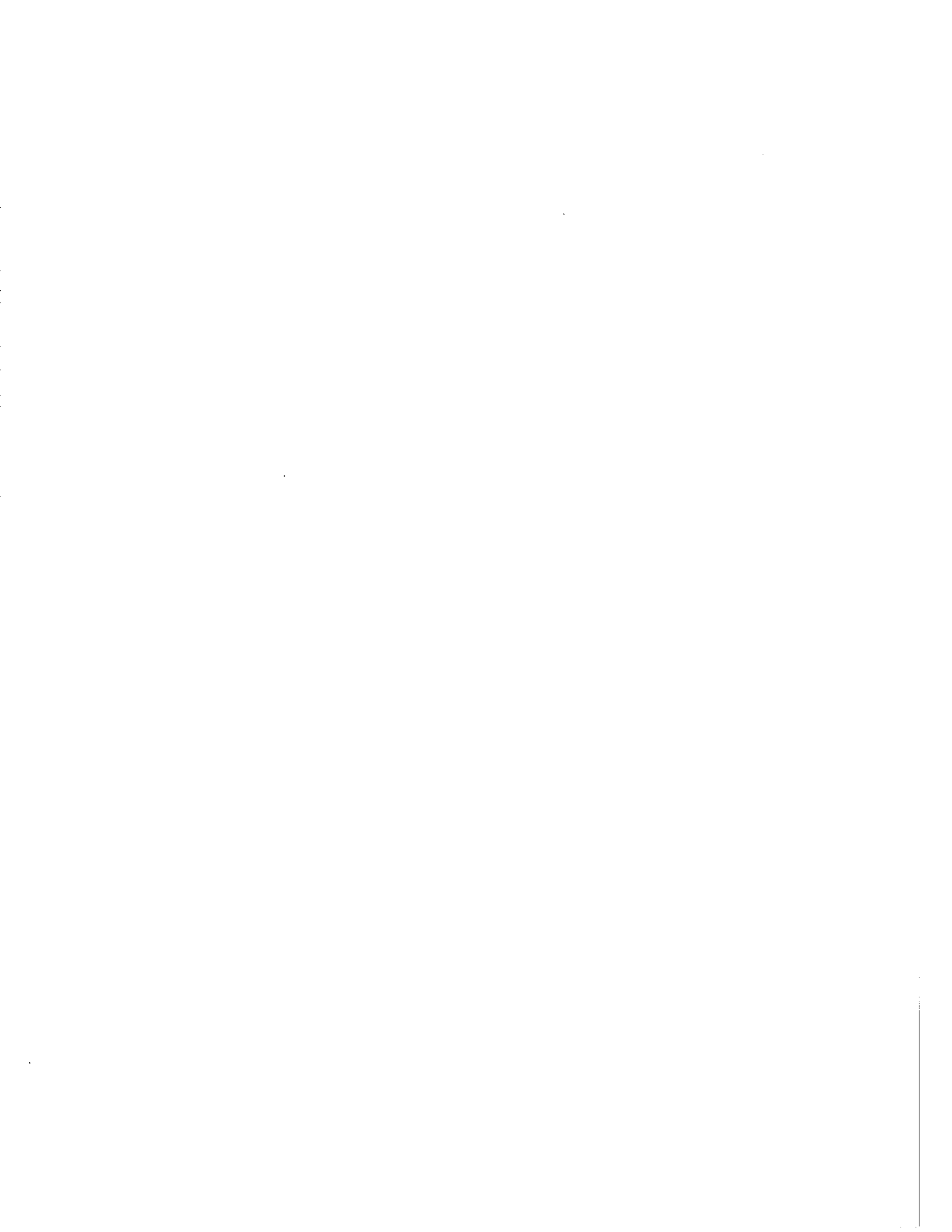




GLOBAL RADIATION: MAC MODEL  
ALBUQUERQUE

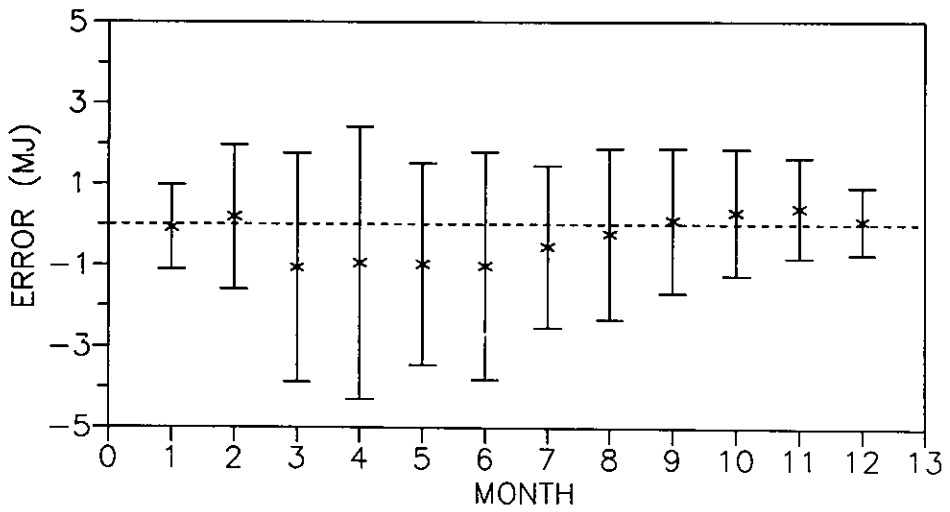
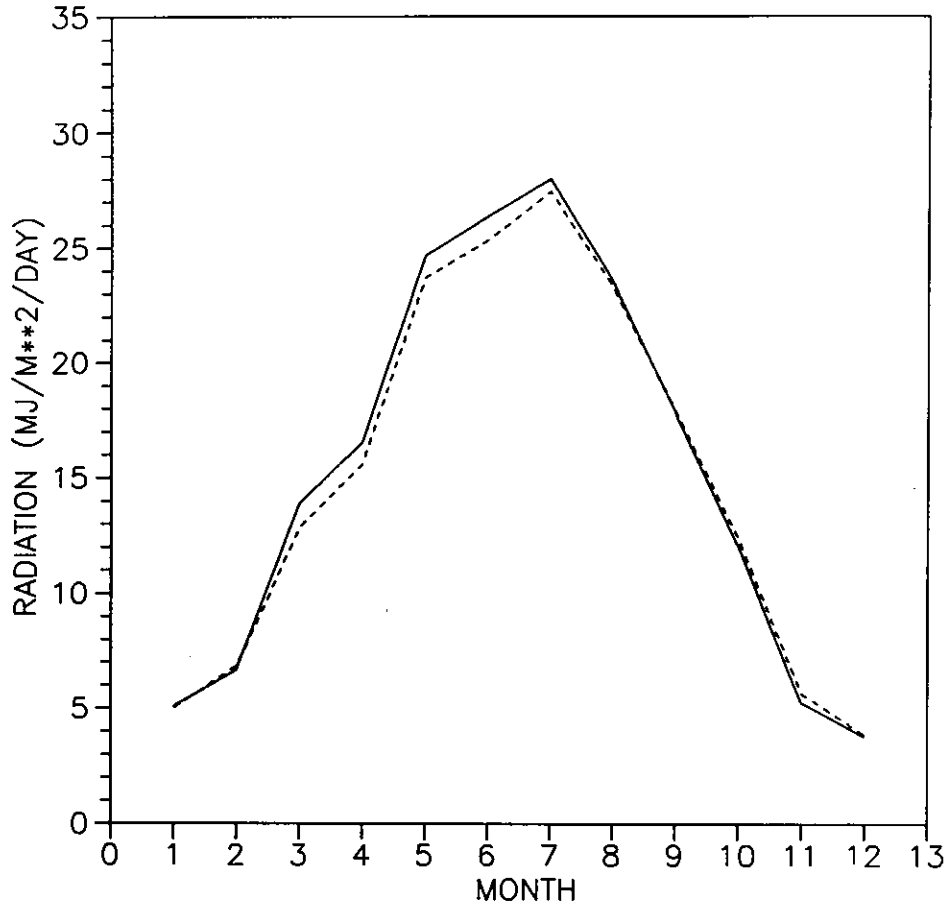






GLOBAL RADIATION: JOS MODEL

MEDFORD





GLOBAL RADIATION: MAC MODEL

MEDFORD

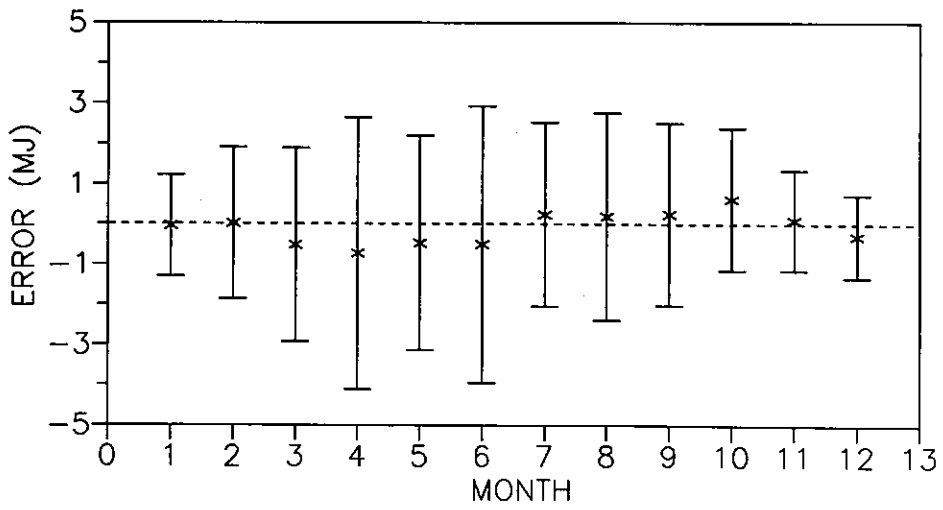
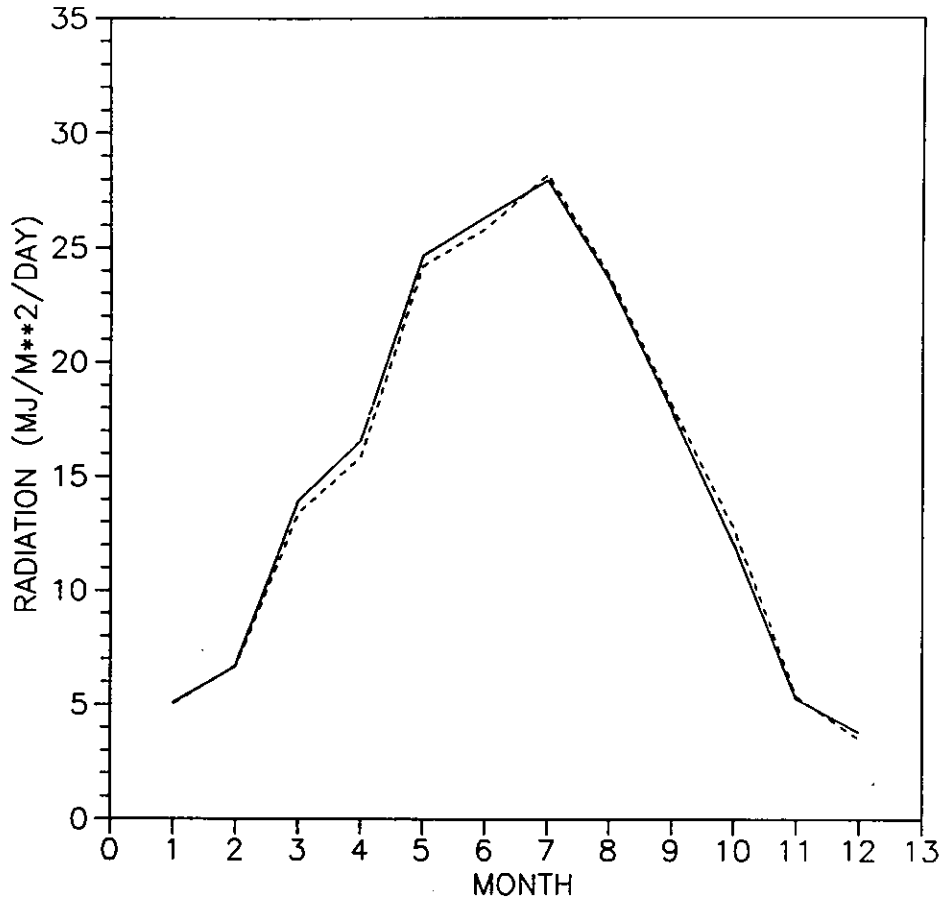


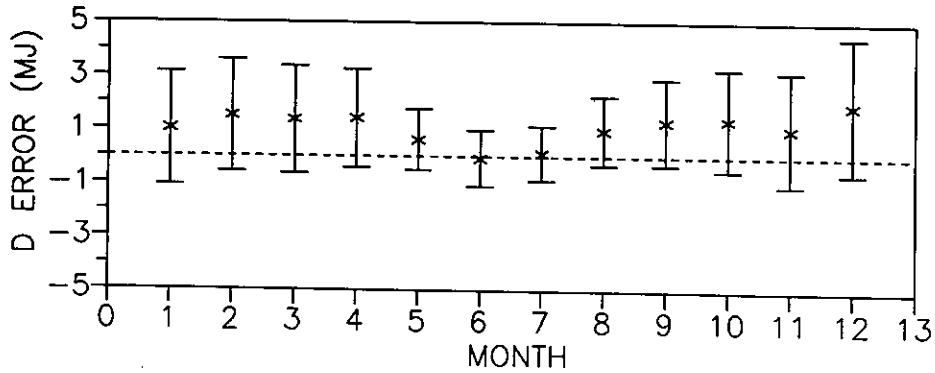
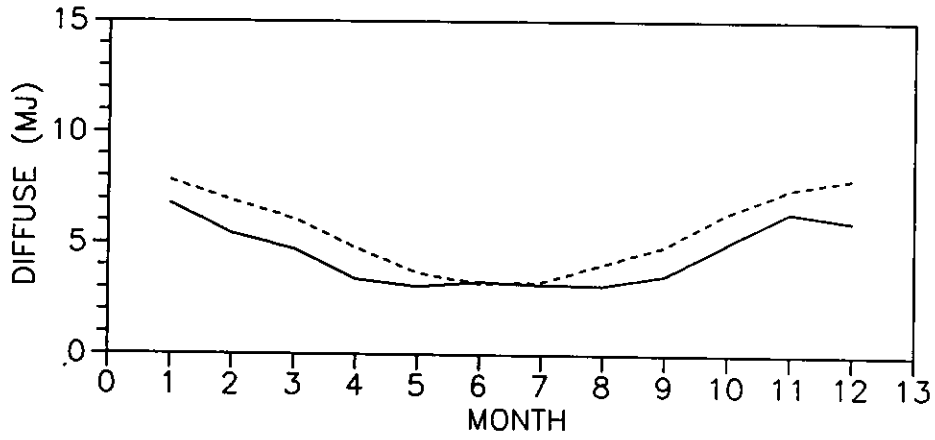
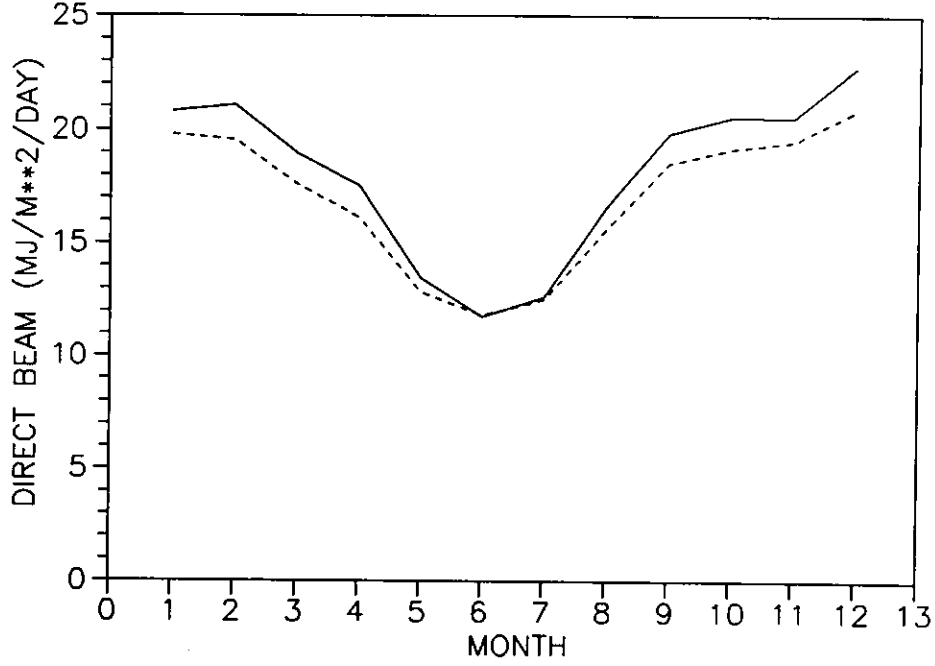


Figure 3b Monthly variation in measured radiation (solid line) and EKDD and EKDH model estimates (dashed line) for selected stations. MBE values are shown as crosses and RMSE values as vertical bars. There is no separate error diagram for direct beam radiation since MBE values differ from diffuse radiation MBE only in sign while RMSE values are the same as for diffuse.

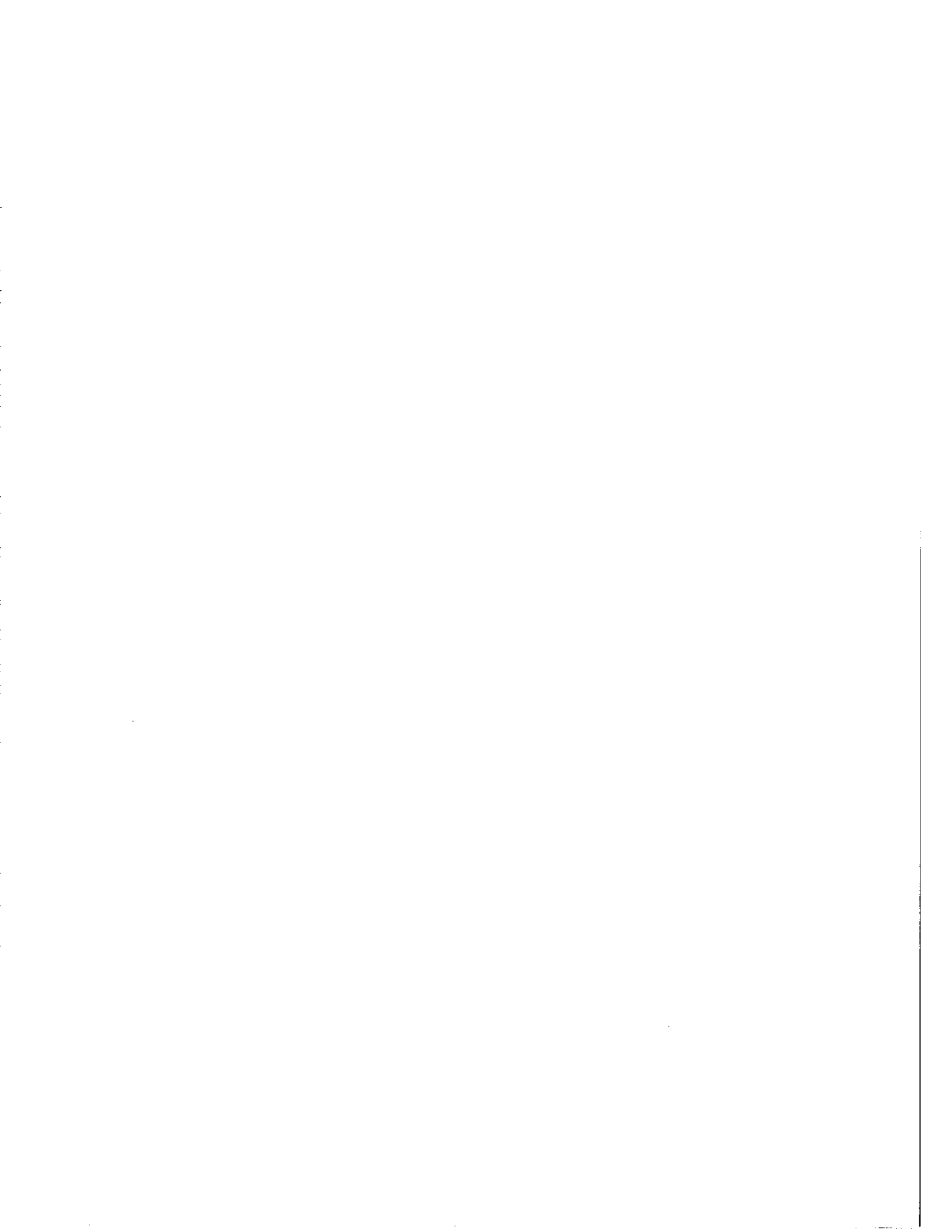


# DIFFUSE AND DIRECT BEAM RADIATION

EKDD MODEL: ALICE SPRINGS

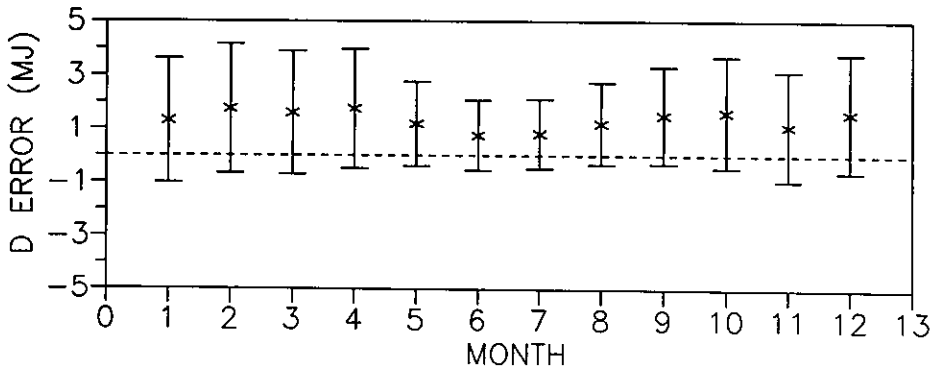
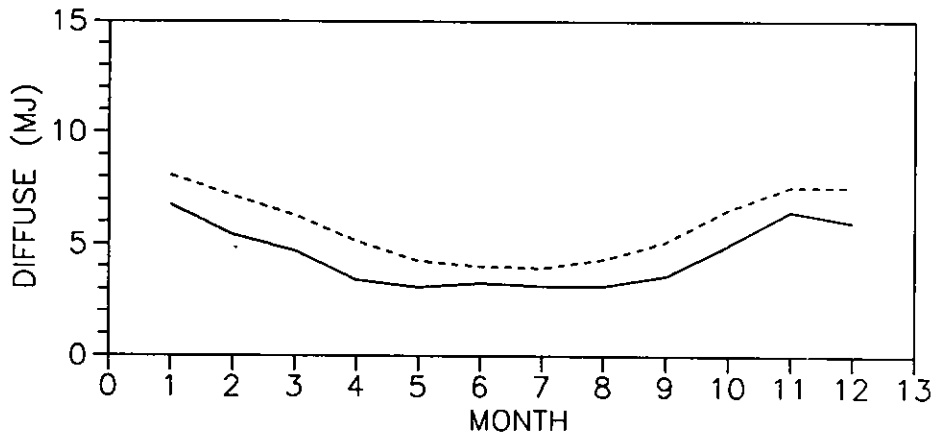
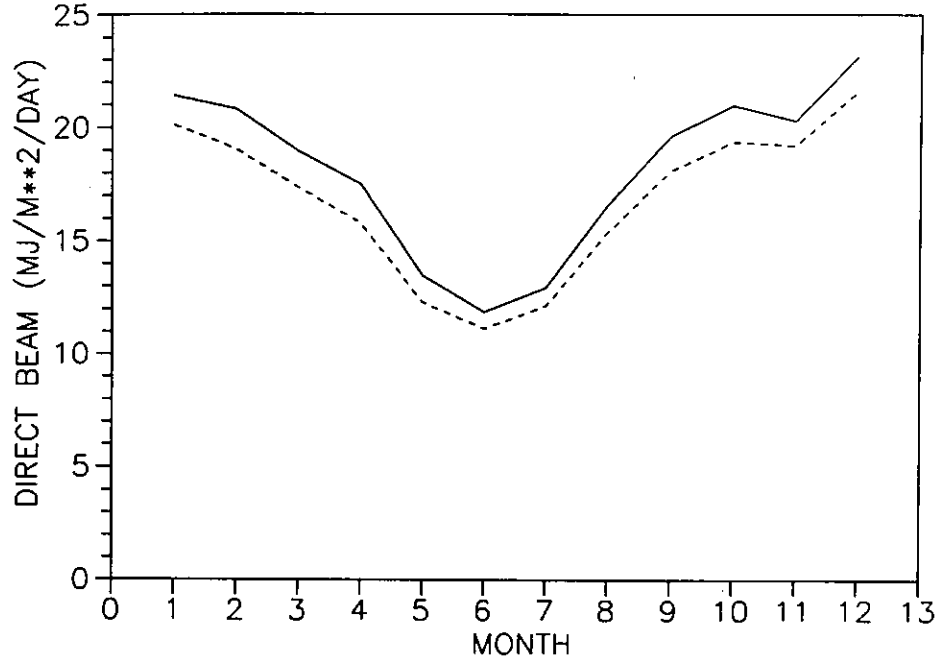






DIFFUSE AND DIRECT BEAM RADIATION

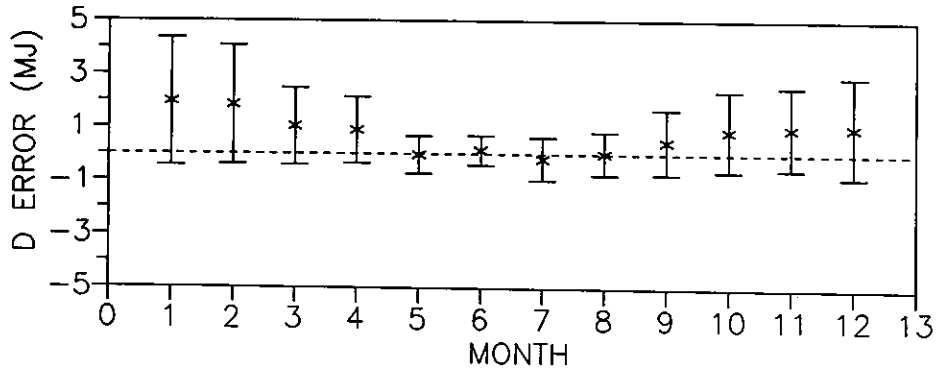
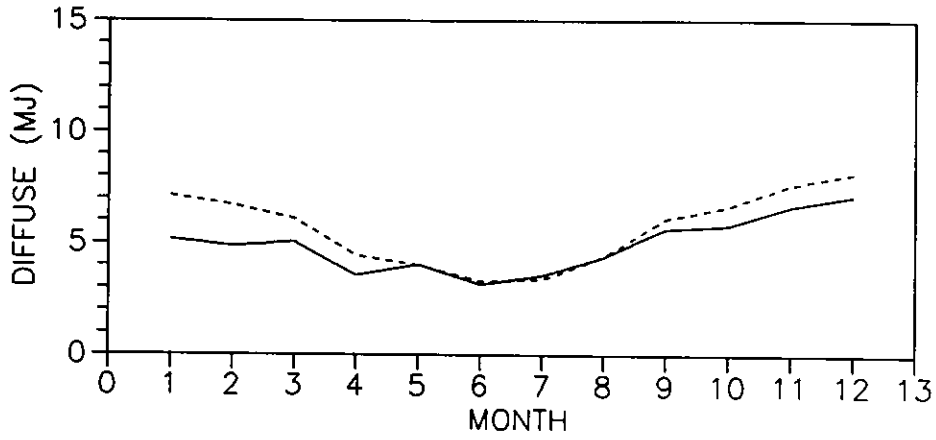
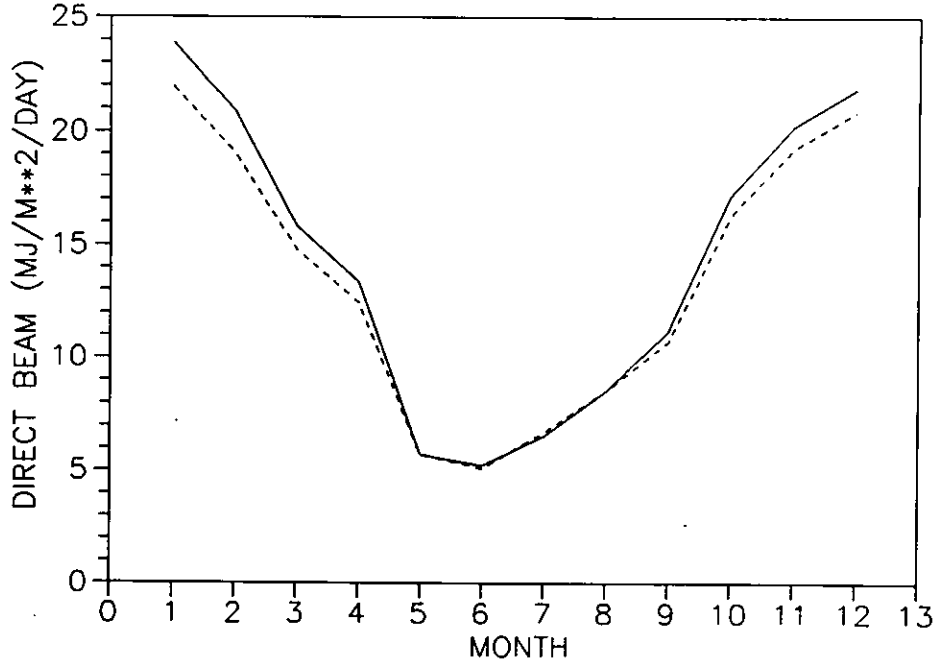
EKDH MODEL: ALICE SPRINGS





DIFFUSE AND DIRECT BEAM RADIATION

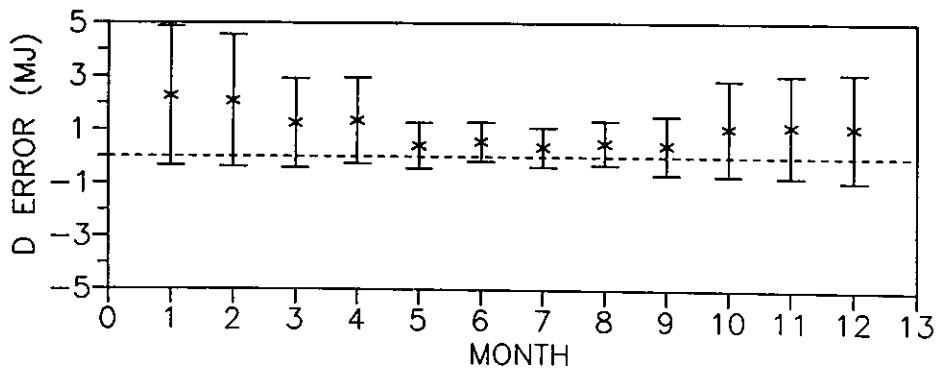
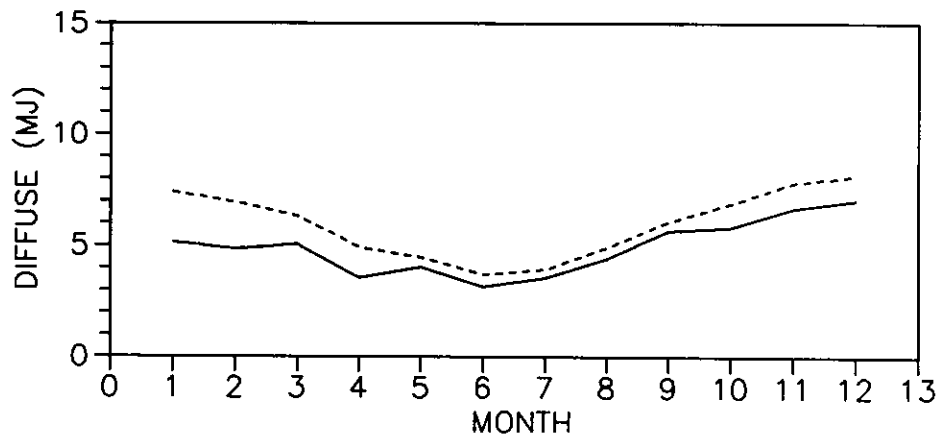
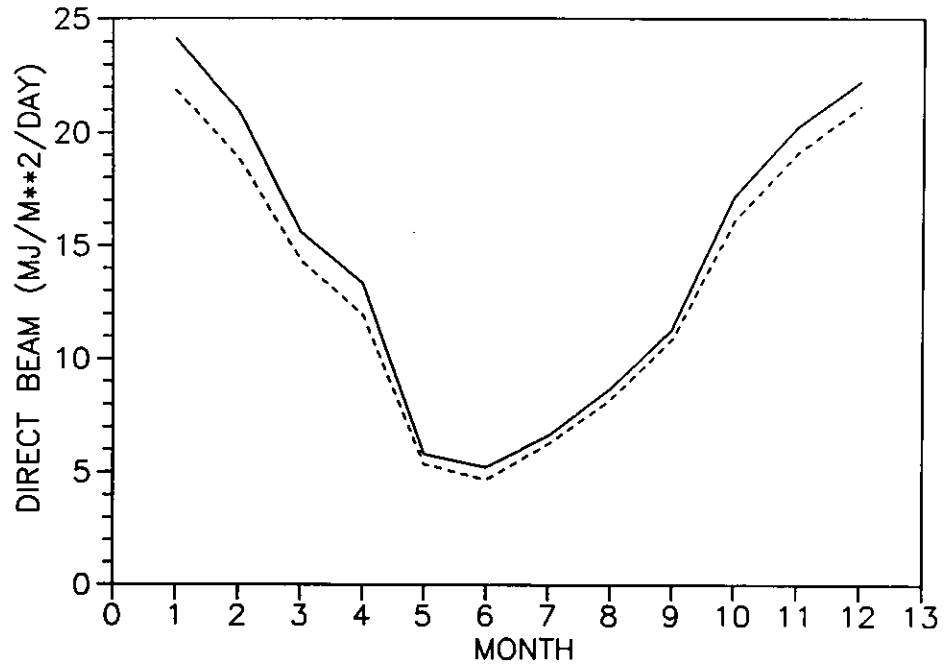
EKDD MODEL: MILDURA

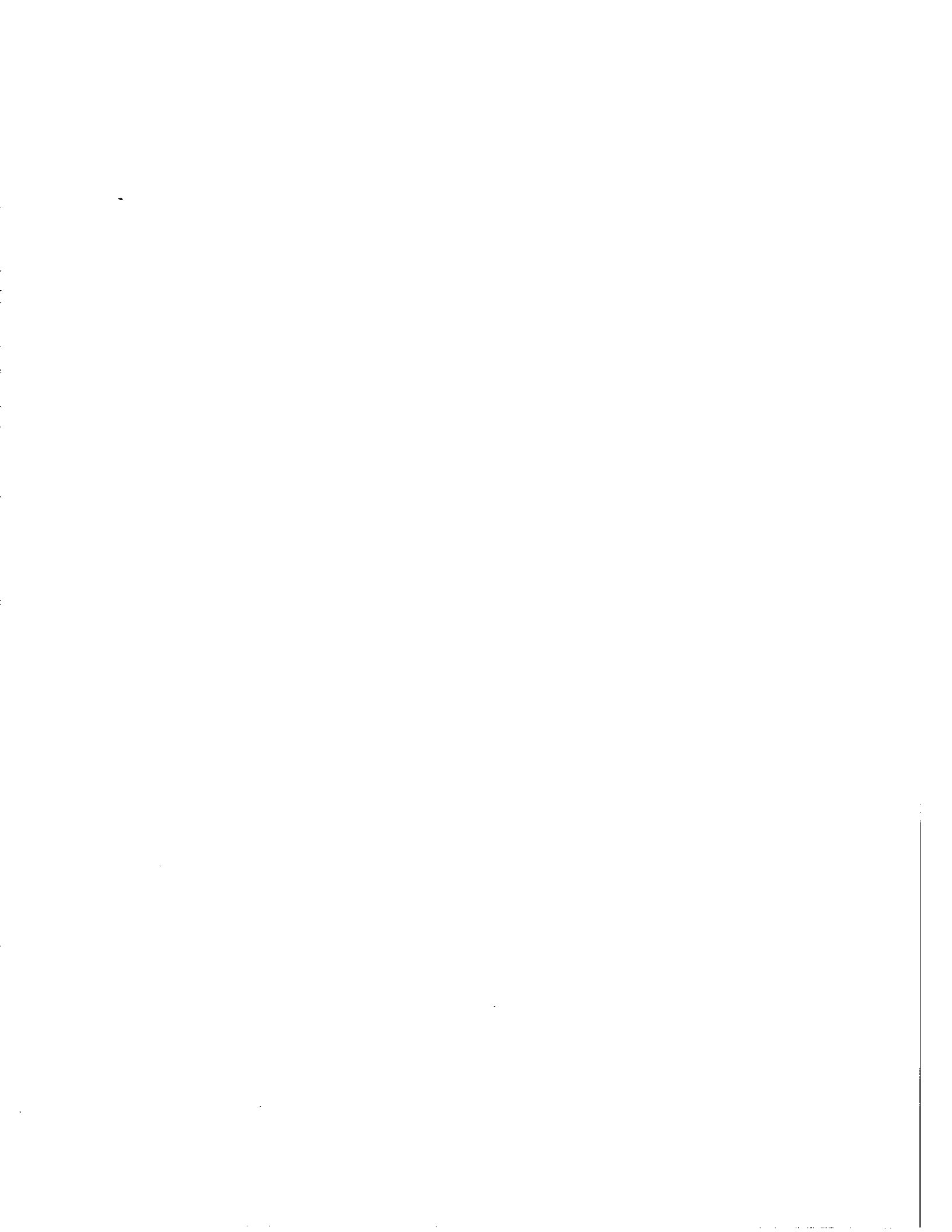




# DIFFUSE AND DIRECT BEAM RADIATION

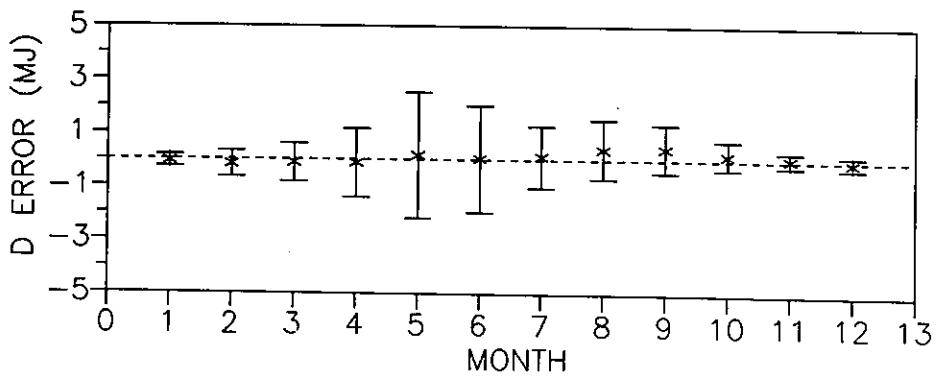
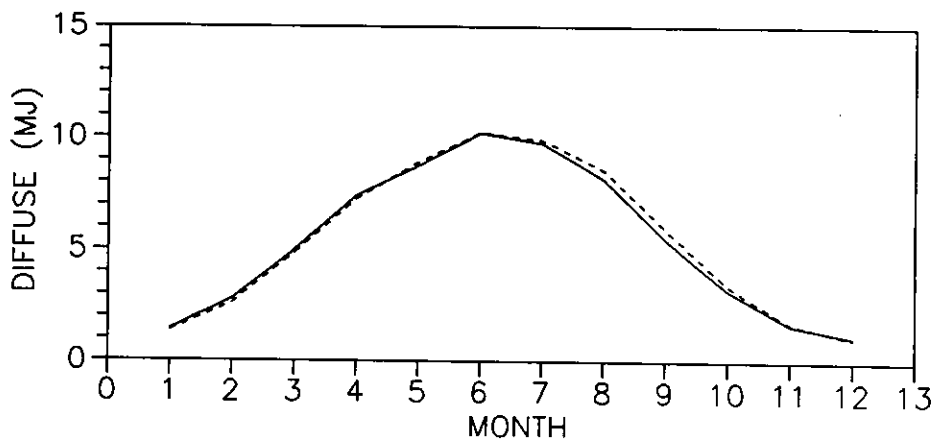
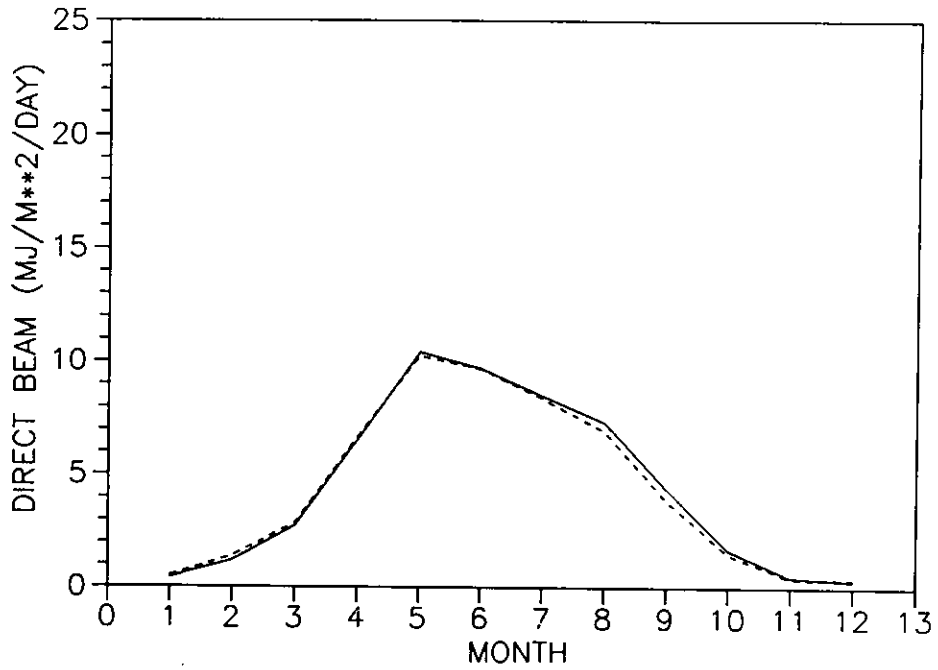
EKDH MODEL: MILDURA



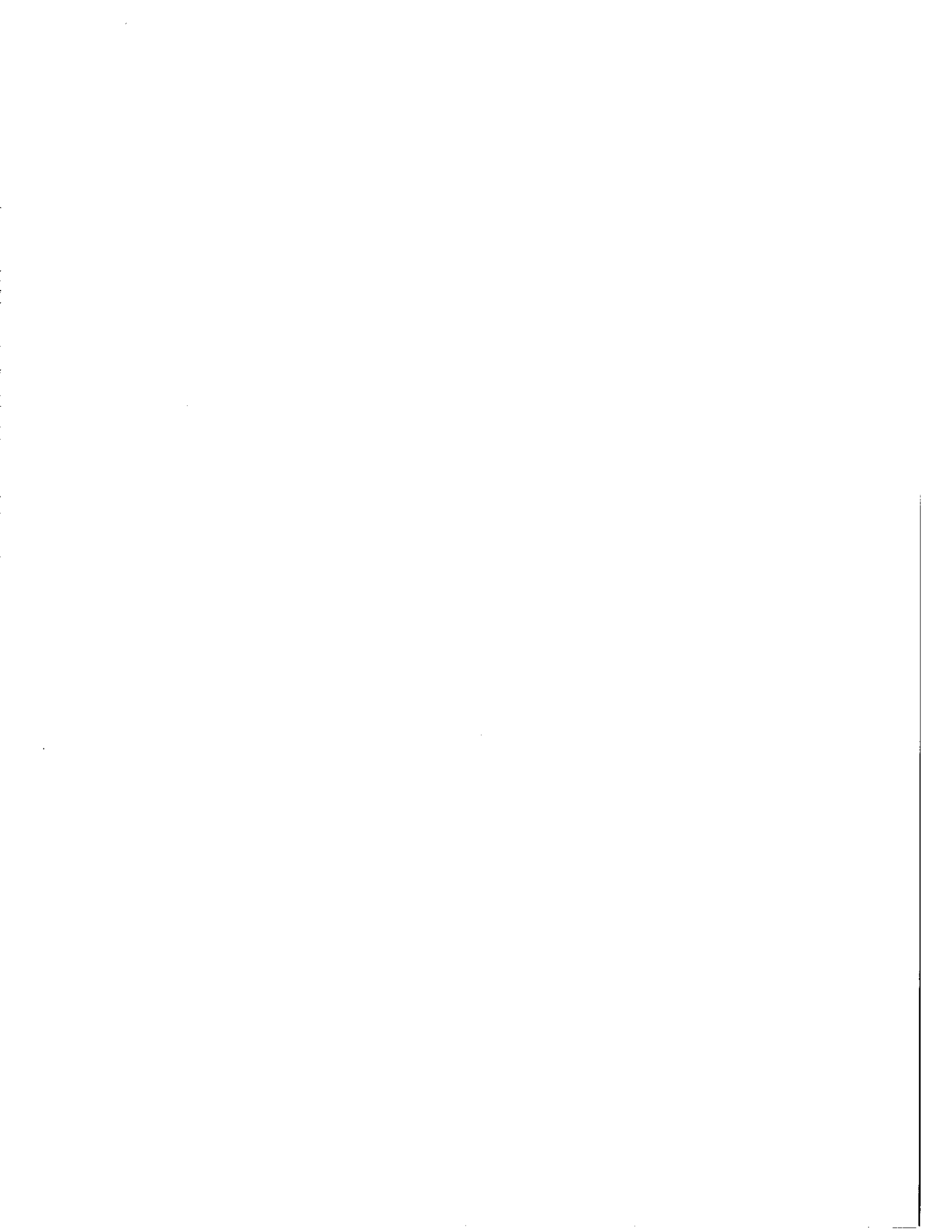


DIFFUSE AND DIRECT BEAM RADIATION

EKDD MODEL: HAMBURG

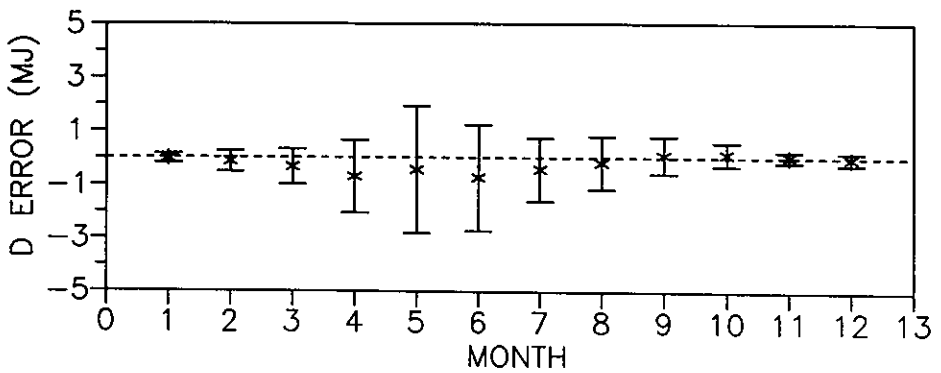
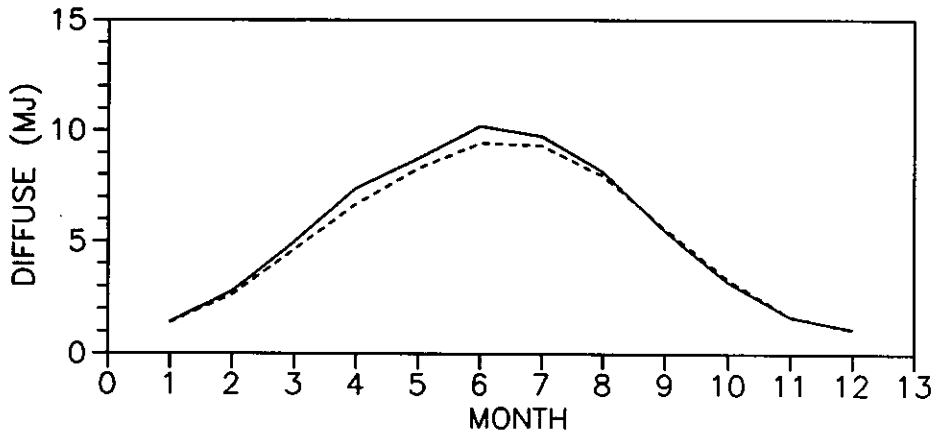
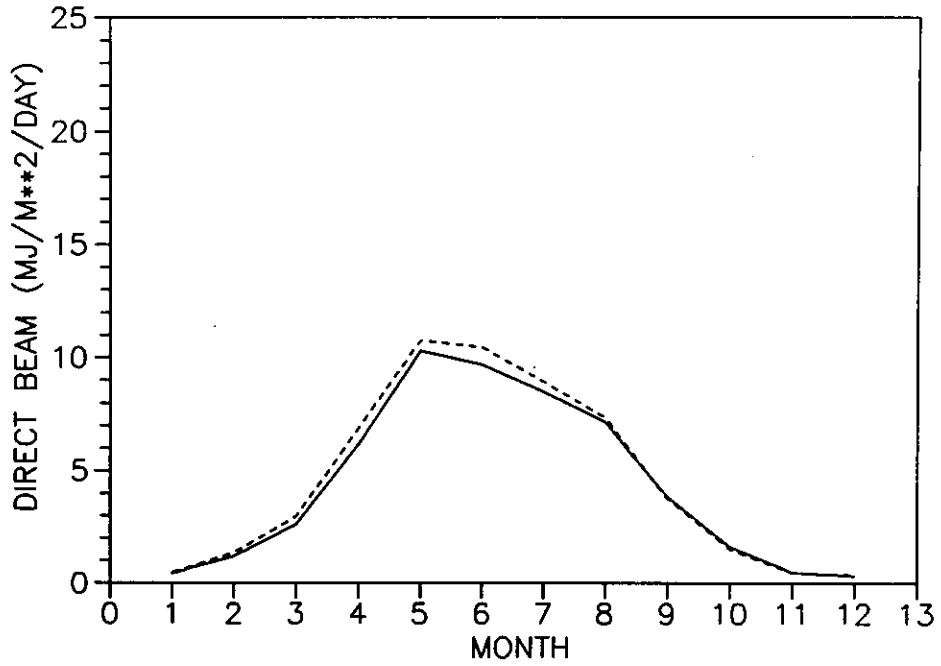


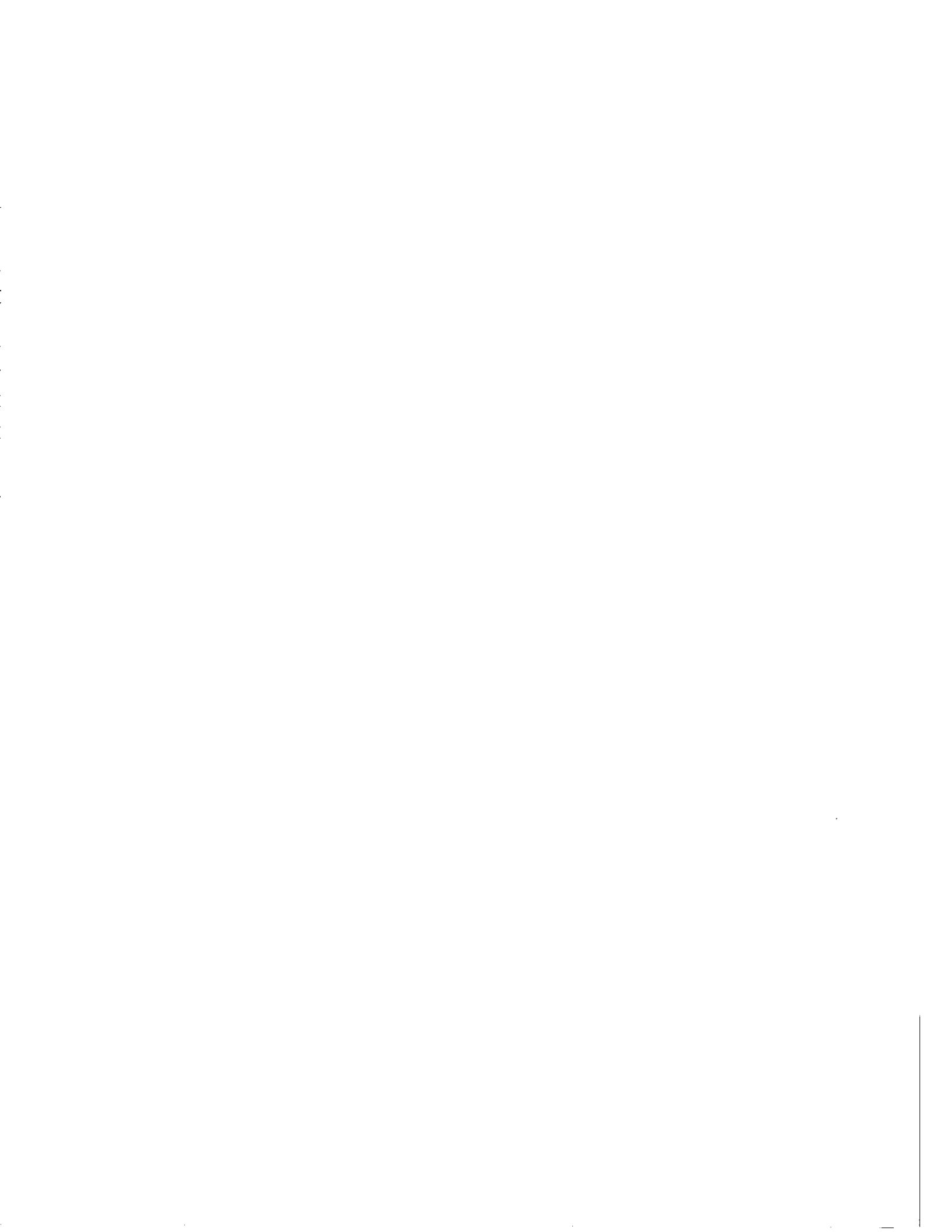




DIFFUSE AND DIRECT BEAM RADIATION

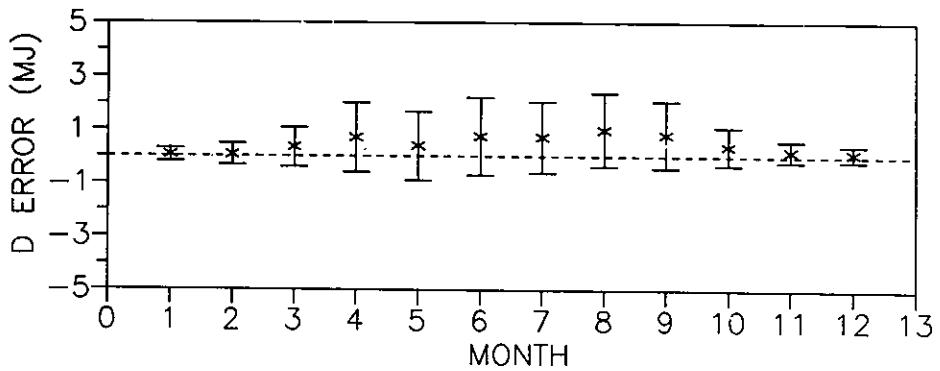
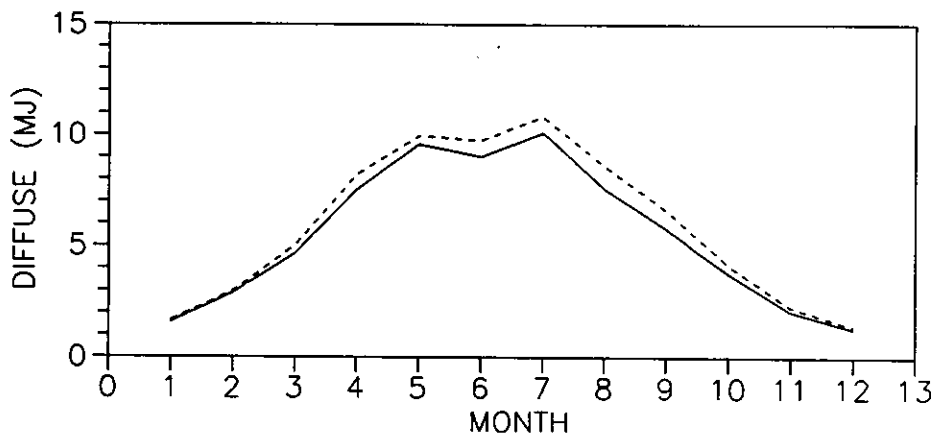
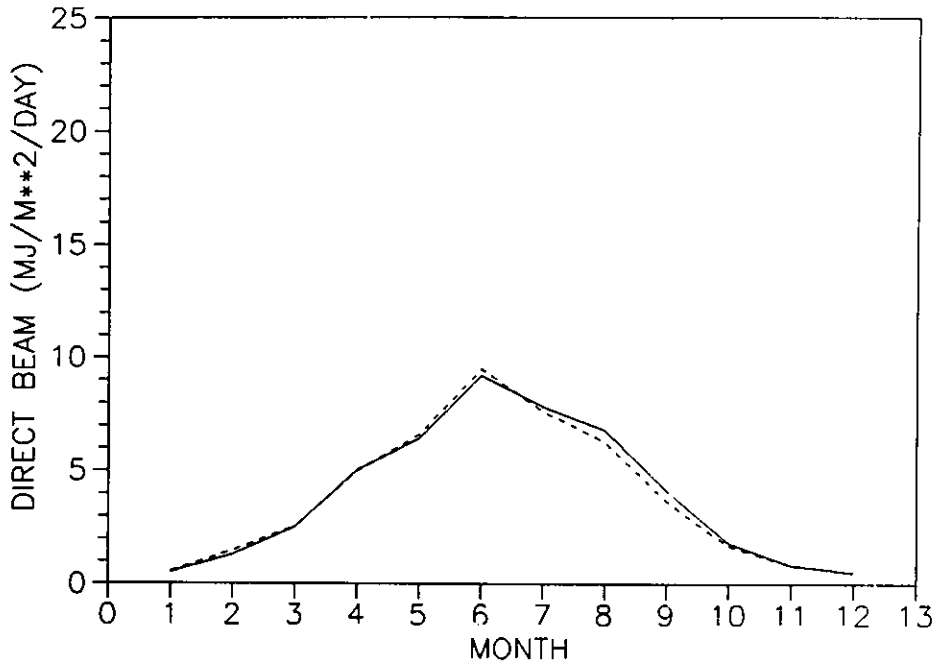
EKDH MODEL: HAMBURG





DIFFUSE AND DIRECT BEAM RADIATION

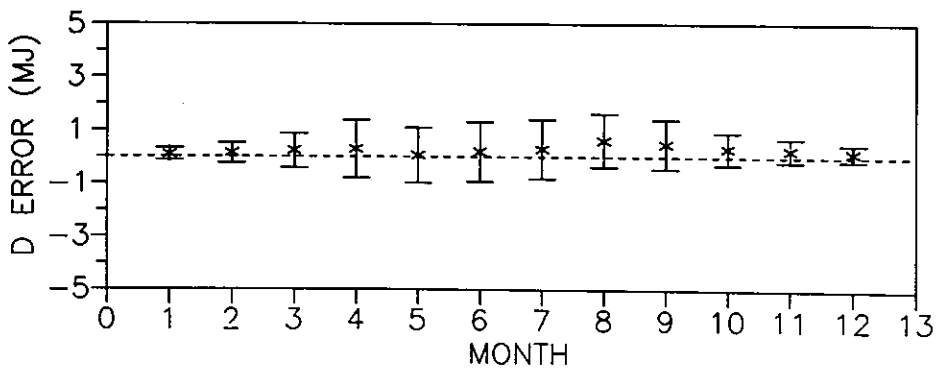
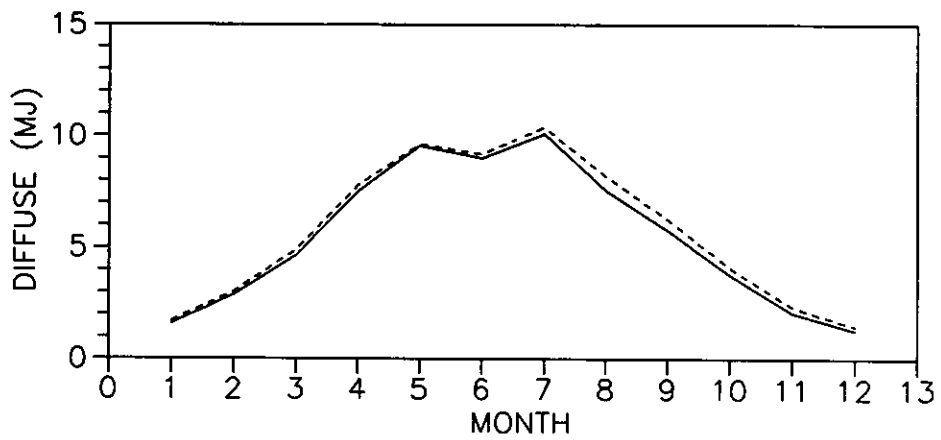
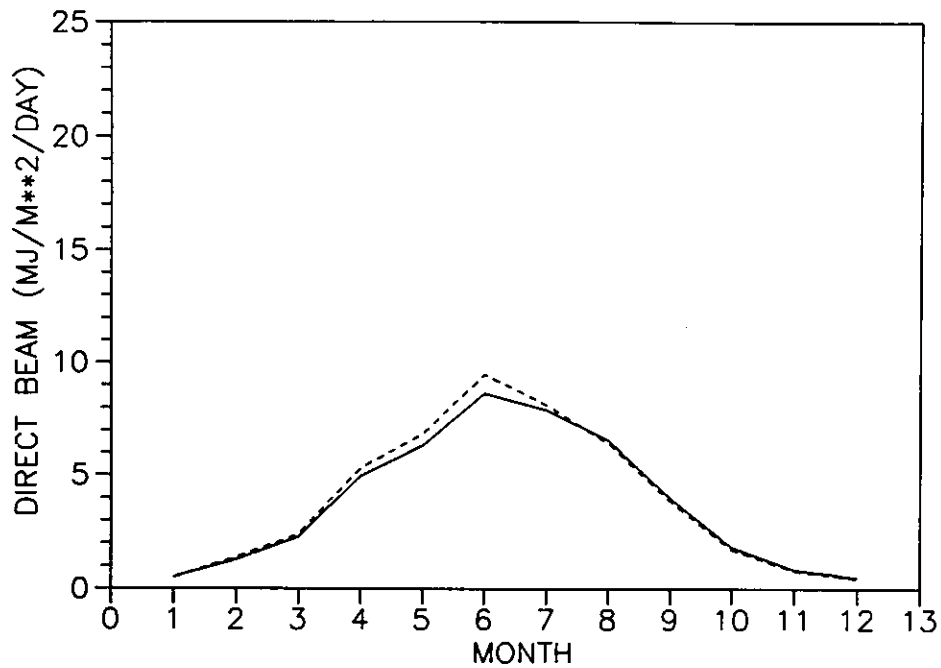
EKDD MODEL: KEW

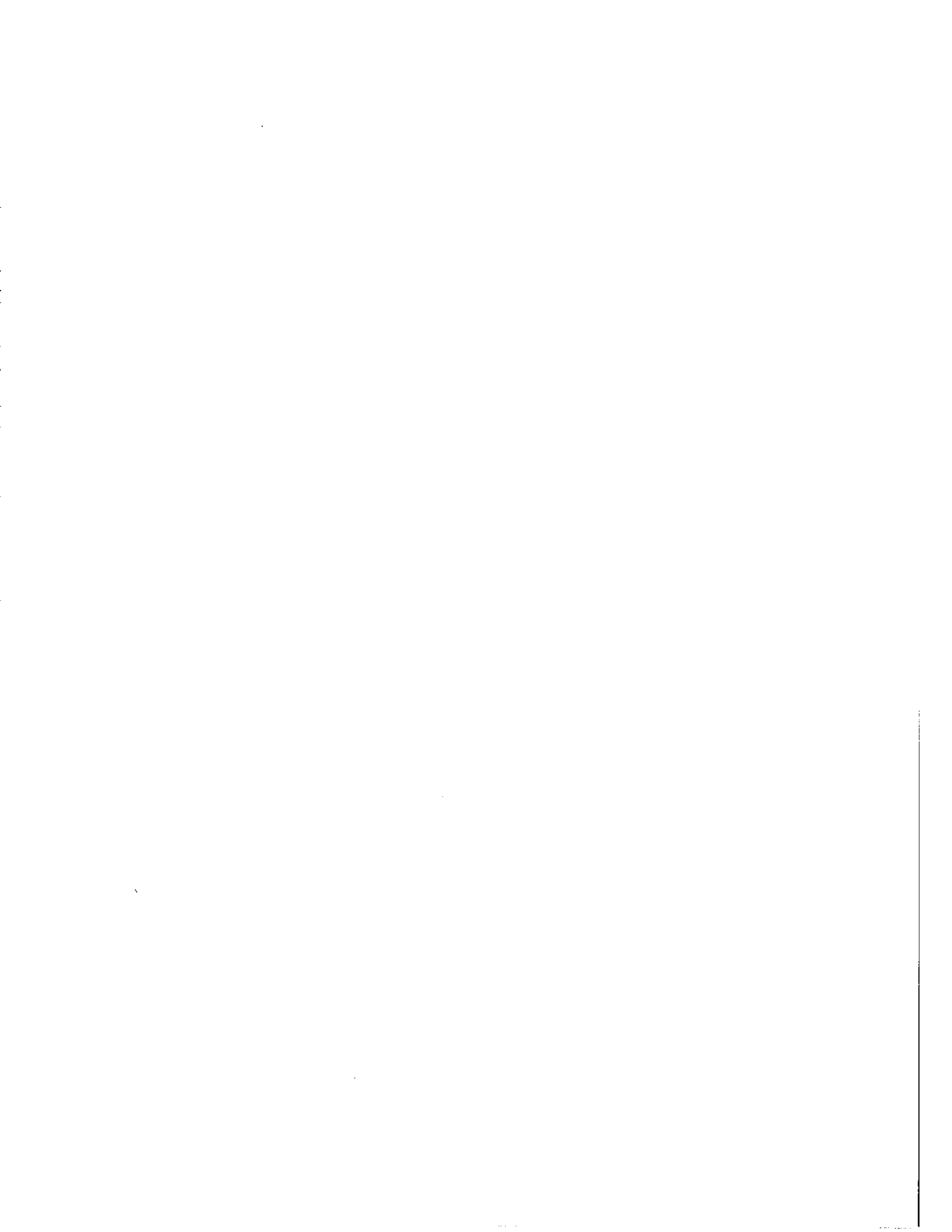




# DIFFUSE AND DIRECT BEAM RADIATION

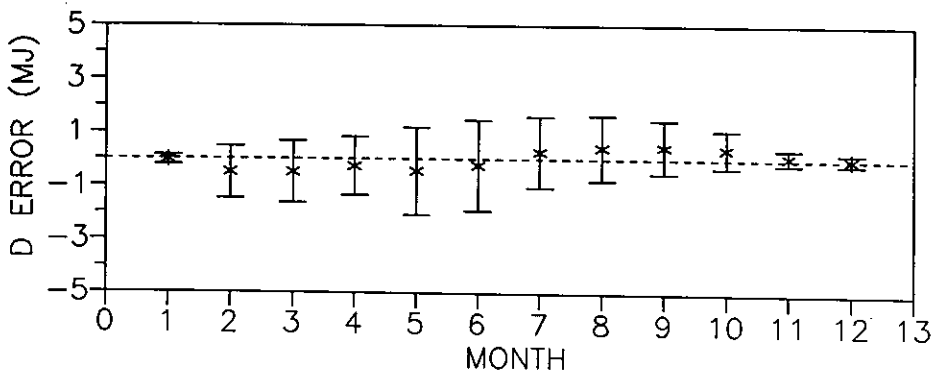
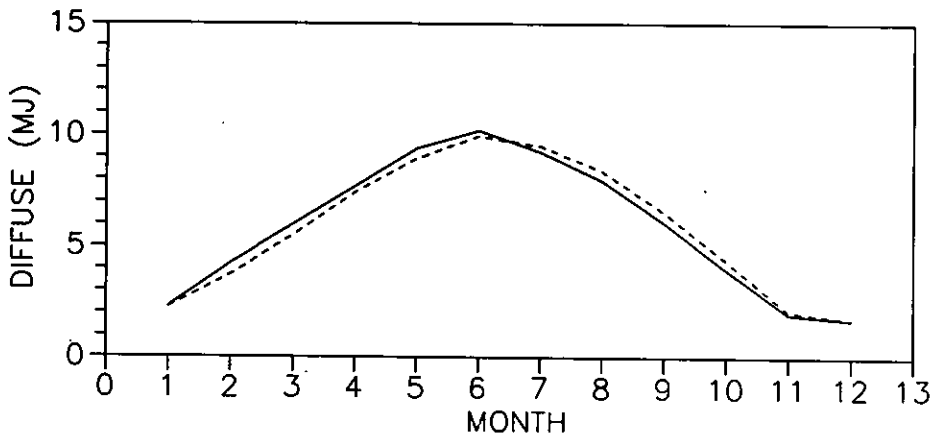
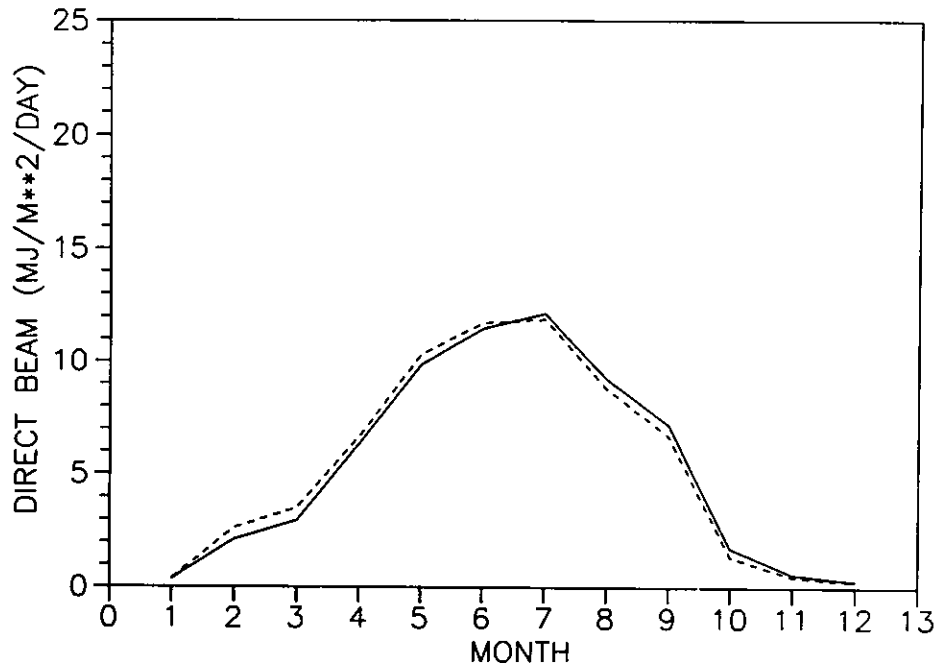
EKDH MODEL: KEW





DIFFUSE AND DIRECT BEAM RADIATION

EKDD MODEL: ZURICH

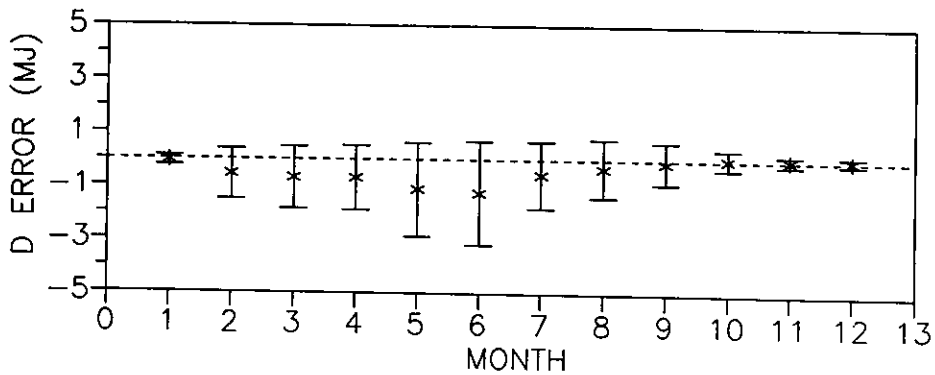
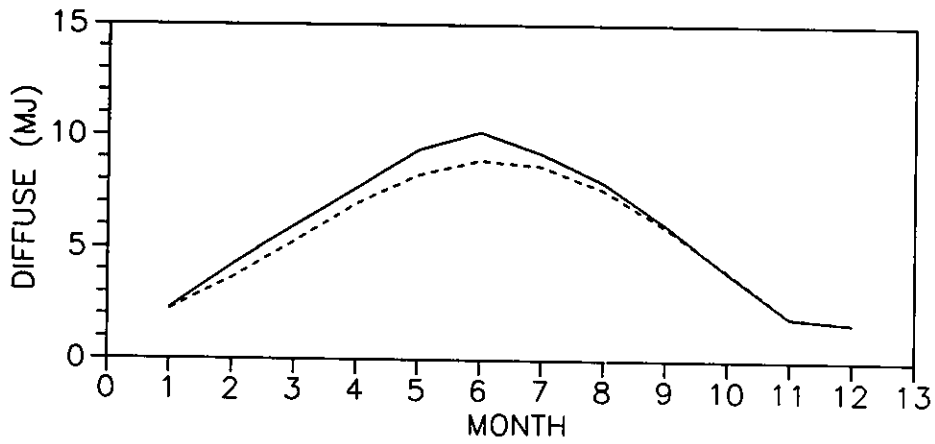
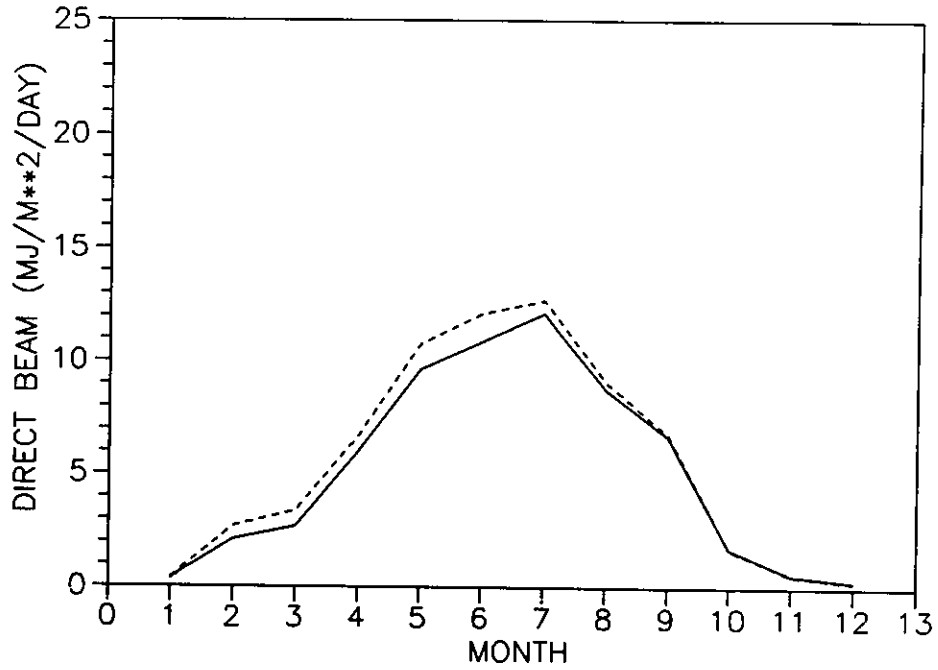






DIFFUSE AND DIRECT BEAM RADIATION

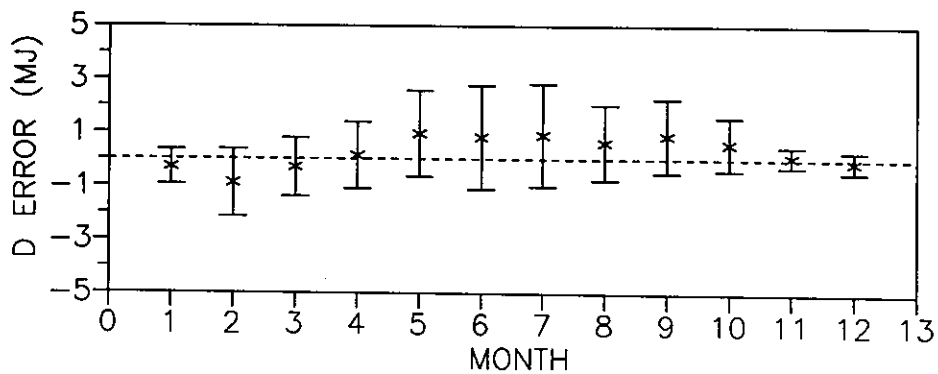
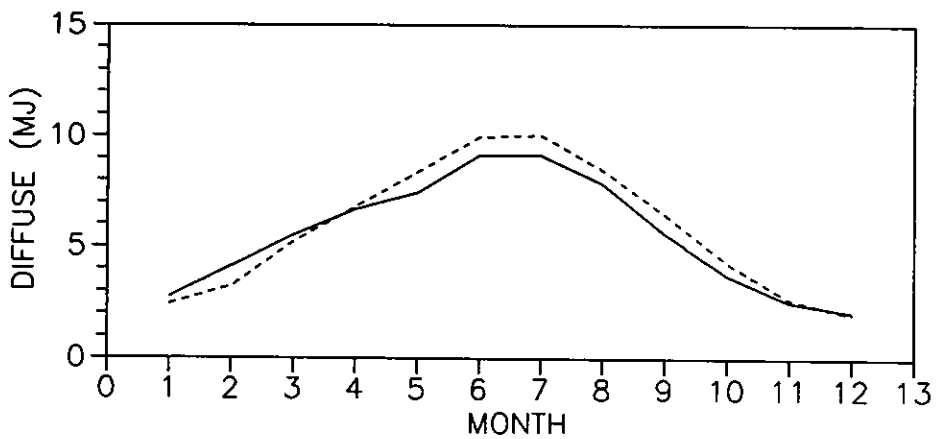
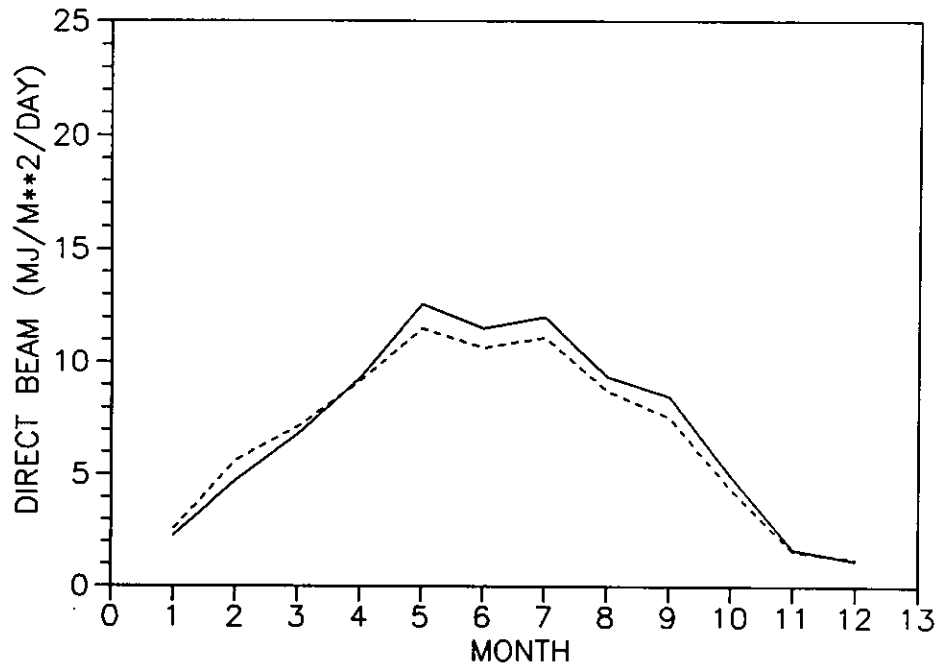
EKDH MODEL: ZURICH

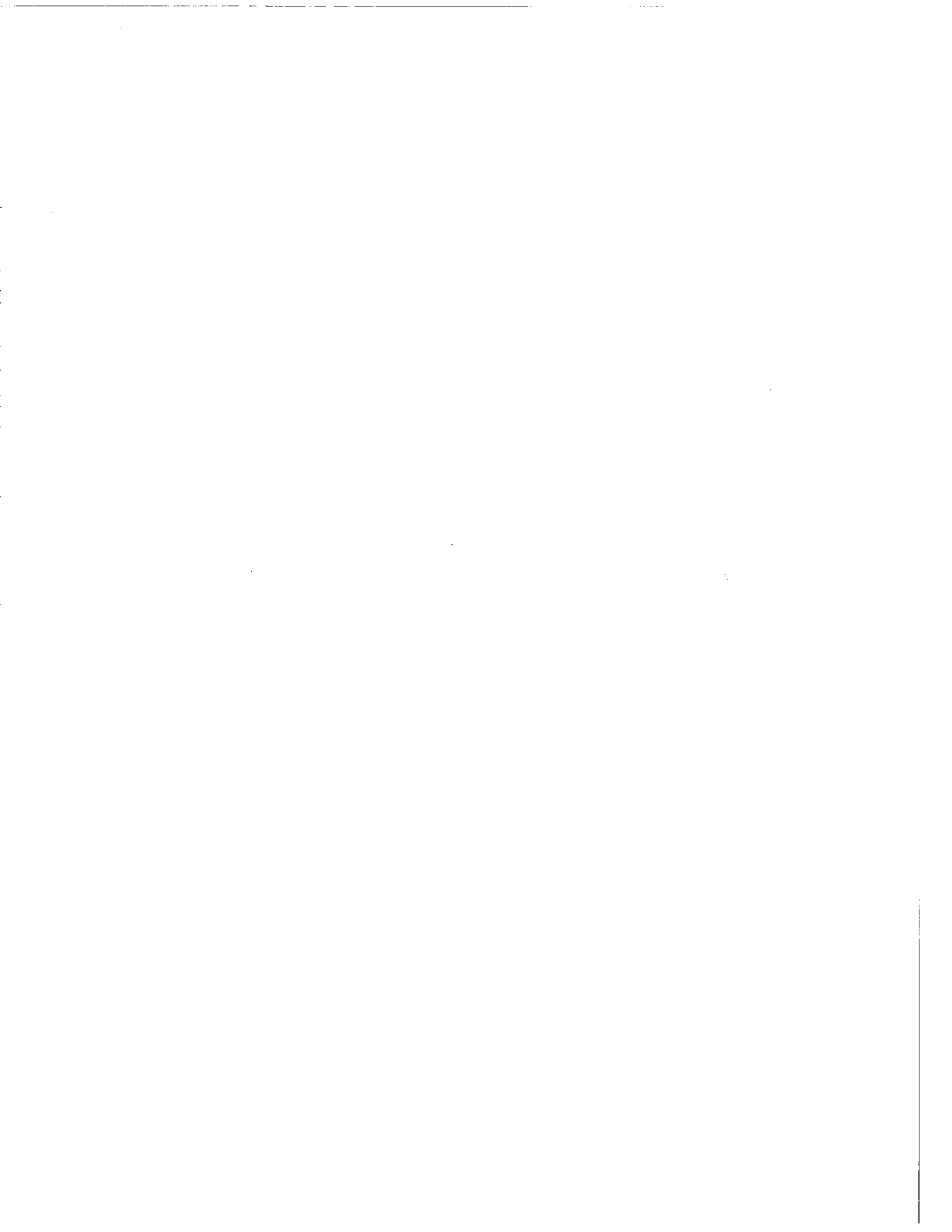




# DIFFUSE AND DIRECT BEAM RADIATION

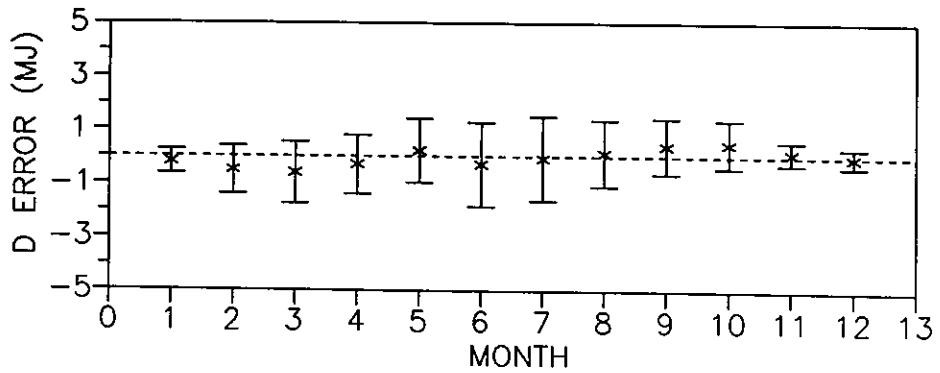
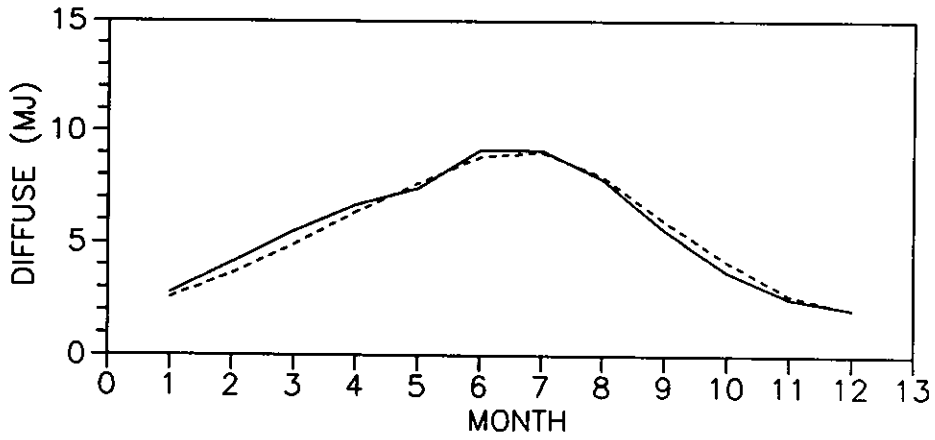
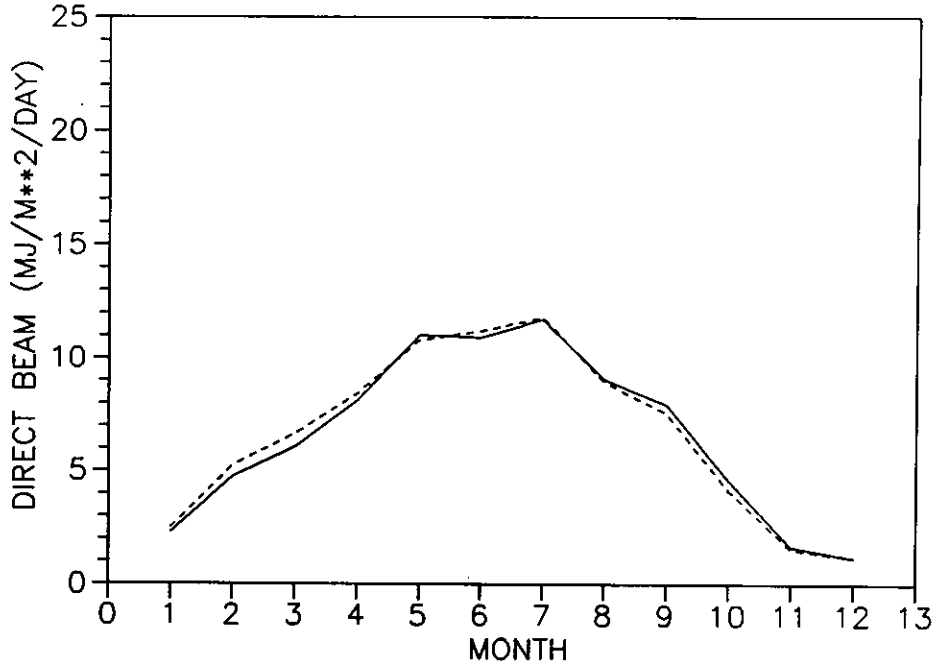
EKDD MODEL: MONTREAL





DIFFUSE AND DIRECT BEAM RADIATION

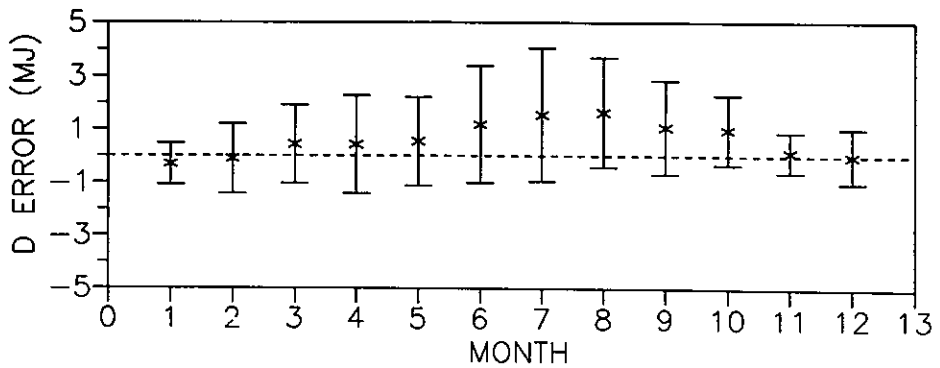
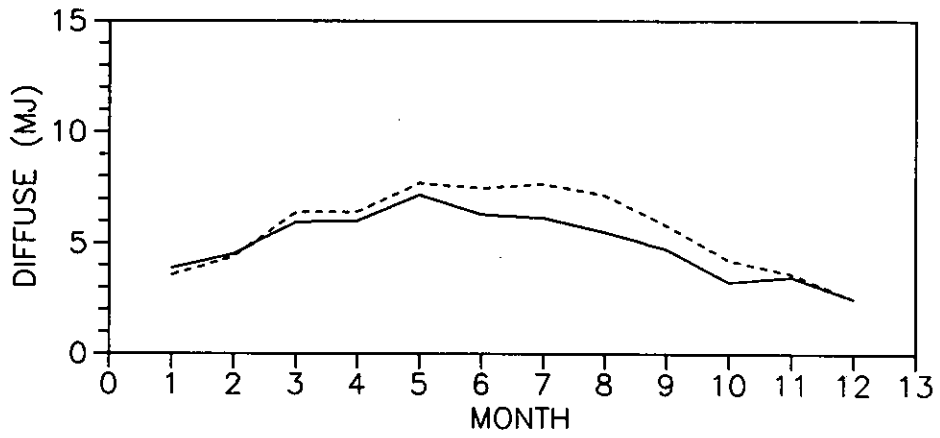
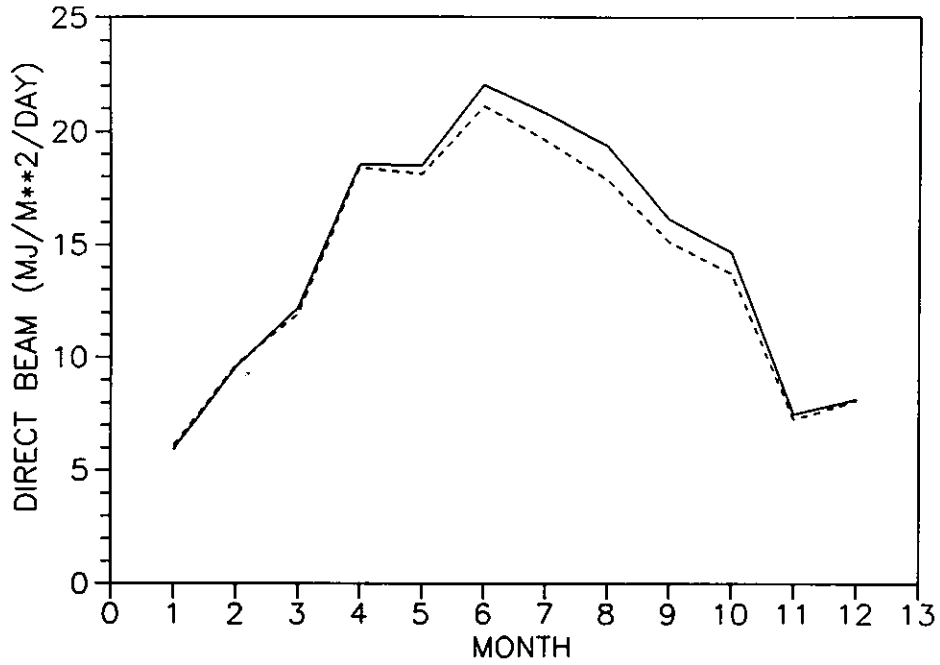
EKDH MODEL: MONTREAL





DIFFUSE AND DIRECT BEAM RADIATION

EKDD MODEL: ALBUQUERQUE

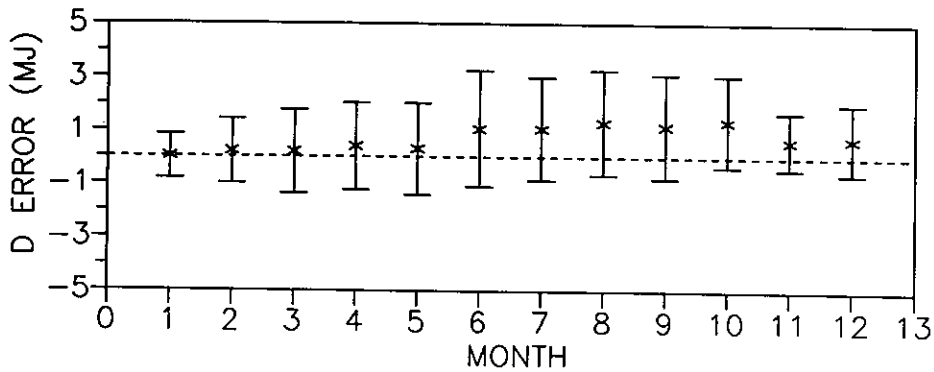
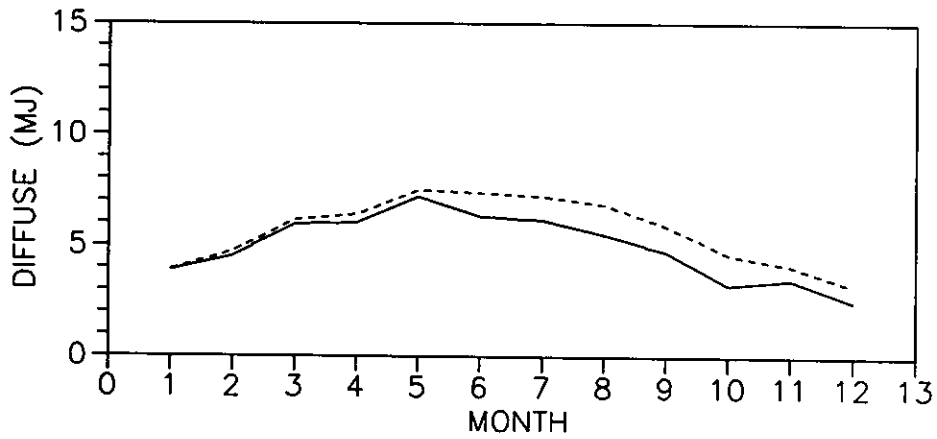
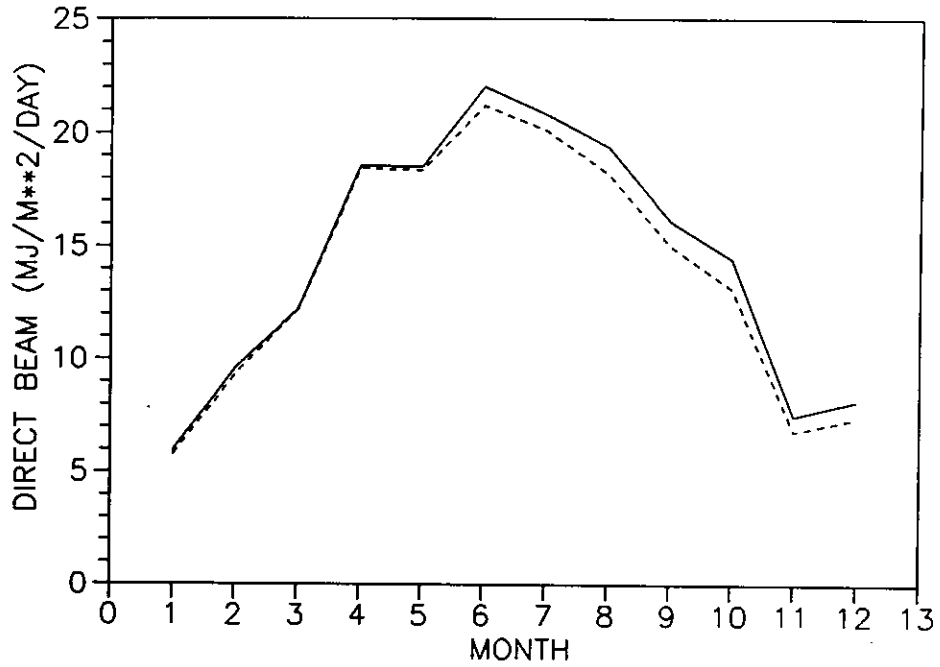


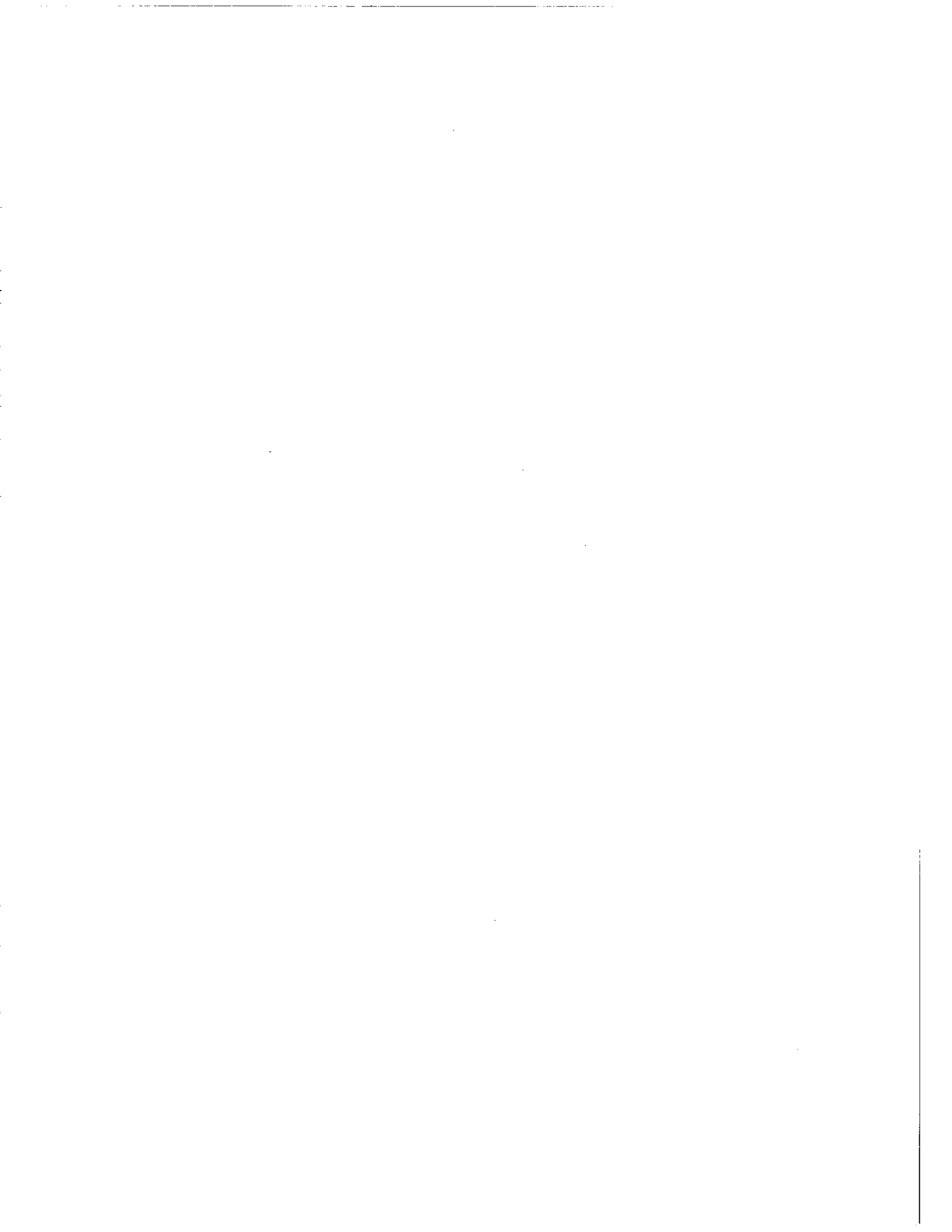




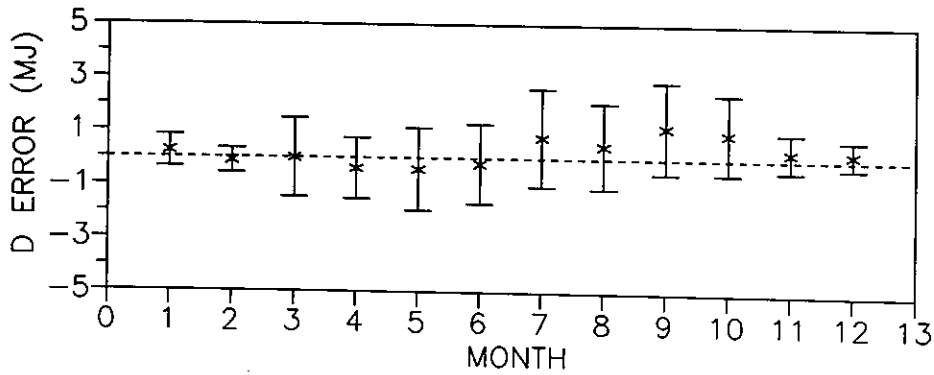
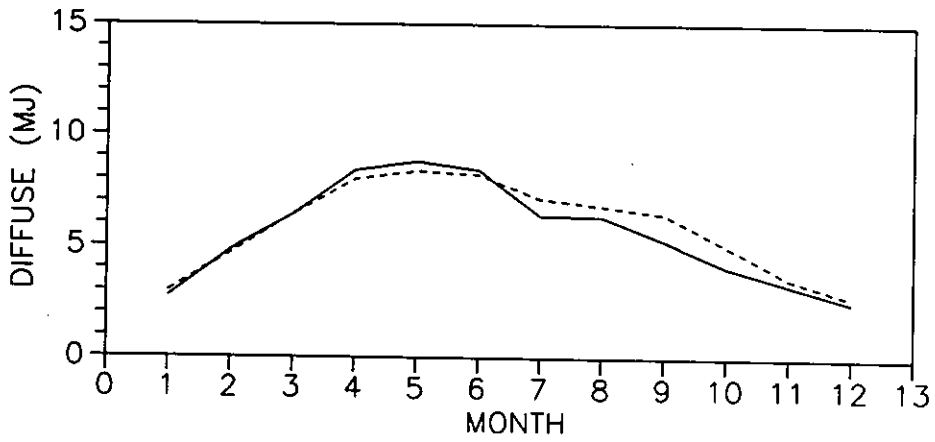
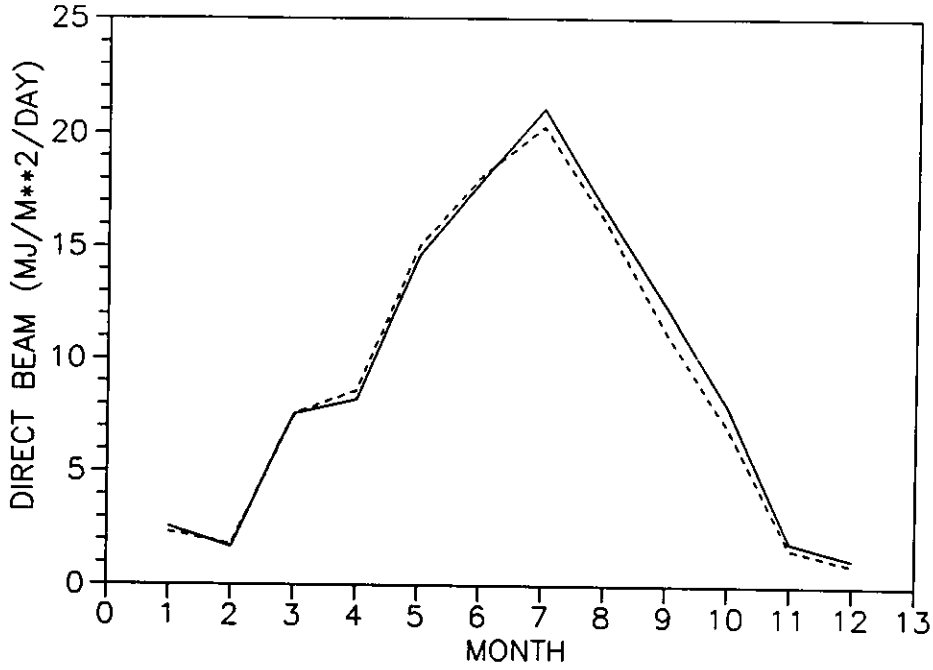
DIFFUSE AND DIRECT BEAM RADIATION

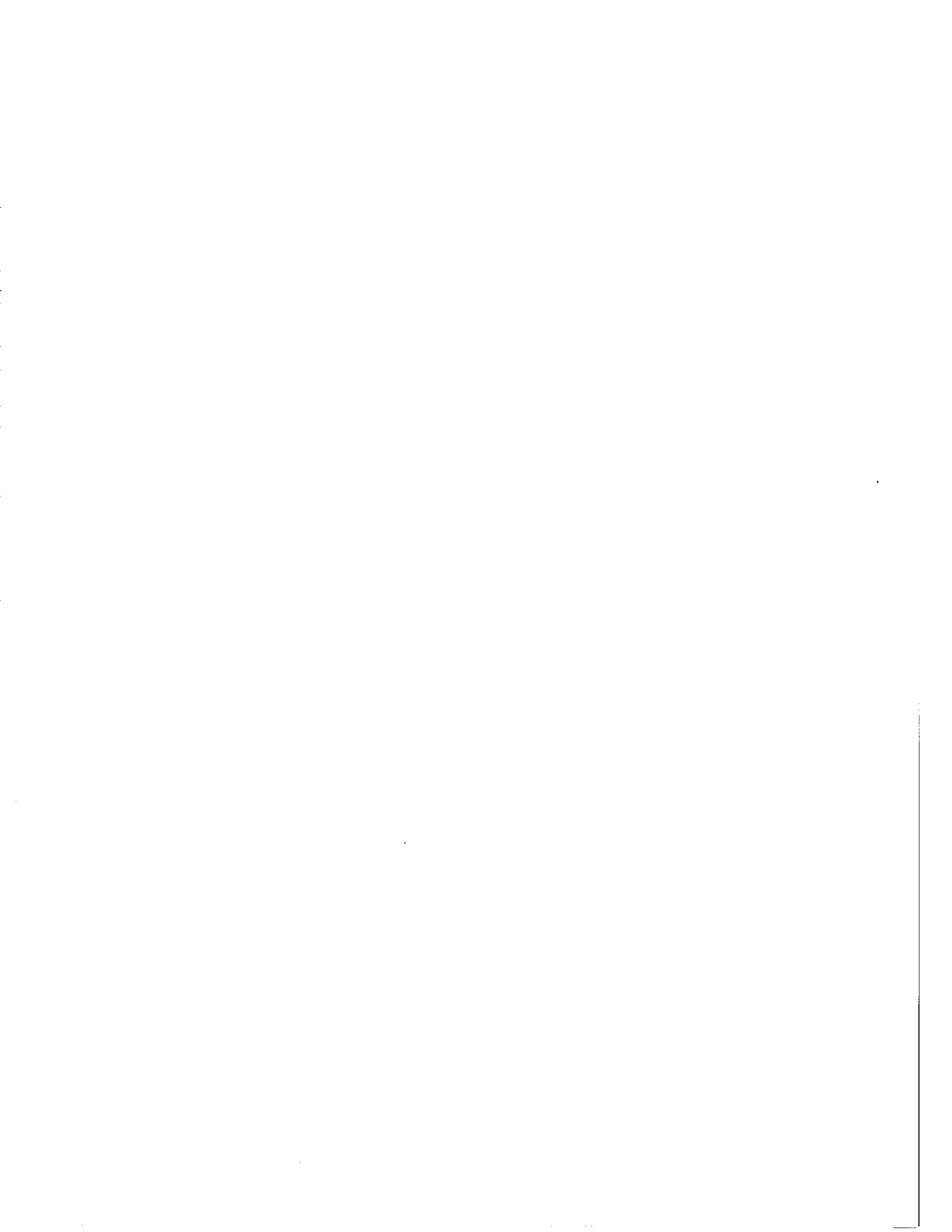
EKDH MODEL: ALBUQUERQUE



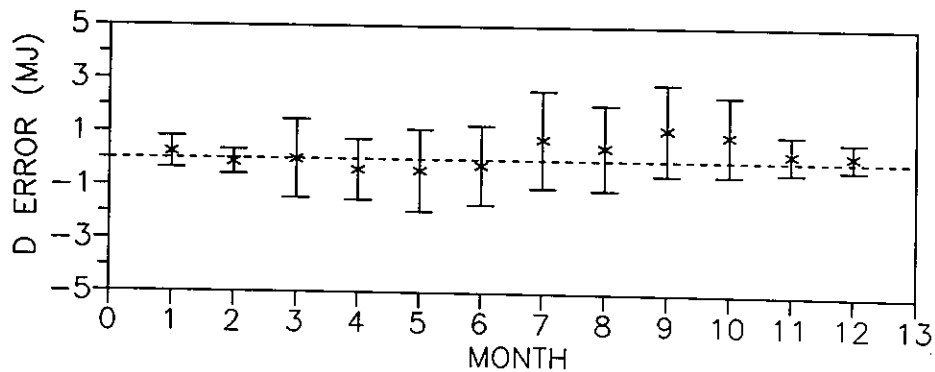
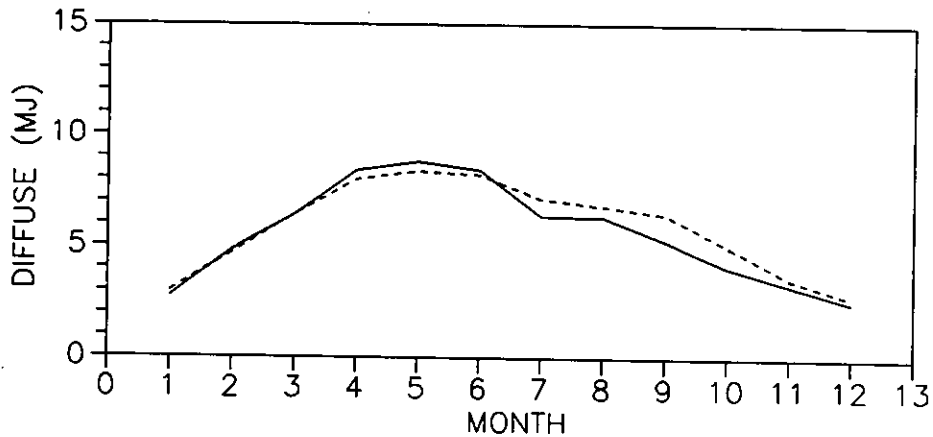
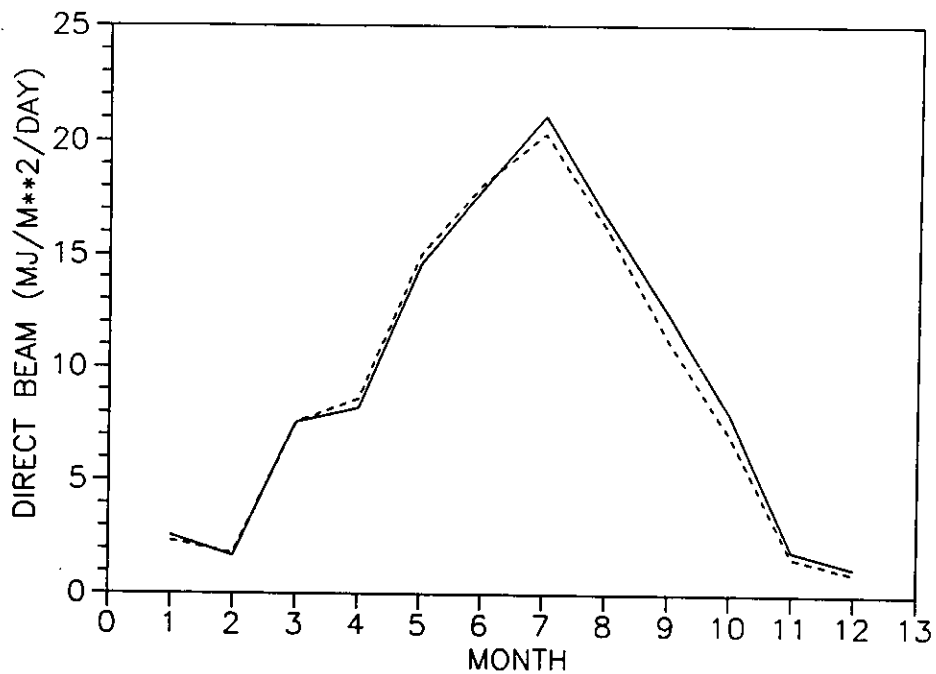


DIFFUSE AND DIRECT BEAM RADIATION  
EKDD MODEL: MEDFORD





DIFFUSE AND DIRECT BEAM RADIATION  
EKDD MODEL: MEDFORD





conditions. Thus, the curves for diffuse radiation estimates are often smoother than those for the corresponding measurements. Their statistical nature may account for the systematic overestimation at the two Australian stations: similar radiation regimes were probably not represented by the data used to fit them. With the exception of Albuquerque, where diffuse radiation is overestimated from spring onwards, there is good agreement between measured and calculated radiation.

#### 4.6 MODEL PERFORMANCE AND CLOUDINESS

Cloud exerts major control on day-to-day variation in global radiation and partitioning into diffuse and direct beam components. Variation in model performance was examined in two ways: (1) using hourly measured and estimated radiation and cloud cover; (2) using daily measured and estimated radiation and atmospheric transmissivity.

At the stations used in this study, cloud cover was recorded in one of three ways: (1) hourly, in tenths; (2) hourly, in oktas; (3) three-hourly, in oktas. Observations in oktas were converted to decimal fractions, and linear interpolation was used to fill gaps between three-hourly observations. Since conversion of okta to decimal leaves two unrepresented cells in the 0 to 10 range, results for stations with hourly oktal observations will be presented in oktas, not tenths. However, tenths are used for cloud interpolated from three-hourly observations in oktas.

We present results for *MAC* and *JOS* for global radiation (Figure 4a) and for *MAC*, *JOS* and *EKDH* for direct beam radiation (Figure 4b) for Alice Springs, Mildura, Albuquerque, Medford, Montreal, Kew, Hamburg and Zurich. Frequency distributions of cloud amounts are included in Figures 4a and 4b below plots of measured and calculated radiation against cloud amount.

Although a perfect model should produce radiation estimates which match

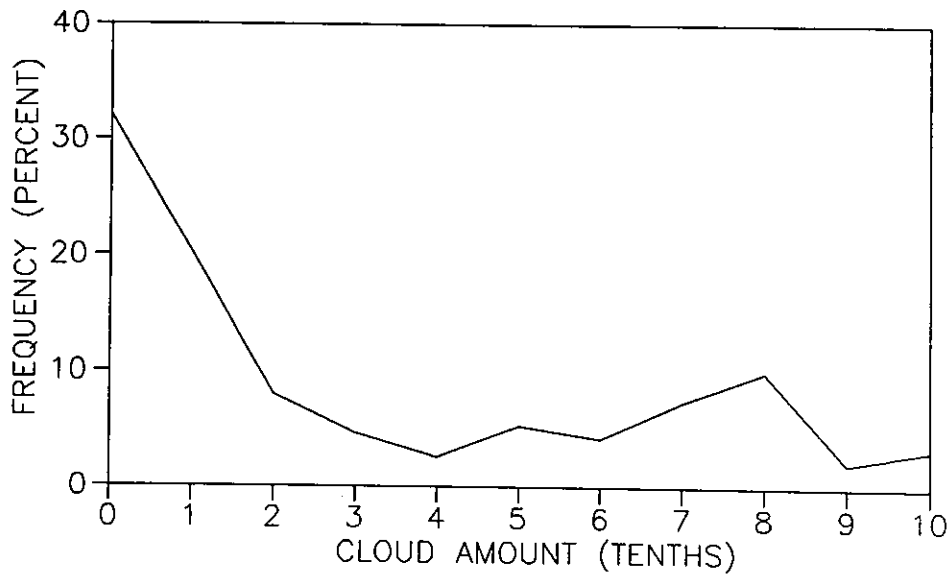
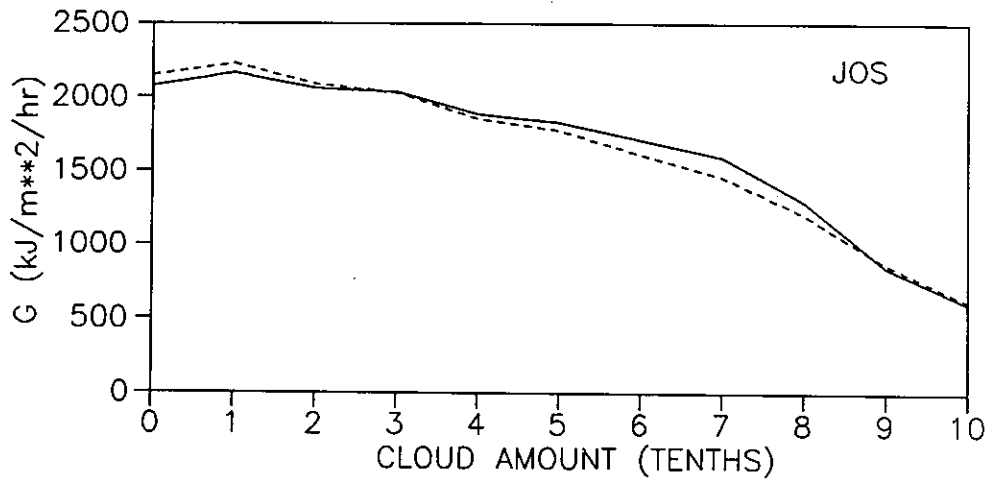
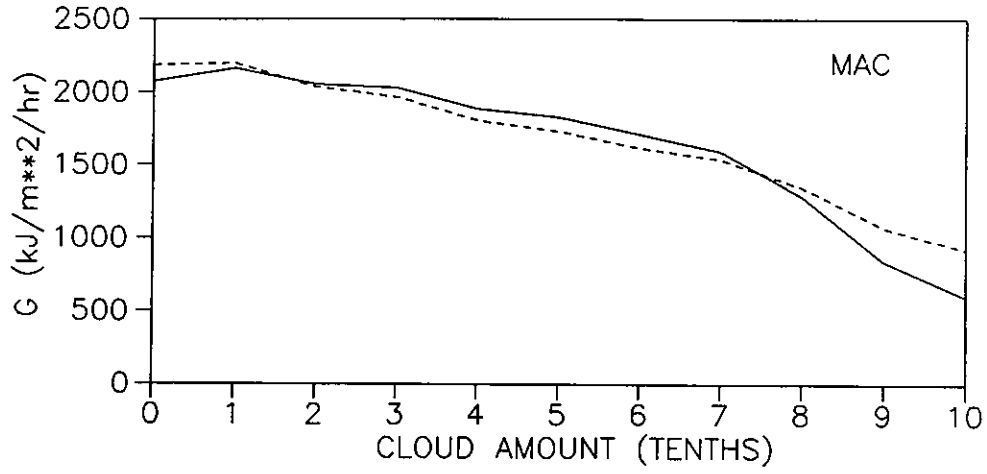


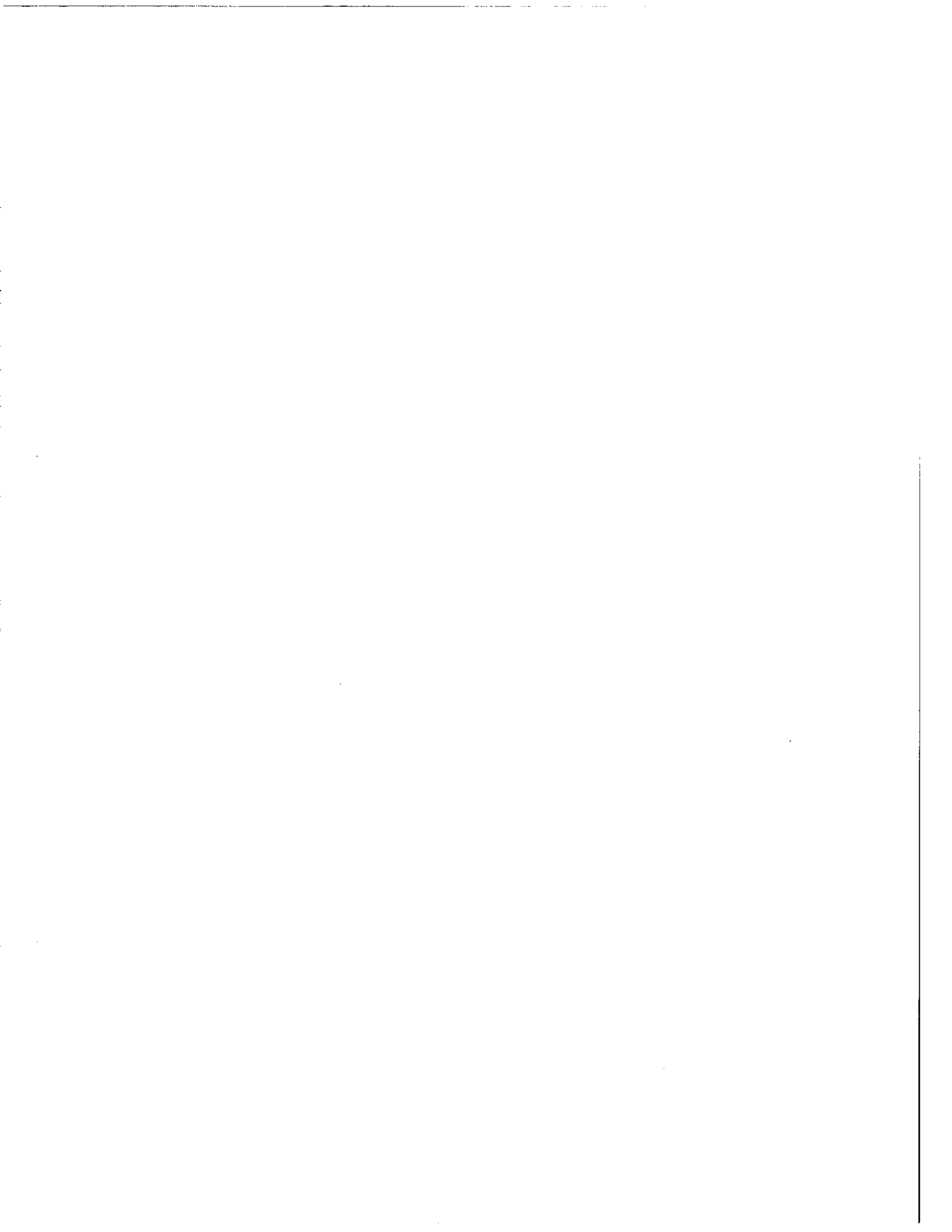


Figure 4a Model performance and cloudiness: a comparison of measured global radiation (solid line) and layer model estimates (dashed line) for selected stations

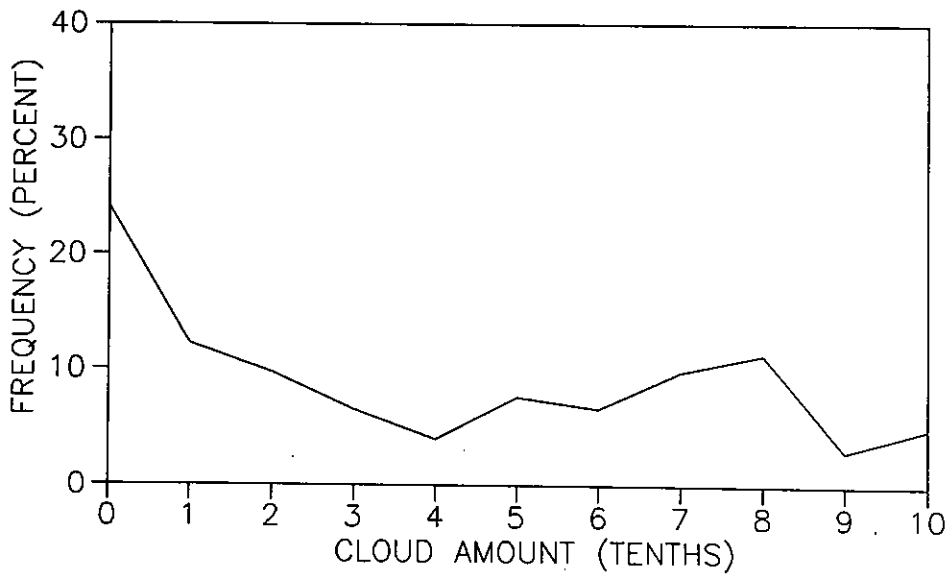
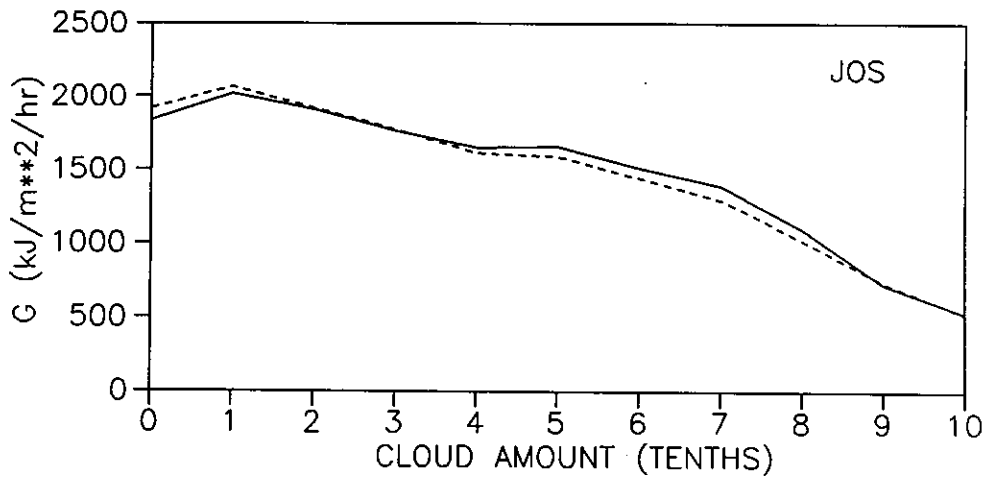
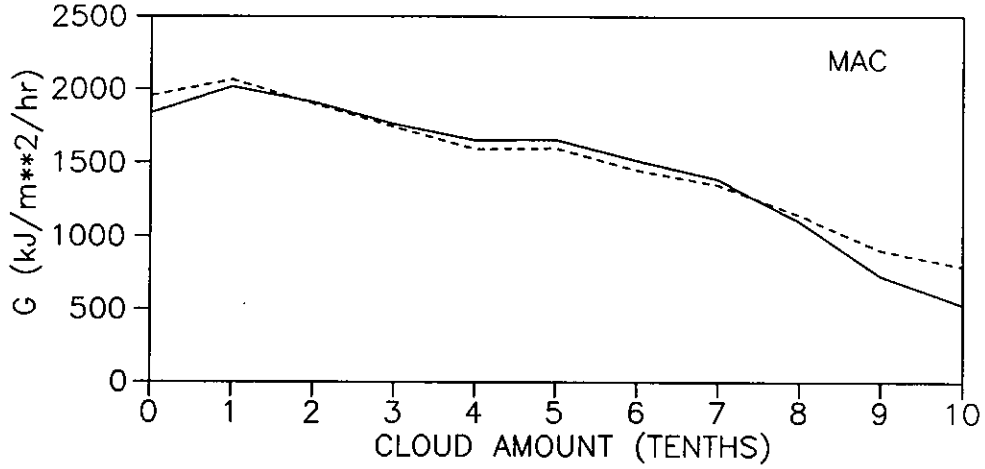


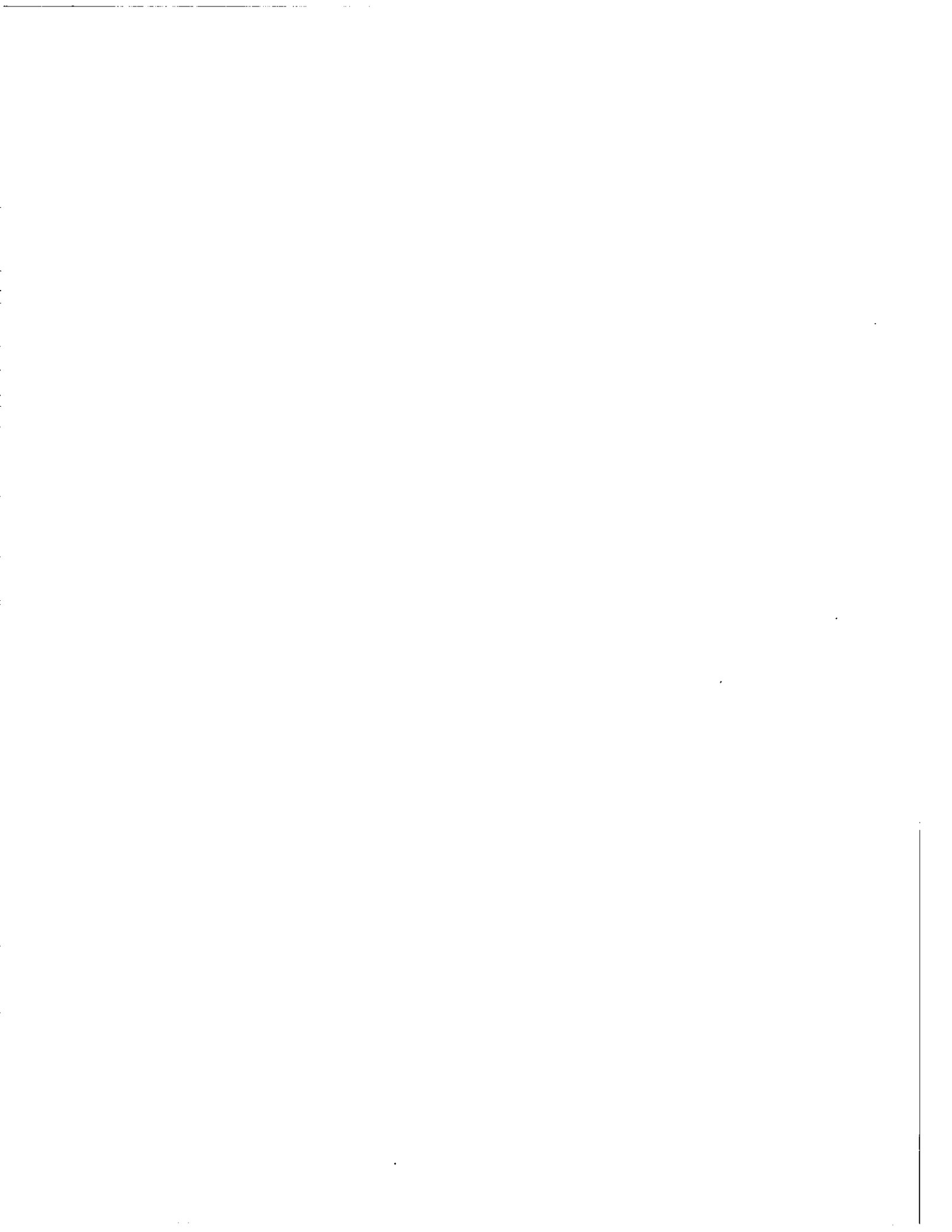
GLOBAL RADIATION AND CLOUD  
ALICE SPRINGS



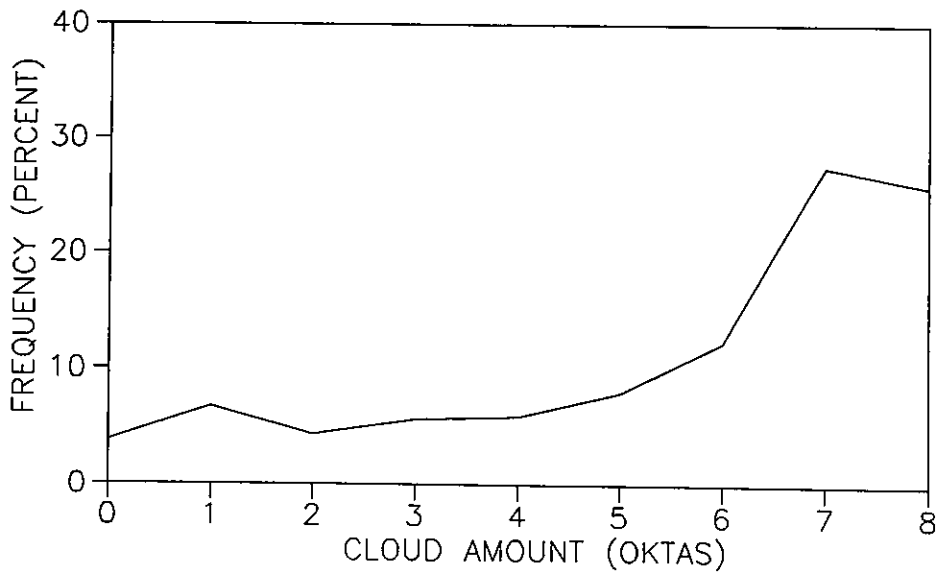
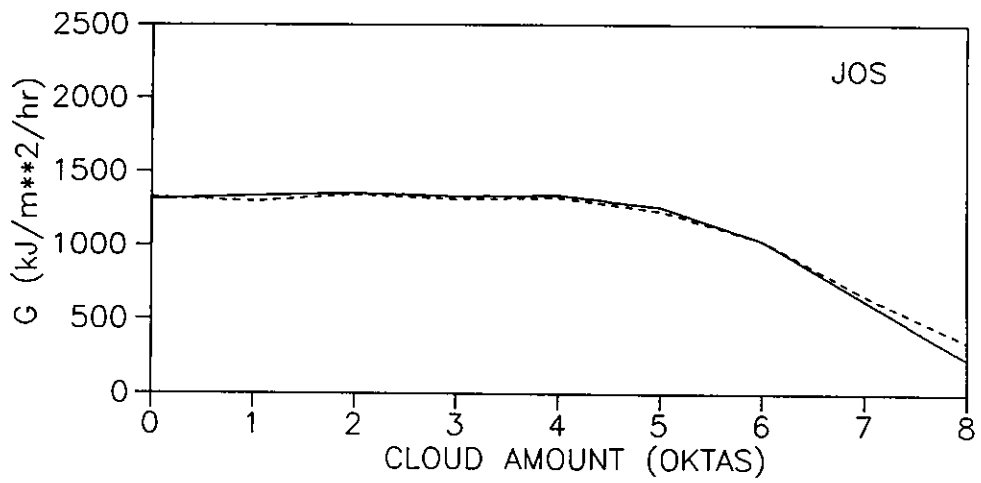
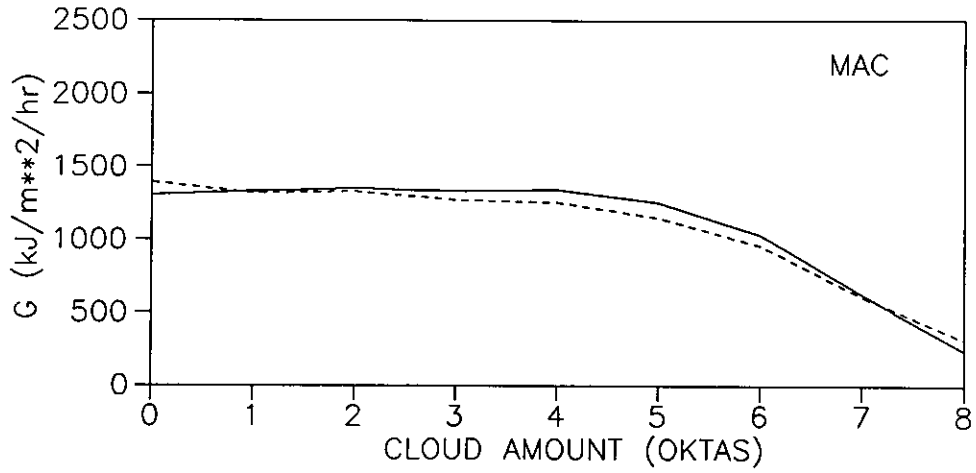


GLOBAL RADIATION AND CLOUD  
MILDURA





GLOBAL RADIATION AND CLOUD  
HAMBURG

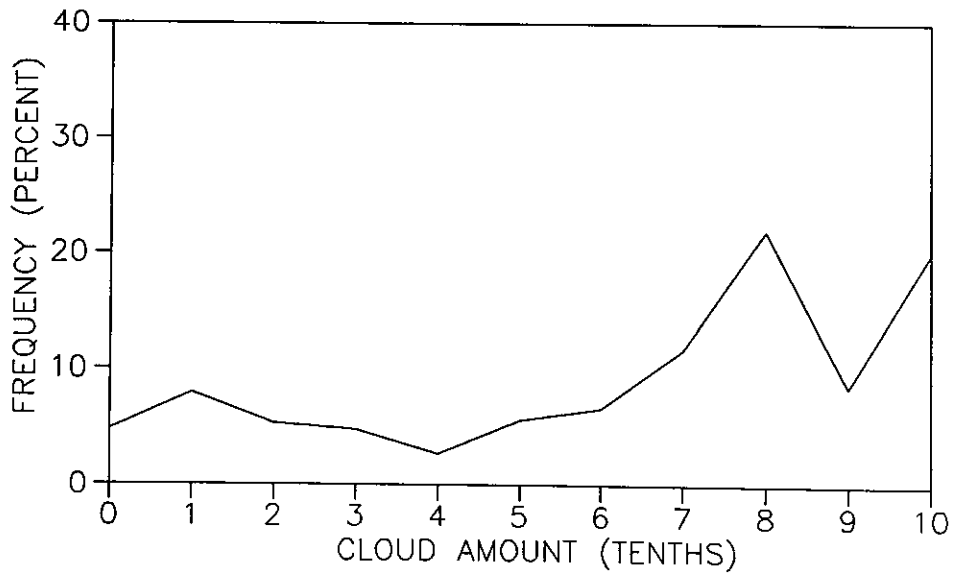
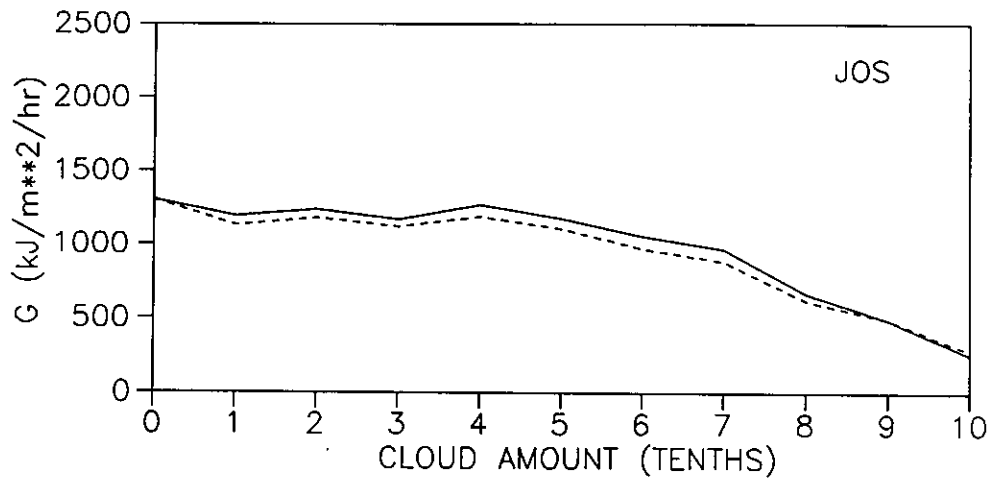
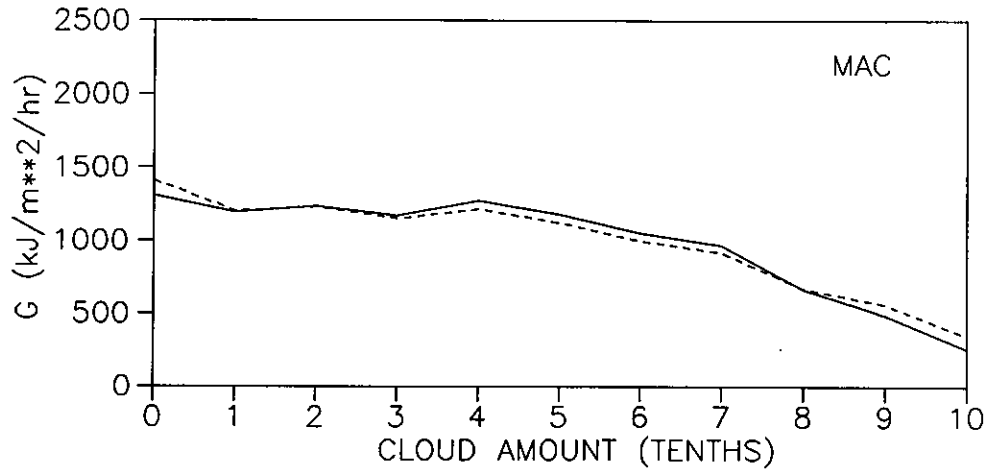


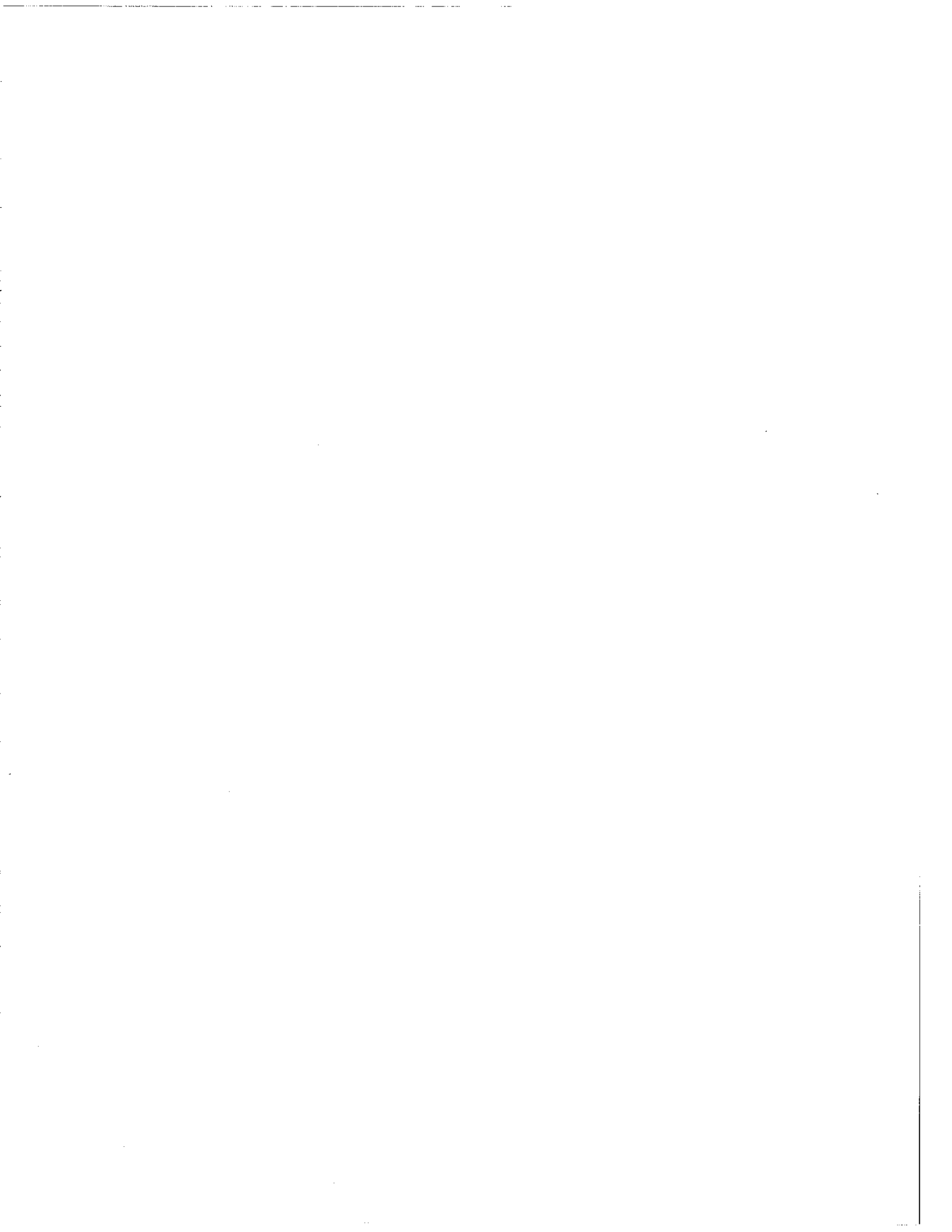




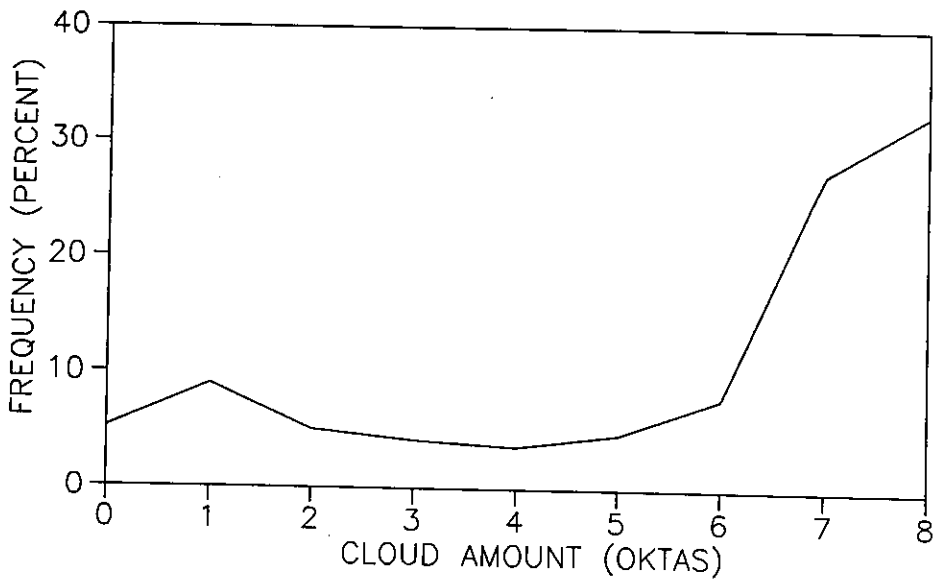
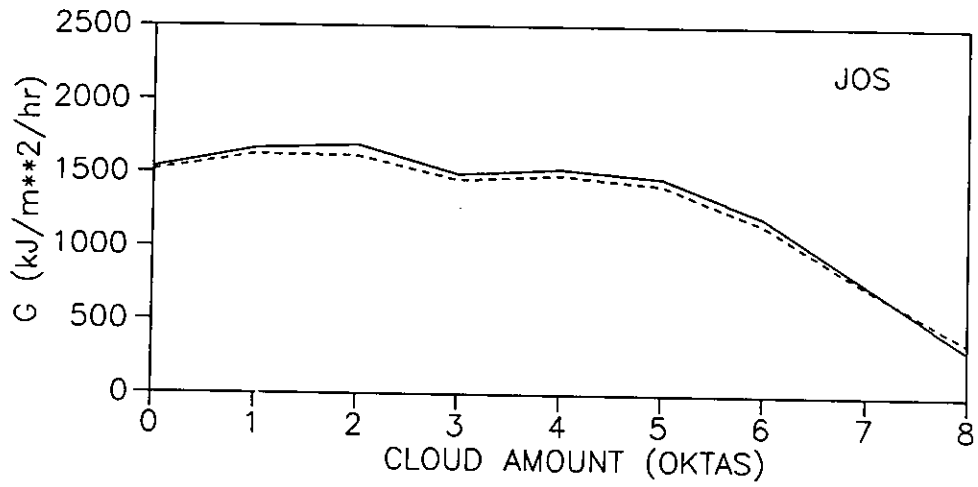
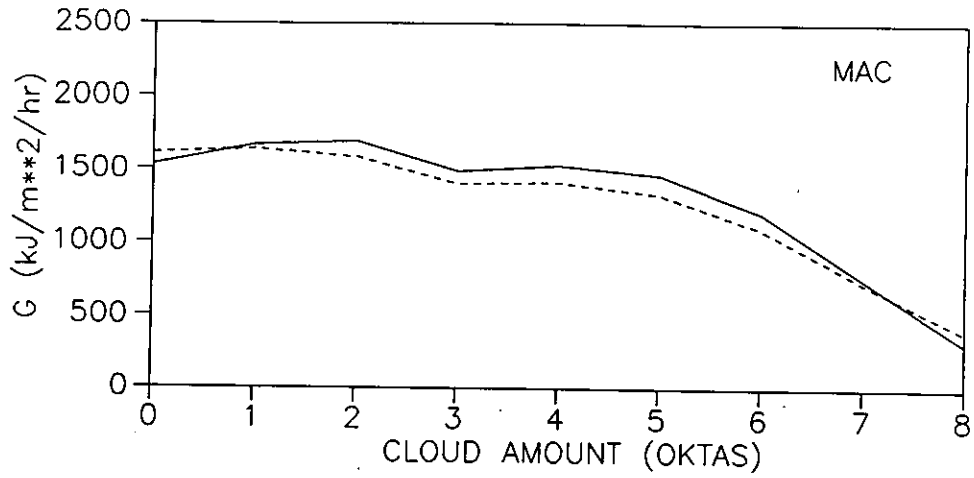
# GLOBAL RADIATION AND CLOUD

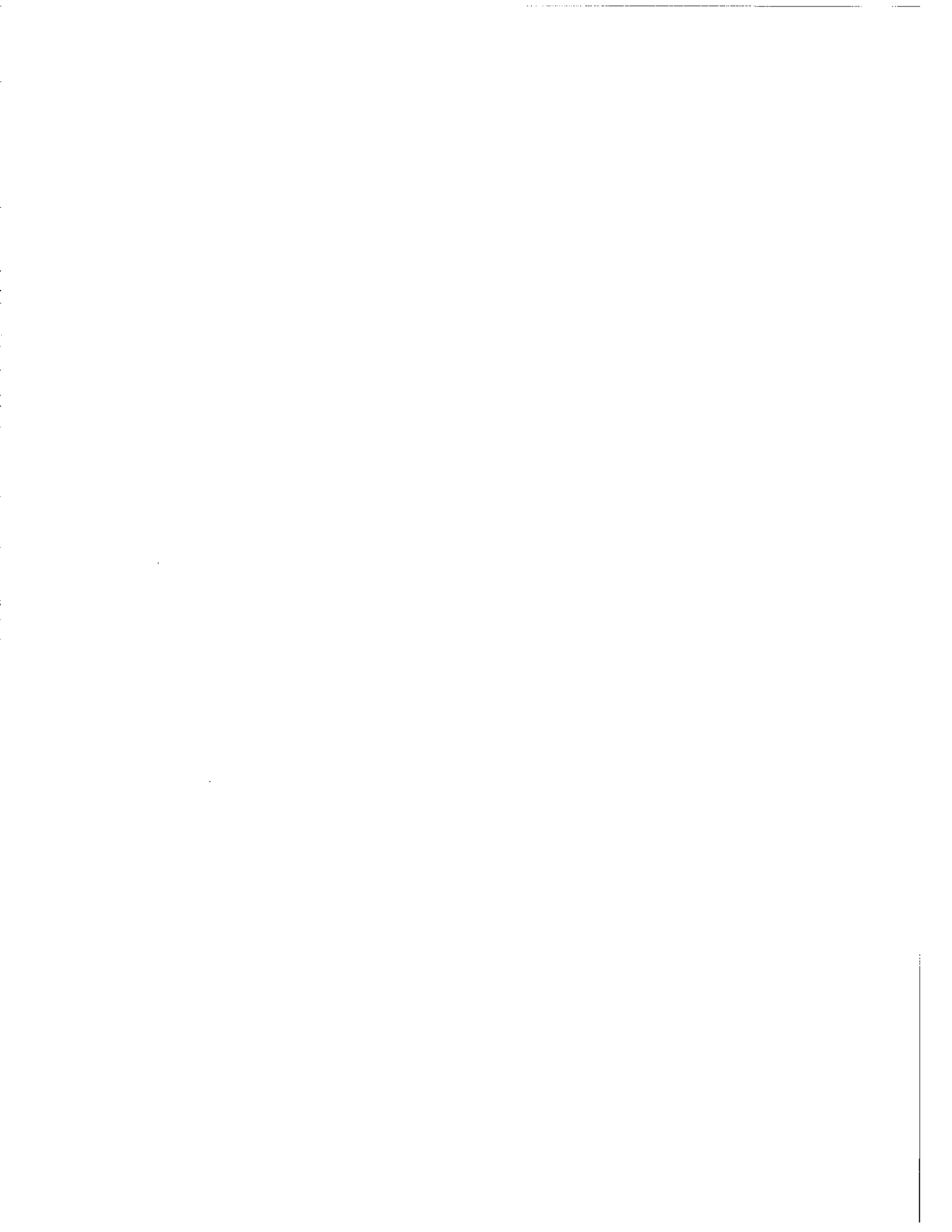
KEW



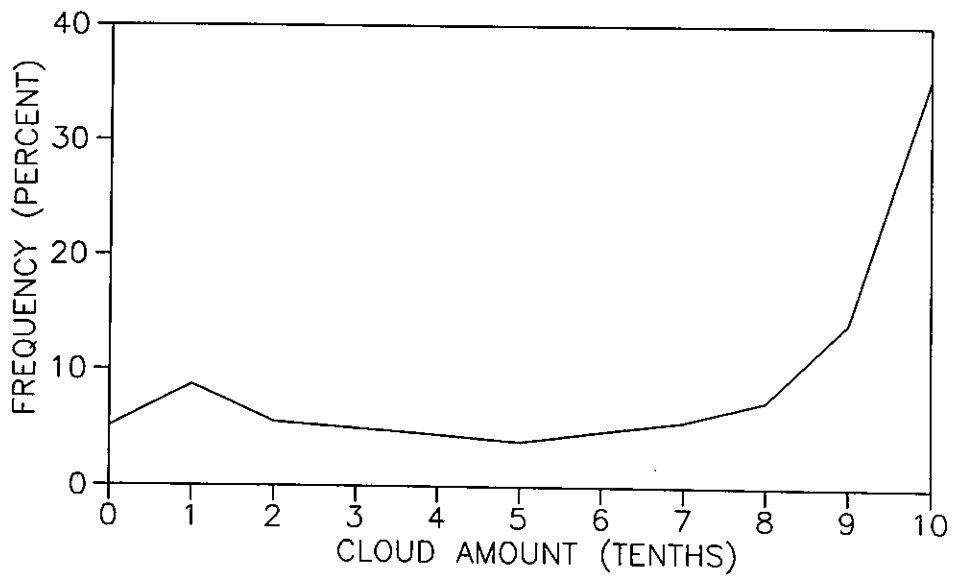
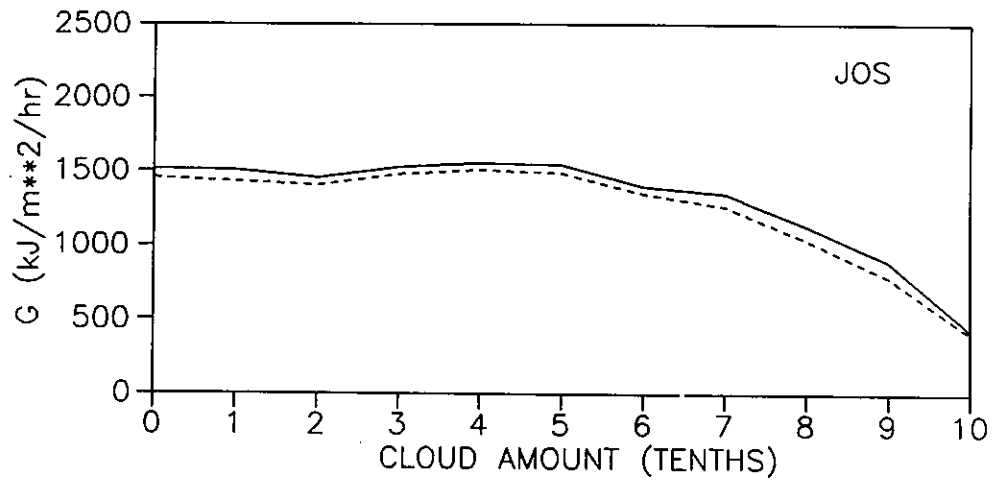
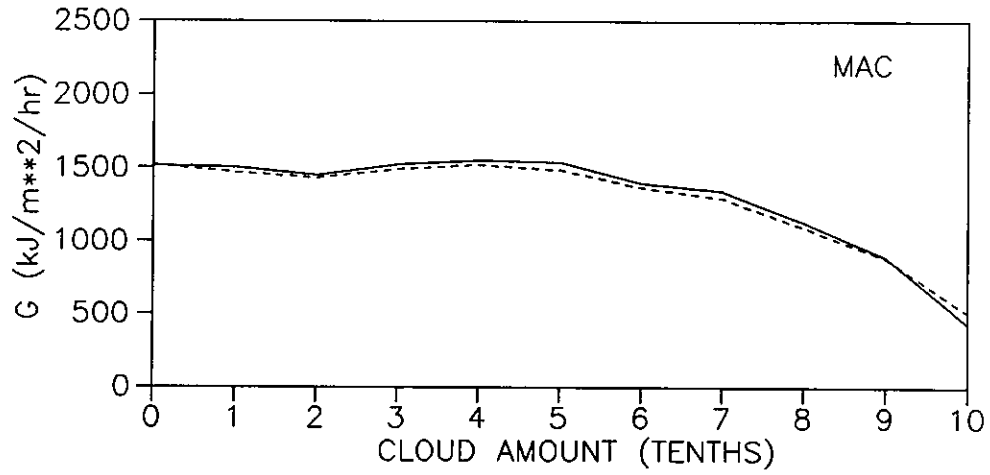


GLOBAL RADIATION AND CLOUD  
ZURICH



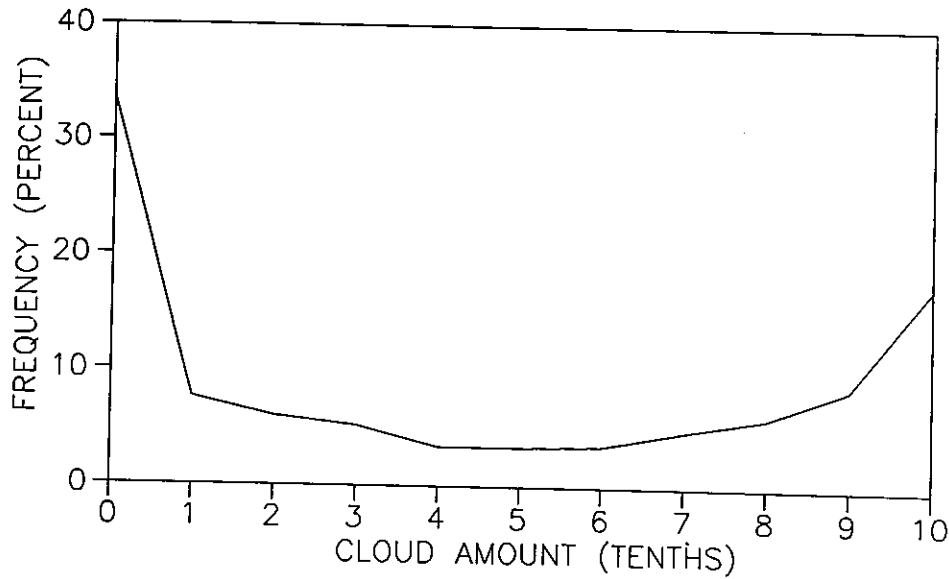
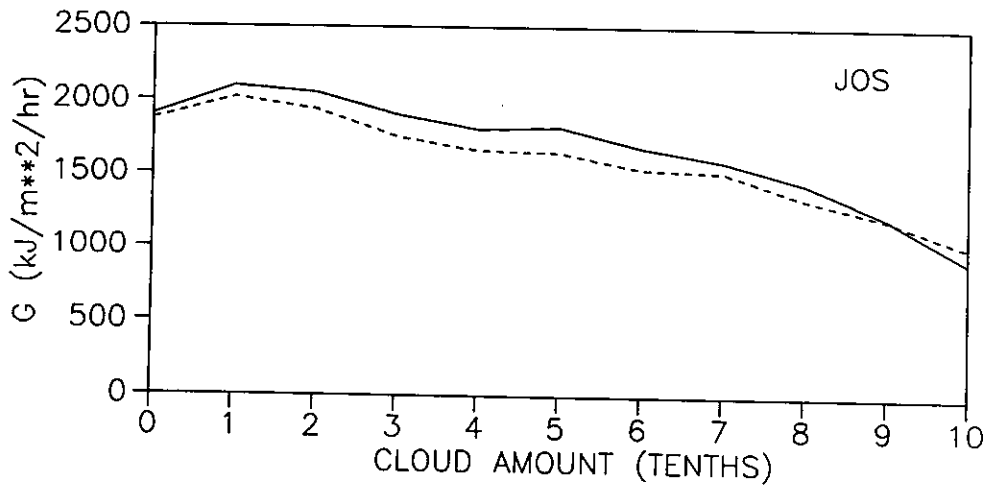
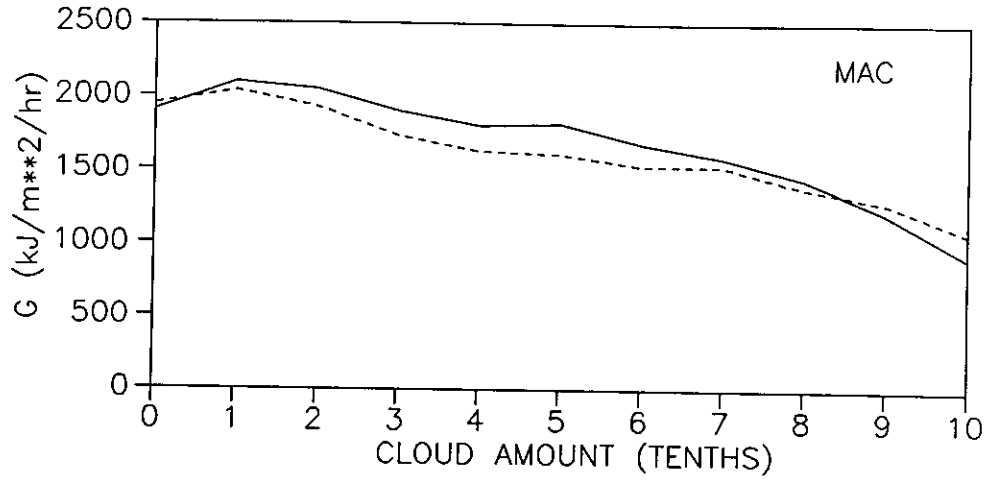


GLOBAL RADIATION AND CLOUD  
MONTREAL

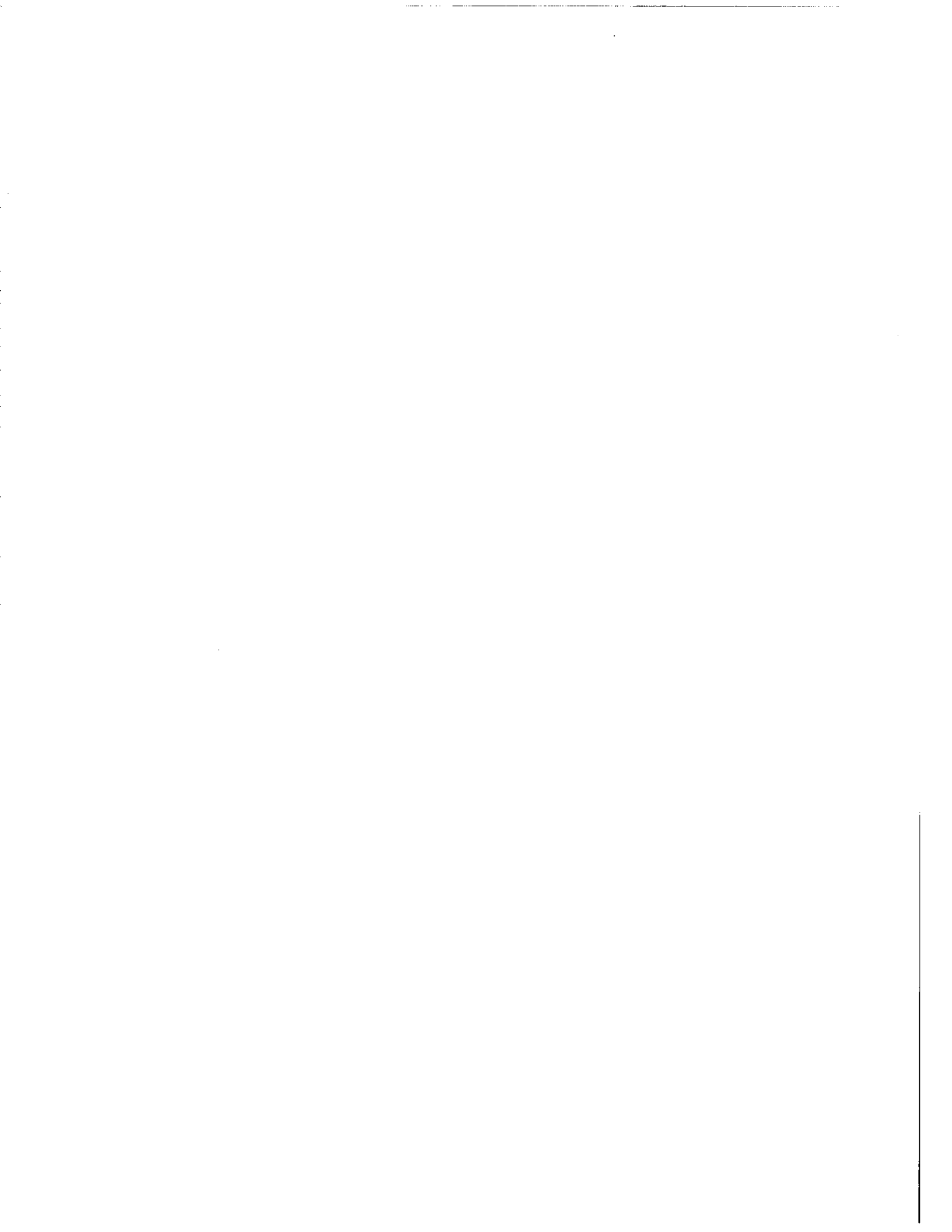




GLOBAL RADIATION AND CLOUD  
ALBUQUERQUE

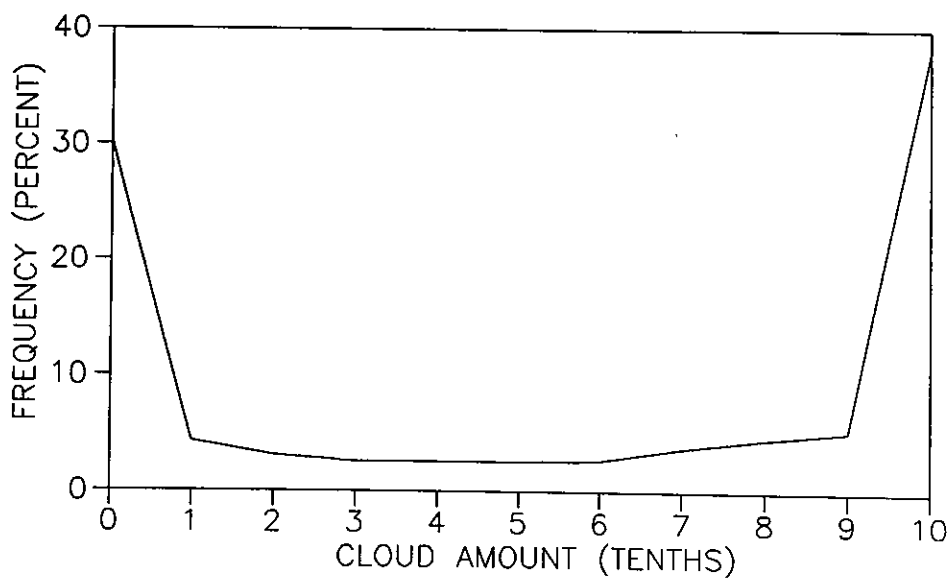
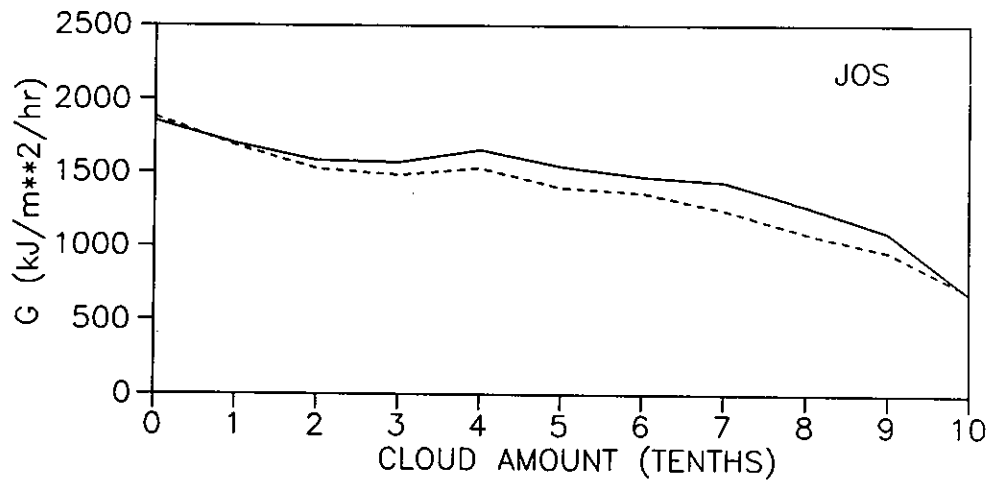
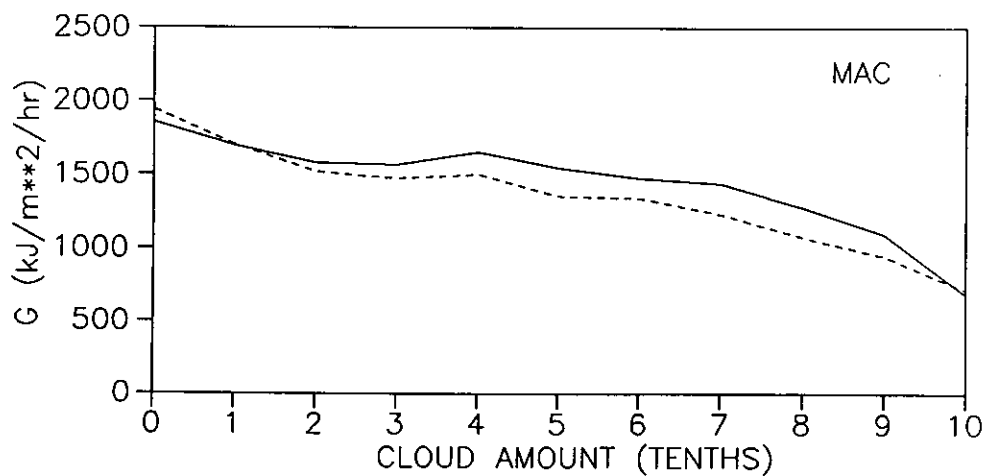






# GLOBAL RADIATION AND CLOUD

## MEDFORD



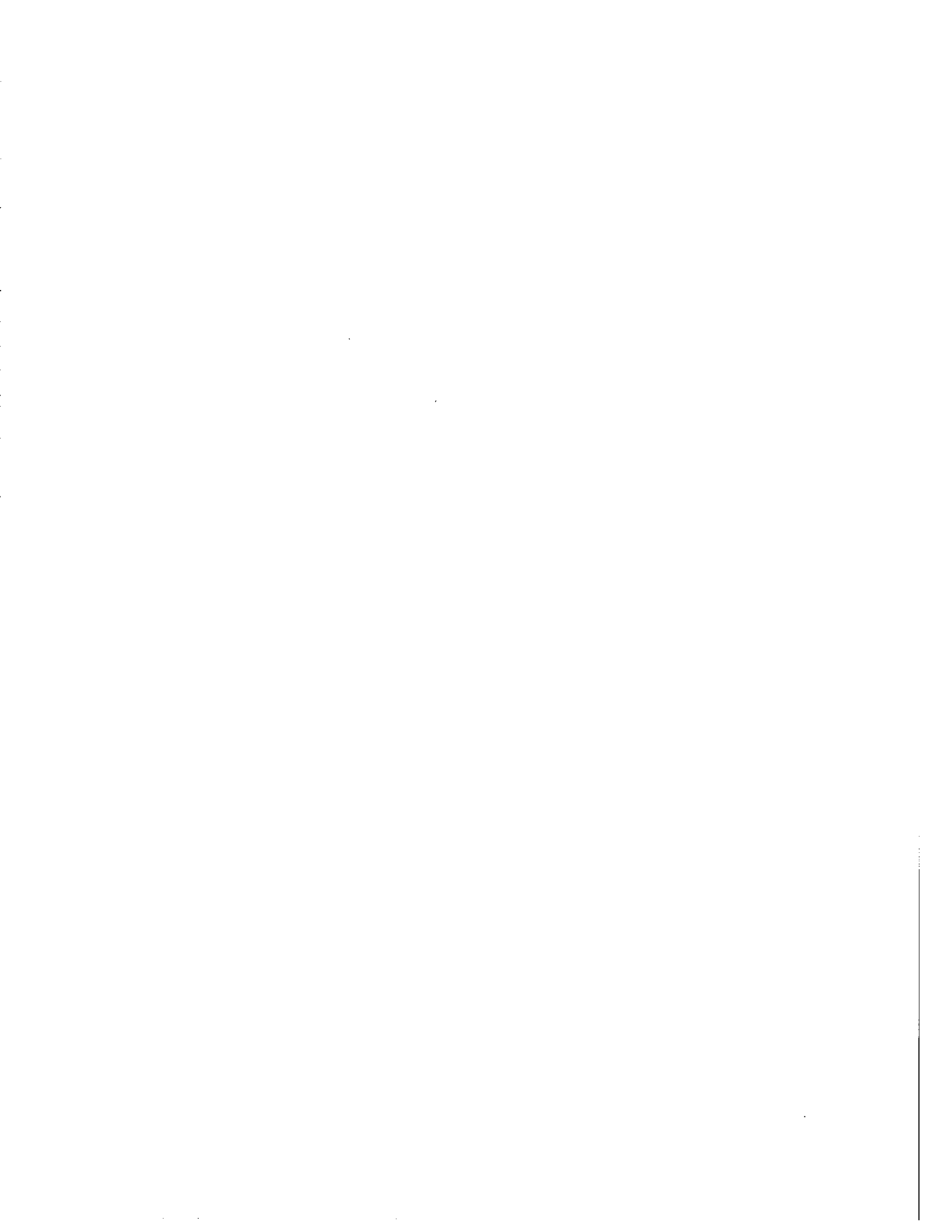
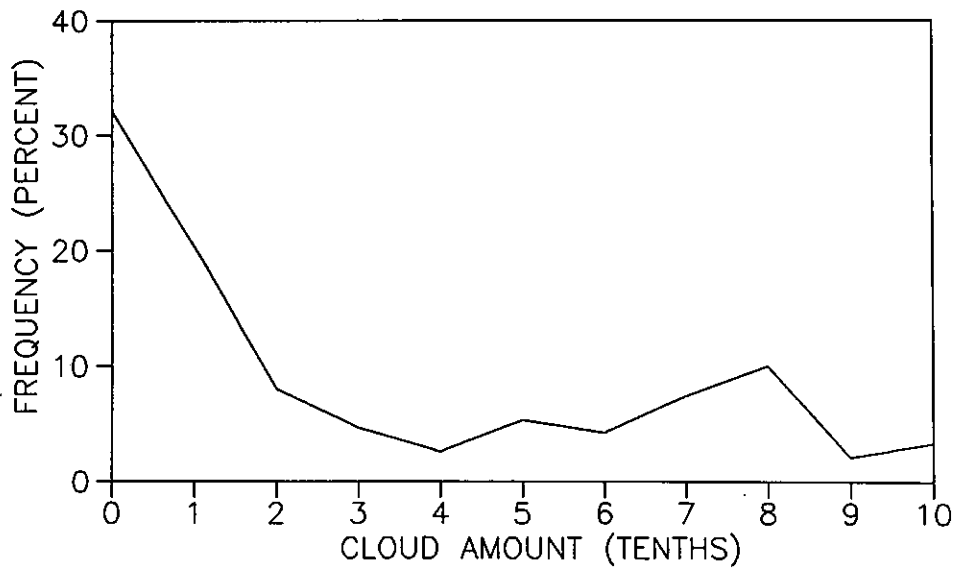
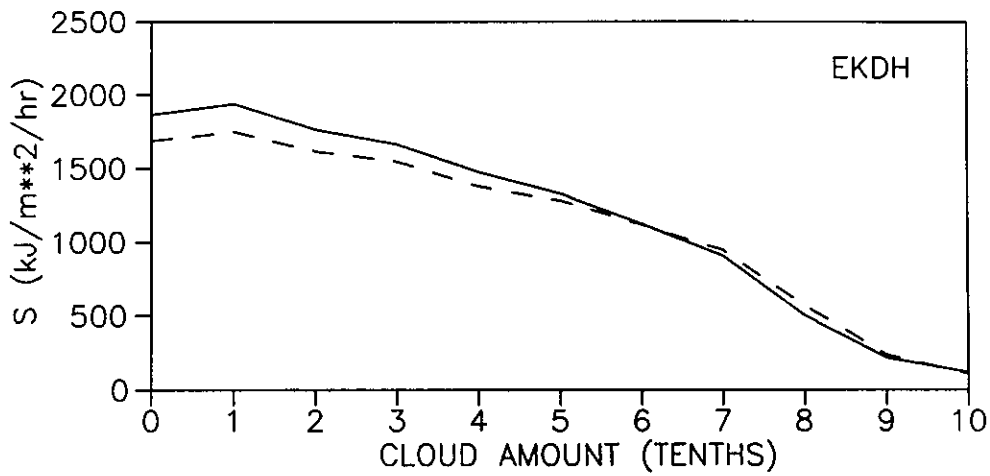
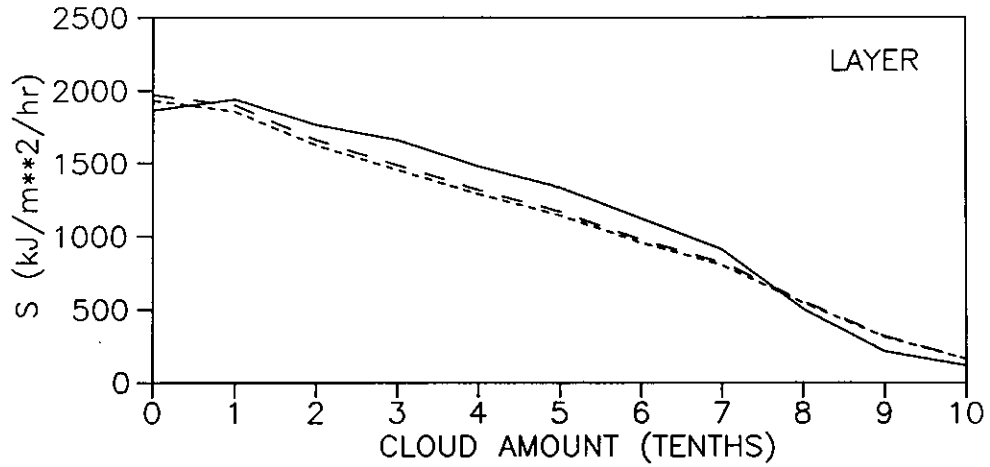
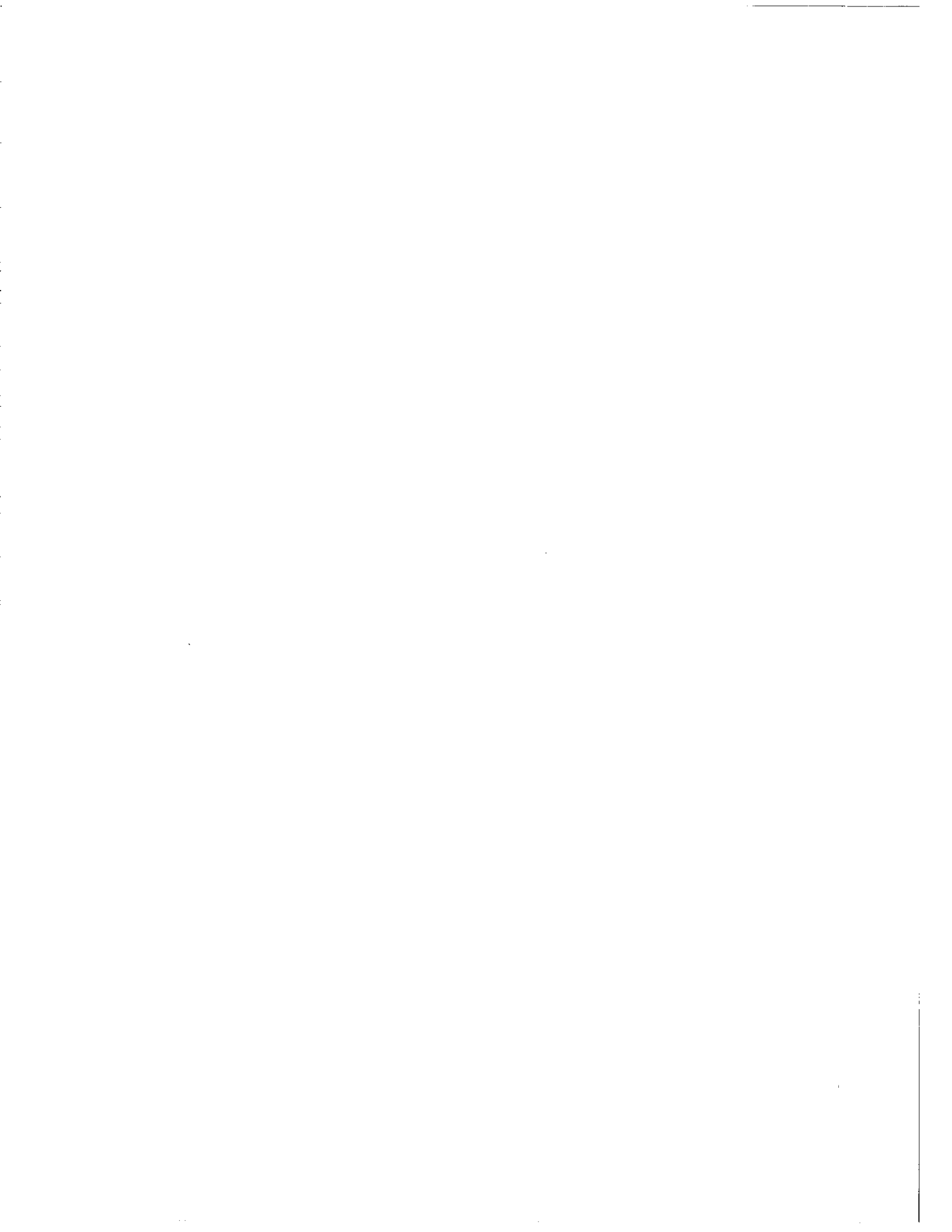


Figure 4b Model performance and cloudiness: a comparison of measured diffuse and direct beam radiation (solid line) with model estimates (dashed lines) for selected stations. The longer dashed line represents the MAC estimates and the shorter dashed line the JOS estimates in the layer model diagram



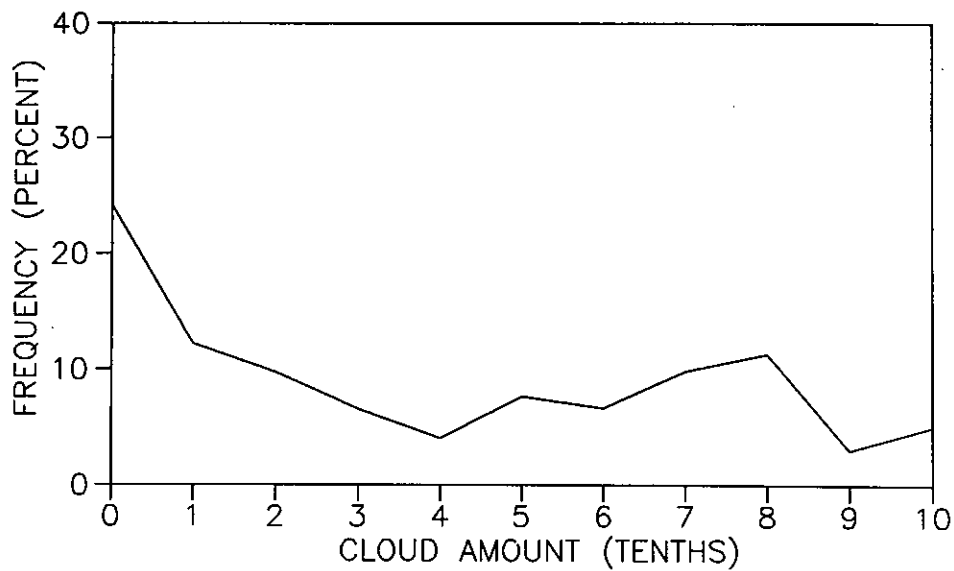
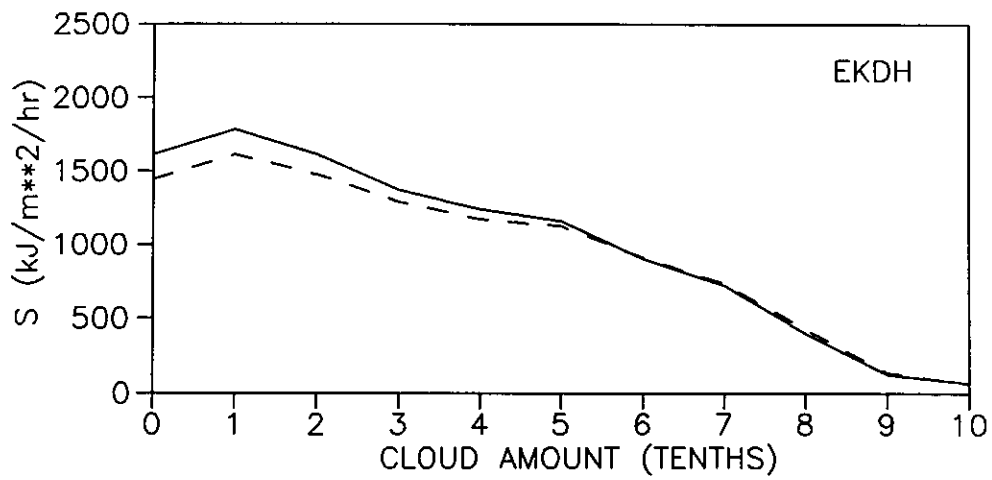
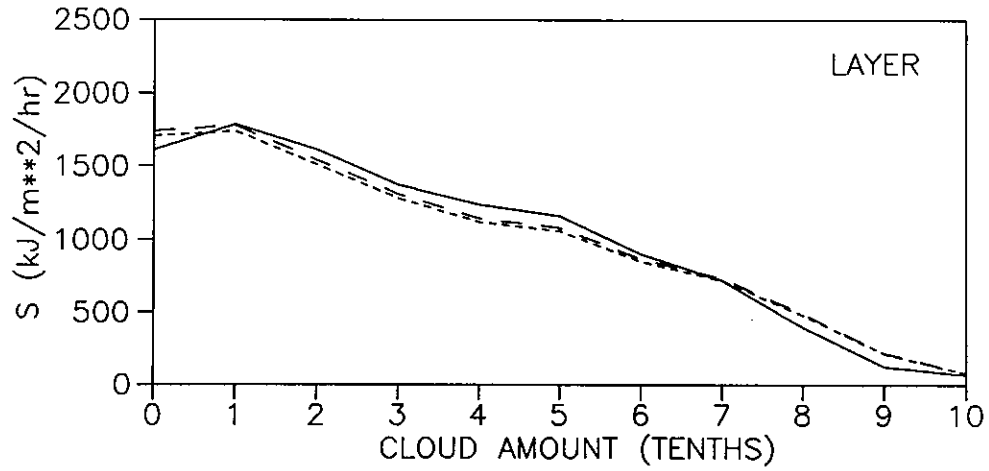
DIRECT BEAM RADIATION AND CLOUD  
ALICE SPRINGS



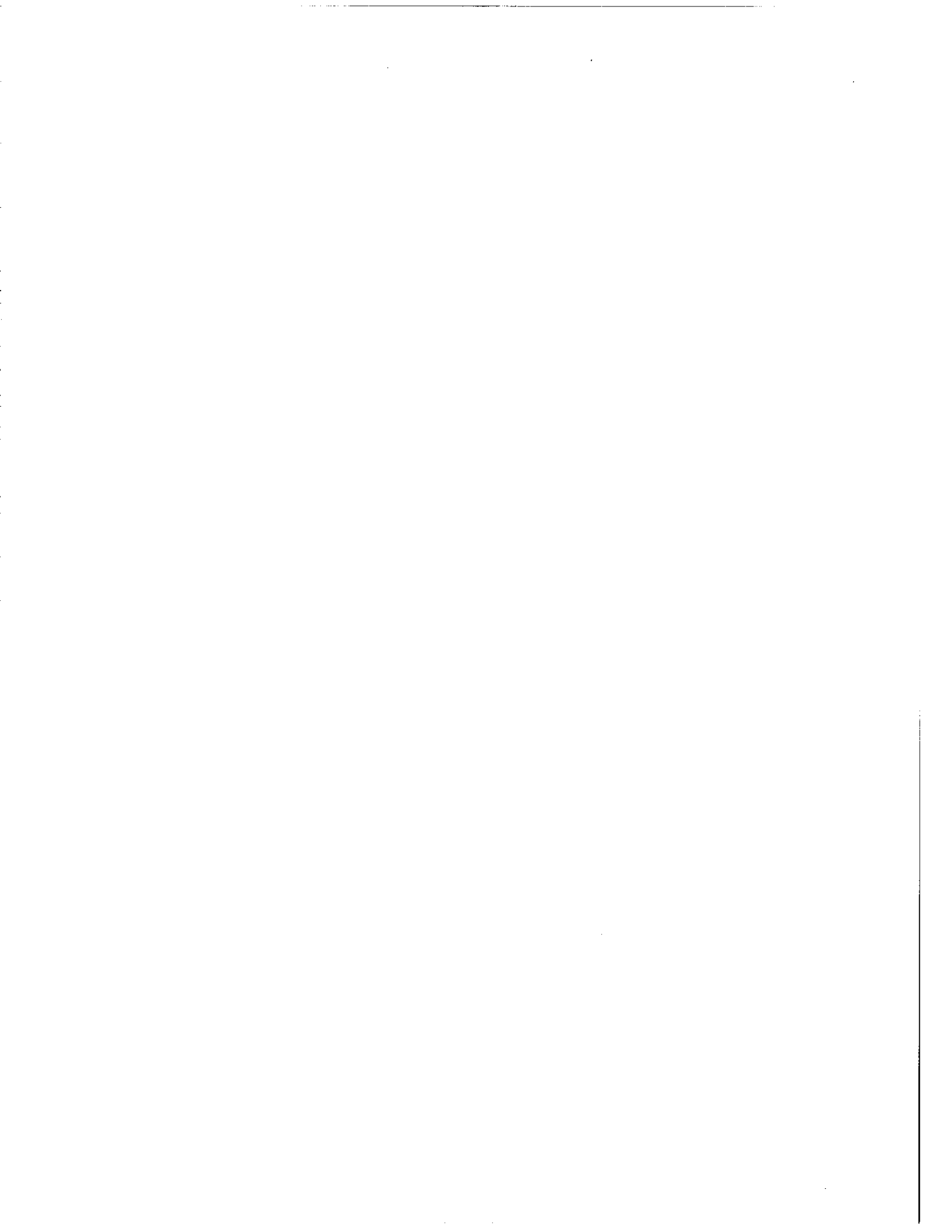


# DIRECT BEAM RADIATION AND CLOUD

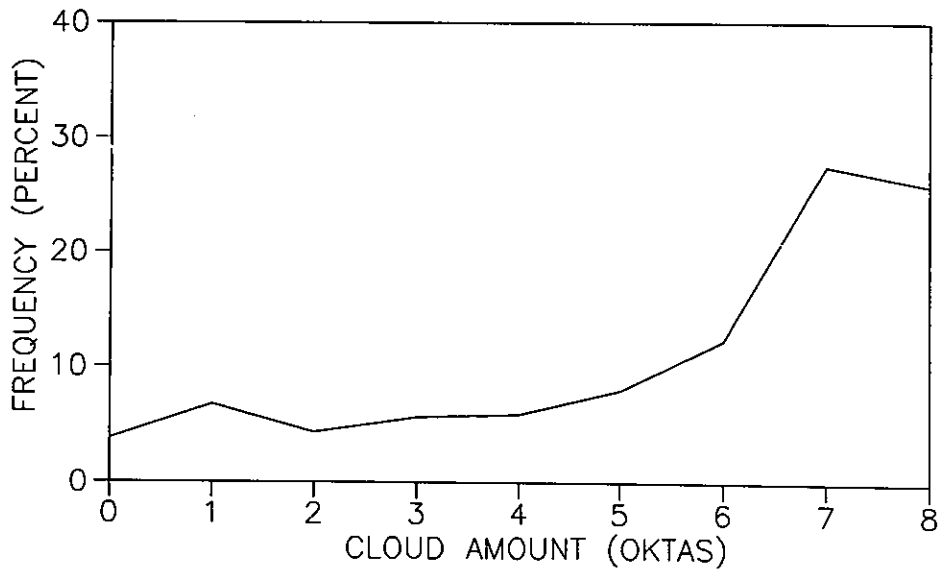
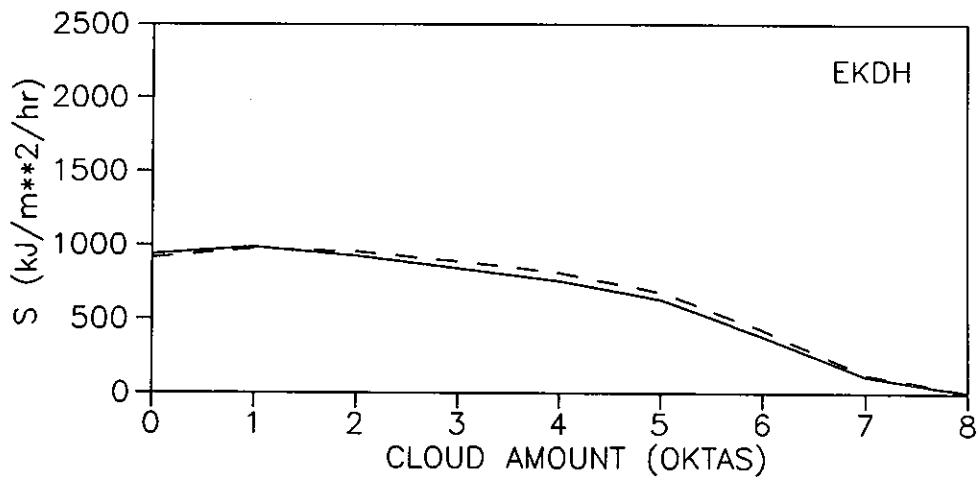
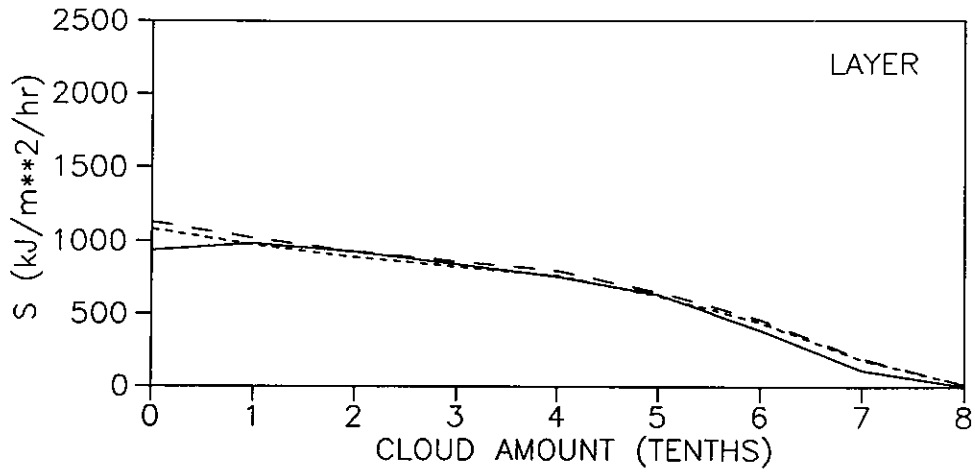
## MILDURA

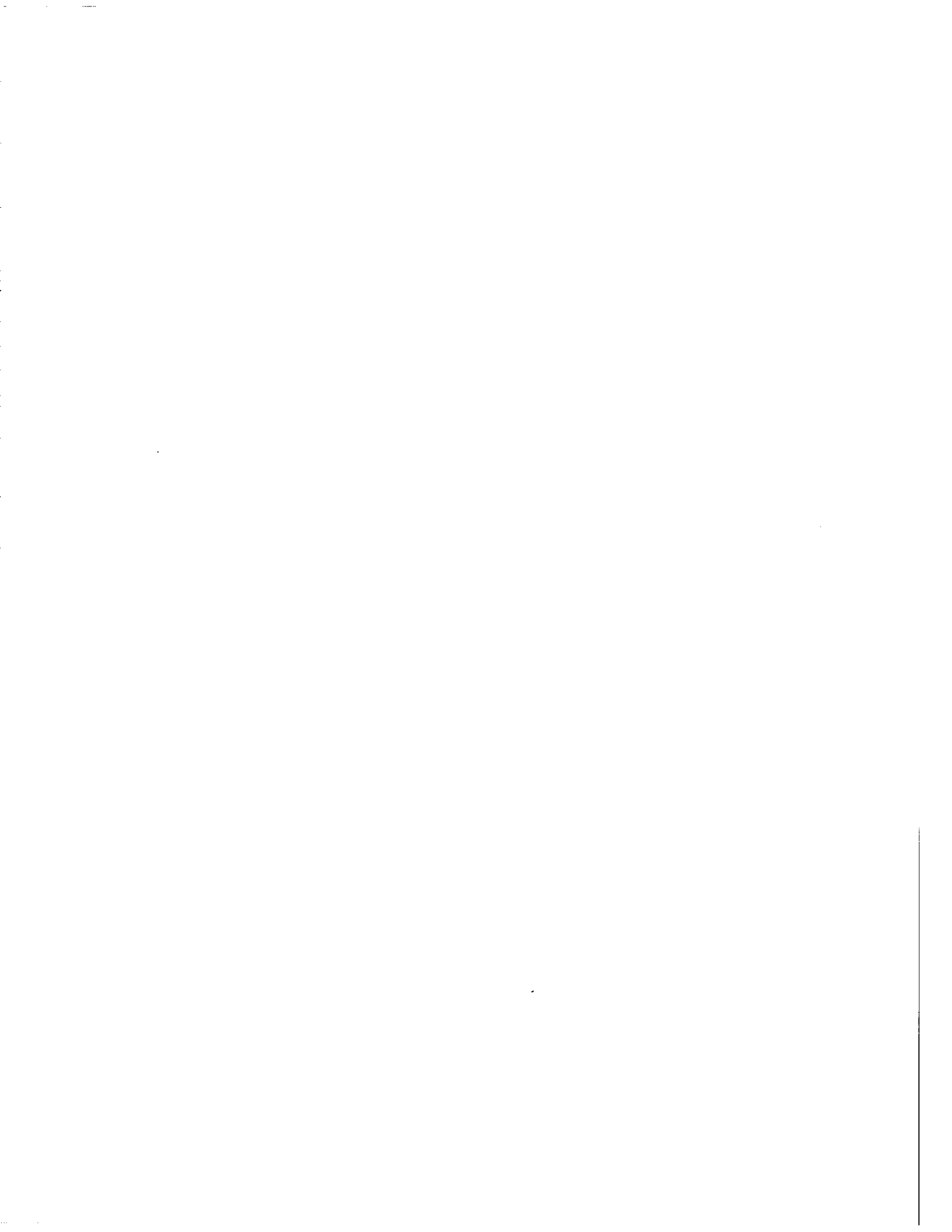






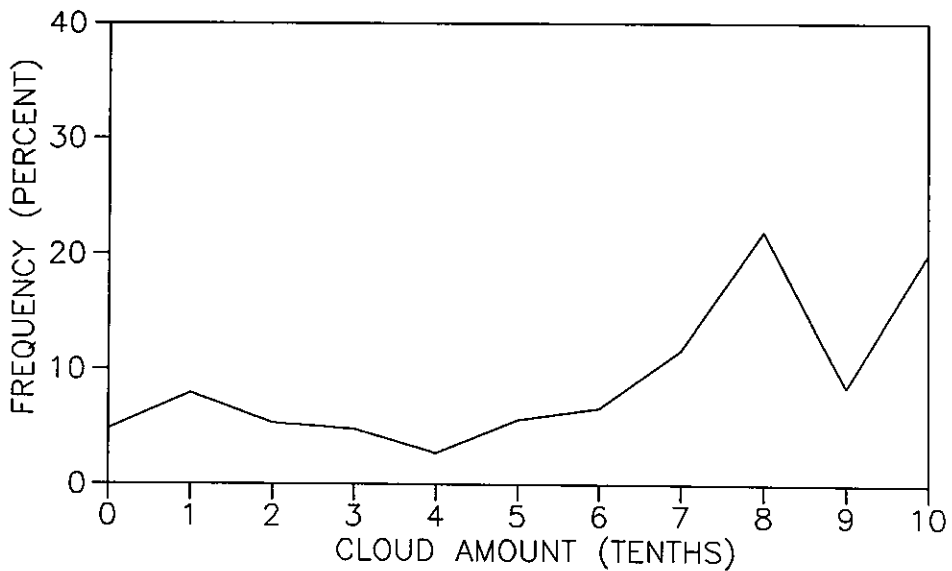
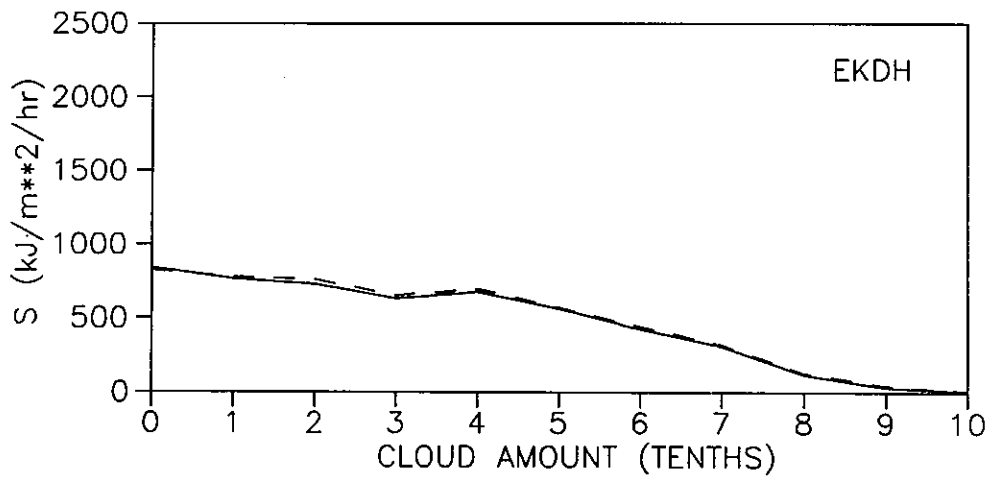
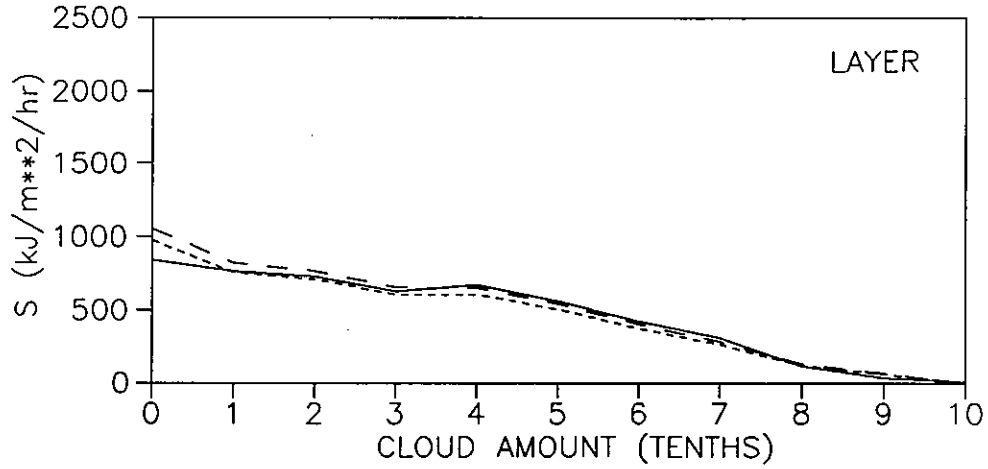
DIRECT BEAM RADIATION AND CLOUD  
HAMBURG

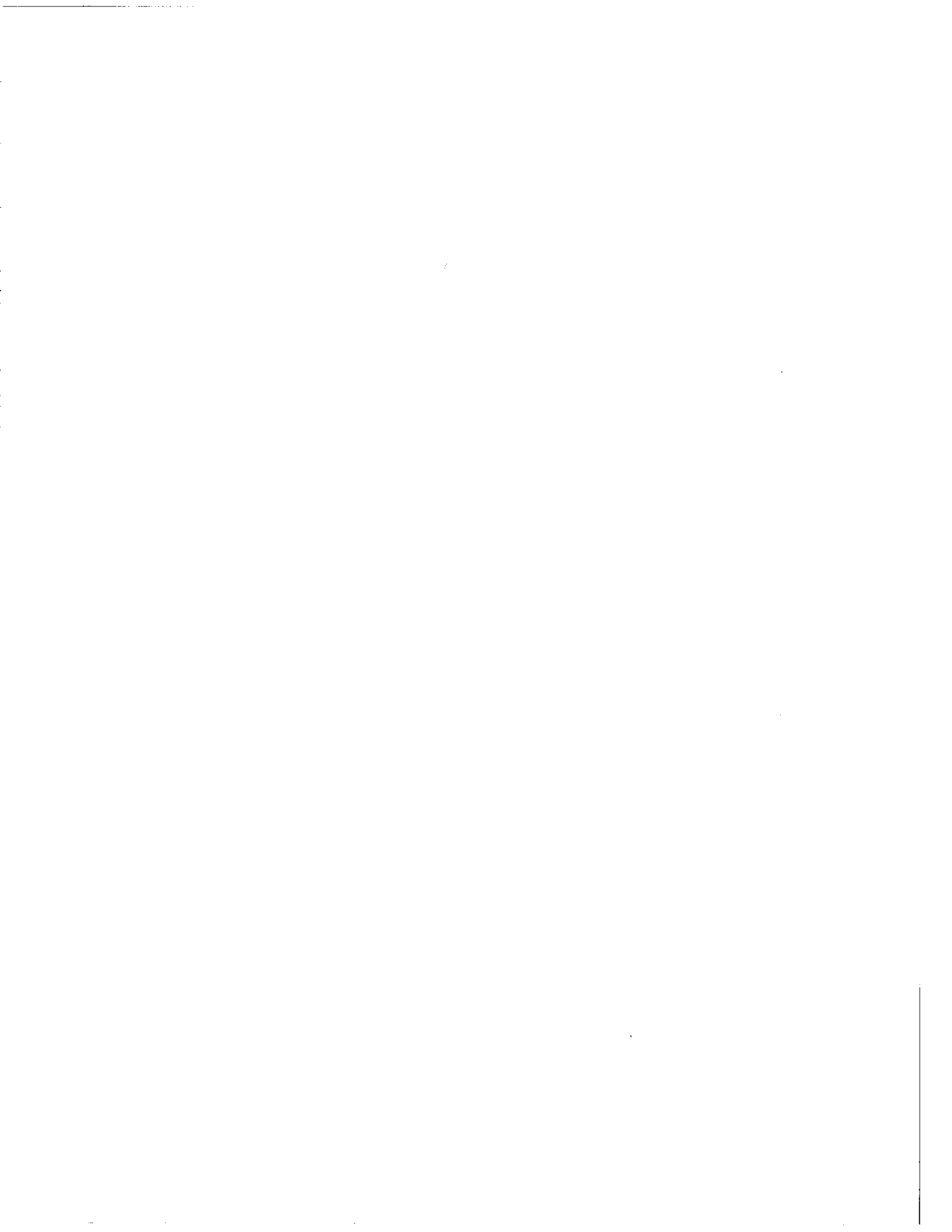




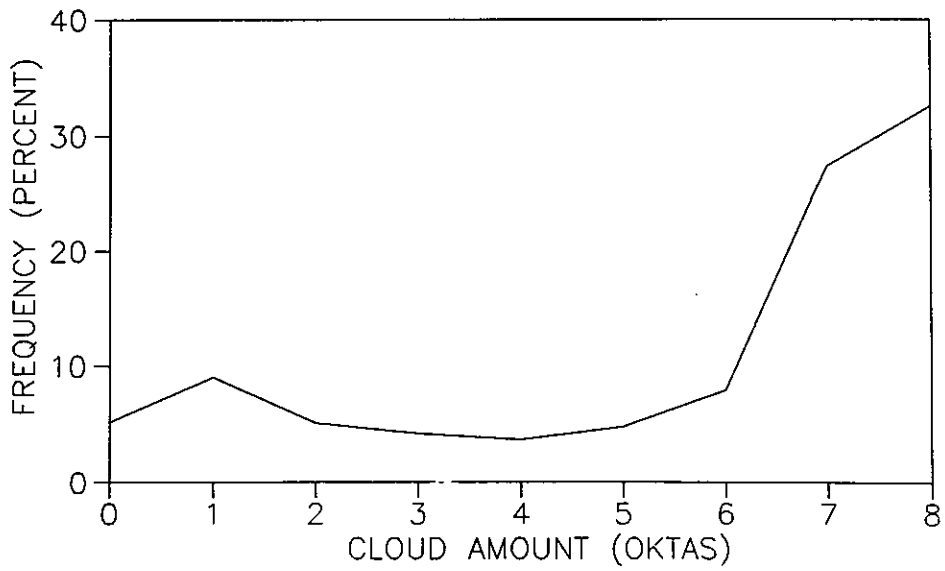
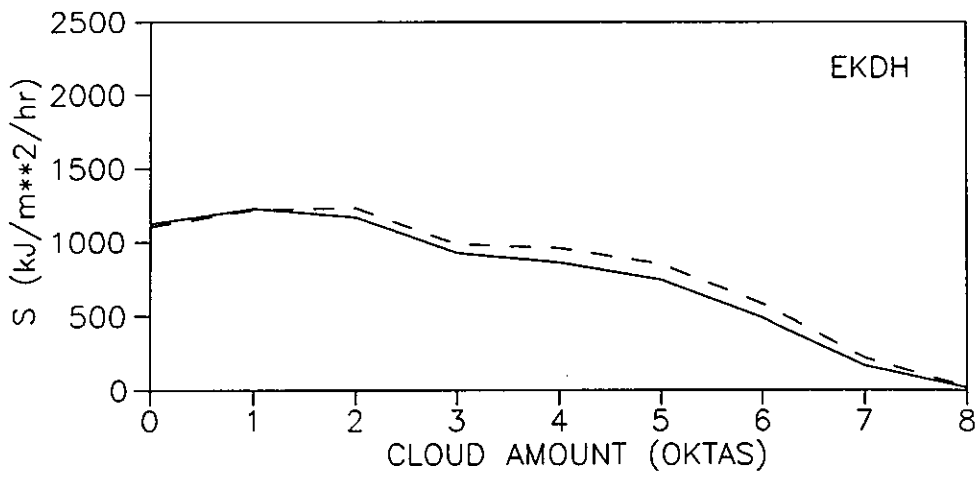
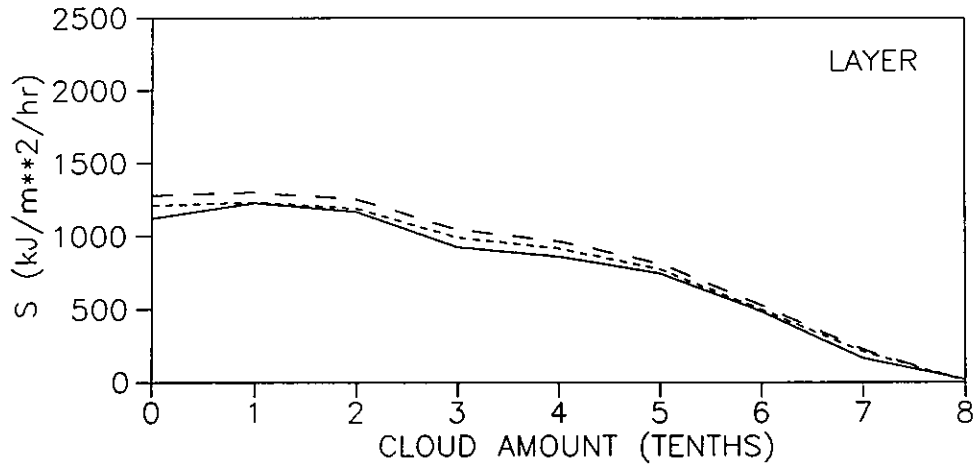
DIRECT BEAM RADIATION AND CLOUD

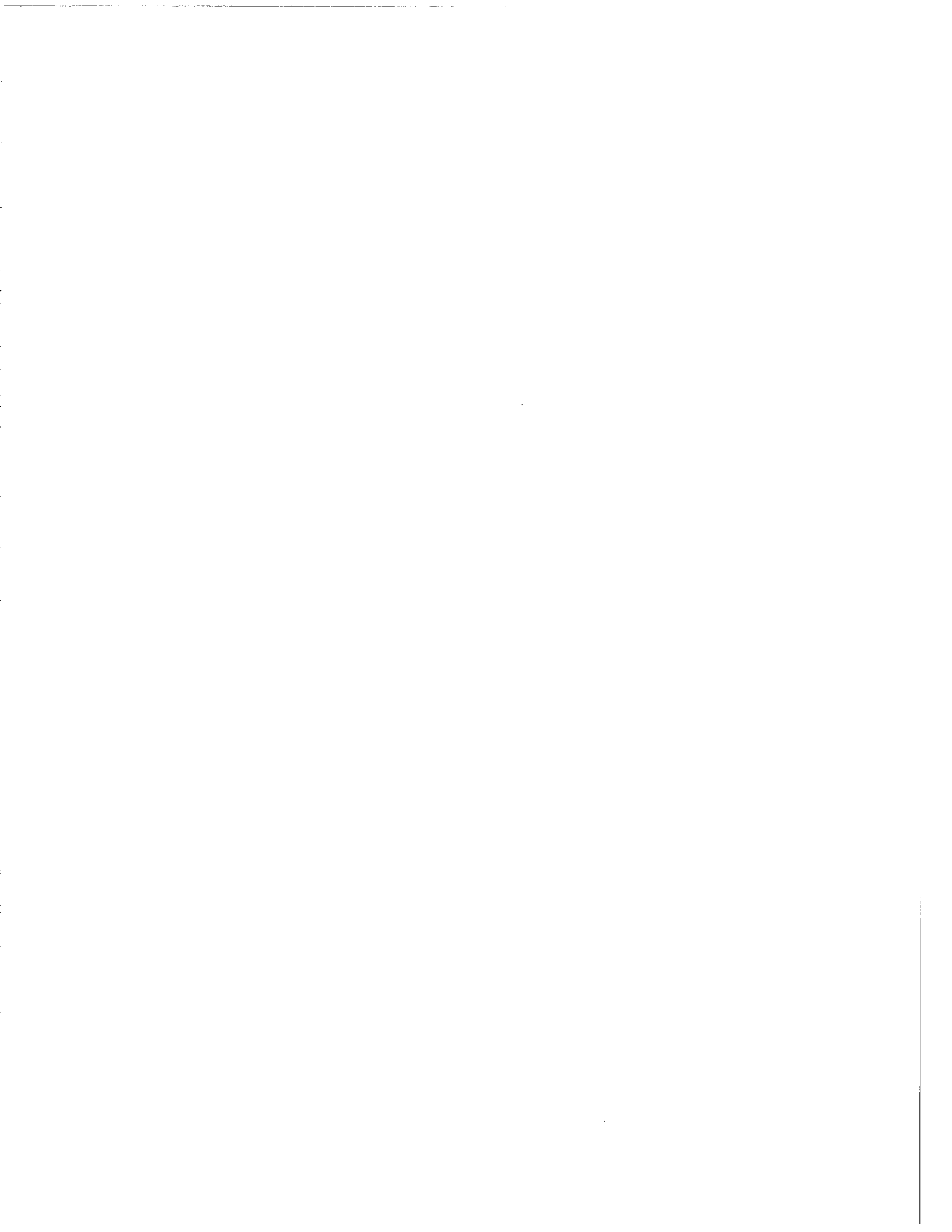
KEW



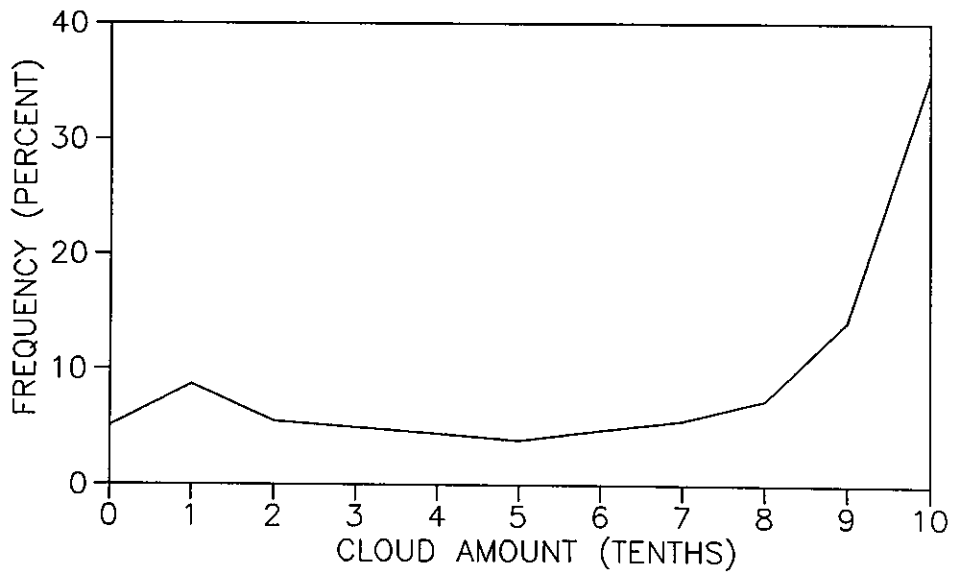
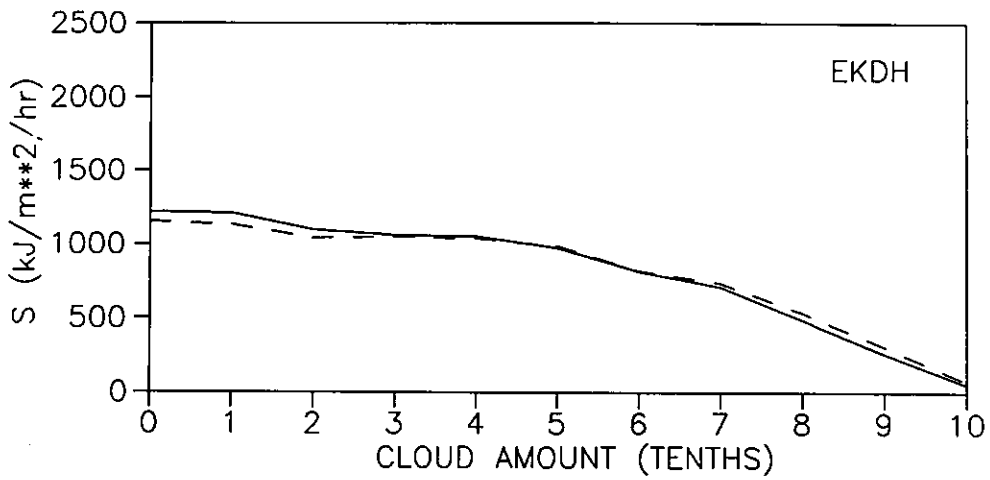
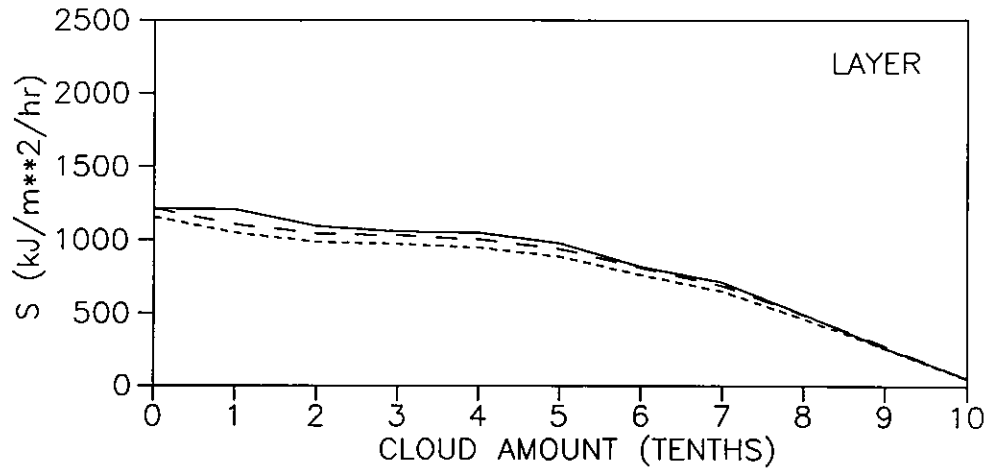


DIRECT BEAM RADIATION AND CLOUD  
ZURICH

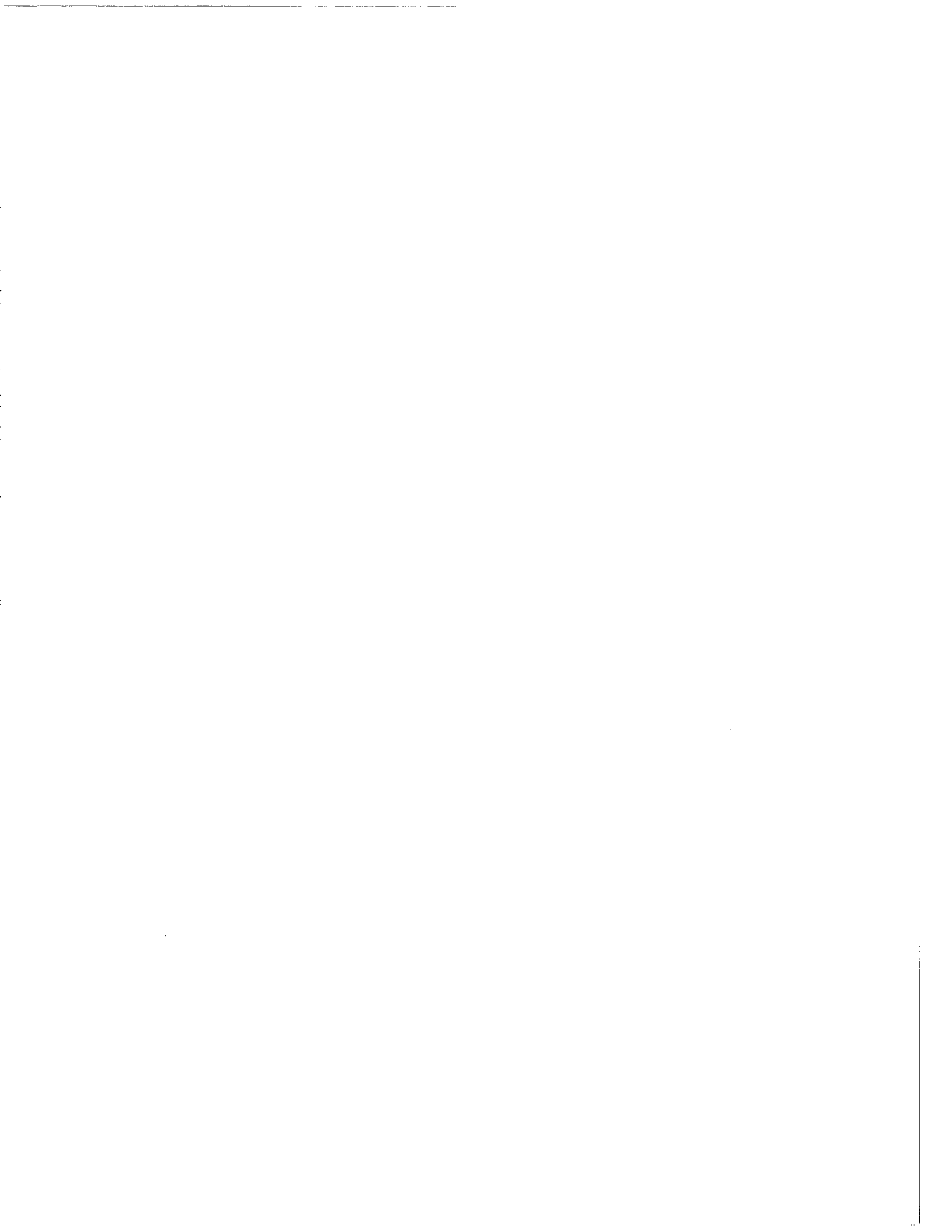




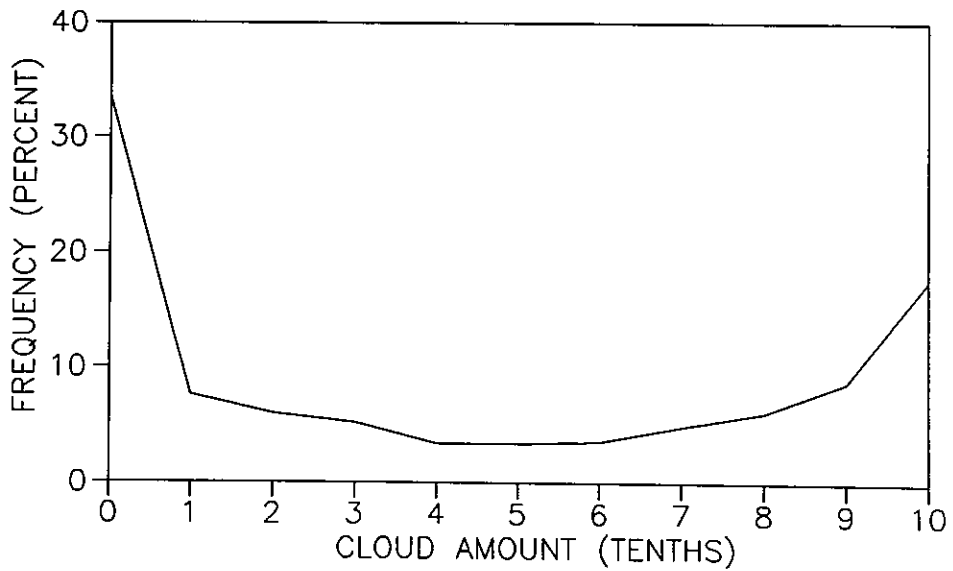
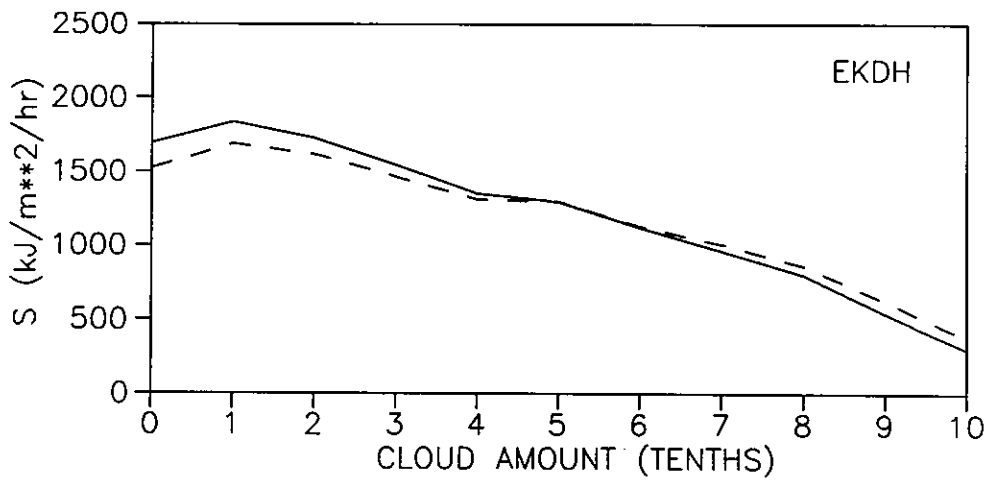
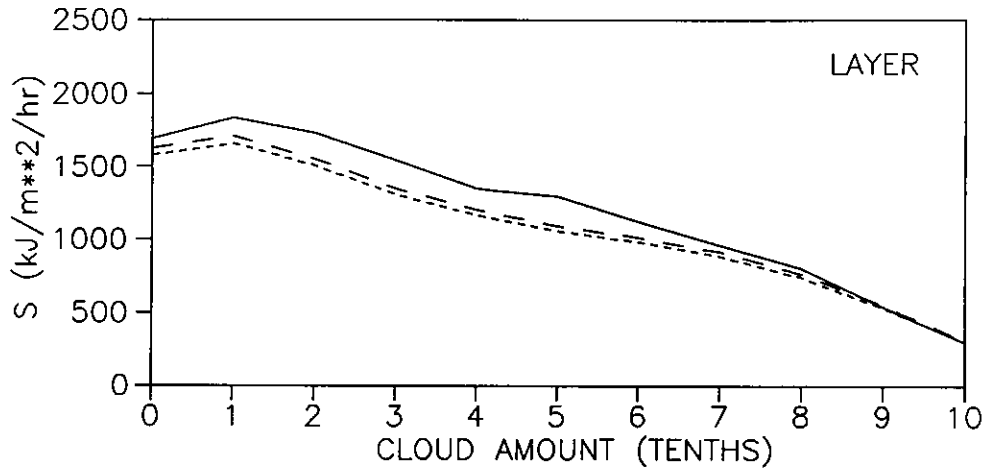
DIRECT BEAM RADIATION AND CLOUD  
MONTREAL

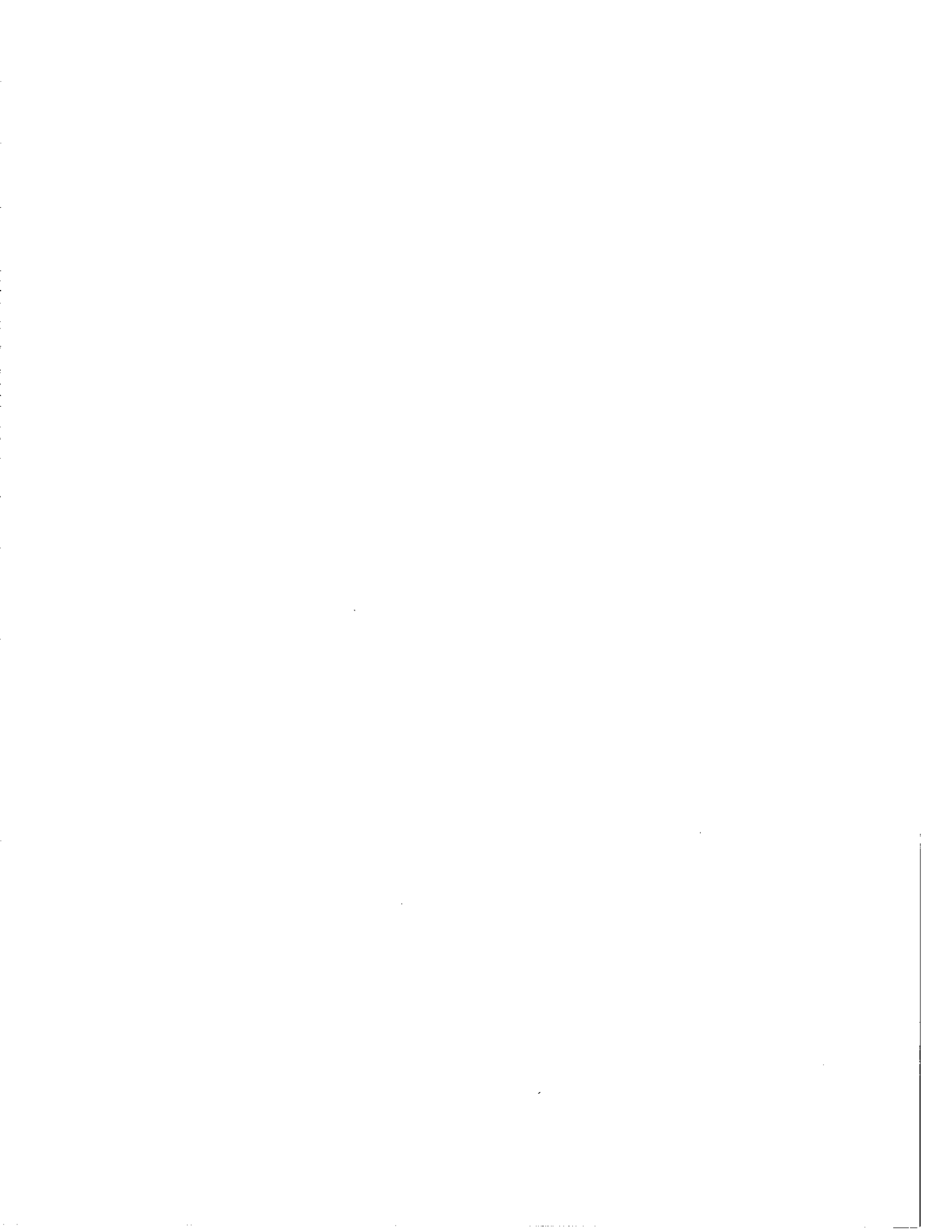




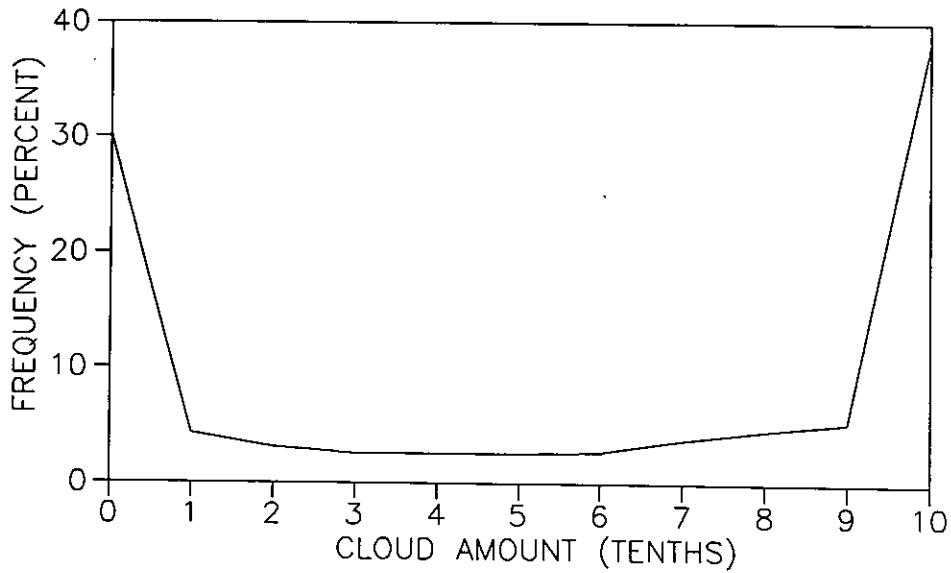
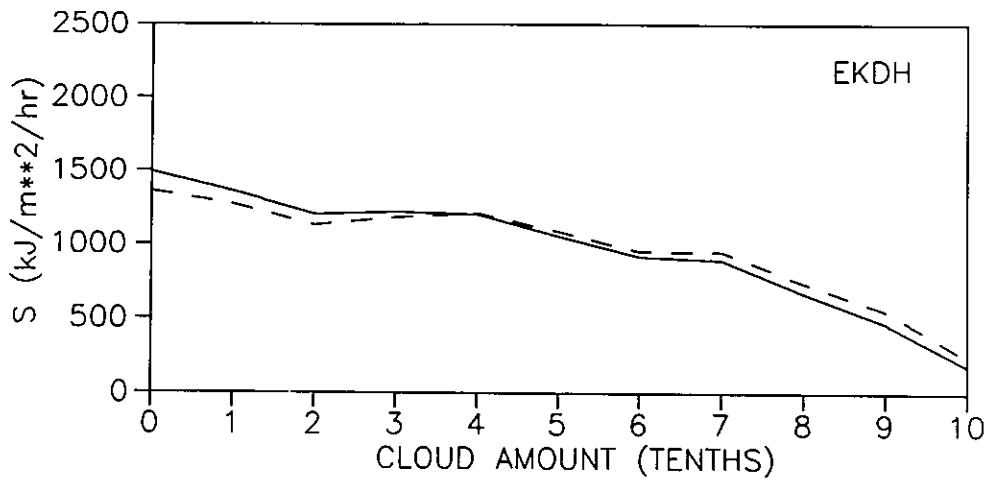
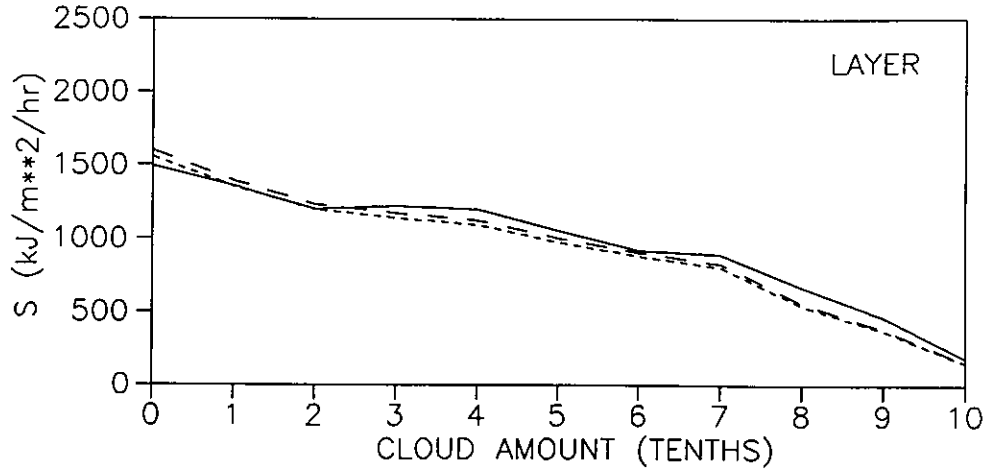


DIRECT BEAM RADIATION AND CLOUD  
ALBUQUERQUE



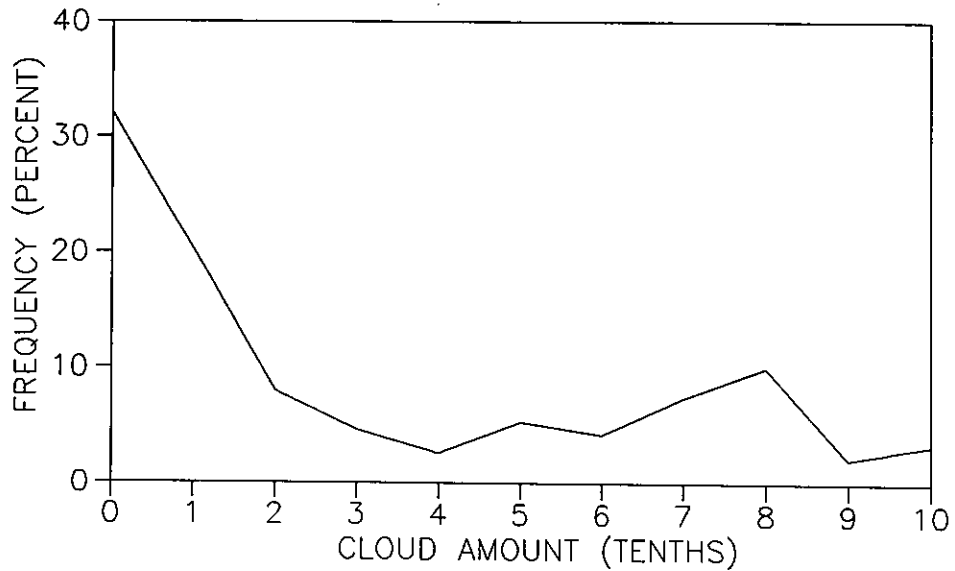
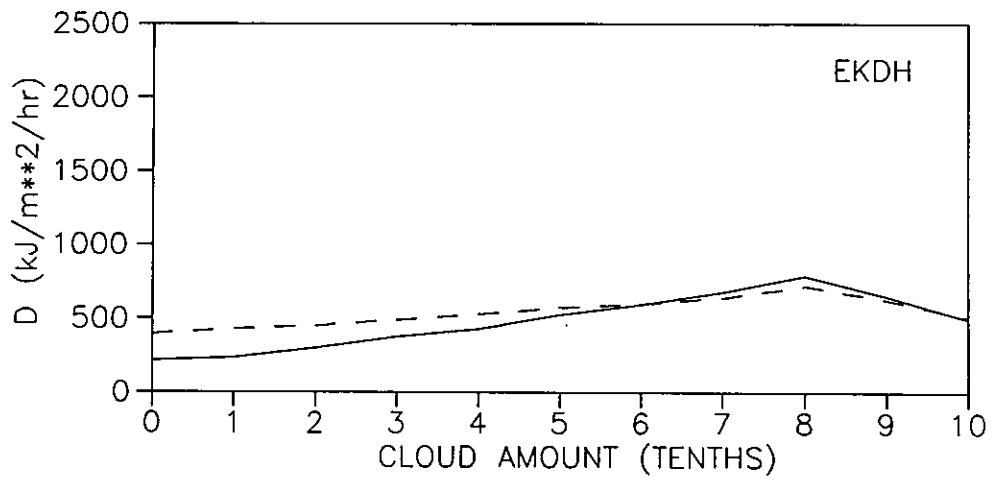
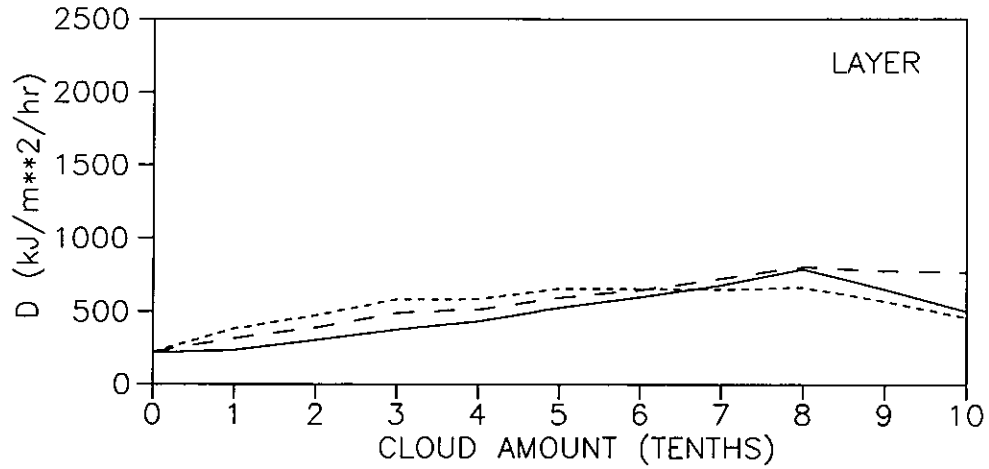


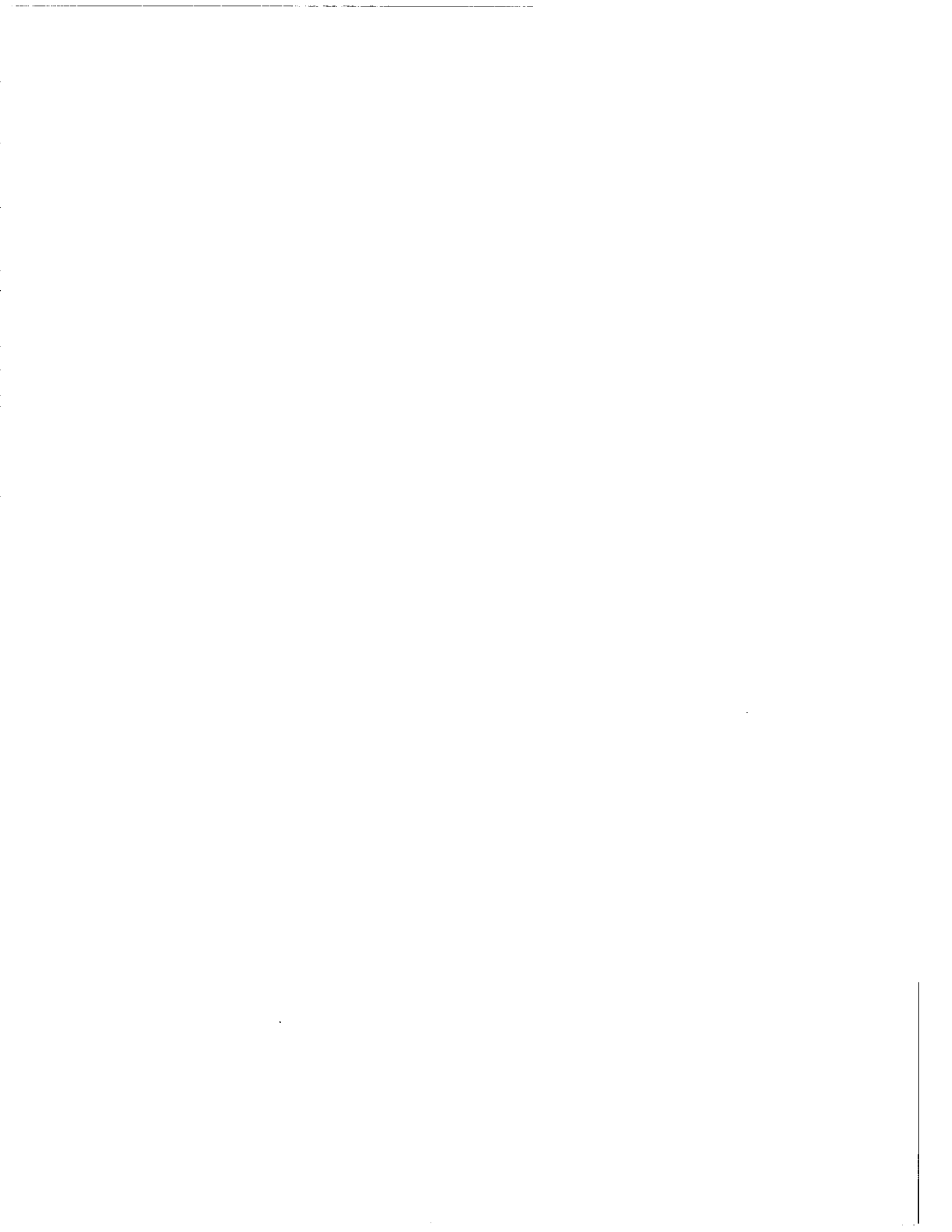
DIRECT BEAM RADIATION AND CLOUD  
MEDFORD





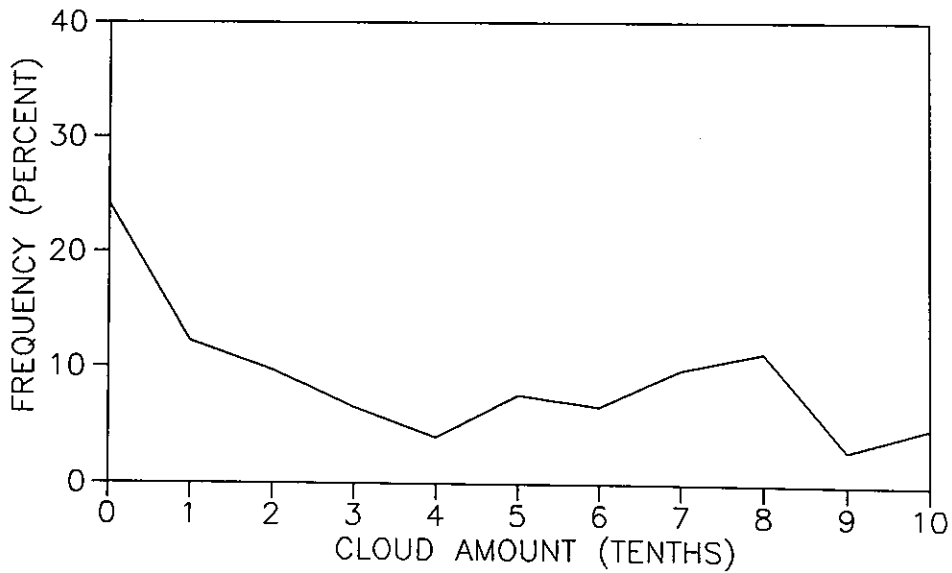
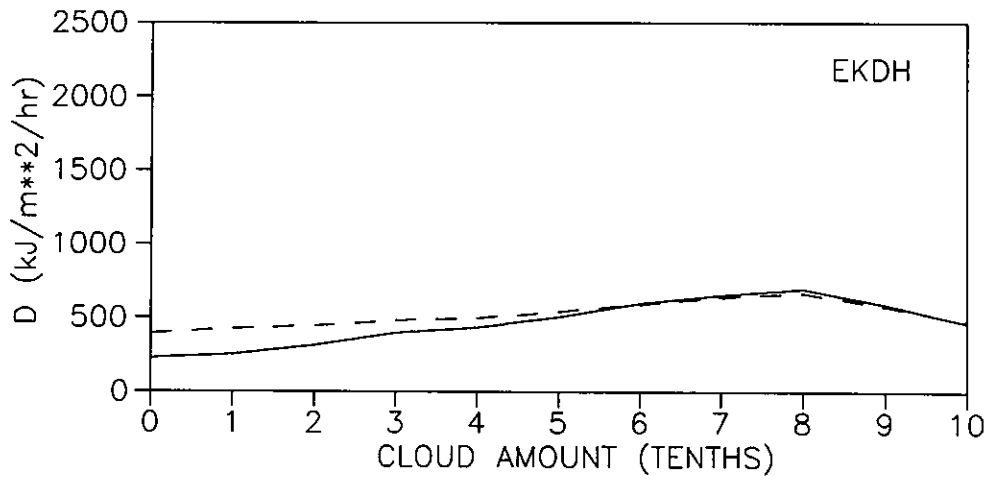
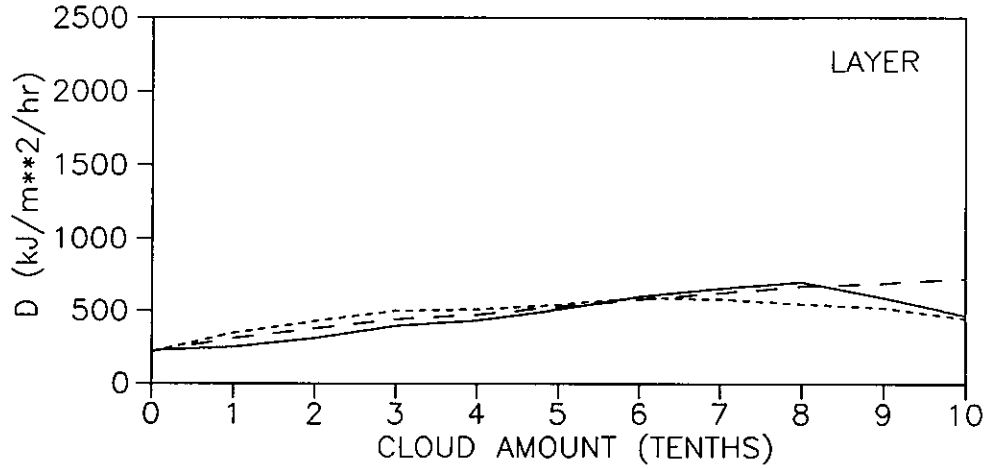
DIFFUSE RADIATION AND CLOUD  
ALICE SPRINGS



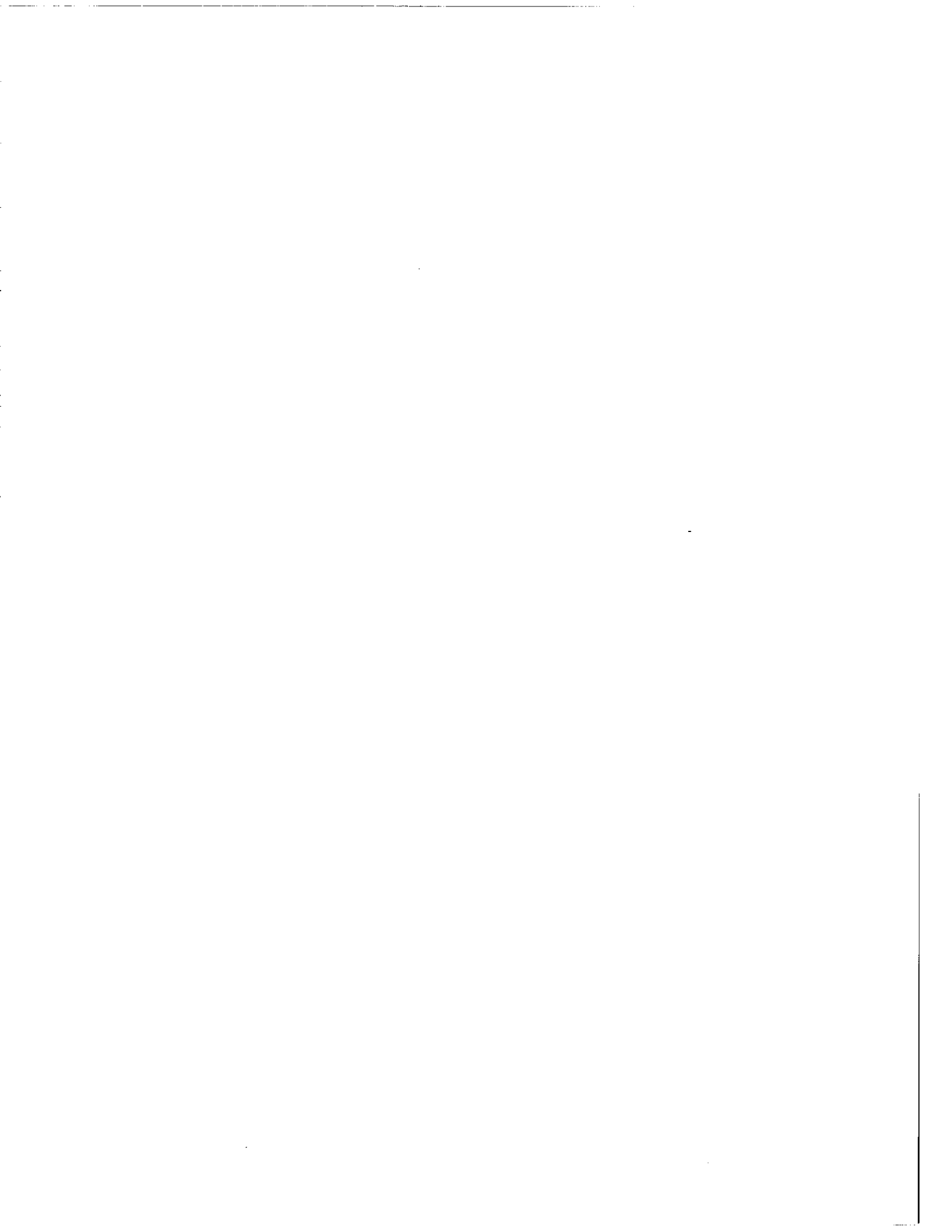


# DIFFUSE RADIATION AND CLOUD

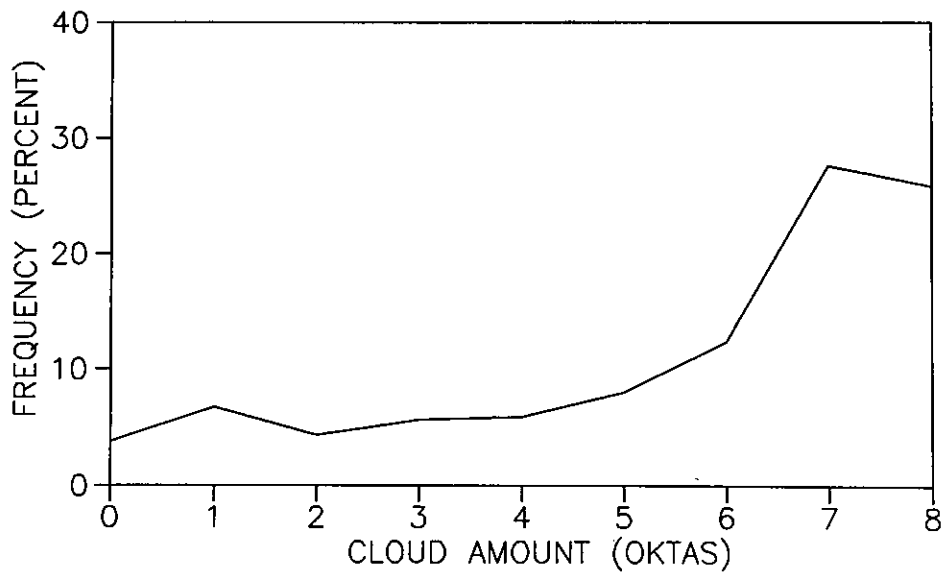
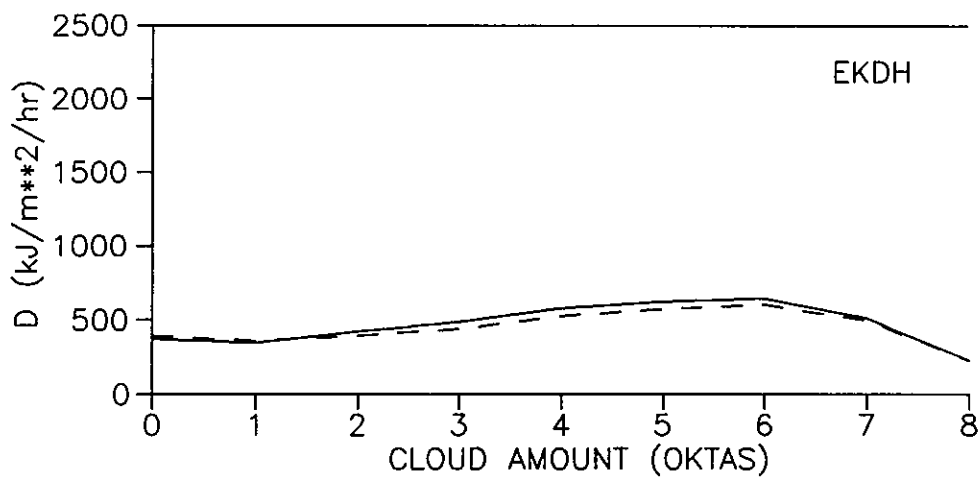
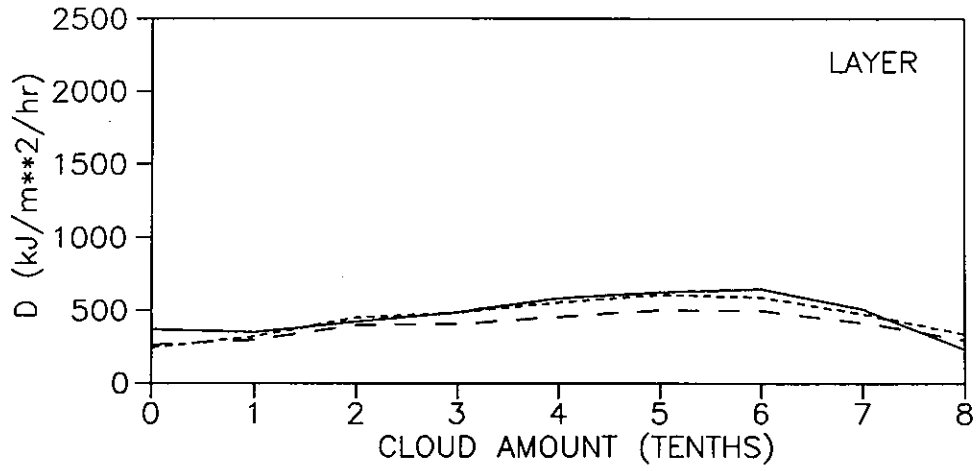
## MILDURA







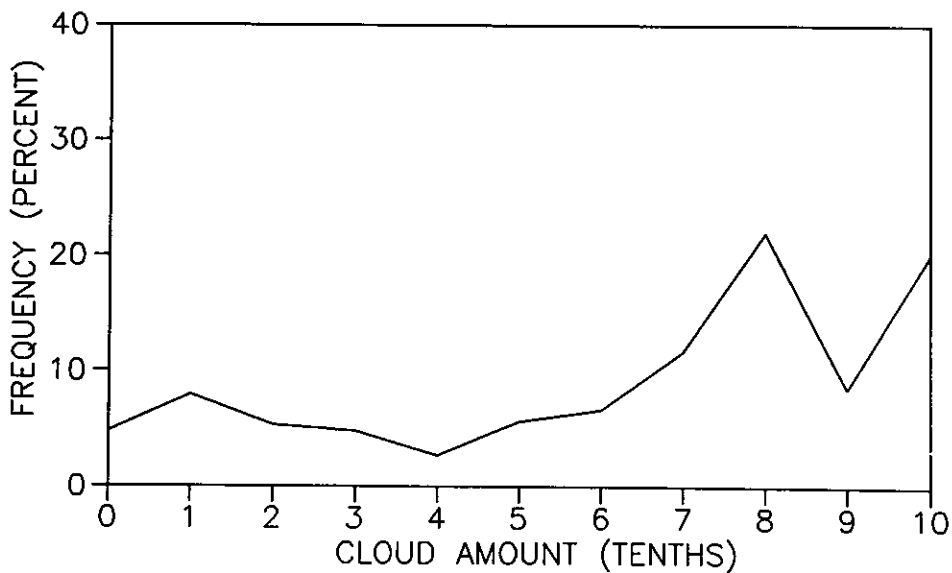
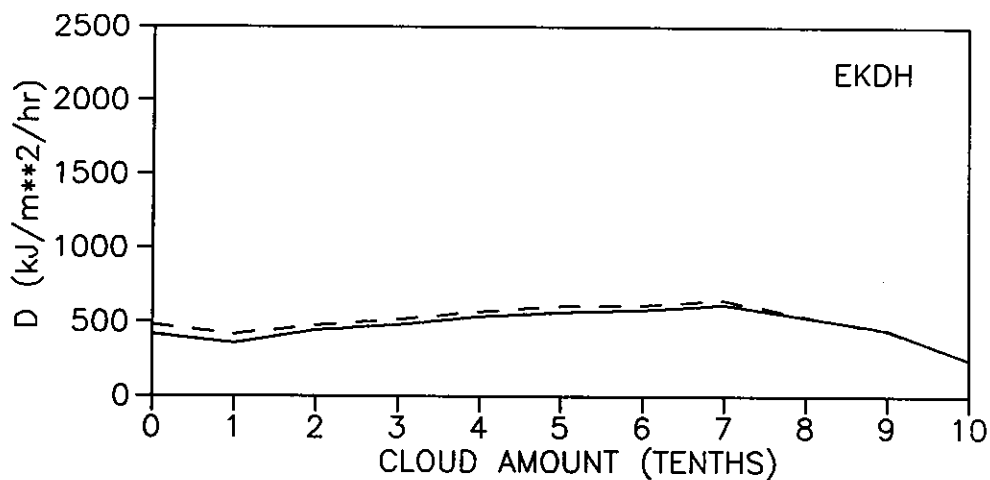
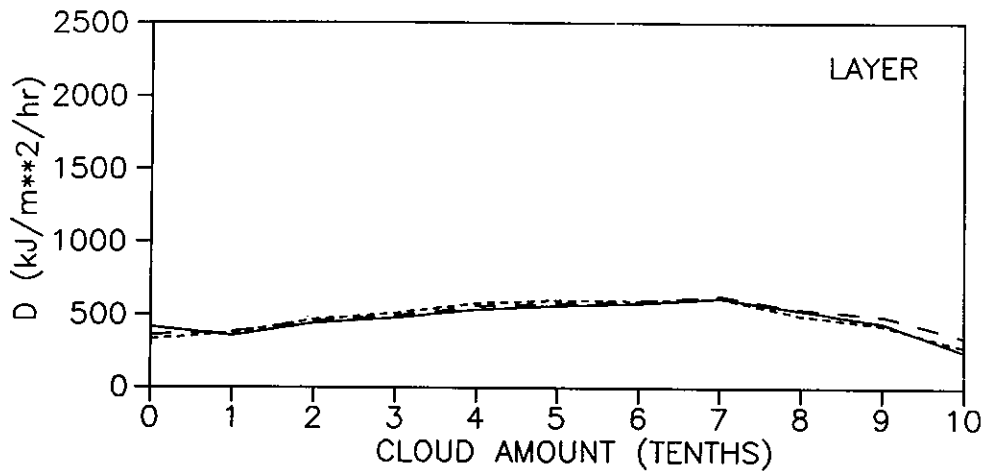
DIFFUSE RADIATION AND CLOUD  
HAMBURG

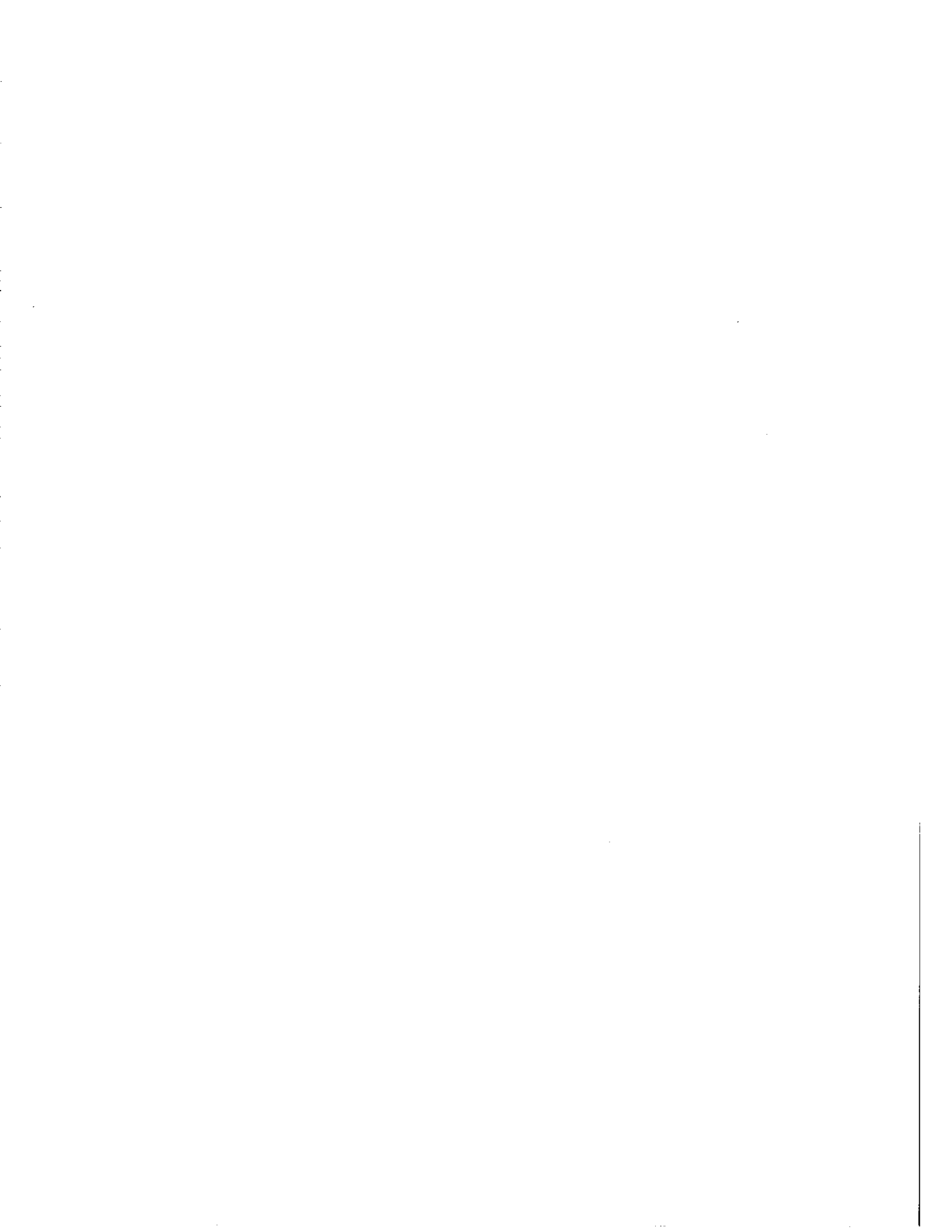




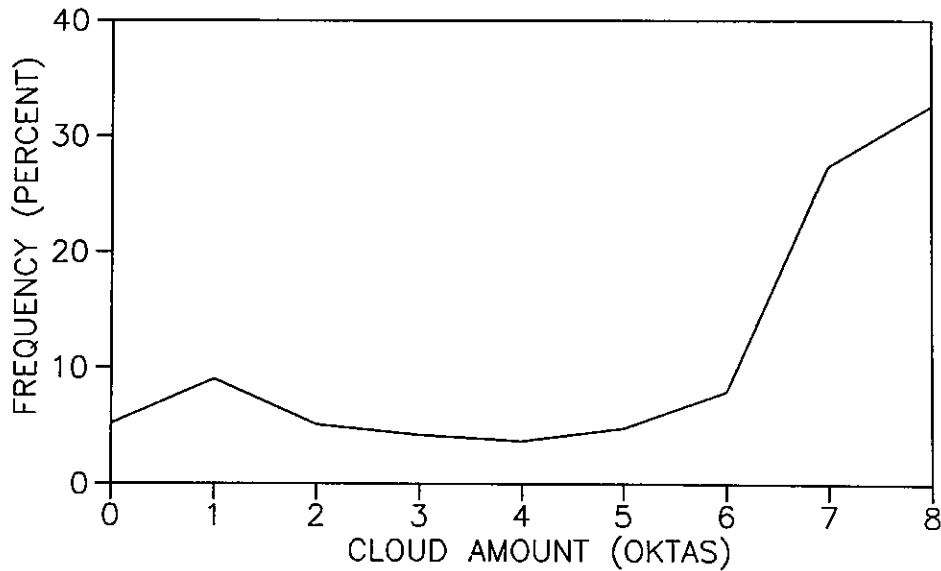
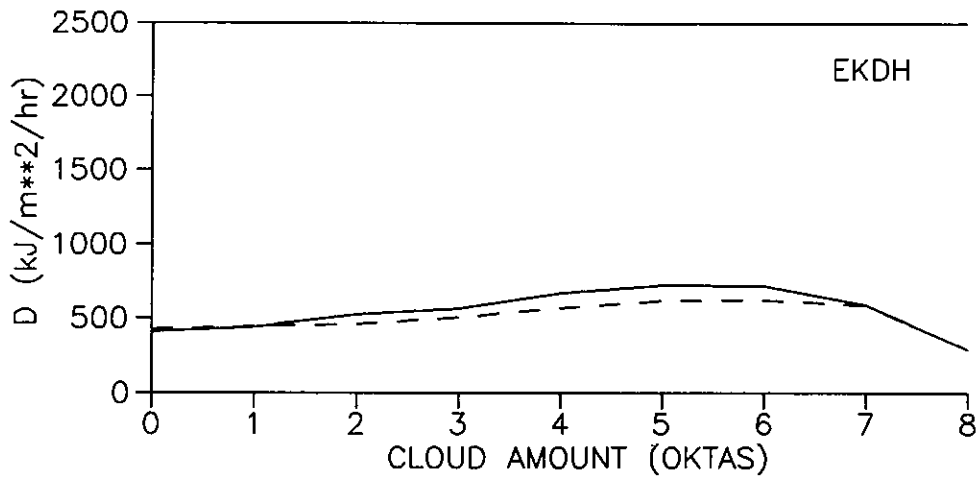
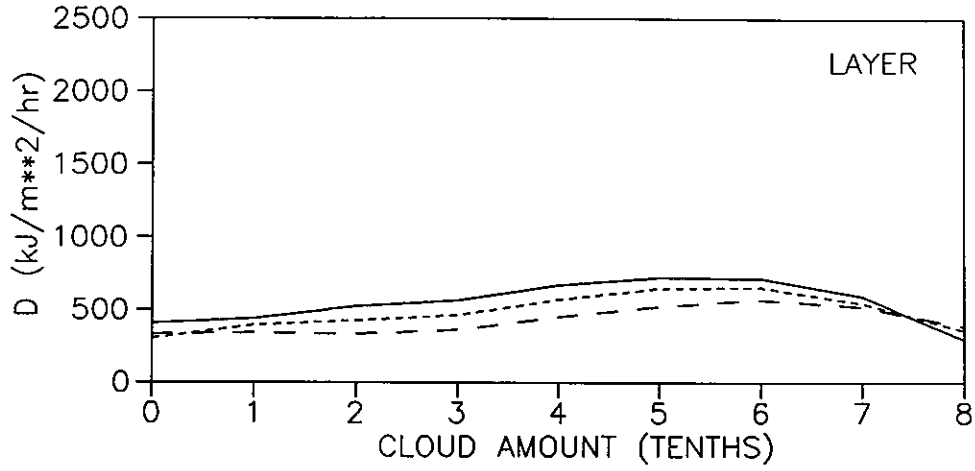
# DIFFUSE RADIATION AND CLOUD

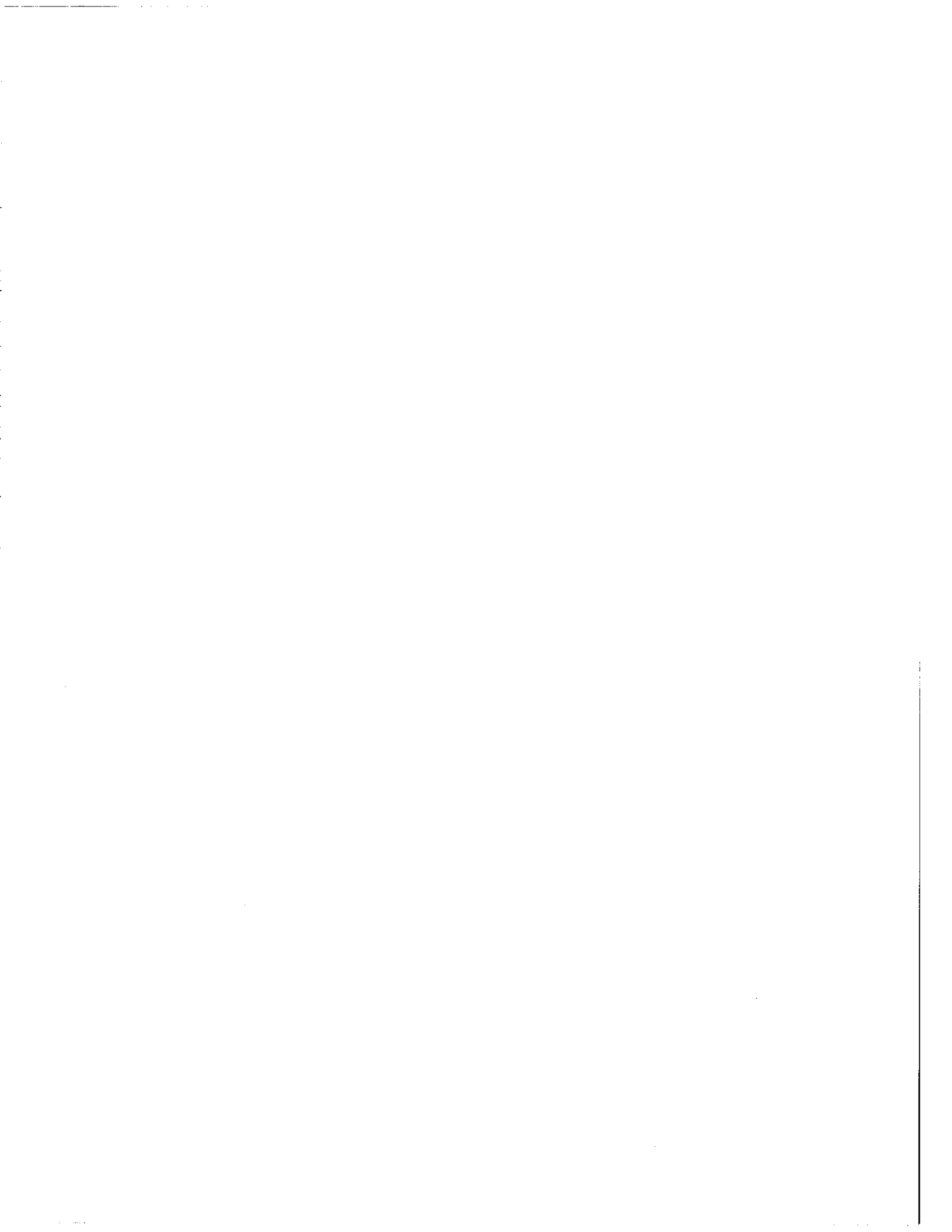
KEW



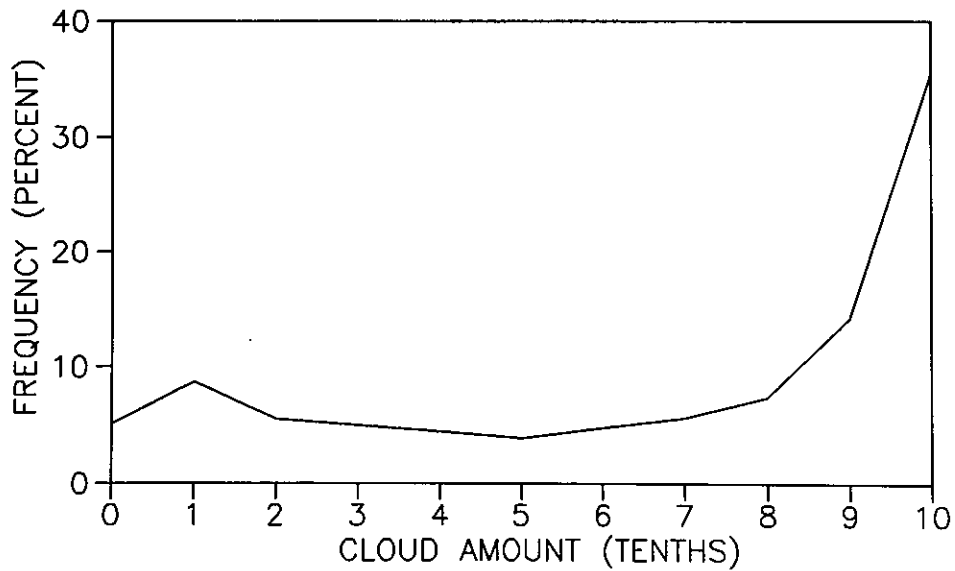
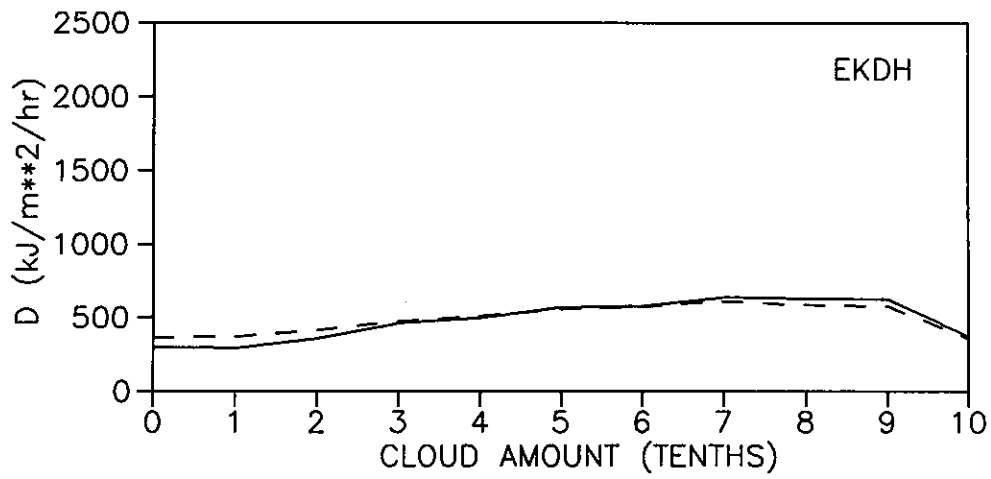
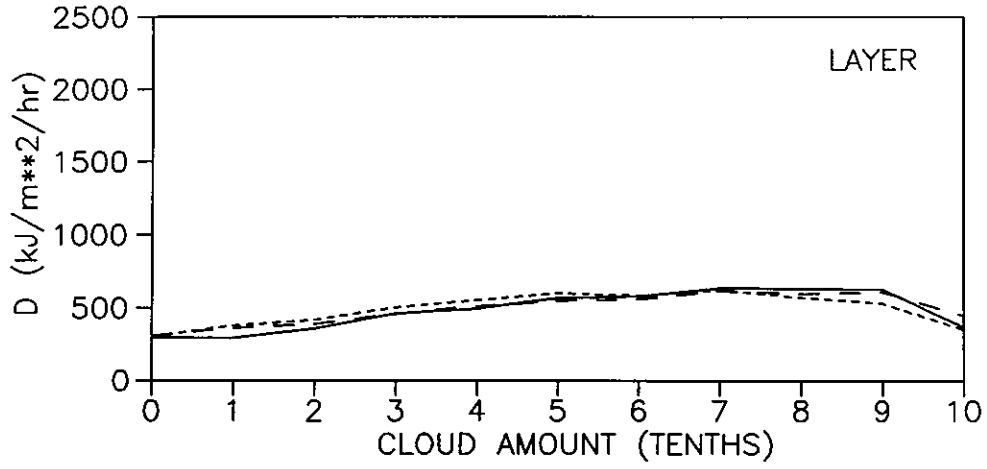


DIFFUSE RADIATION AND CLOUD  
ZURICH





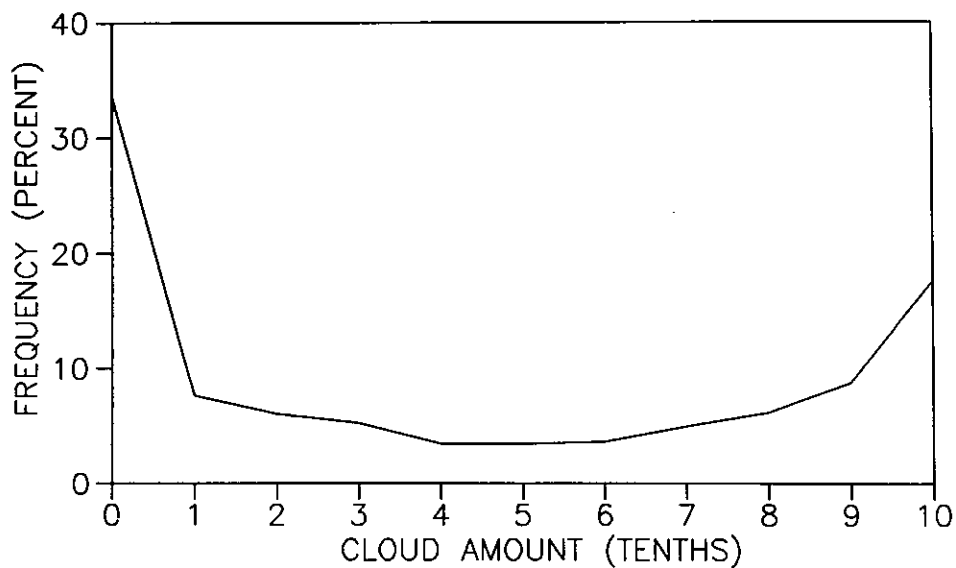
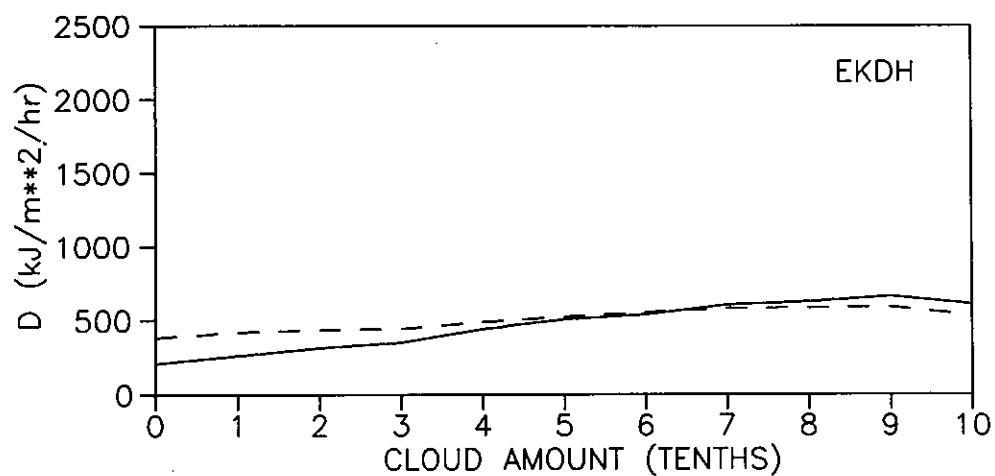
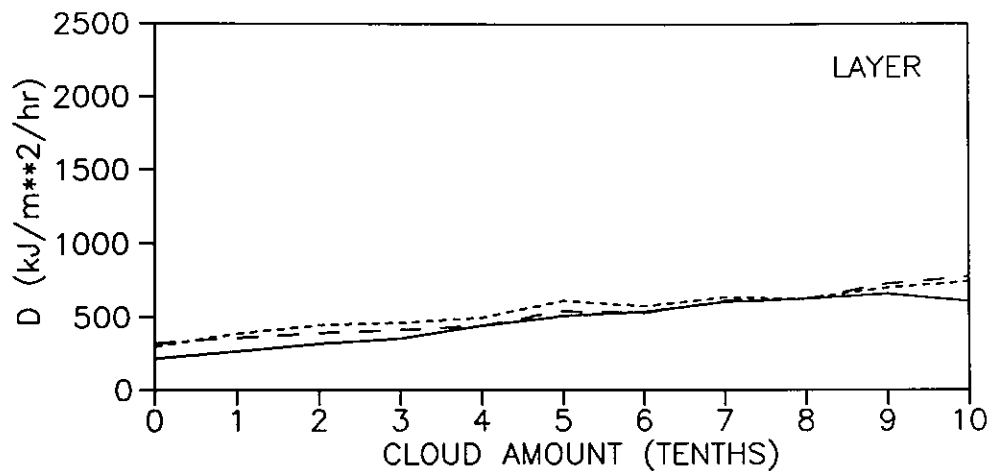
DIFFUSE RADIATION AND CLOUD  
MONTREAL

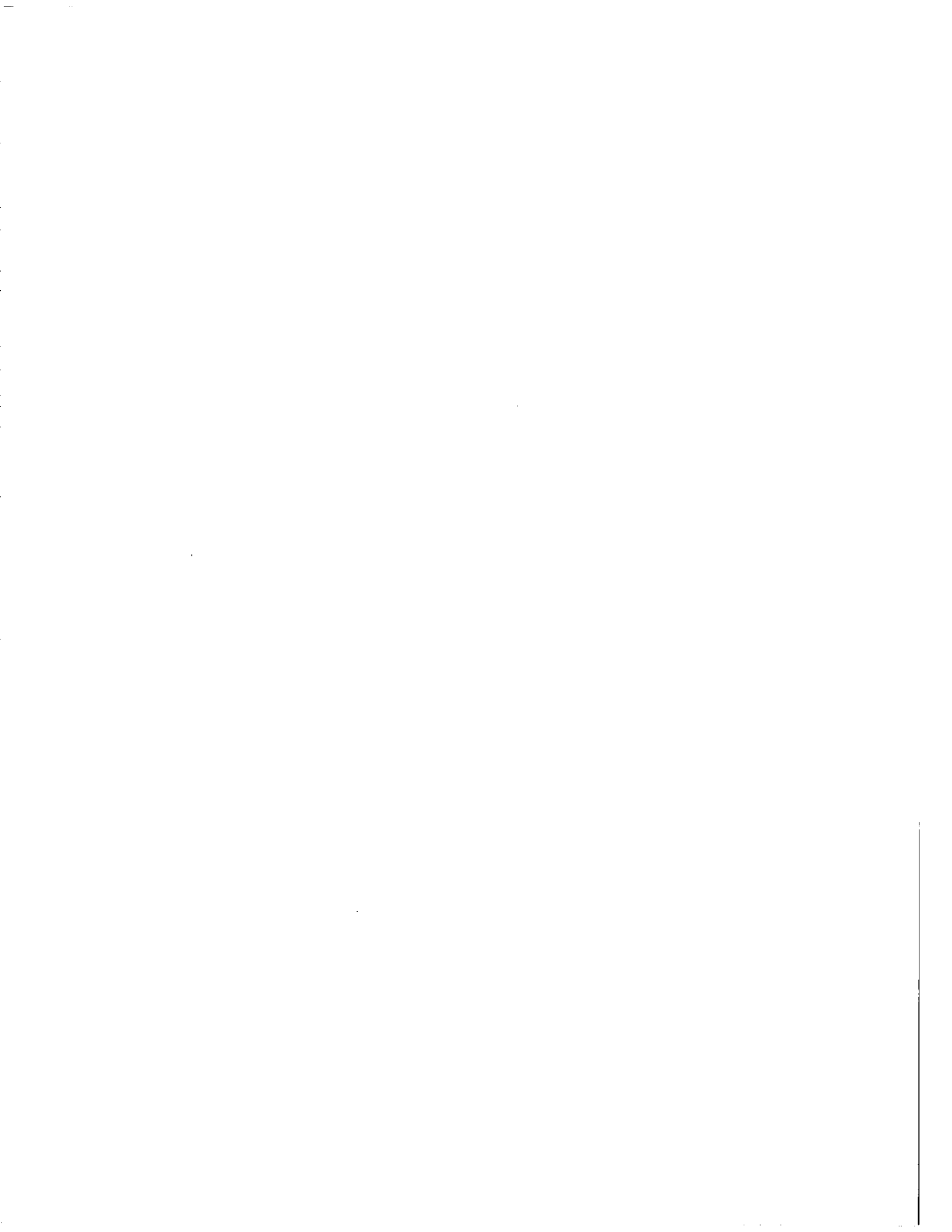




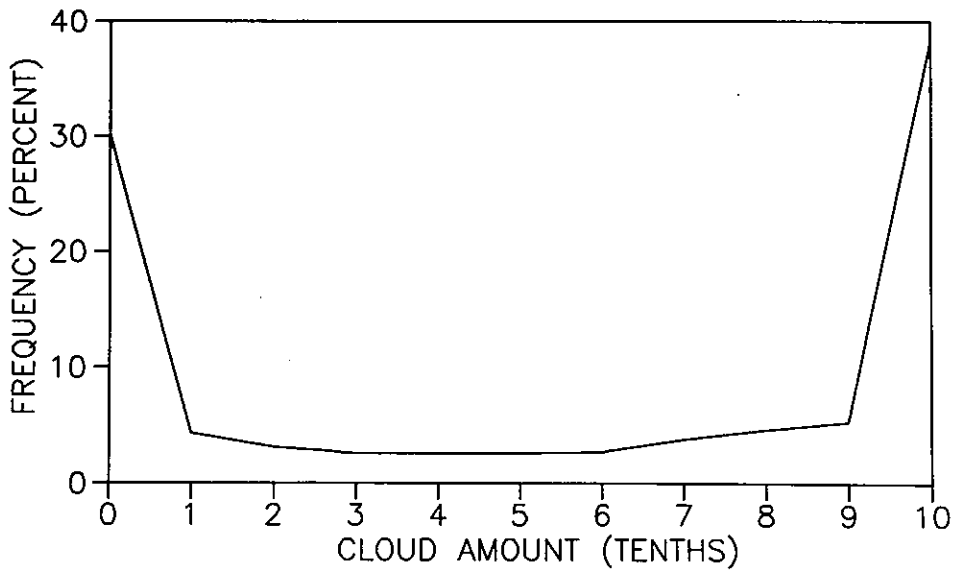
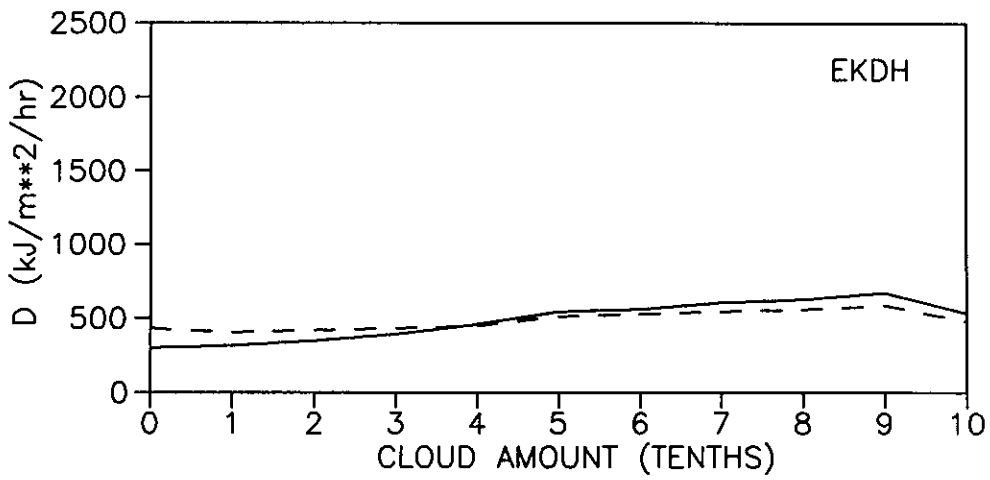
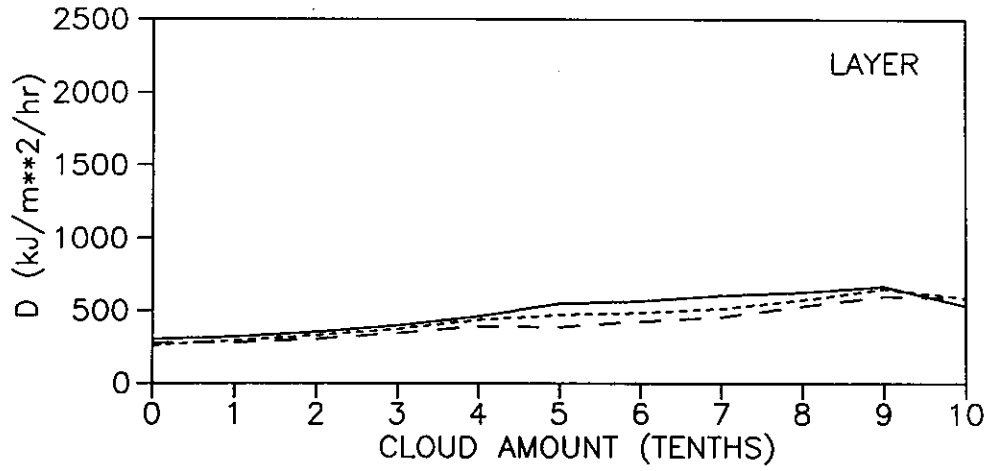


DIFFUSE RADIATION AND CLOUD  
ALBUQUERQUE





DIFFUSE RADIATION AND CLOUD  
MEDFORD



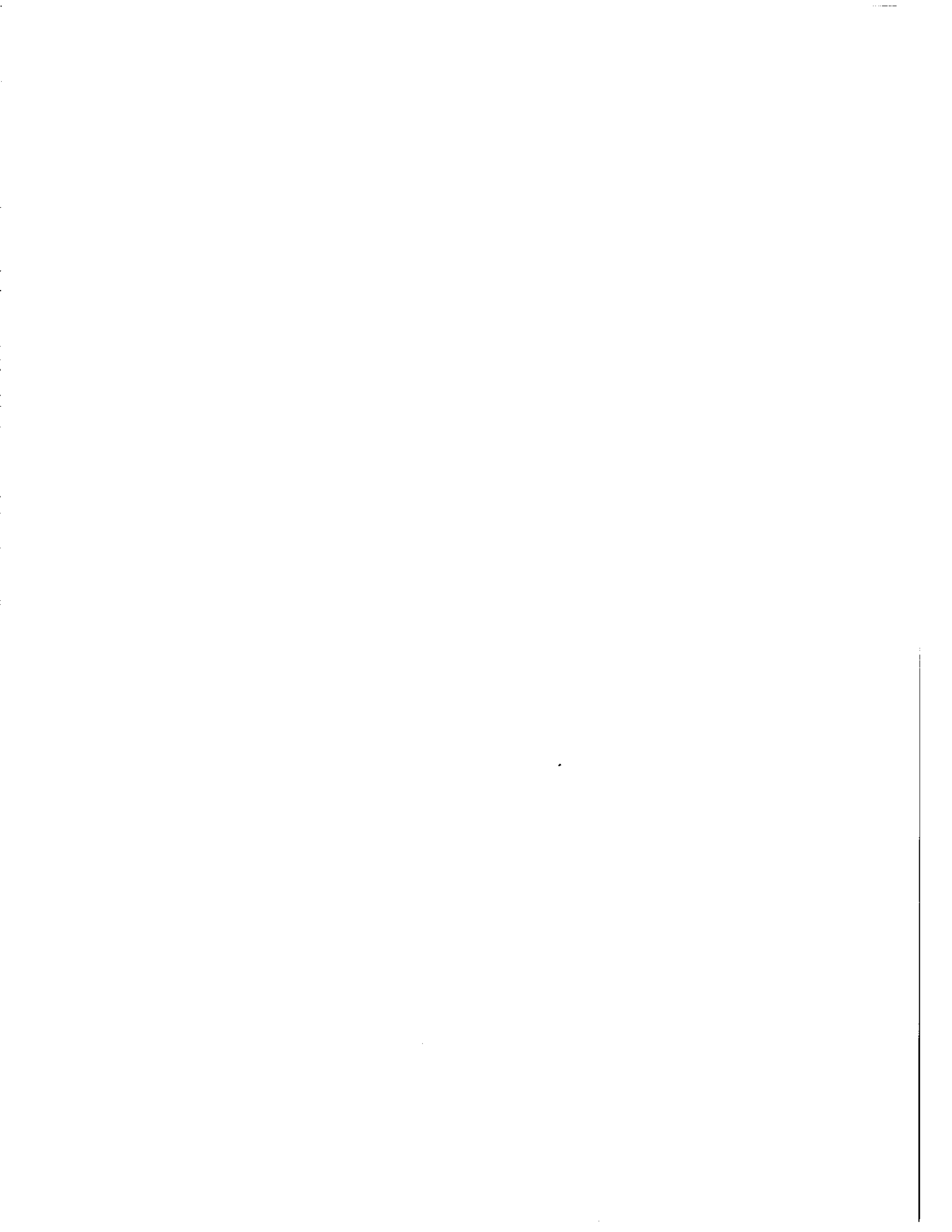


Table 12 Global radiation frequencies according to atmospheric transmission. Frequencies are expressed as percentages of the total number of measurements at each station

STATION	ATMOSPHERIC TRANSMISSION (PERCENT)							
	10	20	30	40	50	60	70	80
Alice Springs	1	2	3	4	7	9	32	42
Guildford	1	3	5	12	16	18	44	
Mildura	1	3	5	7	12	20	45	9
Rockhampton	1	2	4	8	15	26	42	1
Kew	13	16	17	17	17	15	5	
De Bilt	12	18	15	15	16	15	8	
Hamburg	15	16	17	16	14	13	9	1
Zurich	14	20	14	13	12	14	13	
Montreal	14	11	13	11	14	17	20	2
Winnipeg	3	8	10	12	14	17	31	6
Vancouver	16	13	10	11	11	16	23	
Albuquerque	1	2	4	5	8	16	44	19
Medford	4	11	11	12	11	13	36	2
Columbia	5	10	8	11	15	21	28	3
Sterling	8	7	10	13	16	26	19	
Averages								
Group 1	1	2	4	7	12	18	41	10
Group 2	8	10	10	13	14	18	25	2
Group 3	14	18	16	16	15	13	7	

measured values for all cloud amount categories, it is more important for practical purposes that the model perform well for the most frequently observed cloud amounts. Therefore, frequency distributions of cloud amounts are included in Figures 4a and 4b. These diagrams show that a successful model must perform well under low cloudiness at Alice Springs and Mildura; under both low and high cloudiness at Albuquerque and Medford; and under high cloudiness at Montreal, Kew, Hamburg and Zurich. Both *MAC* and *JOS* satisfy these conditions, although both tend to underestimate global radiation at the less frequently observed cloud amounts between 2 and 7 tenths.

In Figure 4b, the longer dashed line represents the *MAC* model estimates of diffuse and direct beam radiation in the layer model diagram and the shorter dashed line represents *JOS*. The results for the layer models are similar to the results for global radiation. With the exception of the two Australian stations, the agreement between *EKDH* model values and measurements is good. These results do not suggest serious deficiencies with these models.

Since cloud observations are, in some instances, incomplete and made on inconsistent scales (tenths and oktas), cloudiness was also represented by atmospheric transmission, which was calculated as the ratio of daily measured radiation to daily extraterrestrial radiation. Daily results for all years for each station were pooled. For each radiation flux, *MAB*, *MBE* and *RMSE* were calculated for atmospheric transmissions between 10% and 80% in 10% intervals. Each range was centred on a transmission value. For example, 30% includes transmissions greater than 25% and less than 35%. The number of days, the mean and standard deviation of the measured daily radiation were also calculated for each transmission range. The results are given in Appendix D. Results for measured global radiation suggested that the stations selected for this study fall into three

groups (Table 12):

- Australian stations and Albuquerque
- European stations
- Canadian stations and the remaining three US stations.

The first is the most cloud free and, therefore, has the largest occurrence of high transmissions; the second is the most cloudy with a uniform distribution of transmission frequency, and the third falls between the first two. Therefore, the European stations may provide the best test of model performance in all cloud conditions.

As with the previous examination of model performance with hourly cloudiness, we found no evidence of variations in model performance with atmospheric transmissivity.

#### 4.7 EFFECT OF USING INCOMPLETE CLOUD COVER DATA ON GLOBAL RADIATION ESTIMATES.

Consistent performance by the two layer models indicates that three-hourly cloud information can be used as successfully as hourly information. Changes in the performance of the MAC model are examined when the cloud field transmittance function is linearly interpolated between cloud observations at intervals from 2 to 6 hours. Meteorological data for the stations with hourly cloud observations (Montreal, Winnipeg, De Bilt, Hamburg and Zurich) were used. Calculations were made first for hourly observations, then repeated with observations selected every 2,3,4,5 and 6 hours. Cloud observations for the first and last daylight hours were always included.

The error statistics are given in Table 13. RMSE for 10-day and 30-day radiation averages are included. The *MBE* decreases systematically as interpolation



Table 13. MAC model performance statistics for different intervals between cloud observations. Statistics refer to pooled data for all years for each station.  $\langle G \rangle$  is the mean measured radiation for the period. RMSE(1), RMSE(10) and RMSE(30) are RMSE values for daily, 10-day mean and 30-day mean radiation.

	CLOUD DATA INTERVAL				
	1	3	4	5	6
MONTREAL: $\langle G \rangle = 12.10 \text{ MJ/m}^2/\text{day}$					
MBE	0.10	-0.01	-0.02	-0.19	-0.21
RMSE(1)	1.85	1.98	2.04	2.13	2.25
RMSE(10)	0.65	0.69	0.66	0.80	0.74
RMSE(30)	0.52	0.54	0.50	0.61	0.53
WINNIPEG: $\langle G \rangle = 13.11 \text{ MJ/m}^2/\text{day}$					
MBE	0.07	-0.05	-0.12	-0.22	-0.38
RMSE(1)	1.85	1.91	1.95	2.03	2.14
RMSE(10)	0.76	0.79	0.81	0.81	0.96
RMSE(30)	0.45	0.48	0.49	0.50	0.67
DE BILT: $\langle G \rangle = 9.96 \text{ MJ/m}^2/\text{day}$					
MBE	-0.08	-0.07	-0.13	-0.17	-0.14
RMSE(1)	1.62	1.75	1.81	1.95	1.98
RMSE(10)	0.66	0.69	0.74	0.73	0.81
RMSE(30)	0.41	0.49	0.50	0.445	0.58
HAMBURG: $\langle G \rangle = 9.87 \text{ MJ/m}^2/\text{day}$					
MBE	-0.13	-0.21	-0.25	-0.26	-0.30
RMSE(1)	1.67	1.78	1.81	1.88	2.02
RMSE(10)	0.76	0.79	0.89	0.82	0.86
RMSE(30)	0.49	0.50	0.60	0.48	0.50
ZURICH: $\langle G \rangle = 10.95 \text{ MJ/m}^2/\text{day}$					
MBE	-0.12	-0.16	-0.26	-0.35	-0.34
RMSE(1)	1.72	1.87	2.00	2.14	2.13
RMSE(10)	0.75	0.79	0.72	0.87	0.87
RMSE(30)	0.45	0.54	0.55	0.60	0.63

interval increases: the model underestimates increasingly. For 3-hourly cloud observations, the shift in bias is insignificant: less than 1% of the mean measured radiation. The tendency towards increased underestimation may be due to the linear interpolation of the cloud field transmission function, since in the model, the cloud transmissivity varies exponentially with optical air mass, which, in turn, varies non-linearly with time. For intervals longer than 3 hours, a non-linear interpolation would probably reduce this tendency.

*RMSE* increases with length of interpolation interval but for the 3-hourly case, the increase is less than 10% and for 10-day and 30-day averages differences between hourly and 3-hourly results are insignificant. Even for 6-hourly data, increases in *RMSE* are quite small especially for 10-day and 30-day averages.

Cloud regimes must be persistent to allow successful radiation estimates with cloud observations made less frequently than hourly. Changes in observed cloud amount were calculated for hourly, 3-hourly and 6-hourly intervals. Pooled results are shown separately for the Canadian and European stations in Figure 5. Persistence is confirmed: even for 6-hourly observations most changes in total cloud amount are within 1 tenth or 1 okta.

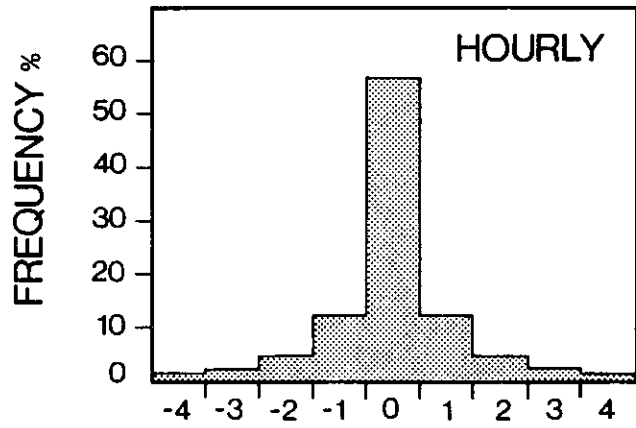
These results confirm that little error is introduced into model calculations when 3-hourly cloud observations are used. Results for 6-hourly cloud observations suggest that useful radiation estimates from this type of model may be obtained for remote locations, such as oceans, using single pass cloud data from satellites. Successful application depends on the persistence of the cloud field at a location.



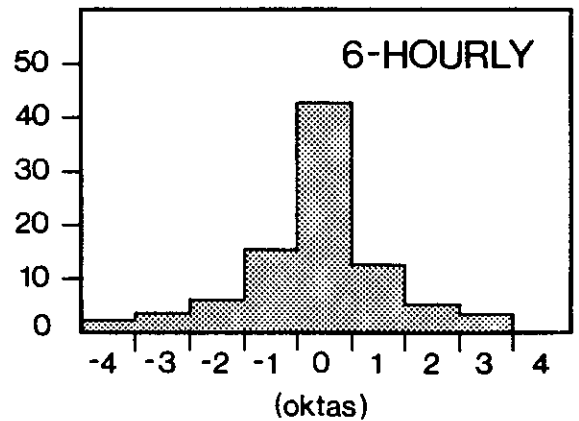
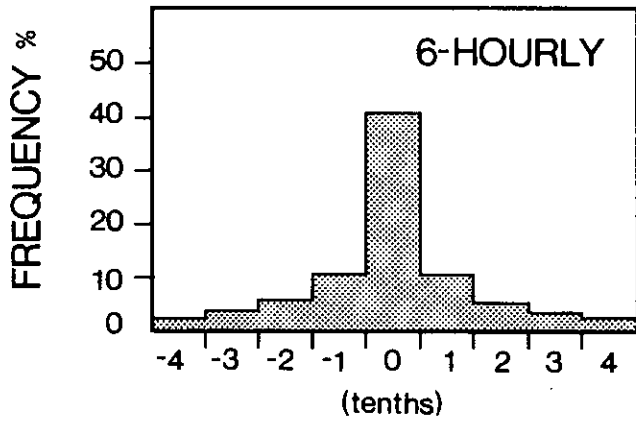
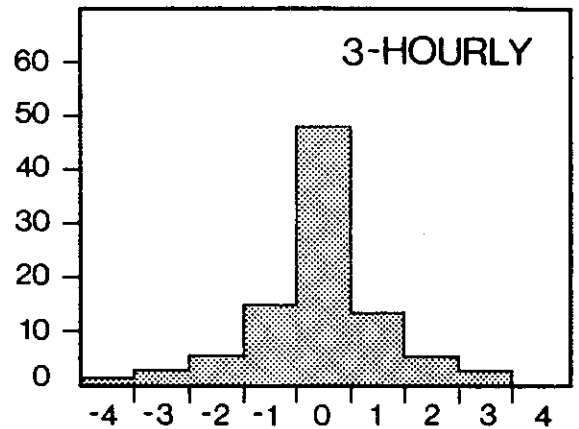
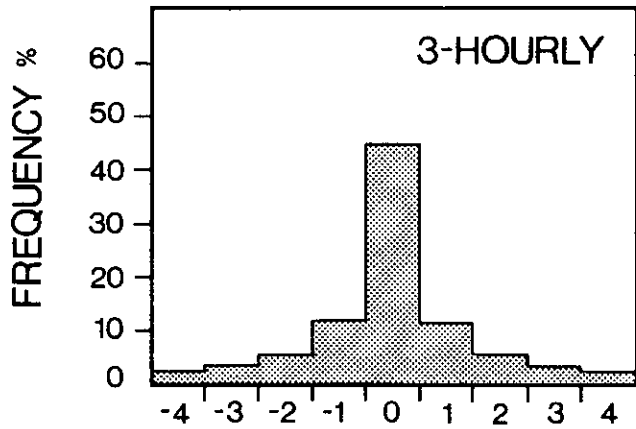
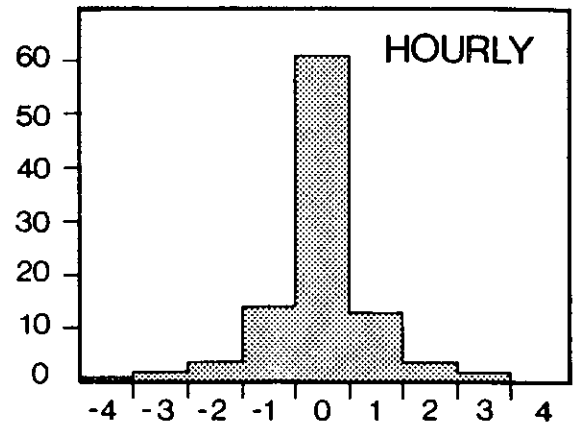
Figure 5 Frequency distributions of changes in observed cloud amount for hourly, 3-hourly and 6-hourly intervals for Canadian and European stations



CANADA



EUROPE



CHANGE IN CLOUD AMOUNT



#### 4.8 EFFECT OF INCLUDING MONTHLY VARIATIONS IN TURBIDITY ON GLOBAL RADIATION ESTIMATES FOR HAMBURG

Climatological estimates of Linke's index were available for Hamburg (Kasten, personal communication). The effect on *MBE* and *RMSE* of including them in Kasten's model on *MBE* and *RMSE* was determined for Hamburg for three years. Table 14 identifies the months (expressed numerically) where inclusion of a variable turbidity index improved or degraded each statistic and shows the overall effect in performance for each year. Improved performance was obtained only in 1978. The monthly distributions of better or worse performance do not show any clear pattern. Thus, it is unlikely that our general use of a fixed turbidity has produced significant error.

#### 4.9 EFFECT OF USING ESTIMATES OF INCIDENT RADIATION TO CALCULATE RADIATION ON TILTED SURFACES

This question was not considered using the data sets for this study but was addressed in a previous study using experimental tilted surface radiation data for Vancouver and the Meteorological Research Station at Woodbridge, Ontario in 1981 and 1982 (Davies and Abdel-Wahab, 1984). Global radiation on surfaces of different tilt and azimuth was calculated from the Hay model (Hay and Davies, 1980)

- using measured incident radiation;
- using *MAC* model estimates of incident radiation.

Average *RMSE* and *MBE* values for 1981 and 1982 for daily data and for 30-day means are given in Table 15. Davies and Abdel-Wahab concluded that:

- Daily *RMSE* values for tilted surface radiation using *MAC* model input are 20–30% larger than *MAC* model *RMSE* values for global radiation on a



Table 14 Effects on MBE and RMSE at Hamburg of including monthly variation in the Linke turbidity index in Kasten's model for global radiation. Months are identified numerically

		MBE	RMSE
1976	Months		
	Better in	1,2,3,10,11,12	1,10,11,12
	Worse in	4,5,6,7,8,9	2,3,4,5,6,7,8,9
	Year	Worse by -1.4 to -8.1%	Worse by 4.2%
1977	Months		
	Better in	2,7,9,10,	1,2,7,9,10,12
	Worse in	3,4,5,6,8,11,12	3,4,5,6,8,11
	Year	Worse by -4.1 to 2.8%	Worse by 2.3%
1978	Months		
	Better in	3,7,8,9,10	1,3,7,9,10,12
	Worse in	1,2,4,5,6,11,12	2,4,5,6,8,11
	Year	Better by -2% to 5%	Better by 0.2%

horizontal surface.

- *RMSE* increase by up to a factor of two when the *MAC* model results are used.
- In percentage terms, *RMSE* values for the different tilted surfaces are similar.
- *RMSE* values for radiation estimates using *MAC* input are less than 10% for monthly averages.

Hourly *RMSE* values are up to seven times as large as values calculated from measured input data. Such values can be predicted *a priori* by standard error analysis (Bevington, 1969) if the *RMSE* of the radiation input data for a numerical model is known (Davies and Abdel-Wahab, 1984). Using *MAC* model hourly *RMSE* values for global, diffuse and direct beam radiation, estimates of the *RMSE* for tilted surfaces were calculated for each month in 1981 for both Vancouver and Woodbridge. Figure 6 shows that these anticipated values are in reasonable agreement with actual *RMSE* values obtained when tilted surface radiation values were calculated from *MAC* model radiation inputs. Since differences between the *RMSE* values of the *MAC* and *JOS* models are small, both must yield similar *RMSE* values for radiation estimates on tilted surfaces.

Davies and Abdel-Wahab (1984) also calculated tilted surface radiation using the *OH* model to partition global radiation. Two sets of calculations were made: one using measured global radiation (*OH1*) and the other using *MAC* model estimates (*OH2*). Table 16 summarizes the results for Vancouver and Woodbridge for hourly radiation for *OH1*, *OH2*, *MAC* and *HAY* (calculations using measured direct beam and diffuse radiation input). Differences in *MBE* between the four methods are small. For south-facing surfaces, *RMSE* for *OH1* is less than twice *RMSE* for *HAY*, but increases to 3–4 times the *HAY* value for east-facing and

Table 15 MBE and RMSE values ( $\text{MJ}/\text{m}^2/\text{day}$ ) for estimated radiation for tilted surfaces using MAC model (upper row) and measured (lower row) input. Data were averaged for both stations for both years.  $\langle G \rangle$  is mean measured radiation for a given surface. RMSE(1) and RMSE(30) are RMSE for daily values and 30-day means

	TILTED SURFACE				
	30S	90S	90E	90W	90N
$\langle G \rangle$	13.94	9.88	7.97	7.21	4.79
MBE	-0.37 0.14	-1.08 -0.10	-0.06 -0.58	-0.02 1.00	-0.19 -0.78
RMSE(1)	2.82 0.95	2.18 0.99	1.71 0.87	1.58 0.75	1.15 0.79
RMSE(30)	1.31 0.45	1.03 0.43	0.71 0.37	0.66 0.37	0.39 0.33

Figure 6 Comparison between actual and estimated values of RMSE for radiation on tilted surfaces at Vancouver and Woodbridge



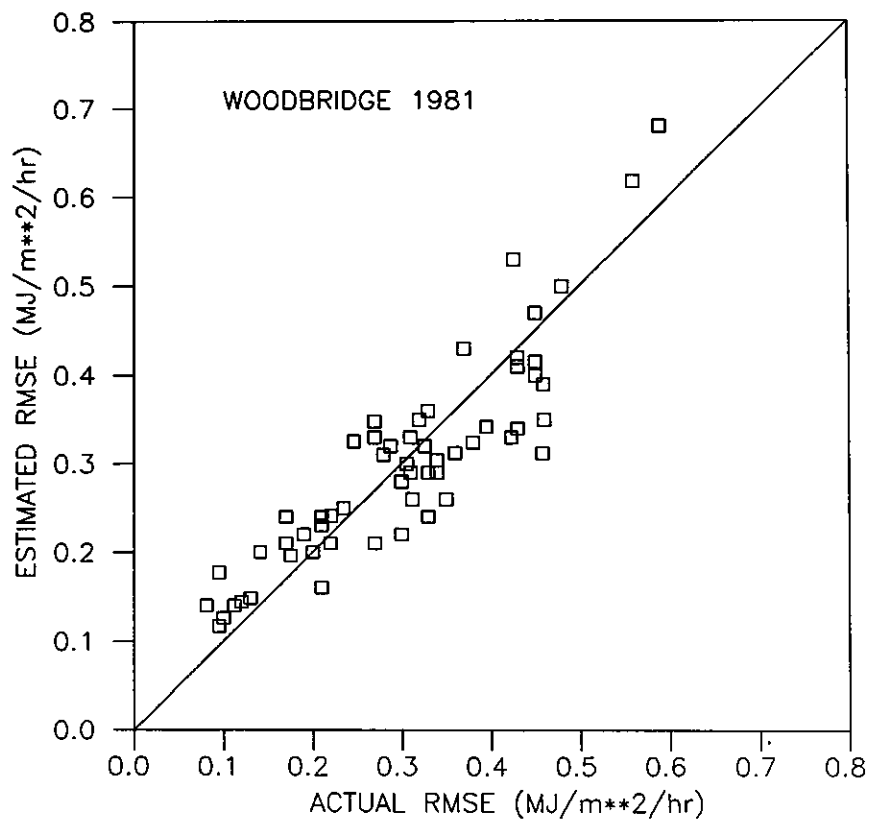
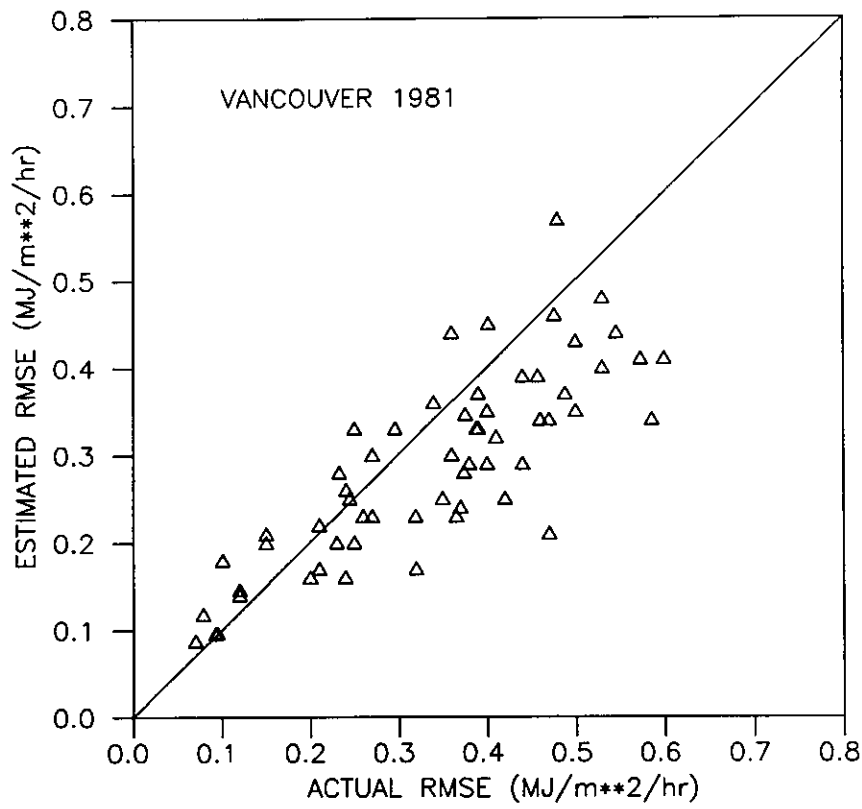




Table 16 MBE and RMSE values ( $\text{MJ}/\text{m}^2/\text{hr}$ ) for estimates of tilted surface radiation using measured input (HAY), measured global radiation with partitioning by the OH model (OH1), numerical model input (MAC), and numerical model global radiation with partitioning by the OH model (OH2). The results are for Vancouver and Woodbridge in 1981.  $\langle G \rangle$  is the mean measured radiation for a given surface

	30S	TILTED SURFACE			
		90S	90E	90W	90N
<b>MBE</b>					
<b>VANCOUVER</b>					
$\langle G \rangle$	1.162	0.847	0.634	0.527	0.286
HAY	-0.017	-0.015	0.006	0.036	0.022
OH1	0.003	0.005	0.010	0.043	0.003
MAC	-0.077	-0.053	0.002	0.044	0.013
OH2	-0.067	-0.050	0.000	0.053	0.015
<b>WOODBIDGE</b>					
$\langle G \rangle$	1.139	0.768	0.623	0.646	0.362
HAY	0.026	-0.039	-0.044	-0.008	-0.014
OH1	0.034	-0.027	-0.012	0.023	0.029
MAC	0.030	-0.044	-0.029	0.034	0.003
OH2	0.038	-0.023	0.011	-0.068	-0.025
<b>RMSE</b>					
<b>VANCOUVER</b>					
HAY	0.050	0.071	0.078	0.089	0.090
OH1	0.085	0.146	0.354	0.262	0.153
MAC	0.399	0.326	0.321	0.302	0.202
OH2	0.582	0.484	0.412	0.457	0.158
<b>WOODBIDGE</b>					
HAY	0.132	0.153	0.199	0.142	0.116
OH1	0.167	0.228	0.415	0.440	0.333
MAC	0.416	0.357	0.291	0.287	0.170
OH2	0.475	0.433	0.311	0.341	0.151



west-facing surfaces. For surfaces other than south-facing at Woodbridge the *RMSE* for *OH1* exceeds *RMSE* for *MAC* and *OH2*, while at Vancouver, the three sets of *RMSE* values are similar. There is no advantage in using *OH2* instead of the *MAC* model, and *OH1* only gave better results than the *MAC* model for south-facing slopes.

## CHAPTER 5: SUMMARY AND CONCLUSIONS

### 5.1 Global radiation

- Model rankings using either hourly or daily radiation are the same. In general, the cloud layer models (*JOS*, *MAC*) provide the best estimates with *JOS* usually best. Except for Australia, they perform similarly. This is expected since differences between the models are slight. *RMSE* results for 30-day means show even more clearly the superiority of layer models. With the exception of Australian stations, the *MAC* model has smallest *RMSE* for global radiation. The best *RMSE* values for global radiation are 3–5 times larger than those for *BEST*.

- Even incomplete cloud layer information can be successfully used in layer models. Model performance is not degraded when multi-layer cloud information is not available for all levels. Since cloud cover is persistent, little error is introduced if three-hourly rather than hourly cloud observations are used. Useful layer model estimates of global radiation may be obtained even from six-hourly cloud observations.

- Rietveld's procedure for estimating the  $a$  and  $b$  parameters for the Ångström equation did not improve upon radiation estimates from Page's model which uses fixed parameter values. *PAGE* and *KAS* performed similarly.

- The performance of Kasten's model was not improved either by introducing water vapour absorption explicitly or by including a monthly varying Linke turbidity factor.

- There is one surprising regional discrepancy. *MON* is the best performer for the USA but the worst for EUR and EURCAN.

- The *BCLS* model performed surprisingly poorly.

## 5.2 Diffuse and direct beam radiation

- As expected, Liu and Jordan models provided the best estimates; *OH* and *EKDH* for hourly radiation and *EKDD* for daily. However, daily estimates from *EKDH* were superior for North America. *CPR* did not perform as well as the other three models of this type. In Australia, both *CPR* and *OH* failed to match the performance of the layer models. Differences in uncertainty between Liu and Jordan models and layer models is about 25% for daily estimates. The magnitude of this difference may be offset by the Liu and Jordan models' requirement for measured global radiation.

- Layer model estimates improve significantly, and possibly to the point of acceptance, for radiation averaged over periods longer than a day. For 30-day means, diffuse and direct beam radiation layer model values are often similar or even better than values for Liu and Jordan models. Monthly estimates of these components from the two types of models have comparable accuracy. This is an important result for applications where monthly radiation estimates are sufficient.

## 5.3 Variation in model performance with season and cloudiness

Although the stations selected for this study represented a wide range of atmospheric conditions, there was no consistent evidence of variations in the performance of the better models from month to month or with cloudiness and atmospheric transmissivity. This suggests that these models may have general application.

## 5.4 Effect of using MAC model estimates of incident radiation to calculate radiation on tilted surfaces with the Hay model at Vancouver and Woodbridge

- Daily *RMSE* values for tilted surface radiation are 20–30% larger than *MAC* model *RMSE* values for global radiation on a horizontal surface. Generally,

*RMSE* increase by up to a factor of two when the *MAC* model results are used. For monthly averages *RMSE* are less than 10%.

- Hourly *RMSE* values are up to seven times as large as values calculated from measured input data. Knowing the *RMSE* of model input data error analysis can be used to estimate hourly *RMSE* values for radiation calculations for tilted surfaces.

- There was no advantage in partitioning numerical model estimates of global radiation with the *OH* model and little advantage in partitioning measured global radiation.

### 5.5 General

- Differences between the statistical measures of error for the best and worst performing models may not be sufficiently large to be significant for solar energy or any other purpose. Because there is no clear statement on the required accuracy of radiation estimates, it is impossible to assess whether these results, or others, are sufficient for recommending one or more models. Since the performance of *BEST* is not much better than that of the layer models, one possible interpretation of the results is that models are close to the limit of prediction. The difference in *RMSE* between *JOS* (1.67 MJ/day) and *BEST* (1.42 MJ/day) for EURCAN may be insufficient to justify further modelling efforts. The performance of models which use surface meteorological measurements and observations is probably limited more by the inadequacy of this information than by modifiable defects in the models themselves. Nor do models which use satellite information provide surface global radiation estimates which are always superior to layer model estimates (Davies *et al.*, 1984).

- There is little to recommend sunshine-based models. Even though the Ångström equation can be easily tuned to a location's climatic conditions by simple

regression, it requires the existence of radiation measurements in the first place to produce the prediction equation and faith that the regression can be applied to sunshine data for another place or time. Its computational simplicity is irrelevant in the age of the microprocessor. All models used in this study are computationally simple. We see little virtue in any further empirical studies with the Ångström equation.

## 5.6 Recommendations

- Layer models should be used for estimating global radiation wherever possible. These models, which have their origins in early attempts to model radiation for large scale climate modelling (Houghton, 1954; Manabe and Strickler, 1964), might be refined further with parameterizations from modern climate models. However, present performance limits for these and other models may be set by inadequacies of meteorological input data rather than inadequacies in models. Even the use of satellite information to estimate surface global radiation has not yet shown substantial improvement in estimates (Davies et al., 1984).

- Liu and Jordan models, particularly *EKDH* and *EKDD*, are generally best for estimating direct beam and diffuse components. Since they are statistical they can not have general applicability.

- Further modelling effort would benefit from clear guidelines from the solar energy community concerning the required accuracies of radiation estimates that are permissible.

## CHAPTER 6: AVAILABILITY OF MODELS AND DATA

The FORTRAN programs used to calculate radiation fluxes and produce statistical results are available either on 9-track computer tape or on floppy disks (360K or 1.2MB formats). All programs were run on either an IBM XT compatible (Compaq Deskpro) or an IBM AT compatible (Texas Instruments Business Professional) microcomputer using the Microsoft FORTRAN 77 Version 3.2 compiler. Computer time to process one year of data, which includes calculations of hourly and daily radiation fluxes for all models and monthly and annual statistics, varied between 15 and 30 minutes on the AT computer. The range in times is due to different sizes of meteorological data input files. This range was reduced to 2 to 6 minutes using Microsoft FORTRAN Version 4.1 on a Compaq 386/20 machine.

The programs' READ statements use the standard format for each country's meteorological data. For use on microcomputers, the FORTRAN programs have been split into two parts (eg. UK1.FOR and UK2.FOR) for separate compilation within the limits of the Microsoft compiler. After compilation, they are linked to create a single executable file as specified in Microsoft's manuals. Combined source codes for mainframe use are also included (for example, UK.FOR). Input/output statements must be amended for the appropriate system. The READ statements only apply to the formats of the tapes provided to us for this study by various agencies.

In addition, we have created files of hourly meteorological data, including measured and calculated radiation fluxes, for all stations using a common format. Hence, the data and results from this study can be accessed easily for other uses. These files only include hourly data for the daylight period. For one year at one station, a file is typically less than 700K. These data can be read with the following

READ and FORMAT statements (a sample OPEN statement is included):

```

OPEN(7,FILE='ALICE80.DAT',STATUS='OLD')
READ(7,1)ISTA,MYR,MON,IDAY,J,ST,ISH,ITCA,ITCO,
+(ICA(L),ICT(L),L=1,4),IDBT,INDIC,IHUM,IPRESS,IVIS,
+IRAIN,IRF1,IG,IRF2,ID,IRF8,IS
1  FORMAT(5I2,F5.2,I2,2I4,4(I4,I2),I4,I1,I4,I5,2I3,23I4)

```

The variables are:

ISTA Station identifier:

#### AUSTRALIA

02	Alice Springs
07	Guildford
13	Mildura
19	Rockhampton

#### EUROPE

70	DeBilt
75	Hamburg
62	Kew
40	Zurich

#### NORTH AMERICA

32	Albuquerque
30	Columbia
31	Medford
51	Montreal
34	Sterling
52	Vancouver
50	Winnipeg

MYR	Year (e.g. 82)
MON	Month (ie.1,2,3,...,12)
IDAY	Day of the month (ie.1,2,3,...,31)
J	Hour of the day (ie.1,2,3,...,24)
ST	Solar time (e.g. 10.00)
ISH	Fraction of the hour with bright sunshine (X10) Divide by 10. Missing data: -99.
ITCA	Total cloud amount (X1000) Divide by 1000. Missing data: -99.
ITCO	Total cloud opacity (X1000) Divide by 1000. Missing data: -99.
ICA(L)	Cloud amount (tenths) in the lth layer (X1000) Divide by 1000. Missing data: -99.
ICT(L)	Type of cloud in the lth layer
IDBT	Dry bulb temperature (Celsius)(X10) Divide by 10. Missing data: -999.
INDIC	= 1 Relative humidity recorded = 0 Dew point temperature recorded
IHUM	Relative humidity or dew point temperature (X100) Divide by 100. Missing data: -999.
IPRESS	Station pressure (kPa)(X100)

IVIS Divide by 100. Missing data: --999.  
 Visibility (km)(X10)  
 IRAIN Divide by 10. Missing data: -99.  
 Precipitation. Missing data:-99)

IRF1 Measured global radiation ( $\text{kJ}/\text{m}^2/\text{hr}$ )

ESTIMATED GLOBAL RADIATION

IG(1)	MAC
IG(2)	KAS
IG(3)	JOS
IG(4)	KASM
IG(5)	MON

IRF2 Measured diffuse radiation ( $\text{kJ}/\text{m}^2/\text{hr}$ )

ESTIMATED DIFFUSE RADIATION

ID(1)	MAC
ID(2)	KAS
ID(3)	JOS
ID(4)	KASM
ID(5)	OH
ID(6)	EKDH

IRF8 Measured direct beam radiation ( $\text{kJ}/\text{m}^2/\text{hr}$ )

IS(1)	MAC
IS(2)	KAS
IS(3)	JOS
IS(4)	KASM
IS(5)	OH
IS(6)	EKDH

Missing data for measured and calculated radiation fluxes: -99.

Cloud type codes are not standardized. We have used the codes employed by each country. Table 17 lists these codes. Canada, the Netherlands, U.S.A, Switzerland and West Germany employ codes that correspond to single cloud types which are independent of layer. However, Australia and the United Kingdom use layer-specific codes.



Table 17 Summary of cloud codes

Canada, U.S.A., Netherlands, Switzerland and West Germany			
Cloud type	Canada	U.S.A	Net./Switz./W. Ger.
Fog	15	1	10
Stratus	14	2	7
Stratocumulus (Sc)	13	3	6
Cumulus	8	4	8
Cumulonimbus	7	5	9
Altostratus (As)	3	6	4
Alto cumulus (Ac)	1	7	3
Cirrus	6	8	0
Cirrostratus	5	9	2
Stratus fractus	10	10	
Cumulus fractus	9	11	
Cumulonimbus Mamm.		12	
Towering cumulus	11		
Nimbostratus (Ns)	12	13	5
Alto cumulus cast.	2	14	
Cirrocumulus	4	15	1
OOTF	16	16	
Australia and U.K			
Code	Low	Middle	High
0	None	None	None
1	Cumulus fractus	Altostratus	Cirrus
2	Cumulus	Alto/Nimbostratus	Denser cirrus
3	Cumulonimbus	Alto cumulus	Densest cirrus
4	Stratocumulus	Alto cumulus	Cirrus
5	Stratocumulus	Alto cumulus cast.	Cirrostratus
6	Stratus	Alto cumulus	Cirrostratus
7	Stratus/Ns	As/Ns/Ac	Cirrostratus
8	Cumulus/Sc	Alto cumulus	Cirrostratus
9	Cumulonimbus Mamm.	Chaotic sky	Cirrocumulus

These data are available on 9 track tape. Individual years for any station can be provided on 1.2 Mb floppy disk, which can only be read on 286 (i.e. AT) and 386 microcomputers.

All requests for data and programs should be addressed to:  
Dr.D.C.McKay, Canada Climate Centre, The Atmospheric Environment Service,  
4905 Dufferin Street, Downsview, Ontario, M3H 5T4,Canada.



## CHAPTER 7: REFERENCES

- AES (1980). Define, develop and establish a merged solar and meteorological computer data base. *Canadian Climate Centre Report No.80-8*. Available from the Atmospheric Environment Service, Downsview, Ontario, Canada.
- Ångström, A.(1924). Solar and Terrestrial radiation. *Q.J.R.Meteorol.Soc*, 50, 121-5.
- ASHRAE (1972). *Handbook of Fundamentals*. American Society of Heating, Refrigerating and Air Conditioning Engineers, New York, 688p.
- Atwater, M.A. and J.T.Ball (1976). Comparison of radiation computation using observed and estimated precipitable water. *J. Appl. Meteorol.*,15, 1319-1320.
- Atwater. M.A. and J.T.Ball (1978). A numerical solar radiation model based on standard meteorological observations. *Solar Energy*,21, 163-170.
- Ball, R.J. and G.D.Robinson (1982). The origin of haze in the central United States and its effect on solar irradiance. *J. Appl.Meteorol.*,21, 171-188.
- Barbaro,S., S.Coppolino, C.Leone and E. Sinagra (1979). An atmospheric model for computing direct beam and diffuse solar radiation. *Solar Energy*,22, 225-228.
- Berland, T.G. and V.Y. Danilchenko (1961). *The continental distribution of solar radiation*. Gidrometeoizdat, Leningrad.
- Bevington, P.R.(1969). *Data reduction and error analysis for the physical sciences*. McGraw-Hill, New York, 336p.
- Collares-Pereira, M. and A. Rabl (1979). The average distribution of solar radiation correlations between diffuse and hemispherical and between daily and hourly insolation values. *Solar Energy*,22, 155-164.
- Davies, J.A. (1965). Estimation of insolation for West Africa. *Q. J. R. Meteorol. Soc.*,91, 359-363.

- Davies, J.A., W. Schertzer and M. Nunez (1975). Estimating global solar radiation. *Boundary-Layer Meteorol.*,9, 33-52.
- Davies, J.A. and T.C. Uboegbulam (1979). Parameterization of surface incoming radiation in tropical cloudy conditions. *Atmosphere-Ocean*,17, 14-23.
- Davies, J.A. and J.E. Hay (1980). Calculation of the solar radiation incident on a horizontal surface. *Proc. First Canadian Solar Radiation Data Workshop*, edited by T.Won and J.E.Hay, 32-58.
- Davies, J.A. (1981). Models for estimating incoming solar irradiance. *Canadian Climate Centre Report No. 81-2*. Available from the AES, Downsview, Ontario, Canada.
- Davies, J.A. and D.C. McKay (1982). Estimating solar irradiance and components. *Solar Energy*,29, 55-64.
- Davies, J.A., M. Abdel-Wahab and J.E. Howard (1984). Cloud transmissivities for Canada. *Mon. Weather. Rev.*,113, 338-348.
- Davies, J.A. and M.Abdel-Wahab (1984). *Further evaluation of the MAC model*. Report to the AES. Available from the AES, Downsview, Ontario, Canada.
- Davies, J.A. (1987). Parameterization for Rayleigh scattering. *Solar Energy*,39,31-32.
- Erbs, D.G., S.A. Klein and J.A. Duffie (1982). Estimation of the diffuse radiation fraction for hourly, daily and monthly average global radiation. *Solar Energy*,28, 293-302.
- Haurwitz, G.(1948). Insolation in relation to cloud type. *J.Meteorol.*,5, 110-113.
- Hay, J.E. (1970). *Aspects of the heat and moisture balance of Canada*. Ph.D thesis, University of London, 322p.
- Hay, J.E. (1979). Calculation of monthly mean solar radiation for horizontal and inclined surfaces. *Solar Energy*,23, 301-307.
- Hay, J.E. and J.A. Davies (1980) Calculation of the solar radiation incident on an

- inclined surface. Proc. First Canadian Solar Radiation Data Workshop, edited by T.Won and J.E. Hay, 59–72.
- Houghton, H.G. (1954). The annual heat balance in the northern hemisphere. *J.Meteorol.*,11, 1–19.
- Hoyt, D.V. (1978). A model for the calculation of solar global insolation. *Solar Energy*,21, 27–35.
- Kasten, H. (1966). A new table and approximation formula for the relative optical air mass. *Archiv fur Meteorol. Geophys. und Bioklim.*,B,206–223.
- Josefsson, W. (1985). Modelling direct and global radiation from hourly synoptic observations. Unpublished manuscript.
- Kasten, F. and G. Czeplak (1980). Solar and terrestrial radiation dependence on the amount and type of cloud. *Solar Energy*,34, 177–190.
- Kasten, F. (1980). A simple parameterization of the pyrhelimetric formula for determining the Linke turbidity factor. *Meteorol. Rdsch.*,33, 124–127
- Kasten, F. (1983). Parametrisierung der globalstrahlung durch bedeckungsgrad und trubungsfaktor. *Ann. Met.*,20, 49–50.
- Kimura, K. and D.G. Stephenson (1969). Solar radiation on cloudy days. Research Paper No. 418, Division of Building Research, National Research Council, Ottawa, 9p.
- Lacis, A.A. and J.E. Hansen (1974). A parameterization for the absorption of solar radiation in the earth's atmosphere. *J. Atmos.Sci.*,31, 118–133.
- Lettau, H. and K. Lettau (1969). Short-wave radiation climatology. *Tellus*,21, 208–222.
- Liu, B.Y.H. and R.C. Jordan(1960). The interrelationship and characteristic distribution of direct, diffuse and total solar radiation. *Solar Energy*,4, 1–19.
- Manabe, S. and R.F.Strickler (1964). Thermal equilibrium of the atmosphere with convective adjustment. *J.Atmos.Sci.*,21, 361–385.

- Monteith, J.L.(1961). An empirical method for estimating long wave radiation exchanges in the British Isles. *Q.J.R. Meteorol.Soc.*,87, 171–179.
- Monteith, J.L. (1962). Attenuation of solar radiation: a climatological study. *Q.J.R. Meteor.Soc.*,88, 508–521.
- Orgill, J.F. and K.G.T. Hollands (1977). Correlation equation for hourly diffuse radiation on a horizontal surface. *Solar Energy*,19, 357–359.
- Page, J.K. (1961). The estimation of monthly mean values of daily total shortwave radiation on vertical and inclined surfaces from sunshine records for latitudes 40°N–40°S. *Proc. U.N. Conference on New Sources of Energy, Paper No. 35/S/98*, 378–390.
- Painter, H.E.(1981). The performance of a Campbell–Stokes sunshine recorder compared with a simultaneous record of the normal incidence irradiance. *Meteorol. Mag.*,110, 102–109.
- Rietveld, H.R.(1978). A new method to estimate the regression coefficients in the formula relating radiation to sunshine. *Agric. Meteorol.*,19, 243–252.
- Robinson, G.D.(1962). Absorption of solar radiation by atmospheric aerosol, as revealed by measurements from the ground. *Arch. Meteorol. Geophys. Bioklimatol.*, B,12, 19–40.
- Rogers, C.D.(1967). The radiative heat budget of the troposphere and lower stratosphere. *Report No. A2, Planetary Circulation Project, Dept. of Meteorology, M.I.T.*,99p.
- Spencer, J.W.(1971). Fourier series representation of the position of the sun. *Search*,2, 172.
- Suckling, P.W. and J.E.Hay (1976). Modelling direct, diffuse and total solar radiation for cloudless skies. *Atmosphere*,15, 298–308.
- Suckling, P.W. and J.E.Hay (1977). A cloud layer–sunshine model for estimating direct,diffuse and solar radiation. *Atmosphere*,15, 194–207.

- Tomasi, C. (1981). Determination of the total precipitable water by varying the intercept of Reitan's relationship. *J. Appl. Meteorol.*,20, 1058–1069.
- Won, T.K.(1977). *The simulation of hourly global radiation from hourly reported meteorological parameters—Canadian Prairie area*. Third Conference, Canadian Solar Energy Society, Edmonton, Alberta.



